Living on the Edge:

Protective Mechanisms Underlying Thermal Tolerance in High Latitude *Symbiodinium* spp.

Stefanie Pontasch

A thesis submitted to Victoria University of Wellington in fulfilment of the requirements for the degree of Doctor of Philosophy in Science

Victoria University of Wellington

2014

ABSTRACT

The association between symbiotic dinoflagellates (*Symbiodinium* spp.) and corals extends to subtropical and temperate regions, where sea surface temperatures (SSTs) are generally lower than in the tropics and can vary substantially over the course of the year due to seasonal changes. These high latitude coral-dinoflagellate symbioses might be better able to withstand thermal variability and might be particularly well equipped to cope with lower SSTs compared to their tropical relatives.

The aim of this thesis was to analyze the cellular mechanisms that underlie heat and/or cold tolerance in a range of reef-building corals (*Acropora yongei*, *Acropora solitariensis*, *Isopora palifera*, *Pocillopora damicornis*, *Porites heronensis* and *Stylophora* sp.), as well as the symbiotic sea anemone *Entacmaea quadricolor*. In particular, the study focussed on protective mechanisms in their dinoflagellate symbionts as a potential determinant of thermal sensitivity (i.e. bleaching) or resistance of the intact symbiosis. High latitude reef-building corals were analyzed at the world's southernmost coral reef at Lord Howe Island, while *E. quadricolor* was sampled at the subtropical coral community at North Solitary Island; both sites are located in New South Wales, Australia.

The specific objectives were to assess the roles of: (1) xanthophyll de-epoxidation; (2) thylakoid fatty acid composition; (3) *Symbiodinium* superoxide dismutase (SOD) and ascorbate peroxidase (APX) activity; and (4) D1 repair on the photophysiology, bleaching susceptibility and survivorship of a range of high-latitude coral-*Symbiodinium* associations from Lord Howe Island when exposed to elevated or decreased temperature. Furthermore, I aimed to: (5) characterise *Symbiodinium* diversity in the anemone *E. quadricolor* on the west coast of Australia; and (6) measure the dynamics of *Symbiodinium* ITS2 populations and SOD activity in two *E. quadricolor* phenotypes (green and pink colour phenotypes) in response to elevated temperature.

I showed that thermal responses in high latitude corals and their dinoflagellate symbionts are highly variable, depending on host species (or phenotype) and *Symbiodinium* genotype, and that the activation of protective mechanisms in

Abstract

Symbiodinium was not necessarily correlated with sub-lethal bleaching susceptibility or survivorship of their coral hosts. More specifically: (1) In response to short-term heat stress and cold stress, xanthophyll de-epoxidation increased in some but not all bleaching susceptible (e.g. *P. damicornis*) *and* bleaching tolerant (*P. heronensis*) corals; (2) overall unsaturated thylakoid fatty acids increased in symbionts of a bleaching tolerant coral association, yet was not correlated with PSII photochemical efficiency; and (3) SOD and APX activity remained unchanged in the majority of *Symbiodinium* types regardless of bleaching susceptibility of the coral host, but decreased in bleaching susceptible *Pocillopora damicornis* when exposed to short-term heat stress. Elevated temperatures resulted in enhanced D1 turnover in two warm-water bleaching susceptible *Symbiodinium*-host combinations; however a direct link between increased dependence on D1 turnover and bleaching susceptibility was not demonstrated. From the results obtained it seems unlikely that the specific cellular adaptations in *Symbiodinium* alone determine the tolerance of Lord Howe corals to thermal variations. In contrast, the results highlight the significance of the particular host-symbiont combination and it appears that the host is important in determining, at least in part, the thermal response of the coral.

Additionally, this study revealed a high diversity of *Symbiodinium* ITS2 (internal transcribed spacer 2) types in *E. quadricolor* from five locations on the west coast of Australia. *E. quadricolor* predominantly associated with six types of clade C (four of which were novel) and most anemones harboured multiple types simultaneously. At North Solitary Island, anemones simultaneously harboured *Symbiodinium* C25 and C3.25 (a novel variant of C3). Experimentally, I showed that anemones shuffled the relative proportions of C25 and C3.25 in response to elevated temperature, but not in both anemone colour phenotypes analyzed. Furthermore, baseline photobiological characteristics were distinct in the two different anemone colour morphs but were not correlated with the ratio of *Symbiodinium* C25 to C3.25, suggesting that host mechanisms such as pigmentation were involved in regulating light utilization by the symbionts. My hypothesis that symbiont shuffling was related to SOD activity, as such that those symbionts with enhanced SOD activity and increased capability to scavenge superoxide anion would increase in relative abundance in response to short-term heat stress, could not be proved.

Abstract

In summary, this thesis provides detailed information on some key cellular mechanisms that could underpin thermal sensitivity and resistance in high latitude *Symbiodinium*, and most importantly highlights the significance of the host-symbiont combination in determining the response to thermal stress. The various mechanistic findings described here further our understanding of the coral bleaching process in general and particularly give insight into physiological and cellular responses to cold-water stress in reef-building corals at high-latitude sites. The results of this thesis indicate that in light of ongoing climate change, as episodes of cold-water and warm-water anomalies will become more frequent, branching corals such as *Acropora yongei* or *Pocillopora damicornis* and their symbionts will experience physiological stress more frequently than massive species such as *Porites heronensis*. This might have profound impacts on the long-term stability and species composition of high latitude coral reefs.

CONTRIBUTIONS AND PUBLICATIONS

This thesis is written as a series of manuscripts which are currently in review or to be submitted in the near future. The thesis is my own intellectual and analytical work except as acknowledged below and throughout the text. It has been prepared specifically for the PhD degree while under supervision at Victoria University of Wellington and has not been submitted for another degree or diploma at this or any other university.

My PhD supervisors Assoc. Prof. Simon Davy and Dr. Paul Fisher provided advice on experimental design throughout, and intellectual and editorial support for all chapters. Additional support and assistance was provided as described below.

Chapter 2: This chapter is formatted as a standalone manuscript and will be submitted for publication: Pontasch S, Fisher PL, Krueger T, Dove S, Hoegh-Guldberg O, Leggat W, and SK Davy. The impact of decreased and increased temperature on Lord Howe Island corals and the pigment profile of their symbionts.

Fieldwork was conducted with P.L. Fisher, who also contributed to experimental design. T. Krueger, S. Dove, O. Hoegh-Guldberg and W. Leggat provided intellectual and editorial support.

Chapter 3: This chapter is formatted as a standalone manuscript and will be submitted for publication: Pontasch S, Fisher PL, Keyzers RA, Wilkinson SP, Krueger T, Dove S, Hoegh-Guldberg O, Leggat W, and SK Davy. Thylakoid fatty acid composition and response to short-term cold and heat stress differs in high latitude *Symbiodinium* spp.

Fieldwork was conducted with S.P. Wilkinson. GC-MS analysis was conducted with R.A. Keyzers. T. Krueger, provided intellectual and editorial support. S. Dove, O. Hoegh-Guldberg and W. Leggat provided intellectual support.

Chapter 4: This chapter is formatted as a standalone manuscript and will be submitted for publication: Pontasch S, Fisher PL, Wilkinson SP, Krueger T, Dove S, Hoegh-Guldberg O, Leggat W, and SK Davy. PSII activity and antioxidant capacity in high latitude *Symbiodinium* spp. exposed to short-term cold and heat stress.

Contributions and Publications

Fieldwork was conducted with S.P. Wilkinson. T. Krueger advised on the procedures for SOD and APX assays. S. Dove, O. Hoegh-Guldberg and W. Leggat provided intellectual support.

Chapter 5: This chapter is formatted as a standalone manuscript and will be submitted for publication: Pontasch S, Fisher PL, Wilkinson SP, Krueger T, Dove S, Hoegh-Guldberg O, Leggat W, and SK Davy. Differential rates of photoinhibition, photorepair and photoprotection in high latitude *Symbiodinium* spp. from Lord Howe Island.

Fieldwork was conducted with S.P. Wilkinson. T. Krueger, S. Dove, O. Hoegh-Guldberg and W. Leggat provided intellectual support.

Chapter 6: This chapter is formatted as a standalone manuscript and is in press in *Coral Reefs* (2014): Pontasch S, Scott A, Hill R, Bridge T, Fisher PL, and SK Davy. *Symbiodinium* diversity in the sea anemone *Entacmaea quadricolor* on the east Australian coast.

Samples were collected by S. Pontasch, A. Scott, R. Hill, T. Bridge, S. Dalton, B. Edgar, M. Harrison, E. Roberts, and S.P. Wilkinson. Sample analysis was performed by S. Pontasch and A. Scott. A. Scott, R. Hill and T. Bridge provided intellectual and editorial input.

Chapter 6: This chapter is formatted as a standalone manuscript and is and will be submitted for publication: Pontasch S, Deschaseaux E, Hill R, Fisher PL, Davy SK, and A Scott. *Symbiodinium* genotypic flexibility and antioxidant capacity during thermal stress in the anemone *Entacmaea quadricolor* are dependent on host pigmentation

Fieldwork was conducted with E. Deschaseaux, R. Hill, and A. Scott, who also gave intellectual input on experimental design and analysis, and editorial support.

Financial support for the core research of this thesis was provided by a Royal Society of New Zealand Marsden Fund grant (contract number VUW0902) to S.K. Davy, S. Dove, P.L. Fisher, O. Hoegh-Guldberg and W. Leggat. Additional financial assistance was provided by a Wellington Botanical Society Grant to Graduate Students, a Faculty

Contributions and Publications

Strategic Research Grant awarded by Victoria University of Wellington, and a Victoria University Submission Scholarship.

Acknowledgement

ACKNOWLEDGEMENTS

There are numerous people I would like to thank, either because they inspired me to choose this journey, or because they walked along or crossed my way and supported me on a professional academic and/or personal level, and ultimately because they believed in me and in the completion of this thesis!

My foremost thank you is to my supervisors Simon Davy and Paul Fisher, for giving me the opportunity to be part of this exciting project, for being patient with me and for giving valued feedback and intellectual and laboratory support. Paul, also thank you for teaching me the art of fieldwork, for always having an open door and ear for my numerous questions, and for keeping the lab running!

A huge thank you is to my field buddies without whom this thesis would not have been possible. Shaun Wilkinson, thank you for your support in the field, for your help with sampling, experimental set-ups, night shifts, unlimited coffee-supply, and your fantastic cooking skills! Sallyanne Gudge, Ian Kerr and Jimmy Maher, thank you for the scientific collection permits, your logistical support and your warm welcome every time we returned to Lord Howe! I am much obliged to the Lord Howe Island Board, and the community of Lord Howe Island for their support. Special thanks go out to Brian “Busty” Busteed and Ian “Fitzi” Fitzgerald. For assistance with fieldwork, logistical or intellectual, I also thank Dr Andrew Baird (James Cook University), Dr Andrew Carroll and Dr Steve Dalton (Southern Cross University), Dr Peter Harrison (Southern Cross University) and Dr Anya Salih (University of Western Sydney).

I can’t say enough thanks to Anna Scott (Southern Cross University, National Marine Science Centre) and Ross Hill (University of New South Wales). Anna, thank you, not only for giving me the opportunity to conduct research at the National Marine Science Centre, but also for your outstanding support and encouragement through all phases of the ‘anemone’-project, for fun times in the lab, and for your valuable advice. Ross, thank you for being part of the project and your expertise! Thank you also to Elizabeth Deschaseaux for all the hard work in the field and for the good spirit you brought to the project!

Acknowledgement

I would like to thank Xavier Pochon for his contagious enthusiasm and advice on *Symbiodinium* genotyping.

I am very thankful to my lab buddies and friends, for their work-related or personal help and support. Thomas, thank you for sharing your vast knowledge with me and being so patient! Susanne, thank you for contributing insightful inputs during many stages of this thesis and for your emotional support when I needed it. Katie and Tom, thank you for sharing the Tongariro experience! Emma thank you for being so positive! Dorota, thank you for Pilates distractions! Jen, thank you for making me smile, for introducing me to the art of circus and Wellington art of life, and for your support throughout the years! Anne, thank you for sharing all the ups and downs, laughter and tears, you are truly a good friend! Sabine, thank you for some adventuresome time in the hills of New Zealand!

Thank you to Maria and Josef Aufschnaiter for giving me a home and place to write the thesis and to Tine for welcome distractions during the write-up phase!

I am truly grateful to my parents and brother, Gerhard, Helene and Christian, for their financial and infinite emotional support. I am grateful that you always believed in me and always supported my ideas! *Mama, Papa, ich bin Euch sehr dankbar für Eure finanzielle aber vor allem emotionale Unterstützung über die Jahre hinweg. Danke, dass ihr an mich glaubt und mich in meinen Vorhaben immer unterstützt.*

Thank you Roland, that you pushed me to live my dream and stuck with me through all these years despite the distance. You are a true inspiration!

TABLE OF CONTENTS

LIST OF FIGURES

LIST OF TABLES

List of Tables

List of Tables

List of Tables

LIST OF ABBREVIATIONS

$^1O_2$	singlet oxygen
2PG	2-phosphoglycolate
3PGA	3-phosphoglycerate
a	alpha, initial slope in light limited region of the rapid light curve
ABH	adaptive bleaching hypothesis
acpPC	chlorophyll *a* – c_2 – protein complex
ADP	adenosine diphosphate
ATP	adenosine triphosphate
ANOVA	analysis of variance
APX	ascorbate peroxidise
BHT	butylated hydroxytoluene
bp	basepair
BSA	bovine serum albumin
CCM	carbon concentrating mechanism
CEF	cyclic electron flow
Chl	chlorophyll
CO_2	carbon dioxide
DCM	dichloromethane
DDE	diadinoxanthin de-epoxidase
Ddn	diadinoxanthin
DEP	diatoxanthin epoxidase
df	degrees of freedom
Dtn	diatoxanthin
DGGE	denaturing gradient gel electrophoresis

List of Abbreviations

dH_2O	distilled water
DMS	dimethylsulfide
DMSO	dimethyl sulfoxide
DMSP	dimethylsulphoniopropionate
DNA	deoxyribonucleic acid
dNTP	deoxynucleotide triphosphate
EAC	East Australian Current
EDTA	ethylenediaminetetraacetic acid
F_0	all PSII reaction centres are oxidised
F_m	all reaction centres are reduced
F_v	variable fluorescence ($F_m - F_0$)
F_v/F_m	dark-acclimated maximum quantum yield of PSII
$\Delta F/F_m'$	light-acclimated effective quantum yield of PSII
FP	fluorescent protein
FSW	filtered seawater
GBR	Great Barrier Reef
GC–MS	gas chromatography-mass spectrometry
GFP	green fluorescent protein
gDNA	genomic deoxyribonucleic acid
GSH	glutathione
GPiR	rate of gross photoinhibition
H_2O	water
H_2O_2	hydrogen peroxide
HPLC	high pressure liquid chromatography
HSD	honestly significant difference
I_k	minimum saturating irradiance
IPAM	imaging pulse amplitude modulated

List of Abbreviations

ITS	internal transcribed spacer
LHC	light-harvesting complex
LHI	Lord Howe Island
Lin	lincomycin
LSU	large subunit (of the ribosomal DNA)
MAA	mycosporineaminoacids
MeOH	methanol
$MgCl_2$	magnesium chloride
ML	maximum likelyhood
MMM	maximum monthly mean
MPA	marine park authority
NaCl	sodium chloride
$NADP^+$	nicotinamide adenine dinucleotide phosphate
NADPH	reduced nicotinamide adenine dinucleotide phosphate
NBT	nitro blue tetrazolium chloride
NH_3	ammonia
NO	nitric oxide
NO_3^-	nitrate
NPQ	non-photochemical quenching
NPiR	rate of net photoinhibition
NSI	North Solitary Island
NSW	New South Wales
nt	nucleotid
O_2^-	super oxide
OEC	oxygen evolving complex
•OH	hydroxyl radical
PAM	pulse amplitude modulated

List of Abbreviations

PAR	photosynthetically active radiation
PASW	predictive analytics software
PC	plastocyanin
PCP	peridinin – chlorophyll *a* – protein complex
PCR	polymerase chain reaction
PO_4	phosphate
ppmv	parts per million volume
PSI + II	photosystem I + II
PSP	pool of photosynthetic pigments
PQ	plastoquinone
Q_A	oxidized primary quinone electron acceptor of PSII
Q_A^-	reduced primary quinone electron acceptor of PSII
Q_B	oxidized secondary quinone electron acceptor of PSII
Q_B^-	reduced secondary quinone electron acceptor of PSII
qE	energy dependent quenching
qI	inhibitory quenching
Q_m	electron pressure over PSII
qPCR	quantitative polymerase chain reaction
qT	quenching associated with state transitions
rDNA	ribosomal DNA
$rETR_{max}$	maximum relative electron transport rate
RLC	rapid light curve
ROS	reactive oxygen species
RR	repair rate
Rubisco	ribulose-1,5-biphosphate carboxylase/oxygenase
RuBP	ribulose-1,5-biphosphate
SDS	sodium dodecyl sulphate

List of Abbreviations

SE	standard error
SIMP	Solitary Island Marine Park
SSU	small subunit (of the ribosomal DNA)
SST	sea surface temperature
SO_4^{2-}	thioredoxin
SOD	superoxide dismutase
TAE	tris-acetat-EDTA
TBE	tris-borate-EDTA
TBS_T	tris buffered saline triton-X100
T_a	annealing temperature
UVR	ultraviolet radiation
VDE	violaxanthin de-epoxidase

Chapter 1:
General Introduction

1.1 The coral reef ecosystem

Coral reefs are among the most productive and most diverse ecosystems on Earth (Connell 1978). Hermatypic corals (phylum Cnidaria, order Scleractinia) contribute significantly to the formation of the physical structure of reefs by accretion of calcium carbonate. The formation of complex three-dimensional structures creates an array of habitats, and spawning and nursery grounds, sustaining a broad diversity of marine flora and fauna with incomparable environmental and biodiversity value. Indeed, although coral reefs cover less than 0.1% of the Earth's surface or less than 0.2% of the oceans' surface (Reaka-Kudla 1997), it is estimated that 35% of marine species inhabit coral reefs (Reaka-Kudla 2005). Furthermore, Reaka-Kudla (1997) estimated that an additional 0.6 - 9 million species are yet to be discovered in and around coral reefs. Coral reefs have an immense economic value, estimated at $U.S. 172 – 375 billion a year (Veron et al. 2009), derived mainly from fishing, recreation, tourism and coastal protection from storms and erosion (Reaka-Kudla 1997; Moberg and Folke 1999; Barbier et al. 2011). Furthermore, coral reefs have a cultural significance to coastal communities around the world.

Due to their environmental requirements, coral reefs generally span coastal areas between approximately 25 °N and 25 °S latitude with the highest species richness in the tropics. At higher latitudes, reef accretion may persist if water temperatures do not fall below 18 °C for extended periods (Johannes et al. 1983; Crossland 1984; Kleypas et al. 1999). At these high latitudes, corals typically show less diversity, lower growth rates, reduced calcium carbonate accretion and limited depth distributions when compared to their tropical counterparts (Harriott and Banks 2002). This is primarily because, at the margins of their distribution, corals live very close to their survival thresholds for

temperature, light and aragonite availability (Kleypas et al. 1999); competition with macroalgae is also considerable at high latitude sites (Hoey et al. 2011). Nevertheless, extensive coral reefs and communities with coral cover comparable to tropical reefs can be found at higher latitudes such as at the Islands of Bermuda in the North Atlantic Ocean (32°N, 64°W; Cook et al. 1990), at the coast of Japan (~ 33.5 °N, 133.5°E; Yamano et al. 2001; Denis et al. 2013), at Lord Howe Island (LHI; 31°32'S, 159°03'E; Veron and Done 1979; Harriott et al. 1995) and at the Solitary Islands (29°55'S, 153°23'E; Harriott et al. 1994) in New South Wales, Australia.

In past decades, the environmental pressure on coral reefs has increased significantly. Local threats such as overfishing, destructive fishing, chemical and oil pollution, sedimentation and eutrophication resulting from coastal development, deforestation and agricultural runoff have led to a decline in the abundance and diversity of corals and other reef associated species worldwide (Hughes 1994; Reaka-Kudla 1997; Jackson et al. 2001; Hughes et al. 2003; Pandolfi et al. 2003). The deleterious effects of these more localized impacts are magnified by global threats associated with climate change: ocean acidification and rising sea surface temperatures (Wilkinson 2004; Hoegh-Guldberg et al. 2007; Veron et al. 2009; Pandolfi et al. 2011). During the 20th Century, seawater temperatures have increased by 0.74 °C and a further rise of approximately 1.8 C – 4 °C over the next century is expected (Solomon et al. 2007). The observed and predicted increases in sea surface temperature might be high enough to have significant effects on the health of corals that live close to their upper thermal limits (Connell 1978; Fitt et al. 2001).

There has been some discussion that high latitude reefs may provide refugia for tropical corals in an era of warming oceans (Greenstein and Pandolfi 2008). Yamano (2011) demonstrated that the distributions of *Acropora hyacinthus*, *A. muricata*, *A. solitariensis* and *Pavona decussata* have expanded polewards in Japan over the last 80 years at a pace of up to 14 km per year. Likewise, a recent expansion of acroporids towards higher latitudes has been observed in the Western Atlantic (Precht and Aronson 2004) and Indo-Pacific (Greenstein and Pandolfi 2008). It remains to be shown whether expanded populations will persist at higher latitudes where seasonal changes in

temperature and diurnal light exposure are more pronounced compared to the tropics (Muller-Parker and Davy 2001). If they succeed and develop resilience, then high latitude coral reefs might experience fundamental modifications in their species assemblages, where tropical species might replace subtropical and cold-adapted species (Precht and Aronson 2004). In this scenario, a shift of coral assemblages seems more likely than an overall increase of species diversity at high latitudes (Dalton and Carroll 2011). It is therefore crucial to understand the response of high latitude corals to environmental stressors such as temperature (and in the long-term how this response is influenced by additional local or global environmental stressors), to shed light on their potential to persist in a future that will be characterized by warmer sea temperatures (Solomon et al. 2007), lower aragonite availability (Orr et al. 2005; Doney et al. 2009; Meissner et al. 2012), and more frequent warm and cold sea temperature anomalies (Timmermann et al. 1999; Abram et al. 2008).

1.2 Coral-algal symbiosis

Most scleractinian and many soft-bodied corals, among a large number of other marine organisms, associate with symbiotic unicellular algae, dinoflagellates of the genus *Symbiodinium* (Freudenthal 1962) (phylum Dinophyta, order Gymnodiniales) (Venn et al. 2008; Weis 2008; Stambler 2010). The association of heterotrophic animals with autotrophic algal cells is widespread within the phyla Ciliophora and Foraminifera (single celled eukaryotes), Porifera (sponges), Cnidaria (corals, jellyfish and anemones), Mollusca (snails and clams) and Plathyhelminthes (flatworms) (Lobban 2002; Coffroth and Santos 2005; Stat et al. 2006). The association between hermatypic corals and *Symbiodinium* spp. can be dated back to the late Triassic, about 240 million years ago (Stanley and Swart 1995). The entity of animal and associated algae as well as other symbionts found in tissue, mucus and skeleton of corals, including archae and bacteria (Rosenberg et al. 2007), is called the holobiont. Within the coral's endodermal cells, symbionts (6 – 15 µm in diameter, reviewed in Stambler 2010) are located within a symbiosome membrane complex (Figure 1.1), which refers to a vacuole surrounded by an outer membrane layer derived from the coral and several inner membrane layers derived

from the *Symbiodinium* cell (Wakefield et al. 2000; Wakefield and Kempf 2001). *Symbiodinium* cells are transferred maternally (vertical transmission mode) or acquired from the environment (horizontal transmission mode) (Baird et al. 2009b).

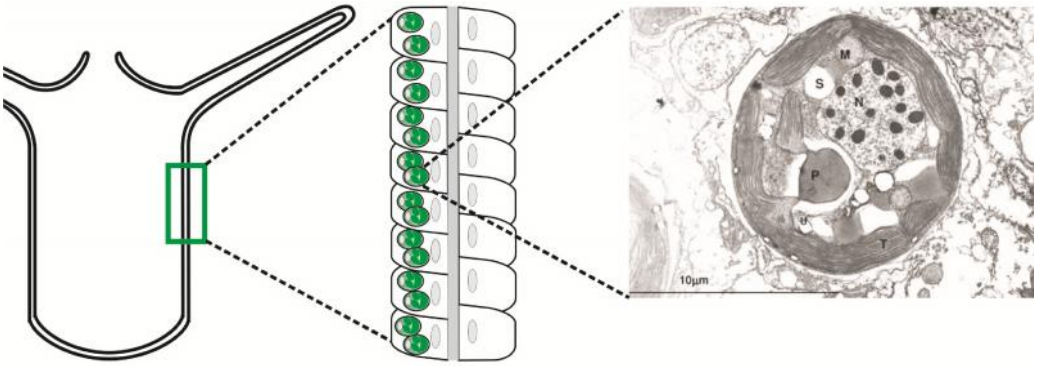

Figure 1.1: Illustration of the coral-*Symbiodinium* association. *Symbiodinium* cells (green) are located within the endodermal cells. The transmission electronic photograph shows the cellular structure of a *Symbiodinium* cell embedded in coral tissue. T, thylakoid; N, nucleus; M, mitochondria; P, pyrenoid; S, starch; U, crystal of uric acid. Transmission electron microscope photograph: Stambler (2011).

The coral-*Symbiodinium* association is a mutualistic symbiosis (Boucher et al. 1982), in which the autotrophic *Symbiodinium* cells provide photosynthetically-fixed carbon to their host and receive inorganic nutrients, such as CO_2, NH_3, PO_4, in return. These nutrients can then be used to synthesize organic compounds such as essential amino acids that further benefit the metabolic demands of the host (Muscatine 1967; Trench 1971; Muscatine and Porter 1977; Trench 1979; Muscatine et al. 1981; Falkowski et al. 1984; Muscatine et al. 1984). More than 95% of photosynthetically-fixed carbon can be translocated through the symbiosome membrane complex and to the coral host in the form of glycerol, glucose, amino acids and lipids (Davy et al. 2012; but see Burriesci et al. 2012) which has the potential to meet >100% of the host's metabolic needs (Muscatine et al. 1984; Davies 1991). Therefore, the association with *Symbiodinium* is considered to be vital for the health, growth, reproduction and survival of corals and other hosts in oligotrophic tropical waters (Davy et al. 2012), while it also promotes coral calcification (Barnes and Chalker 1990). In subtropical and temperate regions, heterotrophic feeding may become more important as a source of carbon for the host,

because nutrients become more available and phototrophy may not be sufficient to meet the metabolic demands of the host due to the lower light availability (Muller-Parker and Davy 2001). The importance of heterotrophy in symbiotic cnidarians is well recognized (Houlbreque and Ferrier-Pagès 2009; Ferrier-Pagès et al. 2011) and recently it has been demonstrated that cultured *Symbiodinium* cells too have the ability to source carbon by feeding on heterotrophic bacteria, cyanobacteria and microalgae (Jeong et al. 2012).

1.3 *Symbiodinium* diversity

Originally described as one ubiquitous species, *Symbiodinium microadriaticum*, by Freudenthal (1962), considerable morphological, physiological and genetic differences have been demonstrated within the genus over the past few decades (reviewed by Coffroth and Santos 2005). Today, molecular tools allow the differentiation of nine divergent lineages or clades (A – I; Figure 1.2) within the genus *Symbiodinium*. To resolve *Symbiodinium* clades, nuclear markers such as the small subunit (SSU) ribosomal rDNA (18S RNA) (e.g. Rowan and Powers 1991; Carlos et al. 1999; LaJeunesse and Trench 2000; Rodriguez-Lanetty et al. 2001; Savage et al. 2002) and the large subunit (LSU) rDNA (28S rDNA) (e.g. LaJeunesse and Trench 2000; Pawlowski et al. 2001; Pochon et al. 2006), as well as the chloroplast 23S domain V (e.g. Santos et al. 2002; Pochon et al. 2006; Stat et al. 2009; Pochon and Gates 2010; Pochon et al. 2010) are used. Pochon et al. (2001; 2004) used partial SSU and LSU fragments that flank the whole internal transcribed spacer (ITS) region (ITS1 + 5.8S + ITS2) to delineate clades. On their own, the rapidly evolving and more variable nuclear markers ITS1 (e.g. van Oppen et al. 2001; Rodriguez-Lanetty et al. 2003) and ITS2 (e.g. LaJeunesse 2001; Thornhill et al. 2006; Pochon et al. 2007; Stat et al. 2009; Pochon et al. 2010) have been widely used to resolve numerous sub-clades or "types" within clades. Scleractinian corals may associate with *Symbiodinium* types clustering in clades A – D, F, and G. Clade C is the most derived lineage and is widely distributed in the Indo-Pacific, whereas clade B dominates the Caribbean-Atlantic region (reviewed in Stambler 2011). *Symbiodinium* spp. may associate with only one specific coral species (i.e. 'specialist'), or associate with a range of coral species (i.e. 'generalist') (LaJeunesse et al. 2003). Furthermore, in one

coral colony, multiple symbiont types may be present (Rowan and Knowlton 1995; Baker 2003; Abrego et al. 2008; LaJeunesse et al. 2008).

Distinct *Symbiodinium* strains show differences in morphology, ultrastructure, growth rate, and physiological capability, including the potential for thermal- and photoacclimation (Schoenberg and Trench 1980a; 1980b; Chang et al. 1983). More recent studies have shown that, even between types, there are differences in physiology and cellular adaptive potential (Robison and Warner 2006; Thornhill et al. 2008; Hennige et al. 2009; Ragni et al. 2010; Krämer et al. 2012). It has been suggested that thermal and light sensitivities might also contribute to the allocation of distinct coral-*Symbiodinium* associations to diverse ecological niches, so sustaining reef diversity and distribution patterns along latitudinal (LaJeunesse and Trench 2000; Rodriguez-Lanetty et al. 2001; Sampayo et al. 2007) or bathymetric (Baker 2001; Iglesias-Prieto et al. 2004) gradients.

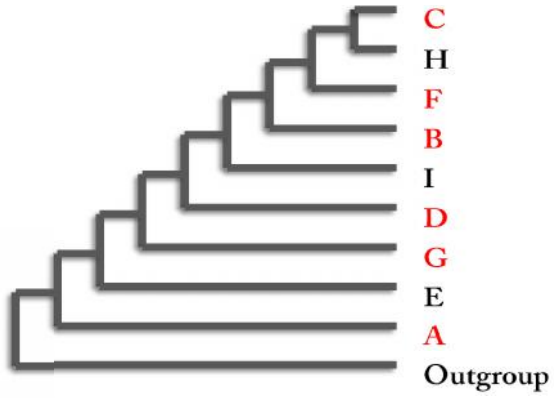

Figure 1.2: Schematic phylogenetic tree of the genus *Symbiodinium*, showing clades A – I. Highlighted in red are those clades/lineages that associate with scleractinian corals. Modified after Coffroth and Santos (2005) and Pochon et al. (2010).

1.4 Coral Bleaching

Thermal stress associated with elevated seawater temperature, combined with increased solar radiation, is now considered to be the principle cause for coral bleaching (Lesser 2011), a phenomenon that has been observed on a global scale since the 1980s (Lessios et al. 1983; Glynn 1984). Coral bleaching describes the coral's loss of some or

all of its algal symbionts or the loss of pigments or pigment-protein complexes within the *Symbiodinium* cells (Falkowski and Dubinsky 1981; Brown 1997; Hoegh-Guldberg 1999; Takahashi et al. 2008). Linked to bleaching is a reduction of photosynthetic performance and carbon fixation (Porter et al. 1989; Brown 1997; Jones et al. 1998; Hoegh-Guldberg 1999; Warner et al. 1999). Hence, bleached corals are deprived of their major source of energy, and persistence or rate of recovery in these conditions is dependent on the coral's ability to acquire carbon heterotrophically (Grottoli et al. 2006). Indeed, bleached corals often show reduced growth rates, and an increased vulnerability to disease and mortality (Jokiel and Coles 1977; Goreau and Macfarlane 1990; Brandt and McManus 2009).

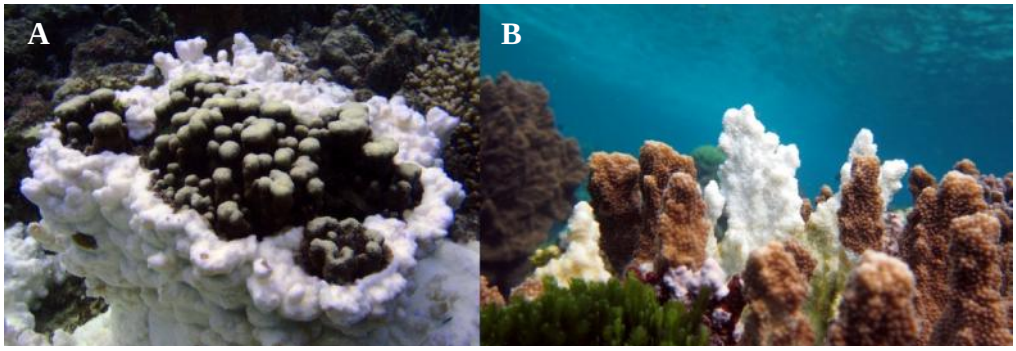

Figure 1.3: Partially bleached *Porites* colony observed in March 2011 (**A**) and partially bleached *Isopora* colony observed in September 2011 (**B**) in the lagoon of Lord Howe Island, New South Wales, Australia. (**A** Photograph courtesy: Shaun Wilkinson).

Although elevated temperature, in conjunction with increased solar radiation, is the main cause of large scale "mass" bleaching events, various environmental stressors may cause bleaching. These include changes in salinity, solar radiation and ultraviolet radiation (reviewed in Banaszak and Lesser 2009; Lesser 2011), and low-temperature thermal stress (Steen and Muscatine 1987; Saxby et al. 2003; Hoegh-Guldberg and Fine 2004; Hoegh-Guldberg et al. 2005). Often, local stressors act synergistically with high light (Saxby et al. 2003; Lesser and Farrell 2004; Lesser 2011). Furthermore, ocean acidification, the decrease of the pH of our oceans due to the uptake of anthropogenically emitted carbon dioxide, may impact the bleaching thresholds of corals and has been shown to lead to bleaching of reef-building corals (Anthony et al. 2008).

1.5 Cellular mechanisms of coral bleaching

At the cellular level, the breakdown of the symbiosis is the ultimate result of multiple mechanisms in both the dinoflagellate symbiont and coral host (Venn et al. 2008; Weis 2008), with no consensus about its initiation or sequential order. It has been postulated that temperature-induced bleaching starts with an initial impairment of photosynthesis in the dinoflagellate, when light harvesting exceeds utilization and "energy absorption is uncoupled from photochemistry" (Iglesias-Prieto et al. 1992). However, there is also evidence that in some instances, cellular changes in the host might precede changes in *Symbiodinium* cells under thermal stress (Ainsworth et al. 2008; Dunn et al. 2012; Paxton et al. 2013). It has been demonstrated that intact host cells containing *Symbiodinium* cells may be released (Gates et al. 1992). Also, it has been shown that released *Symbiodinium* cells can be photosynthetically functional (Ralph et al. 2001; Bhagooli and Hidaka 2004a; Hill and Ralph 2007). Here, the efficiency of photosystem II of expelled *Symbiodinium* cells depended on the time of expulsion and varied between coral hosts (Ralph et al. 2005). Further, long-term viability of expelled *Symbiodinium* cells was limited (Hill and Ralph 2007).

Often, the breakdown of the symbiosis, i.e. the expulsion, degradation, or loss of *Symbiodinium* cells from the host tissue (Gates et al. 1992) is accompanied by photobleaching in *Symbiodinium* cells, i.e. the loss of the major light-harvesting pigments chlorophyll *a*, chlorophyll c_2 and peridinin (Kleppel et al. 1989; Porter et al. 1989). Photobleaching was detected without a concurrent decline of *Symbiodinium* cell density under elevated temperature in the scleractinian corals *Acropora digitifera* (Takahashi et al. 2004) and *Montipora monasteriata* (Dove et al. 2006), and has also been documented for heat-stressed *Symbiodinium* cell cultures (Venn et al. 2006). In *Symbiodinium*, photoinhibition (i.e. the inhibition of the activity of photosystem II [PSII]) is thought to precede photobleaching (Takahashi et al. 2008), although the exact mechanisms of photoinhibition in *Symbiodinium* are largely unknown. In plants and cyanobacteria, it is thought that photoinhibition is a two-step process (Nishiyama et al. 2006). Firstly, strong light (mainly strong ultraviolet and blue light) damages the manganese cluster of the oxygen evolving complex (OEC), and secondly, PSII reaction centres are inactivated by

light absorbed by photosynthetic pigments (Nishiyama et al. 2006; Tyystjärvi 2008). If electrons cannot be transferred from water onto the primary electron donor, P_{680}^{+}, levels of this strong oxidizing compound remain high. Thus, P_{680}^{+} has the potential to oxidize nearby proteins, particularly D1, which comprises together with D2 the core of PSII reaction centres (Nishiyama et al. 2006). Additionally, or alternatively, singlet oxygen ($^1O_2$) might be produced at P_{680}^{+} that oxidizes proteins (Halliwell 2006; Nishiyama et al. 2006). The degradation of damaged D1 proteins results in a loss of functional PSII reaction centres if the rate of *de novo* synthesis and replacement does not meet the rate of damage in the photoinhibition-photorepair cycle (Powles 1984; Aro et al. 1993). In contrast to this model of photoinhibition (manganese mechanism and donor side photoinhibition), the classical acceptor side model assumes that photoinhibition will occur when the plastoquinone pool is fully reduced (Tyystjärvi 2008). The acceptor side photoinhibition assumes that electrons cannot be transferred from Q_A^{-} (reduced primary quinone electron acceptor of PSII located on reaction centre subunit D2) to Q_B (secondary quinone electron acceptor of PSII located on reaction centre subunit D1) due to a lack of vacant Q_B. Q_A^{-} may be double reduced to Q_A^{2-} and be released from the reaction centre resulting in accumulating levels of oxidized P_{680}^{+} (Vass et al. 1992).

In *Symbiodinium*, acceptor side photoinhibition may be of greater importance in coral bleaching than donor side photoinhibition (Hill et al. 2004a; Smith et al. 2005; Hill and Ralph 2006). Although the OEC may be a possible site of PSII damage (Warner et al. 1996; Iglesias-Prieto 1997), it has been shown that symbionts in *Pocillopora damicornis* maintain a functional OEC well above bleaching temperatures (Hill and Ralph 2008). Multiple studies have associated species-specific differences in photoinhibition with distinct susceptibilities to coral bleaching at elevated temperatures (Fitt and Warner 1995; Warner et al. 1996; Warner et al. 1999).

Photoinhibition is enhanced by environmental stressors such as chilling and high temperatures (Long et al. 1994). Elevated temperature is believed to accelerate photoinhibition and photobleaching, either through increased photodamage to PSII proteins (Warner et al. 1999; Hill et al. 2011), or through suppressed photorepair of photodamaged components of PSII (Takahashi et al. 2004; 2009) and light-harvesting

proteins (Takahashi et al. 2008). In *Symbiodinium* cells, the major light-harvesting pigments are bound to antenna proteins that are organized in a water-soluble PCP complex (peridinin – chlorophyll *a* – protein complex) and in a thylakoid integrated acpPC complex (chlorophyll *a* – c_2 – protein complex) (Iglesias-Prieto et al. 1991; 1993). Takahashi et al. (2008) gave evidence that, in cultured *Symbiodinium* cells, heat-induced acceleration of photobleaching is at least partly attributed to the suppression of *de novo* synthesis of these antennae proteins and, importantly, not to their degradation. Furthermore, Takahashi et al. (2009) showed that heat suppressed the synthesis of thylakoid membrane proteins, including D1. Net photoinhibition is determined by the rate of photodamage to PSII reaction centres and its repair (Takahashi et al. 2013). In vascular plants and green algae, these mechanisms consist of the proteolytic degradation of damaged D1, followed by the *de novo* synthesis of D1 precursor proteins that are integrated in the thylakoid membranes and mature to functional D1 proteins embedded in the OEC (Aro et al. 1993; Takahashi and Murata 2008; Takahashi and Badger 2011). In plants and cyanobacteria, reactive oxygen species (ROS), chiefly hydrogen peroxide (H_2O_2) and singlet oxygen ($^1O_2$), have been shown to suppress the synthesis of proteins, including D1, probably by targeting the elongation step at translation (Nishiyama et al. 2006; Takahashi and Murata 2008). These results challenge the paradigm that photoinhibition is accelerated by direct damage of photosynthetic pigments, proteins and thylakoid membranes by ROS (Niyogi 1999). Importantly, Takahashi et al. (2009) also demonstrated that the PSII repair system in *Symbiodinium* differs from that of plants, in that photodamaged PSII can be partly repaired without *de novo* protein synthesis; these authors proposed the presence of 'a unique PSII repair system' which has yet to be identified (Takahashi et al. 2013). In contrast, Hill et al. (2011) showed that photoinhibition under bleaching conditions is a result from increased photoinactivation, rather than an inhibition of photorepair in *Pocillopora damicornis*.

Environmental stressors such as cold and heat negatively impact CO_2 fixation in photosynthetic organisms (Long et al. 1994). Suppressed CO_2 fixation is thought to increase the susceptibility of PSII to photoinhibition by the limitation of electron flow and a resulting generation of ROS which in turn may inhibit the synthesis of proteins in the chloroplast, as experimentally shown in *Chlamydomonas reinhardtii* (Takahashi and

Murata 2005; Murata et al. 2007). Heat-induced down-regulation of ribulose-1,5-bisphospate carboxylase/oxygenase (Rubisco), the carboxylating enzyme of the Calvin cycle, has been observed in *Symbiodinium* spp. (Lesser 1996; Jones et al. 1998). Decreased carboxylating activity of Rubisco is probably due to an increased affinity for O_2 at high temperatures (Badger et al. 2000) that might be particularly exacerbated in *Symbiodinium* spp. which contain a form II Rubisco that is known for a poor discrimination between CO_2 and O_2 (Rowan et al. 1996). Although an inorganic carbon concentrating mechanism (CCM) counteracts this disadvantage (Leggat et al. 1999), elevated temperature might affect the carbonic anhydrase and also cause carbon limitation under high temperature (Leggat et al. 2002). Jones et al. (1998) recognized the importance of CO_2 fixation and other electron sinks for the maintenance of an adequate electron flow and suggested that impaired CO_2 fixation precedes temperature-induced bleaching in *Symbiodinium* spp..

Iglesias-Prieto et al. (1992) hypothesized that the temperature-induced declines in photosynthesis were due to changes in the thylakoid membrane fluidity and an impaired capability of electron transport past PSII. Later it was demonstrated that thylakoid membrane integrity, which depends on the thylakoid lipid composition and the state of lipid saturation, was indeed affected by high temperature, causing the energetic uncoupling of electrons, the loss of the trans-thylakoid ΔpH gradient, and loss of the generation of NADPH as well as ATP (Tchernov et al. 2004). Although this mechanism does not initially involve photoinhibition, excessive ROS can be generated (Tchernov et al. 2004). The composition of thylakoid lipids is different between thermally-sensitive and thermally-resistant *Symbiodinium* types (Tchernov et al. 2004). They showed that the loss of thylakoid membrane integrity initiates bleaching (both photobleaching and loss of cells) and thylakoid lipid composition is diagnostic of bleaching susceptibility or tolerance (Tchernov et al. 2004). However, the usefulness of thylakoid lipids as bleaching indicators in *Symbiodinium* spp. is controversial and the adjustment of thylakoid lipids to changing thermal conditions seems to be a complex process (Díaz-Almeyda et al. 2011). In photosynthetic organisms, the quality of fatty acids (the degree of saturation or unsaturation of lipid fatty acids, and their respective chain length) may determine the membrane fluidity at a given temperature which itself influences the integration of *de*

novo synthesized D1 proteins (Aro et al. 2005). Additionally, the degree of saturation and unsaturation of lipid fatty acids influences lipid peroxidation susceptibility, i.e. the oxidation of their carbon chains by ROS (Halliwell 1987).

In summary, as illustrated in Figure 1.4, three major sites of impact have been described in *Symbiodinium* chloroplasts under bleaching conditions which certainly are interrelated: (1) PSII with D1 protein; (2) the thylakoid membrane; (3) the Calvin cycle. There is overwhelming evidence that ROS play a pivotal role in the process of photobleaching and loss of symbionts (Downs et al. 2002; Smith et al. 2005; Lesser 2006; Suggett et al. 2008; Lesser 2011). The mechanisms by which symbionts are lost from coral tissue during natural bleaching events are not yet fully resolved. However, there is evidence that oxidative damage might disturb inter-partner signalling and play a central role in modifying host signalling pathways that are known to trigger apoptosis (Weis 2008; Tchernov et al. 2011). Here, a key signalling molecule might be nitric oxide (NO), which has been shown to increase in concentration during thermal stress (Perez and Weis 2006). NO interacts with superoxide (O_2^-) to form the highly reactive peroxynitrite $ONOO^-$, a compound that has recently been identified in the model organism *Aiptasia pulchella* (Hawkins and Davy 2013). However, the role of $ONOO^-$ in thermal bleaching is still unclear (Hawkins and Davy 2013). Other than apoptosis, other possible mechanisms of symbiont expulsion/loss include *in situ* degradation followed by digestion or expulsion, exocytosis of symbiont cells into the gastrovascular cavity of the polyp, host cell detachment and host cell necrosis (Gates et al. 1992; Dunn et al. 2002; 2004; 2007a; 2007b; Weis 2008; Dunn and Weis 2009; Paxton et al. 2013).

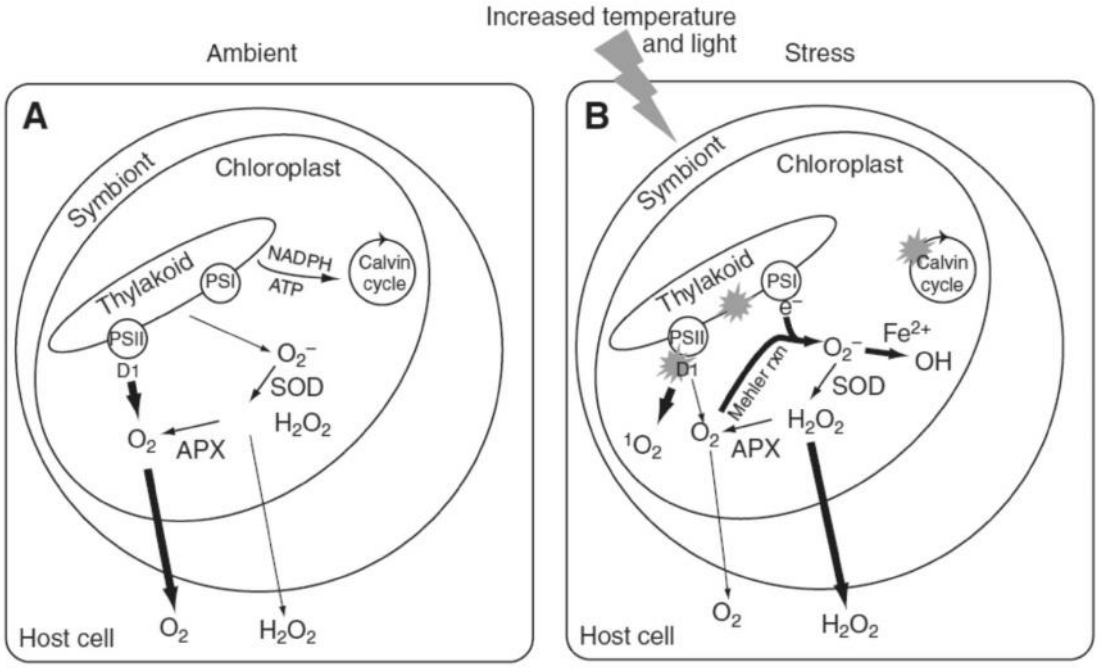

Figure 1.4: Illustration of electron and oxygen pathways in the chloroplast of *Symbiodinium* under ambient conditions (**A**) and high temperature and light conditions (**B**). This schematic representation is not exhaustive because several alternative sinks for electrons exist in the chloroplast, which are not shown. Under ambient conditions, electrons are passed on via the linear electron transport chain to generate NADPH and ATP. Reactive oxygen species (ROS) are converted back to oxygen with superoxide dismutase (SOD) and ascorbate peroxidase (APX). Under excessively high temperature or light, the photosynthetic machinery is thought to be affected on at least three sites (shown as flashes): (1) PSII with D1 protein, (2) the thylakoid membrane, and (3) the Calvin cycle. Excess ROS might overwhelm the detoxification system, act cytotoxic and/or inhibit the repair of D1, and diffuse into host tissues. For a more detailed description refer to the text. Figure obtained from Weis (2008).

1.6 The role of oxidative stress

Oxidative stress defines the imbalance between pro-oxidants (radicals, ROS) and antioxidants, when the former are produced excessively and the production of the latter is decreased or insufficient (Sies 1991). In the coral-algal association, oxidative stress is thought to play a key role in the bleaching response (Downs et al. 2002; Smith et al. 2005; Suggett et al. 2008; Lesser 2011). In plants and animals, the roles of ROS are

multiple: they are (1) cytotoxic; (2) involved in cell signalling, regulating development and pathogen defense (Apel and Hirt 2004; Foyer and Noctor 2005); and (3) involved in the suppression of protein translation in the chloroplast (Nishiyama et al. 2006; Takahashi and Murata 2008). Hence, it is not trivial to elucidate the exact nature of ROS and oxidative stress in the coral-algal symbiosis. In both symbiotic partners, ROS are generated by respiratory activity in mitochondria (Nii and Muscatine 1997; Dunn et al. 2012). In *Symbiodinium*, as in all photosynthetically active organisms, ROS are also generated by photosynthetic activity in the chloroplasts (Apel and Hirt 2004; Lesser 2006). As outlined in Figure 1.5, when adequate photosynthetic electron sinks are missing, electrons can be passed to oxygen and generate O_2^- by this photoreduction (Mehler reaction; Asada 1999; 2000; 2006). The most significant site of O_2^- production in the chloroplast is PSI, due to the high reduction potential of this site. O_2^- is stable but short lived (lifetime 50 µs) and can diffuse through membranes (diffusion distance 320 nm) (Lesser 2006). O_2^- is converted to H_2O_2 by the enzyme superoxide dismutase (SOD) (Asada 1999; 2000; 2006). Uncharged H_2O_2 molecules can diffuse readily through membranes and may react directly with DNA and proteins far from the origin of H_2O_2 synthesis (Lesser 2006). H_2O_2 can be converted to water by the enzyme ascorbate peroxidase (APX) which oxidizes ascorbate to monodehydroascorbate and dehydroascorbate. The oxidized ascorbate products are reduced back to ascorbate in order to maintain the conversion cycle, referred to as the water-water-cycle (Asada 1999; 2000; 2006). H_2O_2 can react with ferrous ions to generate the most harmful and reactive oxygen species, the hydroxyl radical (•OH) (Asada 1999), that can oxidize membranes and denature proteins and DNA in close proximity (diffusion distance 4.5 nm; lifetime 0.1 µs) (Lesser 2006). •OH in turn can be reduced to the harmless hydroxyl ion (OH^-) and water (Asada 1999; Halliwell 2006; Lesser 2006). In addition, singlet oxygen ($^1O_2$) can be produced at PSII by excited chlorophyll molecules that pass their excitation energy to oxygen. $^1O_2$ is highly reactive, has a short lifetime (3.7 µs) and diffusion distance (82 nm), and might be responsible for site-specific damage at PSII (Lesser 2006; Nishiyama et al. 2006).

(1) $O_2 + e^- - - - - - - - - - - - - - - - > O_2^-$ (superoxide anion)

(2) $O_2^- + 2H^+ + e^- - - - - - - - - - - > H_2O_2$ (hydrogen peroxide)

(3) $H_2O_2 + e^- - - - - - - - - - - - - - > OH^-$ (hydroxyl ion) + •OH (hydroxyl radical)

(4) $•HO + e^- - - - - > OH^-$

Figure 1.5: Production and conversion of reactive oxygen species. The superoxide anion (O_2^-) can be reduced to hydrogen peroxide (H_2O_2), which in turn can be reduced to form the hydroxyl radical (•OH). Also, the hydroxyl ion (HO^-) can be reduced to a hydroxyl radical. Modified from Lesser (2011).

Although the cytotoxic nature of ROS is well recognized, it is important to emphasize that the generation of ROS is not necessarily detrimental for the cell. On the contrary, a properly operating water-water-cycle can be considered photoprotective because excessive excitation energy is dissipated effectively (Asada 1999; 2000). What is more, the water-water-cycle creates a trans-thylakoid pH gradient that can aid to maintain energy-dependent heat dissipation in *Symbiodinium* when primary photochemistry is limited (Goss and Jakob 2010).

1.7 Photoprotective mechanisms

A number of mechanisms exist in both the animal host and in *Symbiodinium* cells to alleviate the effects of excess light and mitigate the impacts of environmental stressors such as high or cold temperatures. The major protective mechanisms in chloroplasts of *Symbiodinium* cells are summarized in Figure 1.6 and are discussed in greater detail in the following sections. Protective mechanisms act to avoid excess light absorption to prevent photodamage (see Section 1.5), and promote successful dissipation or utilization of electrons in the *Symbiodinium* chloroplast. This prevents the excessive generation of ROS that are ultimately cytotoxic and/or inhibitory to the protein synthesis machinery (see Section 1.6) (Takahashi and Badger 2011).

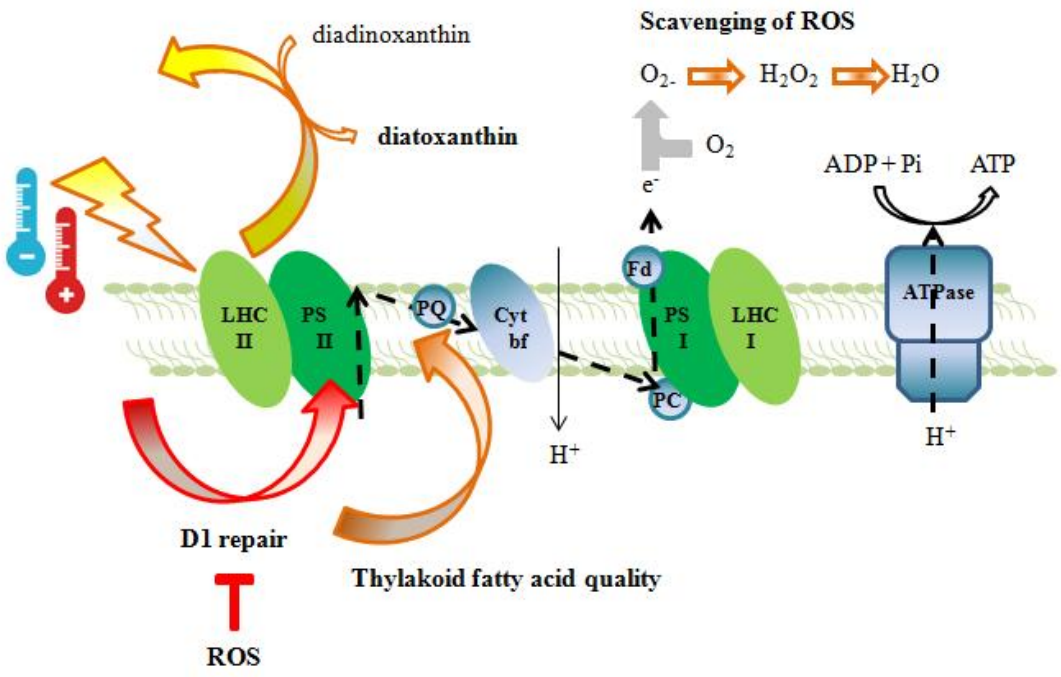

Figure 1.6: Major protective mechanisms in the chloroplast of photosynthetic organisms such as *Symbiodinium*. Illustrated is the photosynthetic membrane with major processes of the light reactions of photosynthesis. In the event of excessively high or low temperature or high light intensity, excessively absorbed light energy can be dissipated as heat (yellow curved arrow), mediated by the conversion from diadinoxanthin to diatoxanthin. Reactive oxygen species (ROS), such as superoxide anion (O_2^-) and hydrogen peroxide (H_2O_2), produced at PSI, are scavenged enzymatically by superoxide dismutase (SOD) and ascorbate peroxidase (APX) or non-enzymatically by ascorbate. ROS can damage D1 or inhibit D1 repair, probably by inhibition of the protein translation machinery (red curved arrow). Finally, the potential to adjust the state of saturation/unsaturation of thylakoid membranes might balance the fluidity of the lipid bilayer at a certain temperature, maintaining the efficiency of the electron transport chain (orange curved arrow). Fd, ferredoxine; LHC, light-harvesting complex; PC, plastocyanine; PQ, plastoquinone;

In the coral host, behavioral or morphological adjustments may provide protection from light or thermal stress, by altering the light environment and therefore reducing the amount of energy that reaches PSII. Anemones (Dykens and Shick 1984) and scleractinian coral polyps (Brown et al. 2002) may avoid light through contraction. Colony morphology can be adjusted to minimize electron flux from sunlight (Anthony et

al. 2005). Furthermore, host tissue thickness, which influences the intensity of light experienced in *Symbiodinium* cells, has been directly correlated with coral survivorship after stress (Loya et al. 2001; Thornhill et al. 2011). In both the coral host and *Symbiodinium*, cellular mechanisms such as scavenging of ROS, and screening of photoradiation are crucial protective mechanisms (Baird et al. 2009a; Takahashi and Badger 2011). In *Symbiodinium* chloroplasts, additional photoprotective mechanisms address the effective dissipation of absorbed light energy as heat (thermal dissipation; Goss and Jakob 2010), and the successful utilization of electrons in photosynthetic processes such as carbon assimilation in the Calvin cycle (Smith et al. 2005). Under carbon limited conditions, respiratory pathways (Crawley et al. 2010), cyclic electron flow (CEF) around PSI (Reynolds et al. 2008), the water-water-cycle (Asada 1999; Asada 2000), possibly dissociation and redistribution of antennae complexes (state transitions; Hill et al. 2005; Reynolds et al. 2008; Hill et al. 2012) and chlororespiration (Hill and Ralph 2005) might act to dissipate energy (Takahashi and Badger 2011; Murata et al. 2012). Furthermore, nitrogen metabolism might constitute an electron sink in carbon limited conditions (Smith et al. 2005). Here, reduced ferredoxin might act as a cofactor for ferredoxin-nitrite reductase which is responsible for the reduction of nitrite (NO_2^-) to ammonia (NH_3) which in turn is protonated to ammonium (NH_4^+). Nitrate and nitrite reductases have been found in *Symbiodinium* (reviewed in Davy et al. 2012).

1.7.1 The antioxidant defense system

Mechanisms that lead to the neutralization or detoxification of ROS are collectively termed the “antioxidant defense system” and include enzymes that directly or indirectly convert ROS to less harmful molecules and low molecular weight compounds that directly scavenge ROS (Halliwell 2006). Antioxidant defense mechanisms evolved in all respiring and photosynthesizing cells, and play a significant role in maintaining the pro-oxidant/antioxidant balance.

1.7.2 Enzymatic antioxidants

Major enzymes involved in the detoxification of reactive oxygen species are shown in Figure 1.7. Superoxide dismutase (SOD) is the first enzyme that intervenes in the chain of ROS production by converting O_2^- to H_2O_2, which in turn can be neutralized by peroxidase (ascorbate peroxidise, APX; and glutathione peroxidase) and catalase activity. SOD is present in three types (CuZn-SOD, Fe-SOD and Mn-SOD) that have all been identified in *Symbiodinium* cells and coral tissues, occurring in several isoforms in both (Richier et al. 2003; 2005; 2008). H_2O_2 can be converted to H_2O by catalase which has been identified in both *Symbiodinium* cells (Tytler and Trench 1986; Lesser and Shick 1989; Leggat et al. 2007) and corals (Merle et al. 2007), or glutathione peroxidase that is present in both, *Symbiodinium* cells (Downs et al. 2005; Downs and Downs 2007) and corals (Downs and Downs 2007).

(1) $O_2^- + O_2^- + 2H^+$	$-----> $	$H_2O_2 + O_2$	Superoxide dismutase
(2) $H_2O_2 + H_2O_2$	$-----> $	$2H_2O + O_2$	Catalase
(3) $H_2O_2 + RH_2$	$-----> $	$2H_2O + R$	Peroxidase

Figure 1.7: Main enzymes involved in ROS detoxification and their corresponding reactions. Modified from Furla et al. (2011).

1.7.3 Non-enzymatic antioxidants

The main non-enzymatic low molecular weight antioxidants are water soluble ascorbic acid and glutathione (GSH), as well as lipid soluble carotenoids and tocopherols (Halliwell 2006). Ascorbic acid and GSH are essential for quenching O_2^-, H_2O_2 and •OH, are therefore vital to maintain a reduced cellular environment. Both reducing compounds are applied in many biological systems to moderate cellular oxidative stress, as they are in corals (Downs et al. 2002). Carotenoids are generally not produced by animals; the presence of carotenes in corals suggests translocation from the *Symbiodinium* cells and/or uptake through heterotrophy (Furla 2011). Xanthophylls such as peridinin, dinoxanthin, diadinoxanthin (ddn) and diatoxanthin (dtn) are present in *Symbiodinium* spp but not the animal host. (Furla 2011). While the major function of peridinin is the energy transfer to

chlorophyll *a*, its ability to quench $^1O_2$ has been shown for marine algae (Pinto et al. 2000). The major protective function of diadinoxanthin and diatoxanthin is energy dissipation in a process termed "xanthophyll de-epoxidation" which can be measured as qE (energy dependent quenching) associated with NPQ (non-photochemical quenching), but a weak antioxidant function has also been proposed for diatoxanthin (Furla 2011). Tocopherols mainly quench $^1O_2$, whereas β-carotene quenches both $^1O_2$ and triplet-excited chlorophyll (Lesser 2006). Further important small-molecule antioxidants in marine algae are dimethylsulfide (DMS) and dimethylsulphoniopropionate (DMSP). DMS has the ability to quench $^1O_2$, while DMSP has the ability to quench •OH (Sunda et al. 2002). DMSP occurs in *Symbiodinium* cells (Hill et al. 1995; Van Alstyne et al. 2009; Yost and Mitchelmore 2009; Yost et al. 2010), where type-specific differences in baseline concentrations (Steinke et al. 2011), and in the activation of this compound, have been shown (Yost and Mitchelmore 2009).

1.7.4 Screening of photoradiation

Mycosporine-like amino acids (MAAs; Dunlap and Chalker 1986) are efficient UV-absorbing and -dissipating compounds (Dunlap and Shick 1998; Banaszak and Lesser 2009). They occur in cultured (Banaszak et al. 2000) and isolated *Symbiodinium* cells (Banaszak et al. 2006), exclusively in the host (Banaszak and Trench 1995; Yakovleva et al. 2004) or in the intact symbiosis (reviewed in Dunlap and Shick 1998; Shick and Dunlap 2002). Indeed, the diversity of MAAs in cnidarians is high (Banaszak 2003), and it is believed that they acquire these compounds heterotrophically and/or from the symbionts (Banaszak and Trench 1995; 2001; Shick and Dunlap 2002).

Further, a large array of fluorescent proteins (FPs) has been identified in corals, with the potential to minimize intracellular energy levels by scattering, absorption or dissipation of light (Salih et al. 2000; Dove et al. 2001), and the potential to quench O_2^- (Bou-Abdallah et al. 2006) and H_2O_2 (Palmer et al. 2009).

1.7.5 Non-photochemical quenching and xanthopyll de-epoxidation

All photosynthetic organisms use non-photochemical quenching (NPQ) to balance the amount of energy absorbed and utilized. This process is particularly important in environments where light intensities change in magnitude and over time, and has been intensely studied in plants and algae (Eskling et al. 1997; Niyogi 1999; Muller et al. 2001; Ort 2001; Goss and Jakob 2010). In vascular plants and green algae, NPQ collectively describes at least three mechanisms that affect chlorophyll fluorescence yield apart from photochemistry (photochemical quenching), and can be distinguished due to distinct relaxation kinetics in the dark (Niyogi 1999; Muller et al. 2001). Thermal dissipation linked with qE involves xanthophyll de-epoxidation and is highly reversible (within seconds to minutes). State transition, linked with qT (transitional quenching), relates to the reorganization of antenna complexes from PSII to PSI, and relaxes within tens of minutes. Photoinactivation, linked with qI (photoinhibitory quenching), is involved with photoinactivation due to PSII core rearrangement or degradation, and shows intermediate to slow relaxation/recovery (within hours) (Niyogi 1999; Muller et al. 2001). In dinoflagellates, such as *Symbiodinium*, NPQ seems to be less heterogeneous compared to vascular plants, and NPQ is strongly correlated with qE (Goss and Jakob 2010). Although there has been some speculation that state transitions might be active in *Symbiodinium* cells (Hill et al. 2005; Reynolds et al. 2008; Hill et al. 2012) there is no evidence of the cellular process (detachment of antenna complexes from PSII upon phosphorylation and reattachment at PSI) in *Symbiodinium* or other dinoflagellates (Goss and Jakob 2010).

Xanthophyll de-epoxidation results from the excitation energy transfer from excited chlorophyll to a de-epoxy xanthophyll which has the capability to energetically return to ground state, thereby directly quenching the energy by dissipation of heat at the light-harvesting complexes (LHC). In *Symbiodinium* cells (as in the algal classes Bacillariophyceae, Xanthophyceae, Haptophyceae and Dinophyceae), the acidification of the thylakoid lumen activates the enzyme diadinoxanthin de-epoxidase (DDE), which catalyzes the conversion of the structural, epoxy-free xanthophyll ddn to dtn. This mechanism is comparable to the conversion of violaxanthin to zeaxanthin via

antheraxanthin, catalyzed by violaxanthin de-epoxiase (VDE), in vascular plants and green algae, although considerable differences exist in the regulation of these two mechanisms. In both systems, light-driven photochemical processes result in an acidification of the thylakoidal lumen which activates DDE and VDE. The pH optimum of isolated VDE is 5.2 and the pH optimum of isolated DDE is 5.5, but more importantly it has been demonstrated that a pH of 7.2 may activate DDE. This means that a weak acidification as generated by chlororespiration or mitochondrial-palstid interactions may be sufficient to maintain ddn ep-oxidation in the dark (Goss and Jakob 2010, Nixon 2000). Indeed, Middlebrook et al. (2010) have shown that the majority of the xanthophyll pool can be in the de-epoxidated state even after 70 min of dark acclimation. Furthermore, Hill et al. (2012) have demonstrated that higher levels of xanthophyll de-epoxidation in a bleaching sensitive coral were sustained at night. These findings have important implications, as xanthophyll de-epoxidation in *Symbiodinium* cells might act efficiently to dissipate energy both when exposed to high light and in low light or darkness (Middlebrook et al. 2010).

1.7.6 Photochemical quenching and alternative electron sinks

Photochemical quenching describes the utilization of the light energy absorbed at light-harvesting complexes (LHC) to drive photochemical processes, and in particular the transfer of electrons from H_2O to NADPH which is necessary for carbon assimilation (assimilatory linear electron transport) (Niyogi 1999). In carbon limiting conditions or when the dark reaction is saturated, NADPH can be used to reduce NO_3^- (nitrate) and/or SO_4^{2-} (thioredoxin) (Niyogi 1999; Smith et al. 2005). In photosynthetic organisms, in non-assimilatory oxygen-dependent electron transport, electrons are transferred to oxygen through: (1) direct transfer at PSI by the Mehler reaction (Asada 1999; 2000) (see Section 1.6); and (2) oxygenase activity of rubisco in the photorespiratory pathway (Ort and Baker 2002). Although in *Symbiodinium* high CO_2 concentrations are maintained through a CCM (Leggat et al. 1999; Leggat et al. 2002), photorespiration might contribute significantly to maintain linear electron transport and utilization of light energy (Crawley et al. 2010). Finally, in the cyclic electron flow (CEF), electrons are cycled from PSI back to PSII, thereby dissipating energy (Niyogi 1999). The water-

water-cycle and the CEF generate and maintain a ΔpH which in turn is needed to activate thermal dissipation through xanthophyll de-epoxidation (Goss and Jakob 2010).

1.8 Effects of decreased temperatures

The complex physiological, cellular and molecular effects of heat stress have been extensively studied in *Symbiodinium* cells when *in hospite* or culture, or in freshly isolated cells. The effects of cold water stress are less well understood, although several events of coral bleaching due to cold water stress have been reported. Coral bleaching has been documented under subnormal temperatures in the Arabian Gulf (Coles and Fadlallah 1991), the Florida Keys (Porter et al. 1982; Kemp et al. 2011), the Gulf of California (LaJeunesse 2010), and the southern Great Barrier Reef (Hoegh-Guldberg and Fine 2004; Hoegh-Guldberg et al. 2005), as well as many other sites (Hoegh-Guldberg 1999). The physiological responses of corals or *Symbiodinium* cells to heat and cold stress are very similar. For example, Jokiel and Coles (1977) reported pigment and tissue loss, and reduced calcification rates in Hawaiian reef corals exposed to decreased temperatures. Similar effects were demonstrated by Roth et al. (2012), who also showed that xanthophyll de-epoxidation was up-regulated in cold-stressed *Acropora yongei*. However, the underlying cellular mechanisms of bleaching and whether they are similar under cold and heat stress are not resolved yet. Steen and Muscatine (1987) reported a decline of photosynthesis when the sea anemone *Aiptasia pulchella* was exposed to 4 °C for 4 hours. Saxby et al. (2003) suggested that cold-induced impairment of photosynthetic efficiency might be caused by the impairment of the Calvin-Benson cycle due to negative effects on enzyme activity. In contrast, Thornhill et al. (2008) hypothesized that cold-induced impairment of photosynthetic efficiency was due to a loss of thylakoid membrane fluidity. Clearly, a consensus about the cellular effects of cold stress, which lead to the impairment of photosynthesis and to the disruption of the symbiosis, is missing. Thus, the direct comparison of cold and heat stress was a focus of this thesis.

1.9 Physiological and cellular plasticity in corals and anemones

In reef habitats, changes in temperature and light (among other environmental parameters) can occur on small areal and temporal scales. In response to these fluctuating environmental conditions, organisms need to adjust their cellular and biochemical properties accordingly to maintain their physiological efficiency. This process, referred to as "acclimatization" is important in symbiotic corals and anemones across their distribution range. The capability for acclimatization depends on the physiological plasticity of the organism concerned (the capability for "phenotypic adaptation") which is the extent to which organisms can respond to environmental changes on cellular and molecular levels (Brown and Cossins 2011). Such adaptations can include the increased expression of protective components such as ROS-scavenging or radiation-screening components, or the differential use of protective pathways in both symbiotic partners (see Section 1.7). These mechanisms are associated with tolerance or susceptibility to bleaching (Brown and Cossins 2011). Short-term (e.g. over the course of one day) and long-term (e.g. over the course of seasons) acclimatization is generally reversible, and the potential for acclimatization of the coral-*Symbiodinium* association is determined by the genotype of both the coral and *Symbiodinium* (Edmunds and Gates 2008; Brown and Cossins 2011) as well as other symbionts such as bacteria and archaea (Rosenberg et al. 2007). Beneficial traits can be manifested in the genotype over generations ['genotypic adaptation', (Brown and Cossins 2011)] resulting in an array of genotypes with different cellular, biochemical and consequently physiological capabilities.

Because of the physiological diversity in *Symbiodinium* clades and types, shifts in the taxonomic composition of *Symbiodinium* populations have been suggested as a potential acclimatory mechanism (Buddemeier and Fautin 1993; Baker 2001; Baker 2004; Buddemeier et al. 2004; Rowan 2004). In the "adaptive bleaching hypothesis" (ABH) it has been hypothesized that bleaching might provide the chance to repopulate a bleached coral with a different *Symbiodinium* partner, that might be more stress-tolerant (Buddemeier and Fautin 1993). The repopulation might result from "symbiont switching", the replacement of sensitive *Symbiodinium* clades/types with resistant clades/types or "symbiont shuffling", the re-organization of existing co-occurring

clades/types with respect to their dominance (Baker 2003). For example, *Pocillopora damicornis* hosting the thermally tolerant *Symbiodinium* clade D has been shown to be more resistant to bleaching than *P. damicornis* hosting clade C (Rowan 2004). Furthermore, the apparently thermally tolerant genotype clade D has been reported to dominate reefs after bleaching events (Baker 2004). However, this concept of "switching" of *Symbiodinium* types is highly controversial and experimental proof of stable *de novo* acquisition of *Symbiodinium* types has not been provided yet. In a recent study, the acquisition of novel *Symbiodinium* types in scleractinian corals was achieved in laboratory conditions, but only temporarily maintained (Coffroth et al. 2010). Hence, rather than a "switching" in *Symbiodinium* types, a "shuffling" of existing *Symbiodinium* types might take place, where corals that host multiple clades or types shift their dominant symbiont(s) (Berkelmans and van Oppen 2006; Mieog et al. 2007; Jones et al. 2008; LaJeunesse et al. 2009).

1.10 High latitude coral reefs and coral communities

Acclimatization is particularly relevant at high latitude locations where sea surface temperatures and light availability vary considerably over the year. However, few studies have analyzed which cellular mechanism, or suite of mechanisms, high latitude corals use to cope with these variable conditions. Moreover, it has been hypothesized that corals at high latitude sites are better equipped to withstand environmental variability (Cook et al. 1990; Wicks et al. 2010b), due to the natural fluctuations of their environment over the course of seasons. At high latitudes, sea surface temperatures vary considerably over the year and can be very low during winter months. For example, at the Iki Islands of Japan corals are exposed to temperatures as low as 14 °C during winter, and as high as 27.5 °C during summer (reviewed in Brown and Cossins 2011). The most extreme example is the Arabian Gulf, where temperatures range from 18 °C to 36 °C (Riegl 2003). Other than Japan and the Arabian Gulf, examples of high latitude coral reefs include Bermuda in the Atlantic Ocean (Cook et al. 1990) and Lord Howe Island (31°33'S, 159°05') in the Pacific Ocean (Harriott et al. 1995). Reef communities occur at high latitude locations when temperatures are too low to allow reef accretion. High coral cover can be found at the

subtropical reef in the Solitary Islands Marine Reserve in Eastern Australia (29°55'S, 153°23') (Harriott et al. 1994).

The coral reef at Lord Howe Island is characterized by relatively high coral species diversity, with 80 scleractinian coral species recorded (Veron and Done 1979; Harriott et al. 1995). The coral reef community is a mixture of tropical species that occur at their southernmost distributional limits, subtropical species and some temperate species (Harrison 2008). Recently, a high diversity of *Symbiodinium* types has also been reported on the reef of Lord Howe, with many types present that have so far not been described from anywhere else (Wicks et al. 2010a). The challenging sea surface temperatures common at this high latitude site (annual sea temperature range 18 – 26 °C), and the presence of novel *Symbiodinium* types have led to the suggestion that these symbionts might be physiologically adapted to these variable circumstances. Indeed, a study by Wicks et al. (2010b) showed that *Pocillopora damicornis* harbouring *Symbiodinium* type C100 seems to be specialized to cooler temperatures than is normally seen at other latitudes.

Studying the physiological capability of these novel symbiont types presents a powerful opportunity to understand the mechanisms regulating bleaching susceptibility of the coral-dinoflagellate association. This topic is therefore the primary focus of this thesis.

The Solitary Islands Marine Reserve (located in New South Wales, eastern Australia) is characterized by a similar high diversity of scleractinian corals, with 90 species described (Harriott et al. 1994). Although at this subtropical reef, soft coral cover is generally low compared to the GBR (Harriott et al. 1994), the bubble-tip anemone *Entacmaea quadricolor* is abundant at North Solitary Island. *E. quadricolor* (Rüppell and Leuckart 1828) is an ecologically important species because it associates with *Symbiodinium* and anemonefish in a three-way-symbiosis (Dunn 1981; Fautin and Allen 1992). At North Solitary Island, this anemone harbours *Symbiodinium* clade C (Hill and Scott 2012). However, symbiont diversity at the sub-cladal level has not been described yet for this species in Australia. Furthermore, it has been demonstrated recently that *E. quadricolor* lives within 1 °C of its thermal threshold (Hill and Scott 2012). However, it is not known whether differences in bleaching susceptibility exist between different

colour phenotypes, or anemones hosting different *Symbiodinium* types. These questions are also addressed in this thesis.

1.11 Aim and specific objectives

Aim: The overall aim of this study was to investigate the importance of, and possible interactions between, protective mechanisms that underlie both heat and cold tolerance in *Symbiodinium* types common at high latitude sites and how these influence bleaching susceptibility or mortality of the cnidarian host.

In this study, a number of *Symbiodinium* types hosted by scleractinian corals common at the high latitude coral reef of Lord Howe Island (New South Wales, Australia, 31°33'S, 159°05') and the sea anemone *E. quadricolor* found around the subtropical Solitary Islands (New South Wales, Australia, 29°55'S, 153°23') were analyzed.

Specific objectives

1. To assess the role of non-photochemical quenching mediated by xanthophyll de-epoxidation on bleaching susceptibility and survivorship of different high latitude coral-*Symbiodinium* associations from Lord Howe Island when exposed to short-term heat and cold stress.

It was hypothesized that corals which are more robust to thermal stress, as demonstrated by survivorship and bleaching tolerance, would host *Symbiodinium* types which have a stronger capability of non-photochemical quenching as estimated by the size and de-epoxidation state of the xanthophyll pool.

2. To determine whether thylakoid fatty acid composition and re-modelling influence the photophysiology of different high latitude coral-*Symbiodinium* associations from Lord Howe Island when exposed to short-term heat and cold stress.

It was hypothesized that short-term heat- or cold-stressed coral-*Symbiodinium* associations would adjust their thylakoid fatty acid composition as such that the overall

relative content of unsaturation would increase in response to cold stress and decrease in response to heat stress.

3. To analyze the relationship between differential bleaching susceptibility or mortality and oxidative stress, by comparing the activity of superoxide dismutase (SOD) and ascorbate peroxidase (APX) in a range of high latitude *Symbiodinium* types *in hospite* a range of scleractinian corals from Lord Howe Island when exposed to short-term heat and cold stress.

It was hypothesized that corals that are more robust to thermal stress, as demonstrated by survivorship and bleaching tolerance, would host *Symbiodinium* types that have a greater pool of SOD and/or APX and/or are able to rapidly adjust these major antioxidant enzyme pools in response to changing temperatures.

4. To compare the impact of short-term heat stress on the damage and repair of PSII reaction centres, specifically the core protein D1, in high latitude *Symbiodinium* types from Lord Howe Island that associate with corals that have different bleaching susceptiblities.

It was hypothesized that bleaching susceptible corals would host *Symbiodinium* types that show greater net-photoinhibition due to lower photorepair rates under bleaching conditions such as short-term heat stress.

5. To provide information on the diversity of *Symbiodinium* types found in the soft-bodied bubble-tip anemone *Entacmaea quadricolor* on the east coast of Australia.

It was hypothesized that *E. quadricolor* would host different types of *Symbiodinium* potentially driven by environmental parameters that change with latitude or site.

6. To analyze the role of symbiont shuffling and SOD activity in two distinct colour phenoptypes of the anemone *E. quadricolor* and its symbionts when exposed to short-term heat stress.

It was hypothesized that short-term heat stress would result in symbiont shuffling. It was further hypothesized that symbiont shuffling would depend on the algal SOD

capacities and that the findings could be generalized across anemones with different host pigmentation.

Chapter 2:
The impact of decreased and increased temperature on Lord Howe Island corals and the pigment profile of their symbionts

2.1 Introduction

Reef-building corals associate with symbiotic dinoflagellates of the genus *Symbiodinium*. This symbiotic relationship is sensitive to environmental stress, exhibiting coral bleaching when stressors such as high temperatures lead to substantial degradation or loss of dinoflagellates symbionts and/or their pigments (Falkowski and Dubinsky 1981; Hoegh-Guldberg 1999). Thermal stress associated with elevated temperature anomalies is the principal cause for episodes of mass coral bleaching throughout the global distribution of reef systems (Hoegh-Guldberg 1999; Lesser 2011). Mass coral bleaching has also been documented under subnormal temperatures in the Arabian Gulf (Coles and Fadlallah 1991), the Florida Keys (Kemp et al. 2011), the southern Great Barrier Reef (Hoegh-Guldberg and Fine 2004), as well as many other sites (Hoegh-Guldberg 1999).

At LHI (31°33′S, 159°05′E) is the world's southernmost barrier coral reef, where seasonal sea surface temperatures annually range between 18 °C and 26 °C, with a minimum of 14.5 °C and a maximum of 28 °C recorded in the past 10 years (www.data.aims.gov.au). LHI coral communities are highly diverse, with at least 83 temperate, subtropical and tropical species (Veron and Done 1979; Harriott et al. 1995) hosting at least 15 distinct *Symbiodinium* types, 12 of which have been proposed as being endemic (Wicks et al. 2010a). It has been shown that the combination of corals and their dinoflagellate and microbial symbionts (i.e. the holobiont) influences bleaching propensity (Sampayo et al. 2008; Fitt et al. 2009; Fisher et al. 2012) and post-bleaching mortality of the host (Sampayo et al. 2008; Fitt et al. 2009).

The symbiotic breakdown caused by thermal stress involves a number of cellular changes within the holobiont whose sequential order is still being elucidated. Early responses within the host include apoptotic cell death in the gastrodermis (Ainsworth et al. 2008; Paxton et al. 2013) and a reduction of the coral epithelium which may precede cellular changes in the symbiont (Ainsworth et al. 2008). Furthermore, integrity, ultrastructure and gene expression in host mitochondria change independently from *Symbiodinium* cell integrity. The suppressed expression of the mitochondrial gene cytochrome *c* may result in reduced scavenging of reactive oxygen species (ROS), so increasing the overall levels of ROS within the holobiont (Dunn et al. 2012). Within the chloroplast of symbionts, it has been proposed that thermal stress directly affects photosystem II (PSII) (Warner et al. 1999), the thylakoid membranes (Iglesias-Prieto et al. 1992; Tchernov et al. 2004; Díaz-Almeyda et al. 2011) and the Calvin Cycle (Jones et al. 1998; Leggat et al. 2002; 2004) promoting electron accumulation in the chloroplast and associated overproduction of ROS (reviewed in Venn et al. 2008; Weis 2008). Further, it has been suggested that excess ROS damage host and symbiont deoxyribonucleic acid (DNA), proteins and lipids, so accelerating the rate of damage to the photosystem and resulting in the breakdown of the symbiosis (reviewed in Venn et al. 2008, Weis 2008). However, re-evaluation of recent studies suggests that the initial production of ROS may not increase photodamage *per se*, but rather inhibit the repair of photodamaged components of PSII such as the major PSII core protein D1. If so, small amounts of ROS could promote photoprotective steps: the down-regulation of the linear electron transport could be preventing the uncontrolled generation of excess ROS in the chloroplast (reviewed in Takahashi and Badger 2011).

ROS-mediated inhibition of protein synthesis is attenuated by an array of ROS-scavenging compounds and by mechanisms alleviating the excess production of ROS. ROS-scavenging compounds in the chloroplast include the enzymes superoxide dismutase and ascorbate peroxidase, and non-enzymatic antioxidants such as ascorbate, α-tocopherol, and carotenoids (reviewed in Halliwell 2006). The carotenoid β-carotene, an important antioxidant in marine algae (Ben-Amotz et al. 1989), is involved in quenching singlet oxygen ($^1O_2$; Asada 2006). Other mechanisms alleviating excess ROS production include thermal dissipation of excitation energy, carbon fixation, and

alternative electron pathways such as cyclic electron flow (CEF) and photorespiration in the light and chlororespiration in the dark (reviewed in Takahashi and Badger 2011; Murata et al. 2012).

Thermal dissipation allows the elimination of excessively-absorbed energy at the light-harvesting complexes of PSII as heat, thus avoiding over-excitation of the photosystem (reviewed in Niyogi 1999; Muller et al. 2001). In dinoflagellates such as *Symbiodinium* spp, thermal dissipation relies on the conversion of the structural epoxy-xanthophyll diadinoxanthin (ddn) to the photoprotective epoxy-free diatoxanthin (dtn, xanthophyll de-epoxidation), catalyzed by diadinoxanthin de-epoxidase (DDE), which is equivalent to the conversion of violaxanthin to zeaxanthin catalyzed by violaxanthin de-epoxidase (VDE) in vascular plants. In both systems, epoxidation is primarily activated by exposure to high light and subsequent acidification of the thylakoid lumen caused by light-driven photosynthetic transport. However, in contrast to vascular plants, in ddn-containing organisms DDE can be activated by a weak acidification of the thylakoid lumen that may be generated by chlororespiration in the dark or in conditions of low light (reviewed in Goss and Jakob 2010). The ability of *Symbiodinium* to maintain ddn epoxidation in the dark has been demonstrated by Middlebrook et al. (2010), who showed that 75% of the xanthophyll pool was in the de-epoxidated state even after 70 min of dark acclimation in the reef-building coral *Acropora formosa*. Reversal from the photoprotective to the light-harvesting state is catalyzed by the enzyme dtn epoxidase (DEP) in dinoflagellates and by zeaxanthin epoxidase (ZEP) in vascular plants. In contrast to ZEP, DEP is inhibited by a proton gradient, which is necessary to ensure dtn accumulation in conditions of high light, because DDE and DEP have highly similar rate constants (reviewed in Goss and Jakob 2010).

In ddn-containing algae, the activity of the xanthophyll cycle is closely correlated to the intensity of non-photochemical quenching (NPQ) of chlorophyll fluorescence, as alternative chlorophyll-quenching mechanisms such as state transitions are absent (reviewed in Goss and Jakob 2010). While several studies have addressed xanthophyll de-epoxidation and/or the role of β-carotene in *Symbiodinium* cells (e.g. Brown et al. 1999; Ulstrup et al. 2008; Hennige et al. 2009) and its protective role in conditions of

high light (Ambarsari et al. 1997; Krämer et al. 2012) and high temperature (e.g. Dove et al. 2006; Abrego et al. 2008; Middlebrook et al. 2008), only one study has investigated xanthophyll de-epoxidation during cold water stress (Roth et al. 2012) and comparable detailed studies from high latitude coral reefs are missing.

This study aimed to examine the photophysiological properties of four typical LHI holobionts *(Porites heronensis* C111*, *Acropora yongei* C3/C111*, *Stylophora* sp. C118, and *Pocillopora damicornis* C100/C118) and their responses to short-term thermal stress. In particular, this study explored the dynamics of photoacclimatory and photoprotective pigments (chlorophylls, xanthophylls and β-carotene) in their symbionts and the possibility that the activation of NPQ in form of xanthophyll de-epoxidation might be a key strategy for withstanding bleaching and host mortality at both short-term high and low temperature fluctuations.

2.2 Materials and methods

2.2.1 Sampling

In October 2010, coral fragments of four coral species were collected from the Lord Howe lagoon site Sylphs Hole (S31°31′249″, E159°03′261″). Corals were identified as *Acropora yongei* (n = 5 colonies), *Pocillopora damicornis* (n = 3), *Stylophora* sp. (n = 2) and *Porites heronensis* (n = 4). In addition, fragments of *P. damicornis* (n = 5) were sampled from the lagoon reef site Stephens Hole (S31°31′937″, E159°03′251″). *P. damicornis* samples originated from two different lagoon locations to increase the chance of sampling different symbiont types, as this coral species has been shown to host *Symbiodinium* ITS2 C100, C103 and C118 at LHI (Wicks et al. 2010a; 2010b). All coral species were identified based on morphological characteristics described in Veron and Stafford-Smith (2000). In addition, *Stylophora* sp. and *P. damicornis* were identified using molecular markers (see Chapter 2.2.6 on page 64) because *Stylophora* sp. shared morphological characteristics common to both pocilloporid species (Figure 2.1). All samples were taken from a depth of 0.5 – 3 m during low tide. Fragments were obtained from the top of the colony to ensure that they had received a similar light regime. Sea

temperatures at the time of collection and experimentation (Austral spring) within the lagoon ranged from 16 – 22 °C at a depth of 2.5 – 5.5 m (AIMS data centre; www.data.aims.gov.au). Irradiance in the lagoon, at a depth of 0.5 – 3 m, peaked at approximately 1750 µmol photons m^{-2} s^{-1} as measured with a submersible HOBO pendant data logger (ENVCO, New Zealand) at noon. The HOBO pendant data logger was calibrated with a Li-Cor LI-189 photometer (Li-Cor, USA).

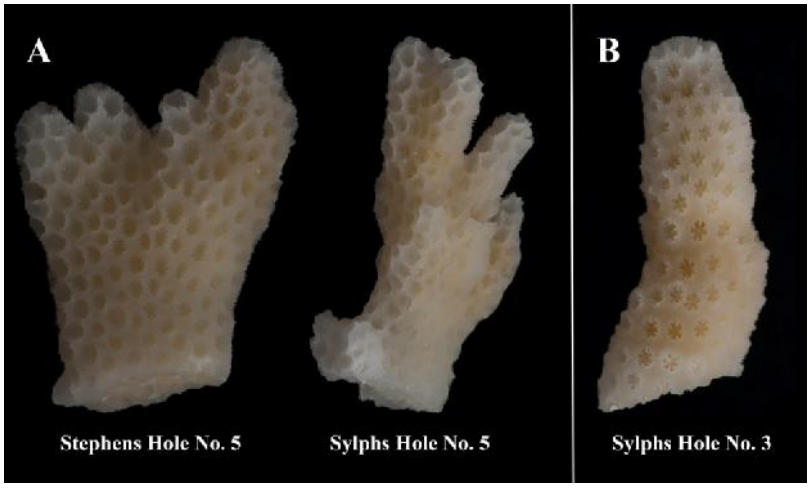

Figure 2.1: Representative skeleton samples of *Pocillopora damicornis* (**A**; representative for samples No. 1 – 6, 9 – 10, see Table 2.1) and *Stylophora* sp. (**B**; representative for samples No. 7 – 8). Explants are approximately 2 cm in length. Photos by Assoc Prof Ken Ryan.

2.2.2 Experimental procedure

Coral explants of 1 – 3 cm length (*A. yongei*. *P. damicornis* and *Stylophora* sp.) or 5 – 7 cm^2 coral surface area (*P. heronensis*) were immediately prepared from fragments following collection (n = 25 per colony). One explant of each coral colony was airbrushed, and *Symbiodinium* cells isolated through repeated washes in 0.22-µm filtered seawater (FSW) and preserved in sodium chloride (NaCl) saturated 20% dimethyl sulfoxide (DMSO) buffer for subsequent genotyping. Remaining coral explants were kept for four days in aerated 50-L tanks that were supplied with unfiltered seawater from the LHI lagoon at regular intervals (approximately every 90 min during daylight hours) for acclimatization. Light intensity was controlled using shade cloth. Temperature and natural light within tanks were monitored using a submersible HOBO pendant logger.

After acclimatization, coral explants were exposed to temperatures averaging: i) 22 ± 0.1 °C (mean ± S.E.), corresponding to the annual temperature average; ii) 29 ± 0.1 °C, corresponding to 5 °C above the annual monthly mean temperature maximum (MMM) and 1 °C below the experimentally determined upper bleaching thermal threshold (Wicks et al. 2010b); and iii) 15 ± 0.1 °C, corresponding to 3 °C below the annual monthly mean temperature minimum and 1 °C above the experimentally determined lower bleaching thermal threshold (Wicks et al. 2010b) (n = 8 for each colony and temperature). Treatment temperatures were based on previous bleaching experiments conducted by Wicks et al. (2010b) at the same location. The chilling/heating to respective treatment temperatures was started at 06:00 h in the morning of Day 1. Treatment temperatures were attained on Day 1 at time 09:10 h (29 °C) and 17:00 h (15 °C). The experiment was terminated at 18:00 h on Day 5. Between 13:00 h and 14:00 h on Days 0, 2, and 5, coral explants were flash frozen in liquid nitrogen. Frozen samples were stored at -80 °C until analysis. For all parameters analyzed, no data points are available for *A. yongei* after Day 2 at elevated treatment due to extensive sloughing of the tissue by Day 3.

2.2.3 Photosynthetic measurements

Chlorophyll fluorescence of PSII was measured using a diving pulse amplitude modulated (PAM) fluorometer (Walz, Germany). Maximum quantum yield of PSII (F_v/F_m) was recorded each day after sunset (18:00 h) on dark acclimated specimen. Effective quantum yield of PSII ($\Delta F/F_m'$) was measured between 12:00 h and 12:45 h noon. Excitation pressure over PSII (Q_m) (Iglesias-Prieto et al. 2004) was calculated as in Fisher et al. (2012):

Q_m = 1 - [($\Delta F/F_m'$) at noon/(F_v/F_m) at dawn of Day 0]

2.2.4 Sample preparation and analysis

Coral fragments were airbrushed in 0.22-µm FSW at 4 °C. Two subsamples of the tissue slurry were removed and frozen at -80 °C for later determination of *Symbiodinium*

cell density. The remaining tissue slurry was processed immediately for pigment identification and quantification. To determine *Symbiodinium* cell density, cells were counted in 10 replicate counts using a haemocytometer and standardized to cells cm^{-2} coral surface area as determined using the paraffin wax method (Stimson and Kinzie 1991).

All steps of pigment extraction were performed at 4 °C and pigment extracts were kept in the dark. The coral/algal homogenate was centrifuged at 4000 × g for 15 min. Supernatant was discarded, and 3 mL of HPLC-grade methanol were added, vortexed and extracted for 10 min. The extract was then centrifuged at 4000 × g for 3 min. The extract was carefully removed in order to not disturb the algal pellet and the extraction repeated with new methanol. Extractions were repeated five times to ensure that all pigments were successfully extracted, and the extracts were combined and filtered through a 0.22-µm cellulose acetate filter prior to pigment analysis. A subsample of the extract was analyzed by high pressure liquid chromatography (HPLC) using an Agilent Technologies, 1200 Series HPLC system, in three replicate measurements (Zapata et al. 2000; Dove et al. 2006). Pigments were quantified by comparison to known concentrations of chlorophyll *a* (chl *a*), chlorophyll c_2 (chl c_2), peridinin, diadinoxanthin (ddn), diatoxanthin (dtn) and β-carotene (β-car). These standards were obtained from DHI, Denmark. Pigment concentrations were normalized to cell and chl *a*.

2.2.5 *Symbiodinium* genotyping

Genomic DNA was isolated following the procedure of Stat et al. (2009) and isolated DNA was stored in Tris buffer (10 mM; pH 8.0) containing ethylenediaminetetraacetic acid (EDTA, 1 mM). The concentration of DNA was measured by absorbance at 230, 260, 280 and 320 nm using a nanophotometer (Implen GmbH, Germany). The ITS2 region of the ribosomal DNA was amplified by polymerase chain reaction (PCR) using the primers itsD (Pochon et al. 2007) and ITS2CLAMP (LaJeunesse and Trench 2000; LaJeunesse 2002) in a final volume of 50 µL PCR reaction. The amplification protocol used a touch-down protocol modified after LaJeunesse and Trench (2000). The initial annealing temperature (T_a) started at 65 °C. Then, T_a was decreased every two cycles by 1 °C and held at the final T_a of 55 °C for an

additional 15 cycles. Amplicons were separated using denaturing gradient gel electrophoresis (DGGE, Biorad DCode system) as performed in Wicks et al. (2010a) except that gels were run at 100 V for 16 h and DNA was stained with ethidium bromide (0.5 µg/mL). DNA from distinct and prominent bands was eluted overnight in 20 µL sterile water. DNA was re-amplified using the primers ItsD and ITS2REVint (5'-CCATATGCTTAAGTTCAGCGGG-3') using 32 amplification cycles at a melting temperature of 94 °C, T_a of 55 °C and elongation temperature of 72 °C, holding each step for 30 s. Amplicons were prepared for sequencing using ExoZap (GE Lifescience, Australia). Samples were sent to Macrogen Inc., South Korea, for sequencing. Each amplicon was sequenced in forward and reverse directions, and both sequences were checked and aligned manually. The resulting consensus sequence was analyzed using BLAST on Genbank (http://blast.ncbi.nlm.nih.gov/Blast.cgi; Altschul et al. 1990) and compared to sequences available on Geosymbio (http://sites.google.com/site/geosymbio; Franklin et al. 2012). Nucleotide sequence alignments were generated using Clustal W (Goujon et al. 2010) and visualized using GeneDoc software (Nicholas et al. 1997).

2.2.6 Host genotyping of Pocilloporidae used in the study

The mitochondrial cytochrome *c* oxidase subunit I (*COI*) was amplified using the universal metazoan primers LCO1490 and HCO2198 (Folmer 1994) in a 12.5 µL PCR reaction using the following conditions: an initial denaturation at 95 °C, followed by 40 cycles at 95 °C for 15 s, 53 °C for 15 s, 72 °C for 15 s, and a final elongation at 72 °C for 7 min. The hyper-variable mitochondrial open reading frame (ORF) was amplified using the coral-specific primers FATP6.1 and ORFR (Flot et al. 2008) in a 12.5 µL PCR reaction using the following conditions: an initial denaturation at 95 °C, followed by 40 cycles at 95 °C for 15 s, 40 °C for 15 s, 72 °C for 15 s, and a final elongation at 72 °C for 7 min. Out of ten pocilloporid colonies, two were successfully identified using ORF and seven were successfully identified using *COI* (Table 2.1).

2.2.7 Statistical analysis

SPSS software (version PASW statistics 18) was used for statistical analysis. Repeated measures analysis of variance (rmANOVA) was performed to determine

significant changes ($p \leq 0.05$) of photophysiological parameters, symbiont density and pigment parameters. These parameters were used as independent variables ('Time'), and the parameters 'Species' and 'Temperature' were used as dependent variables. If assumptions of normality (Kolmogorov-Smirnov test) and assumptions of homogeneity of variances (Levene's test) were violated, data were arcsine (F_v/F_m, Q_m) or log (pigments) transformed. When assumptions of equality of the variances between repeated measures were not met (Mauchly's test of sphericity), the Greenhouse-Geisser correction is reported. After an initial overall analysis including all dependent variables, each coral association and temperature treatment was analyzed separately to reveal significant differences between treatments and between species. When significant interactions were identified ('Time × Species', or 'Time × Temperature', respectively), pairwise comparisons were performed using *post hoc* pairwise comparisons with Bonferroni correction. To analyze differences of any parameter between species on Day 0, an univariate ANOVA test with *post hoc* Tukey's HSD comparison was performed.

Table 2.1: Samples obtained from pocilloporid colonies and their groupings based on skeletal morphology (Figure 2.1), mitochondrial open reading frame (ORF) or cytochrome *c* oxidase subunit I (*COI*) molecular identity. For sequences refer to Appendix A.1 and A.2 on pages 255 – 257. bp = basepair.

site	**Sample No.**	**Skeletal morphology type**	**ORF** closest genbank match accession No. (identity%)	**Genbank accession No.**	***COI*** closest genbank match accession No. (identity%)	**Genbank accession No.**
Stephens Hole	1	A	***Pocillopora damicornis*** EU400213.1 (888/892 bp, 99%)	KF194192	***Pocillopora damicornis*** AY139813.1 (678/680 bp, 99%)	KF194194
	2	A	n/d		***Pocillopora damicornis*** AY139813.1 (695/699 bp, 99%)	KF194195
	3	A	n/d		***Pocillopora damicornis*** AY139813.1 (674/681 bp, 99%)	KF194196
	4	A	n/d		n/d	
	5	A	n/d		***Pocillopora damicornis*** AY139813.1 (674/679 bp, 99%)	KF194197
Sylphs Hole	6	A	n/d		n/d	
	7	B	n/d		***Stylophora pistillata*** EU 400214 (697/708 bp, 98%)	KF194198
	8	B	***Stylophora sp.*** JN558888.1 (863/885 bp, 98%)	KF194193	***Stylophora pistillata*** EU 400214 (673/676 bp, 99%)	KF194199
	9	A	n/d		n/d	
	10	A	n/d		***Pocillopora damicornis*** AY139813 (111/117 bp, 95%)	See Appendix A.1 (Seq7) on page 255

2.3 Results

2.3.1 Genetic identification of *Symbiodinium*

PCR-based amplification and subsequent sequencing of the ribosomal ITS2 region showed that samples from the four coral species hosted a total of four distinct *Symbiodinium* types, all belonging to clade C (Table 2.2 and Figure 2.2). *Acropora yongei* hosted a mixed population of C3 (LaJeunesse 2002) and a symbiont type that showed 99% sequence identity to type C111 (Wicks et al. 2010a). The latter differed by two base-pair mismatches and one base-pair deletion within the ITS2 region, and one base-pair mismatch in the 5.8S rDNA coding region that flanks the ITS2 region (Figure 2.2). This type is hereafter referred to as C111*. *Pocillopora damicornis* hosted a mixture of symbiont types C100 and C118 (Wicks et al. 2010a). Quantitative polymerase chain reaction (qPCR) analysis using type-specific primers showed that the proportion of C118 was always lower than 32% of the total symbiont ITS2 pool (S. Wilkinson, personal communication). The two species *Stylophora* sp. and *Porites heronensis* hosted *Symbiodinium* types C118 and C111*, respectively.

Table 2.2: Coral species and corresponding *Symbiodinium* internal transcribed spacer (ITS) 2 types identified by denaturing gradient gel electrophoresis (DGGE) and subsequent sequencing. bp = basepair.

species	**family**	***Symbiodinium* ITS2 type**	**closest genbank match (identity, %)**	**genbank accession No.**
Acropora yongei	Acroporidae	C3	AF499789 (283/283 bp, 100%)	KF194188
		C111*	HM222438 (279/283 bp, 99%)	KF194187
Pocillopora damicornis	Pocilloporidae	C100	HM222433 (283/283 bp, 100%)	KF194189
		C118	HM222440 (283/283 bp, 100%)	KF194190
Stylophora sp.	Pocilloporidae	C118	HM222440 (283/283 bp, 100%)	KF194191
Porites heronensis	Poritidae	C111*	HM222438 (279/283 bp, 99%)	KF194186

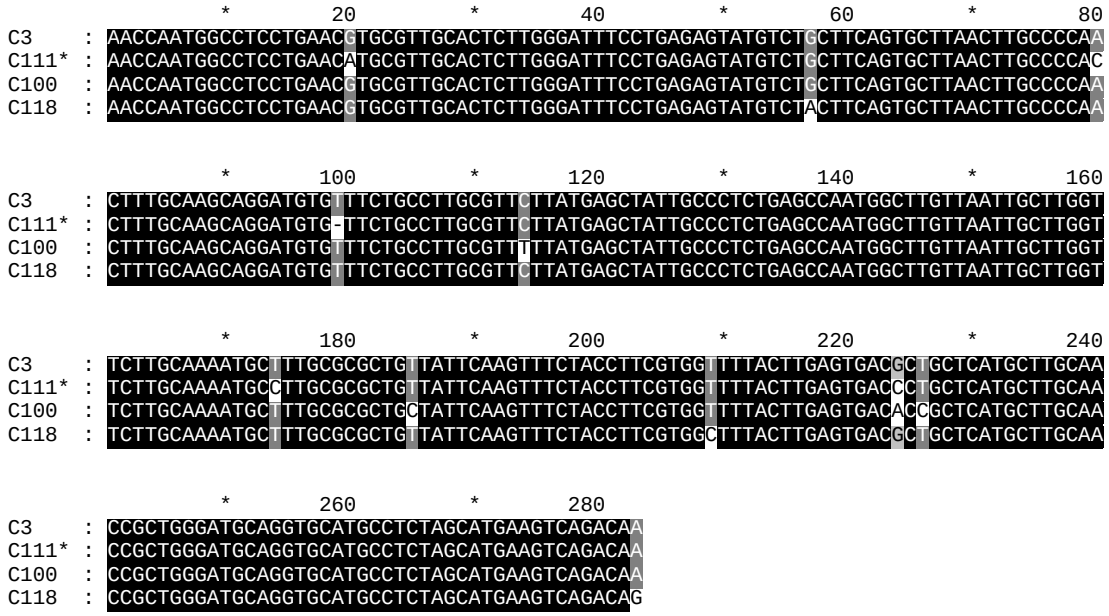

Figure 2.2: Nucleotide sequence alignment of internal transcribed spacer 2 (ITS2) (nucleotide [nt] 69 - 265) flanked 5' by partial 5.8S ribosomal DNA gene (nt 1 – 68) and 3' by partial 28S ribosomal DNA gene (nt 266 – 283) for C3 (*Acropora yongei*), C111* (*Acropora yongei*, *Porites heronensis*), C100 (P*ocillopora damicornis*), and C118 (*Pocillopora damicornis*, *Stylophora* sp.*)* Identical residues in all sequences are highlighted with black background. Identical residues in three sequences are shaded in dark grey. Identical residues in two sequences are shaded in light grey.

2.3.2 Host mortality

A. yongei, but none of the other coral associations, died during the temperature treatment. In the morning of Day 0, 12% of *A. yongei* explants across treatment tanks had extensively sloughed off their tissue so that only the coral skeleton remained. At 29 °C, a total of 56% of *A. yongei* explants had died with identical symptoms by the morning of Day 3. At 22 °C or 15°C, mortality was not observed after Day 0.

2.3.3 Maximum quantum yield of PSII

On Day 0, maximum quantum yield of PSII (F_v/F_m) measured at 18:00 h was 0.682 ± 0.01 (mean ± S.E.) in *P. heronensis*, 0.690 ± 0.01 in *A. yongei*, 0.670 ± 0.01 in *Stylophora* sp. and 0.667 ± 0.01 in *P. damicornis*. Over a period of 5 days, coral species responded differently to a given temperature (significant Time × Temperature × Species interaction, Table 2.3). F_v/F_m in all coral species was affected by temperature, except in *A. yongei* after 2 days of exposure (significant interaction of Time × Temperature, Table 2.4).

Over the 5-day period at 22 °C, F_v/F_m was not significantly different between species (Table 2.5). At both elevated and reduced temperatures, F_v/F_m declined in most coral associations (Figure 2.3 A – D). Exceptions were *A. yongei* after 2 days (Figure 2.3 B) and *Stylophora* sp. after 5 days (Figure 2.3 C) of increased temperature, where no change in F_v/F_m was observed when compared to 22 °C (rmANOVA, $p > 0.05$). At 29 °C, *P. heronensis* reduced its F_v/F_m by 29.2% over 5 days (Figure 2.3 A), *A. yongei* by 16.5% over just 2 days (Figure 2.3 B), *Stylophora* sp. by 22% over 5 days (Figure 2.3 C), and *P. damicornis* by 86.2% over 5 days (Figure 2.3 D). Over 5 days at 15 °C, *P. heronensis* reduced its F_v/F_m by 19.7% (Figure 2.3 A), *A. yongei* by 36.2% (Figure 2.3 B), *Stylophora* sp. by 79.8% (Figure 2.3 C) and *P. damicornis* by 35.6% (Figure 2.3 D).

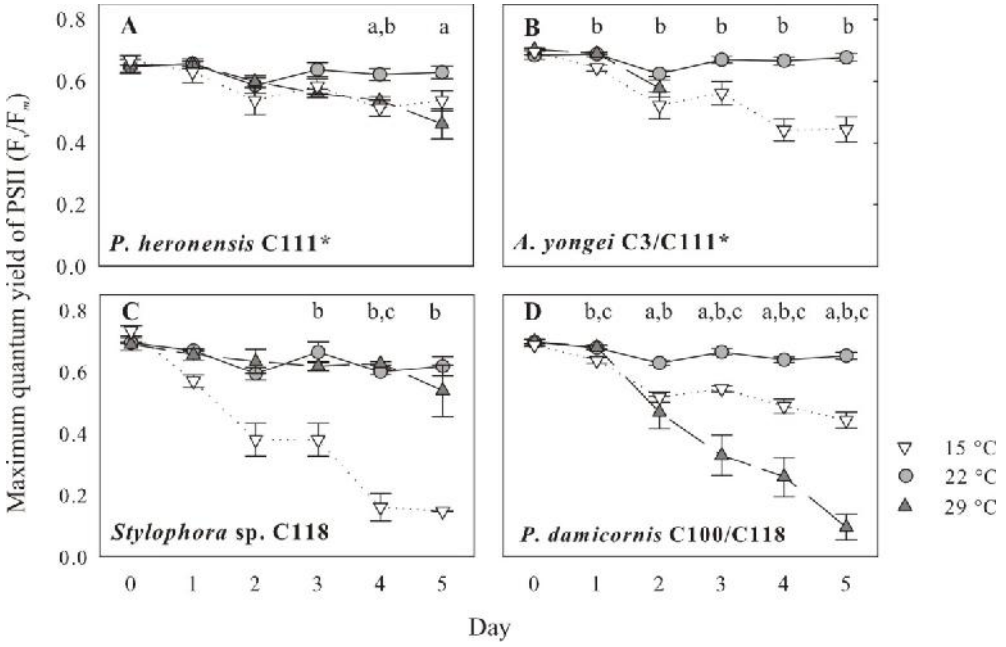

Figure 2.3: Effect of temperature over a 5-day period on maximum quantum yield of PSII (F_v/F_m), in *Porites heronensis* hosting *Symbiodinium* C111* (**A**), *Acropora yongei* hosting C3/C111* (**B**), *Stylophora* sp. hosting C118 (**C**) and *Pocillopora damicornis* hosting C100/C118 (**D**). Presented are mean values ± S.E., n = 2 – 8. Significant differences are reported for (a) 22 °C and 29 °C, (b) 22 °C and 15 °C, and (c) 15 °C and 29 °C at the level of $p \leq 0.05$ (rmANOVA and *post hoc* pairwise comparison with Bonferroni correction).

Table 2.3: Results of rmANOVA analysis for the parameters: photochemical maximum quantum yield of PSII (F_v/F_m); *Symbiodinium* density (SD); concentration of photosynthetic pigments (PSP) per cell; xanthophyll de-epoxidation (dtn/dtn+ddn); concentration of diatoxanthin (dtn) per chlorophyll *a* (chl *a*); and excitation pressure over PSII (Q_m). Bold numbers highlight significant differences ($p \leq 0.05$), grey numbers indicate non-significant differences ($p > 0.05$). † indicates that Greenhouse-Geisser correction is reported.

Variables	**F_v/F_m†**	**SD cm^{-2}**	**PSP cell^{-1}†**	**dtn/(ddn+dtn)**	**dtn/chl *a***	**Q_m†**
Time	**< 0.001**	**< 0.001**	**0.001**	**< 0.001**	**< 0.001**	**< 0.001**
	$F_{3.6} = 106.1$	$F_{2, 37} = 47.1$	$F_{1.7} = 8.4$	$F_{2, 39} = 59.4$	$F_{2, 39} = 24.1$	$F_{3.3} = 114.5$
Time × Temperature	**< 0.001**	**< 0.001**	0.055	**< 0.001**	**0.014**	**< 0.001**
	$F_{7.2} = 19.5$	$F_{4, 74} = 7.1$	$F_{3.5} = 2.5$	$F_{4, 78} = 5.7$	$F_{4, 78} = 3.4$	$F_{6.5} = 13.1$
Time × Species	**< 0.001**	$p = 0.135$	0.109	**0.018**	**0.011**	**< 0.001**
	$F_{10.8} = 5.3$	$F_{6, 74} = 1.7$	$F_{5.2} = 1.9$	$F_{6, 78} = 2.7$	$F_{6, 78} = 3.0$	$F_{9.8} = 5.6$
Time × Temperature × Species	**< 0.001**	**0.004**	0.440	**< 0.001**	**0.001**	**< 0.001**
	$F_{18} = 7.4$	$F_{10, 74} = 1.8$	$F_{8.6} = 1.0$	$F_{10, 78} = 6.0$	$F_{10, 78} = 3.3$	$F_{16.3} = 5.2$
Error (Time)	147.3	37	69.1	39	39	134.0
Temperature	**< 0.001**	**0.016**	**0.003**	**< 0.001**	**0.002**	**< 0.001**
	$F_2 = 33.4$	$F_2 = 4.6$	$F_2 = 6.8$	$F_2 = 16.0$	$F_2 = 7.5$	$F_2 = 86.1$
Species	**0.012**	**< 0.001**	**< 0.001**	**< 0.001**	**0.001**	**< 0.001**
	$F_3 = 4.1$	$F_3 = 18.0$	$F_3 = 161.3$	$F_3 = 10.0$	$F_3 = 6.3$	$F_3 = 33.2$
Temperature × Species	**< 0.001**	$p = 0.099$	**0.014**	0.303	0.687	**< 0.001**
	$F_5 = 11.9$	$F_5 = 2.0$	$F_5 = 3.3$	$F_5 = 1.3$	$F_5 = 0.6$	$F_5 = 11.6$
Error	42	38	40	40	40	41

Table 2.4: Results of rmANOVA analysis (effect of Time × Temperature) when each coral coral-symbiont association is analyzed separately. The parameters are: maximum quantum yield of PSII (F_v/F_m); *Symbiodinium* density (SD); pool of photosynthetic pigments (PSP); xanthophyll de-epoxidation (dtn/(dtn+ddn)); diatoxanthin (dtn) per chlorophyll *a* (chl *a*); pool of diadinoxanthin (ddn) per chl *a*; dtn per chl *a*; and excitation pressure over PSII (Q_m). Only significant effects ($p \leq 0.05$) are shown. [a] shows results for rmANOVA analysis for 2 days of treatment; df = degrees of freedom; ns = not significant on the level $p > 0.05$; [†] indicates Greenhouse-Geisser correction is reported.

parameter		***Acropora yongei*** **C3/C111***	***Acropora yongei*** **C3/C111*[a]**	***Pocillopora damicornis*** **C100/C118**	***Porites heronensis*** **C111***	***Stylophora*** **sp. C118**
F_v/F_m	$F_{(df, Error\ df)}$	**8.0** $_{(2.2,18)}$[†]	ns	**30.2** $_{(5.5, 57.6)}$[†]	**5.1** $_{(4.3,19.5)}$[†]	**12.5** $_{(5, 7.4)}$[†]
	p	**0.005**	ns	**< 0.001**	**0.005**	**0.002**
SD	$F_{(df, Error\ df)}$	**5.6** $_{(2, 6)}$	**4.5** $_{(2, 11)}$	**5.3** $_{(4, 38)}$	ns	**8** $_{(4, 4)}$
	p	**0.042**	**0.038**	**0.002**	ns	**0.035**
PSP	$F_{(df, Error\ df)}$	ns	ns	**5.3** $_{(4, 38)}$	ns	ns
	p	ns	ns	**0.002**	ns	ns
dtn/(dtn+ddn)	$F_{(df, Error\ df)}$	ns	ns	**13.3** $_{(4, 38)}$	**8.5** $_{(4, 16)}$	ns
	p	ns	ns	**< 0.001**	**0.001**	ns
(dtn+ddn)/chl *a*	$F_{(df, Error\ df)}$	ns	ns	**4.3** $_{(2.4, 23.8)}$[†]	ns	ns
	p	ns	ns	**0.021**	ns	ns
dtn/chl *a*	$F_{(df, Error\ df)}$	ns	ns	**6.2** $_{(4, 38)}$	**7.3** $_{(4, 16)}$	**7** $_{(4, 4)}$
	p	ns	ns	**0.001**	**0.001**	**0.043**
Q_m	$F_{(df, Error\ df)}$	**14.7** $_{(2.7, 21.8)}$[†]	**4** $_{(4, 22)}$	**21** $_{(5.7, 59.4)}$[†]	**6.3** $_{(10, 10)}$	ns
	p	**< 0.001**	**0.014**	**< 0.001**	**0.004**	ns

Table 2.5: Results of rmANOVA analysis (effect of Time × Species) when each temperature is analyzed separately. The parameters are: maximum quantum yield of PSII (F_v/F_m); *Symbiodinium* density (SD); pool of photosynthetic pigments (PSP); xanthophyll de-epoxidation (dtn/(dtn+ddn)); diatoxanthin (dtn) per chlorophyll *a* (chl *a*); pool of diadinoxanthin (ddn); dtn per chl *a*; dtn per chl *a*; and excitation pressure over PSII (Q_m). Only significant effects ($p \leq 0.05$) are shown. [a] shows results for rmANOVA analyzes for 2 days of treatment; df = degrees of freedom; ns = not significant on the level $p > 0.05$; [†] indicates Greenhouse-Geisser correction is reported.

parameter		**15 °C**	**22 °C**	**29 °C**	**29 °C[a]**
F_v/F_m	$F_{(df, Error\ df)}$	**3.6 (15, 30.8)†**	ns	**9.5 (5.1, 28.2)**	**3.9 (3.3, 16.7)**
	p	**0.001**	ns	**< 0.001**	**0.025**
SD	$F_{(df, Error\ df)}$	**3.7 (6, 26)**	ns	**3.2 (4, 16)**	ns
	p	**0.008**	ns	**0.040**	ns
PSP	$F_{(df, Error\ df)}$	ns	ns	ns	ns
	p	ns	ns	ns	ns
dtn/(dtn+ddn)	$F_{(df, Error\ df)}$	**3.3 (6, 28)**	**3.6 (6, 28)**	**13.4 (4, 18)**	ns
	p	**0.015**	**0.009**	**< 0.001**	ns
(dtn+ddn)/chl *a*	$F_{(df, Error\ df)}$	**4.3 (6, 28)**	ns	ns	ns
	p	**0.004**	ns	ns	ns
dtn/chl *a*	$F_{(df, Error\ df)}$	**3.1 (4.1, 20.3)†**	**2.8 (6, 28)**	**4.7 (4, 18)**	**3.6 (3, 15)**
	p	**0.038**	**0.030**	**0.009**	**0.039**
Q_m	$F_{(df, Error\ df)}$	**3.2 (15.3, 0.8)**	**3.2 (9.5, 47.3)†**	**8.2 (5.3, 29)†**	**6.9 (4.0, 20.1)**
	p	**0.003**	**0.004**	**0.001**	**0.001**

2.3.4 Population density of symbionts

On Day 0, symbiont densities (mean ± S.E.) were $2.68 \times 10^6 \pm 0.19 \times 10^6$ cells cm^{-2} in *P. heronensis*, $2.02 \times 10^6 \pm 0.09 \times 10^6$ cells cm^{-2} in *A. yongei*, $2.08 \times 10^6 \pm 0.02 \times 10^6$ cells cm^{-2} in *Stylophora* sp. and $1.87 \times 10^6 \pm 0.01 \times 10^6$ cells cm^{-2} in *P. damicornis*. Symbiont density was significantly higher in *P. heronensis* than *A. yongei* and *P. damicornis* (Tukey HSD: $p = 0.007$ and $p < 0.001$, respectively).

Over the 5-day period at 22 °C, symbiont density was stable in all corals (Figure 2.4 A – D) with no significant differences detectable between species (Table 2.5). Over the 5-day period at 29 °C, symbiont density was stable in *P. heronensis*, *A. yongei*, and *Stylophora* sp. (Figure 2.4 A – C), but significantly decreased (by 92%) in *P. damicornis* (Figure 2.4 D, Tables 2.4, 2.5). Symbiont density in this species was significantly lower on Days 2 and 5 at 29 °C than at 22 °C, and lower on Day 5 at 29 °C than at 15 °C (Bonferroni: Day 2: $p = 0.031$, Day 5: $p < 0.001$ for both comparisons). Over the 5-day period at 15 °C, symbiont density remained stable in *P. heronensis* (Figure 2.4 A) but significantly decreased in *A. yongei*, *Stylophora* sp., and *P. damicornis* (Figure 2.4 B – D, Tables 2.4, 2.5). *A. yongei* eventually lost 36% of its symbionts after 5 days ($p = 0.012$). *Stylophora* sp. showed the strongest effect, with its symbiont density reduced by 68% (Day 5 *versus* 0), while *P. damicornis* lost 59% of its symbionts. In these three coral species, the decline in symbiont density resulted in significantly lower values on Day 5 at 15 °C than at 22 °C or 29 °C ($p \leq 0.02$ for both comparisons in all three coral species) (Figure 2.4 B – D).

2.3.5 Photosynthetic pigments

On Day 0, the concentration (mean ± S.E.) of photosynthetic pigments (PSP, pool of chl *a*, chl c_2, peridinin) was 18.0 ± 1.10 pg cell^{-1} in *Symbiodinium* C111* hosted by *P heronensis*, 11.5 ± 0.64 pg cell^{-1} in C3/C111* hosted by *A. yongei*, 7.5 ± 0.27 pg cell^{-1} in C118 hosted by *Stylophora* sp. and 9.2 ± 0.34 pg cell^{-1} in C100/C118 hosted by *P. damicornis* (Figure 2.4 E – H). The concentration in *Symbiodinium* C111* in *P. heronensis* was significantly higher than for the other *Symbiodinium* types/associations (Tukey HSD: $p < 0.001$).

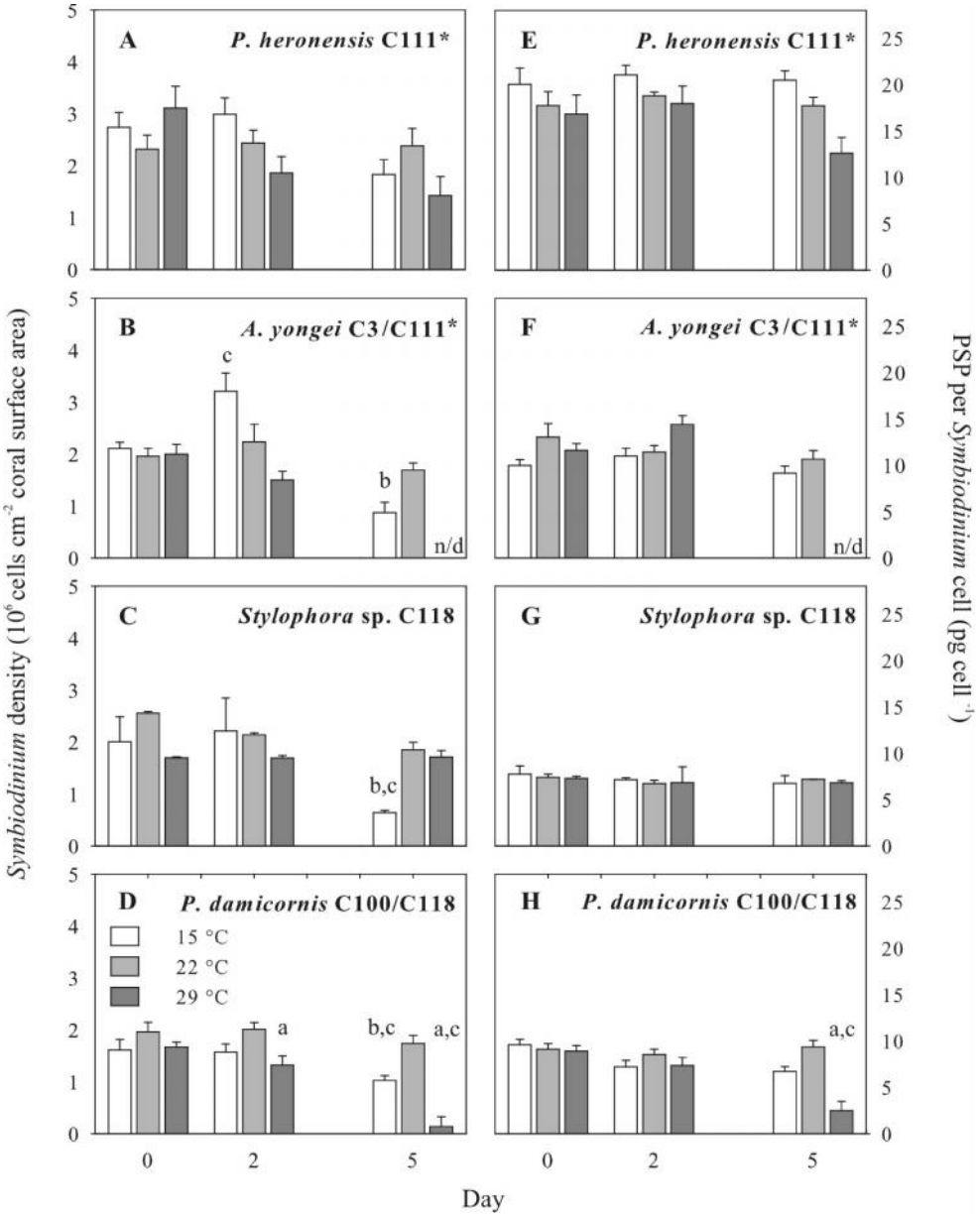

Figure 2.4: *Symbiodinium* cell density in million cells per cm^2 coral surface area (**A – D**) and pool of photosynthetic pigments (PSP, comprising chl *a*, chl c_2, and peridinin) (**E – H**) in pg $cell^{-1}$ for *Porites heronensis* hosting *Symbiodinium* C111* (**A, E**), *Acropora yongei* hosting C3/C111* (**B, F**), *Stylophora* sp. hosting C118 (**C, G**), and *Pocillopora damicornis* hosting C100/C118 (**D, H**). Presented are mean values ± S.E., n = 2 – 8. Significant differences are reported for (a) 22 °C and 29 °C, (b) 22 °C and 15 °C, and (c) 15 °C and 29 °C ($p \leq 0.05$; rmANOVA and pairwise *post hoc* comparison with Bonferroni correction). n/d no data available due to death of the explants.

Over the 5-day period at 22 °C, the PSP pool-size was stable in all *Symbiodinium* types (Figure 2.4 E – H). No significant differences were observed between coral species and their symbionts (Table 2.5). Over 5 days at 29 °C, the overall PSP pool-size remained relatively constant in *Symbiodinium* cells in *P. heronensis*, *A. yongei* and *Stylophora* sp. (Figure 2.4 E – G), though of note, the chl *a* pool-size in C111* hosted by *P. heronensis* declined by 25.3% ($p < 0.001$, mean Day 5 *versus* 0, Table 2.6). In contrast, the PSP pool-size significantly declined in C100/C118 in *P. damicornis* (Figure 2.4 H, Tables 2.5, 2.6), and by Day 5 at 29 °C it was significantly lower than at both 22 °C (Bonferroni: $p = 0.004$) and 15 °C ($p = 0.022$). This decline was associated with a 74.4% loss of chl *a*, 73.3% loss of chl c_2 and 53% loss of peridinin across the 5-day period (Table 2.6). Over 5 days at 15 °C, the PSP pool-size and concentrations of all major photosynthetic pigments were more or less stable in all *Symbiodinium* types (Figure 2.4 E – H, Table 2.6).

2.3.6 Xanthophyll de-epoxidation and β-carotene

On Day 0, xanthophyll de-epoxidation (dtn/dtn+ddn) was 0.25 ± 0.015 (mean ± S.E.) in *Symbiodinium* C111* hosted by *P. heronensis*, 0.27 ± 0.016 in C3/C111* hosted by *A. yongei*, 0.25 ± 0.025 in C118 hosted by *Stylophora* sp. and 0.22 ± 0.013 in C100/C118 hosted by *P. damicornis* (Figure 2.5 A – D).

After 5 days at 29 °C, *Symbiodinium* C111* in *P. heronensis* and *Symbiodinium* C100/C118 in *P. damicornis* enhanced xanthophyll de-epoxidation to 0.43 ± 0.021 and 0.55 ± 0.030, respectively (Figure 2.5 A, D), resulting in a significantly higher rate of xanthophyll de-epoxidation on Day 5 compared to 22 °C and 15 °C (Bonferroni: $p < 0.001$ for both comparisons). C3/C111* in *A. yongei* (Figure 2.5 B) and C118 in *Stylophora* sp. (Figure 2.5 C, Table 2.4) showed no significant increase of xanthophyll de-epoxidation over time in any of the temperature treatments. Over 5 days at 15 °C, *Symbiodinium* C111* in *P. heronensis* was the only type that significantly increased xanthophyll de-epoxidation (Figure 2.5 A), with the rate of xanthophyll de-epoxidation being comparable to that at 29 °C but significantly higher ($p < 0.001$) than that at 22 °C after 5 days (Table 2.4).

Table 2.6: Concentration of light-harvesting pigments chlorophyll *a (*chl *a)*, chlorophyll c_2 (chl c_2), peridinin (pg cell^{-1}) on Days 0, 2 and 5 of the temperature treatment for *Symbiodinium* C111* in *Porites heronensis* (Ph), C3/C111* in *Acropora yongei* (Ay), C118 in *Stylophora* sp. (S) and C100/C118 in *Pocillopora damicornis* (Pd). Significant differences ($p \leq 0.05$) from values at 15 °C ([a]), 22 °C ([b]) and 29 °C ([c]), based on rmANOVA analysis with *post hoc* Bonferroni corrected pairwise comparison, are highlighted in bold.

		chl *a*			**chl c_2**			**peridinin**		
		0	**2**	**5**	**0**	**2**	**5**	**0**	**2**	**5**
Ph	**15 °C**	11.0 ± 0.9	11.3 ± 0.6	11.3 ± 0.4	2.7 ± 0.2	2.8 ± 0.1	2.6 ± 0.3	6.4 ± 0.7	6.9 ± 0.4	6.5 ± 0.4
C111*	**22 °C**	9.8 ± 0.9	10.2 ± 0.2	9.6 ± 0.4	2.3 ± 1.2	2.5 ± 0.1	2.4 ± 0.2	5.7 ± 0.5	6.1 ± 0.2	5.7 ± 0.4
	29 °C	9.1 ± 1.1	9.8 ± 1.0	**6.8 ± 1.0** [a, b]	2.3 ± 0.3	2.4 ± 0.3	1.6 ± 0.3	5.5 ± 0.6	5.8 ± 0.6	4.2 ± 0.5
Ay	**15 °C**	5.8 ± 0.4	6.5 ± 0.5	5.3 ± 0.4	1.3 ± 0.1	1.5 ± 0.1	1.4 ± 0.2	3.0 ± 0.2	3.0 ± 0.2	2.5 ± 0.2
C3	**22 °C**	7.9 ± 0.9	6.5 ± 0.5	6.3 ± 0.6	1.6 ± 0.2	1.2 ± 0.1	1.4 ± 0.1	3.5 ± 0.4	3.2 ± 0.2	2.9 ± 0.3
C111*	**29 °C**	7.0 ± 0.6	8.6 ± 0.6	n/d	1.5 ± 0.1	2.0 ± 0.2	n/d	3.1 ± 0.2	3.8 ± 0.2	n/d
S	**15 °C**	4.6 ± 0.5	4.2 ± 0.1	3.9 ± 0.5	1.2 ± 0.2	1.0 ± 0.1	1.0 ± 0.1	2.0 ± 0.3	1.9 ± 0.1	1.8 ± 0.3
C118	**22 °C**	4.4 ± 0.2	3.8 ± 0.3	4.2 ± 0.1	1.1 ± 0.1	1.0 ± 0.1	1.1 ± 0.1	1.9 ± 0.1	1.9 ± 0.0	1.9 ± 0.1
	29 °C	4.4 ± 0.1	3.8 ± 1.2	4.0 ± 0.2	1.0 ± 0.0	1.2 ± 0.1	1.0 ± 0.0	1.9 ± 0.1	1.9 ± 0.4	1.8 ± 0.1
Pd	**15 °C**	5.2 ± 0.4	3.9 ± 0.4	3.5 ± 0.3	1.5 ± 0.1	1.2 ± 0.1	1.2 ± 0.1	2.9 ± 0.2	2.1 ± 0.2	2.0 ± 0.2
C100	**22 °C**	5.0 ± 0.4	4.7 ± 0.3	5.0 ± 0.3	1.3 ± 0.1	1.5 ± 0.1	1.5 ± 0.2	2.8 ± 0.2	2.4 ± 0.1	2.8 ± 0.2
C118	**29 °C**	4.7 ± 0.4	3.9 ± 0.5	**1.2 ± 0.5** [a, b]	1.5 ± 0.1	1.3 ± 0.1	**0.4 ± 0.1** [a ,b]	2.7 ± 0.2	2.2 ± 0.3	**1.3 ± 0.5** [a, b]

Xanthophyll pool size relative to chl *a* ((dtn+ddn)/chl *a*) was fairly constant between species and remained comparatively constant in all corals at all temperatures except for *P. damicornis* (Table 2.7). After two days exposure to 29 °C *Symbiodinium* C100/C118 hosted by *P. damicornis* had a significantly lower pool-size of xanthophylls compared to 15 °C ($p = 0.042$) but not 22 °C (Table 2.7). However, the concentration of diatoxanthin relative to chl *a* (dtn/chl *a*) increased over time in *P. heronensis* at 15 °C and 29 °C, and in *P. damicornis* at 29 °C (Figure 2.5 F, I, Table 2.4).

β-carotene concentration relative to chl *a* did not vary over time in any coral species (Table 2.7). *P. heronensis* had the highest concentration of β-carotene relative to chl *a*, which was considerably higher than in any other coral association on Day 0 (Tukey HSD: $p \leq 0.026$).

2.3.7 Excitation pressure over PSII

On Day 0, excitation pressure (Q_m) averaged 0.38 ± 0.04 (mean ± S.E.) in *P. heronensis*, 0.34 ± 0.03 in *A.yongei*, 0.51 ± 0.03 in *Stylophora* sp. and 0.42 ± 0.01 in *P. damicornis* (Figure 2.5 J – M).

The temporal response at a given temperature treatment was distinct between corals (significant Time × Temperature × Species interaction, Tables 2.3, 2.4). Over 5 days at 29 °C or 15 °C, all corals except *Stylophora* sp. showed a significantly different temporal response than at 22 °C (Figure 2.5 J – M, Table 2.4). Compared to 22 °C, Q_m at 29 °C was higher in *A. yongei* (Bonferroni: $p = 0.01$) and *P. damicornis* ($p = 0.004$) on Day 2, and higher in *P. heronensis* ($p = 0.047$), and *P. damicornis* ($p < 0.001$) on Day 5. In the latter species, Q_m at 29 °C was also higher than at 15 °C ($p < 0.001$). Compared to 22 °C, Q_m at 15 °C was higher in *P. heronensis* ($p = 0.01$), *A. yongei* ($p = 0.006$) and *P. damicornis* ($p = 0.001$) on Day 2. By Day 5, Q_m at 15 °C remained significantly higher in *A. yongei* and *P. damicornis* ($p < 0.001$) but not in *P. heronensis*.

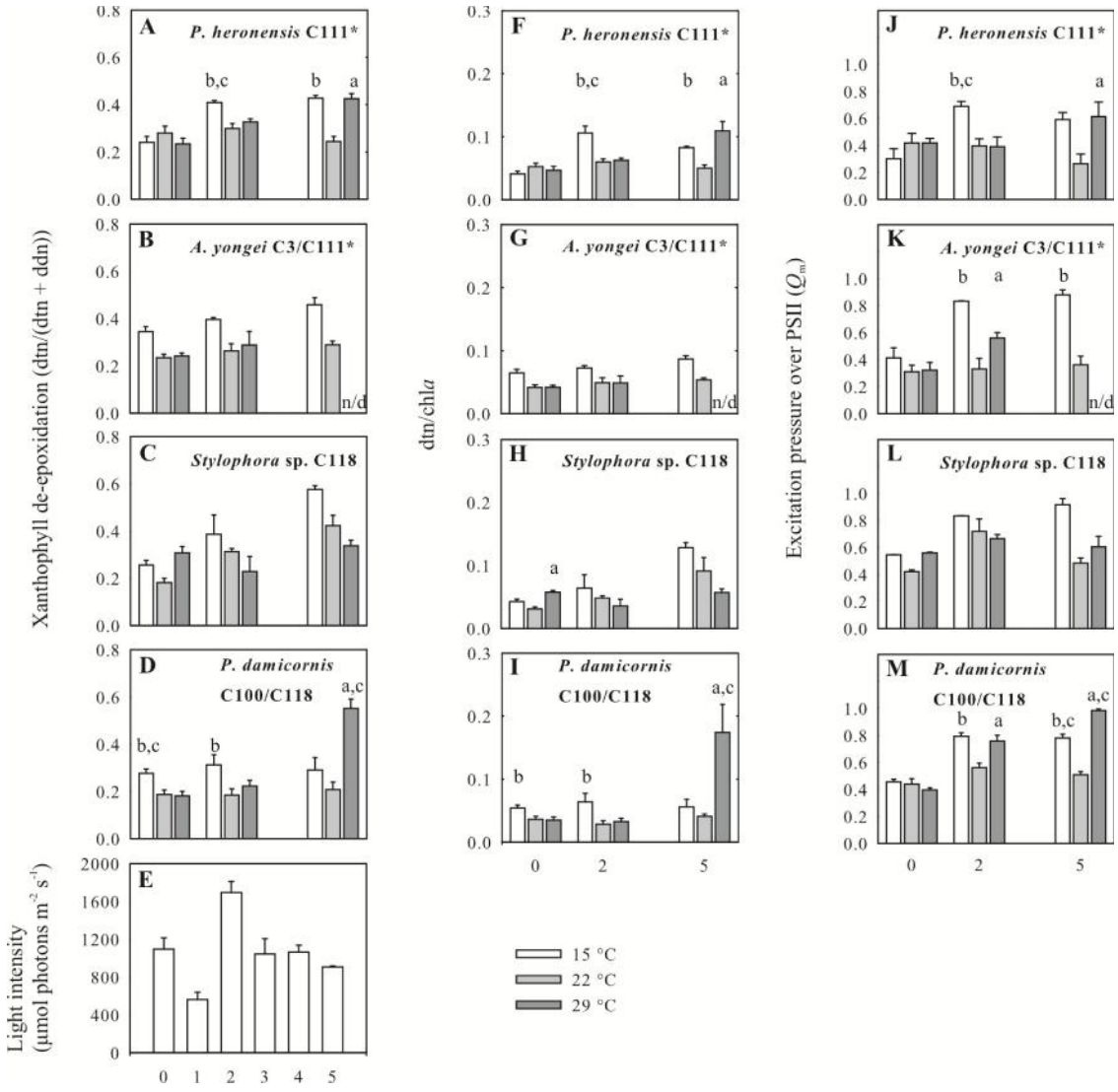

Figure 2.5: Xanthophyll de-epoxidation (**A – D**), light intensity at noon during chlorophyll fluorescence measurement (**E**), concentration of diatoxanthin per chlorophyll *a* (dtn/chl *a*) (**F – I**) and excitation pressure over PSII, Q_m (**J – M**) over a 5-day period in *Porites heronensis* hosting *Symbiodinium* C111* (**A, F, J**), *Acropora yongei* hosting C3/C111* (**B, G, K**), *Stylophora* sp. hosting C118 (**C, H, L**) and *Pocillopora damicornis* hosting C100/C118 (**D, I, M**). Light intensities are mean values ± S.E. between 12:00 h and 13:00 h. All other values are mean ± S.E., n = 2 – 8. Significant differences are reported for (a) 22 °C and 29 °C, (b) 22 °C and 15 °C, and (c) 15 °C and 29 °C at the level of $p \leq 0.05$ (rmANOVA and *post hoc* pairwise comparison with Bonferroni correction).

Table 2.7: Concentration of photoprotective pigments β – carotene/chl *a*, and the xanthophylls diadinoxanthin (ddn) and diatoxanthin (dtn)/chl *a* on Days 0, 2, and 5 of the temperature treatment for *Symbiodinium* C111* in *Porites heronensis* (Ph), C3/C111* in *Acropora yongei* (Ay), C118 in *Stylophora* sp. (S) and C100/C118 in *Pocillopora damicornis* (Pd). Significant differences ($p \leq 0.05$) from values at 15 °C ([a]), 22 °C ([b]) and 29 °C ([c]), based on rmANOVA analysis with *post hoc* Bonferroni corrected pairwise comparison, are highlighted in bold.

		β – carotene/chl *a*			**(ddn + dtn)/chl *a***		
		0	**2**	**5**	**0**	**2**	**5**
Ph	**15 °C**	0.057 ± 0.002	0.062 ± 0.004	0.048 ± 0.004	0.17 ± 0.003	0.21 ± 0.002	0.19 ± 0.003
C111*	**22 °C**	0.075 ± 0.017	0.057 ± 0.004	0.060 ± 0.001	0.19 ± 0.002	0.20 ± 0.005	0.20 ± 0.005
	29 °C	0.060 ± 0.002	0.054 ± 0.003	0.093 ± 0.031	0.20 ± 0.007	0.19 ± 0.005	0.26 ± 0.043
Ay	**15 °C**	0.033 ± 0.008	0.045 ± 0.004	0.033 ± 0.008	0.19 ± 0.005	0.18 ± 0.006	0.19 ± 0.004
C3	**22 °C**	0.044 ± 0.001	0.039 ± 0.004	0.025 ± 0.007	0.18 ± 0.010	0.18 ± 0.013	0.18 ± 0.006
C111*	**29 °C**	0.034 ± 0.007	0.048 ± 0.004	n/d	0.17 ± 0.007	0.17 ± 0.006	n/d
S	**15 °C**	0.043 ± 0.000	0.034 ± 0.001	0.043 ± 0.003	0.17 ± 0.003	0.16 ± 0.020	0.20 ± 0.008
C118	**22 °C**	0.041 ± 0.001	0.031 ± 0.003	0.046 ± 0.004	0.17 ± 0.002	0.15 ± 0.004	0.21 ± 0.029
	29 °C	0.041 ± 0.013	0.021 ± 0.007	0.038 ± 0.005	0.19 ± 0.007	0.15 ± 0.005	0.17 ± 0.005
Pd	**15 °C**	0.040 ± 0.007	0.033 ± 0.009	0.026 ± 0.006	0.19 ± 0.007	0.19 ± 0.016	0.18 ± 0.014
C100	**22 °C**	0.045 ± 0.003	0.028 ± 0.007	0.038 ± 0.007	0.19 ± 0.012	0.15 ± 0.010	0.19 ± 0.010
C118	**29 °C**	0.038 ± 0.006	0.025 ± 0.006	0.031 ± 0.013	0.18 ± 0.009	**0.14 ± 0.008** [a]	0.30 ± 0.063

2.4 Discussion

2.4.1 Lord Howe corals exhibit highly variable responses to thermal stress

High latitude corals might be better able to withstand variability in their thermal environments on account of the broader range of temperatures that they experience over the course of the year (Cook et al. 1990; Wicks et al. 2010b). In addition to prevailing cooler and variable sea temperatures at high latitudes, light penetration is seasonally lower and annually more variable compared to tropical sites (Kleypas et al. 1999). Therefore, the plasticity of light-harvesting and photoprotective parameters might be key parameters to understand the ability of corals to deal with environmental change at these sites. The present study revealed that corals at the high latitude coral reef of Lord Howe Island (LHI) exhibit highly variable responses to short-term heat stress (~ 5 °C above the annual monthly mean temperature maximum (MMM) of 24 °C, ~ 4 °C above the temperature at which heat-stress is accumulated by Coral Watch at www.coralreefwatch.noaa.gov) and short-term cold stress (~ 3 °C below the annual monthly mean temperature minimum of 18 °C). *Porites heronensis* hosting *Symbiodinium* C111* showed similar bleaching and photophysiological responses to cold and heat stress. *Pocillopora damicornis* hosting *Symbiodinium* C100/C118 bleached less severely when exposed to cold stress compared to heat stress. *Stylophora* sp. hosting *Symbiodinium* C118 bleached under cold stress but not under heat stress. Interestingly, A*cropora yongei* died at the highest temperature, without prior bleaching or losses of maximum PSII efficiency in their symbionts, providing an important reminder that the host itself can be more susceptible to thermal stress than its symbionts (Ainsworth et al. 2008; Dunn et al. 2012). Given that *P. heronensis* and *A. yongei*, as well as *P. damicornis* and *Stylophora* sp. shared the same *Symbiodinium* ITS2 type, the observed variability of responses demonstrates that resilience to bleaching or mortality is not determined by symbiont type alone. Although heat susceptible *A. yongei* but not bleaching tolerant *P. heronensis* host *Symbiodinium* type C3, this *Symbiodinium* type does not determine susceptibility as photochemical efficiency and chlorophyll concentrations remained unchanged. Furthermore, bleaching resistance and maintenance of PSII photochemistry

were not consistently associated with enhanced levels of β-carotene and/or xanthophylls and/or enhanced use of xanthophyll de-epoxidation in *Symbiodinium* cells, agreeing with the findings of Venn et al. (2006). Collectively, the results demonstrate that the resilience of a coral to thermal stress is not determined by symbiont type alone or symbiont properties such as the capacity for xanthophyll de-epoxidation.

2.4.2 Mode of bleaching

Although coral bleaching varied in intensity, a similar mode of bleaching across species and temperatures was observed: symbiotic cells were expelled before a significant reduction in the total pool of photosynthetic pigments per cell could be observed. This results agree with earlier findings of symbiont loss due to cold stress (e.g Steen and Muscatine 1987; Saxby et al. 2003; Roth et al. 2012) and heat stress (e.g. Hoegh-Guldberg and Smith 1989), but contrast findings in heat-stressed *Acropora digitifera* or *Montipora monasteriata* that reduced its cell-specific pigment concentration but not its *Symbiodinium* cell density (Takahashi et al. 2004; Dove et al. 2006). Symbiont densities declined in response to cold stress in *A. yongei* and *Stylophora* sp. without concurrent pigment reduction in their symbionts C111*, C3, and C118. In contrast, the mixed population of C100/C118 in *P. damicornis* dramatically reduced cell numbers as well as concentrations of all major photosynthetic pigments when exposed to short-term heat stress and, to a lesser degree, when exposed to short-term cold stress (see Figure 2.4 and Figure 2.6 for summary). Thermally-induced concurrent loss of cells and pigments has been described before (Kleppel et al. 1989) and might exacerbate the process of bleaching that was observed in *P. damicornis*: the reduction of cells and pigments increases light scattering from the underlying coral skeleton, and enhances the internal light intensity (Enríquez et al. 2005).

2.4.3 Chlorophyll fluorescence and photoprotection

Although it has been shown that symbionts expelled from *P. damicornis* due to manipulative thermal stress can be fully photosynthetically functional (Ralph et al. 2001), a decline in photosynthetic performance in remaining symbionts, which can be estimated by chlorophyll fluorescence of PSII, has been shown to associate with coral bleaching

(Hoegh-Guldberg 1999). In this study, in both pocilloporid corals as well as in surviving *A. yongei*, the loss of symbiotic cells was accompanied by a pronounced decline in maximum quantum efficiency of PSII (F_v/F_m). At 29 °C, *P. damicornis* showed the fastest and steepest decline. *P. heronensis* decreased F_v/F_m to a lesser extent and *Stylophora* sp. (over 5 days) and *A. yongei* (over 2 days) maintained F_v/F_m at a level comparable to the control. At 15 °C, *Stylophora* sp. showed a faster and steeper decline compared to *A. yongei*, *P. damicornis* and *P. heronensis*. The underlying cause of the decline of F_v/F_m cannot be decoded with the methods employed in this study. Possible underlying causes are (1) enhanced diatoxanthin (dtn) accumulation and thermal dissipation which might be sustained in the dark by a trans-thylakoidal ΔpH gradient generated by chlororespiration, which may operate in *Symbiodinium* (Hill and Ralph 2005; Reynolds et al. 2008); and/or (2) the inactivation of PSII reaction centres likely coupled with reactive oxygen species (ROS)-mediated inhibition of their repair and the inability to transfer electrons past PSII (Tyystjärvi 2008; Takahashi and Badger 2011).

I estimated the need for photoprotection by calculating the excitation pressure over PSII (Q_m), a parameter that depends on photochemical and non-photochemical quenching processes. In this study, all corals with the exception of *Stylophora* sp. had higher Q_m values at 29 °C and 15 °C compared to the control temperature (see Figure 2.6 for summary). The increase of Q_m was due to a decrease in the effective quantum yield ($\Delta F/F_m'$) at peak solar radiation, which has been described in previous studies (Gorbunov et al. 2001; Warner and Berry-Lowe 2006). *Stylophora* sp. showed a temperature-independent increase in Q_m, indicating an increased quenching under high light that was not exacerbated by thermal stress. In previous studies, the drop in $\Delta F/F_m'$ at noon has been associated with increased NPQ associated with xanthophyll de-epoxidation (Brown et al. 1999; Warner and Berry-Lowe 2006). Further, in diadinoxanthin/diatoxanthin (ddn/dtn) containing algae, NPQ associated with thermal dissipation is directly correlated with the concentration of dtn (Goss and Jakob 2010). In this study, only *P. heronensis* consistently increased xanthophyll de-epoxidation and dtn/chl *a* with Q_m at both 15 °C and 29 °C (Figures 2.5, 2.6), perhaps demonstrating that at both temperatures NPQ is efficiently activated through xanthophyll de-epoxidation. *P. damicornis* enhanced xanthophyll de-epoxidation, dtn/chl *a* and Q_m at 29 °C. In contrast, at 15 °C, Q_m but not

xanthophyll de-epoxidation or dtn/chl *a* was increased over time in *P. damicornis* and *A. yongei*, suggesting that at low temperatures alternative quenching mechanisms are activated in these species. These may include reaction centre inactivation due to PSII core rearrangement or degradation.

The excitation pressure of PSII is affected by NPQ mechanisms such as thermal dissipation and by the rate at which reducing equivalents are consumed downstream of PSII (Ort and Baker 2002). The latter is affected by the availability of electron sinks such as CO_2 and O_2 (Badger et al. 2000; Ort and Baker 2002). At high temperatures, the affinity of Rubisco for CO_2 decreases due to changed kinetic properties of the enzyme, and in these conditions the electron pressure over PSII may be reduced by: (1) the reduction of O_2 by the Mehler reaction which generates O_2^- and other ROS in subsequent reduction processes as part of the water-water-cycle (Asada 1999); or (2) the reduction of O_2 in the photorespiratory pathway (Ort and Baker 2002). Ribulose-1,5-bisphosphate carboxylase oxygenase (rubisco) catalyzes the initial oxygenation in the photorespiratory cycle and its efficiency is temperature-dependent: while high temperatures decrease the affinity of Rubisco for CO_2 and increase the affinity for O_2, low temperatures lead to a decreased affinity for both CO_2 and O_2 uptake. Hence, at low temperatures the water-water-cycle might become more important for photoprotection than photorespiration (Ort and Baker 2002). Although the present study does not provide evidence, the potential saturation of the water-water-cycle and/or the photorespiratory pathway might have influenced the dtn-independent increase of Q_m that was observed in *A. yongei* and *P. damicornis* at low temperature. With ongoing cold stress the expected quantitative increase of the water-water-cycle could have resulted in an imbalance of ROS and detoxifying enzymes, which may have caused inhibition of the repair of photodamaged PSII reaction centres (Takahashi and Badger 2011) and consequently decreased the linear electron transport rate. In this case, cyclic electron flow (CEF) would have become more important for maintaining ATP production (Rumeau et al. 2007). Since both the water-water-cycle and CEF result in an increased acidification of the thylakoid lumen (Rumeau et al. 2007; Foyer et al. 2012), it is intriguing that in *A.yongei* and in *P. damicornis* a significant dtn accumulation was absent at decreased temperatures. Because even a weak change in pH can activate diadinoxanthin de-epoxidase (DDE) and because a trans-

thylakoid proton gradient inhibits diatoxanthin epoxidase (DEP), this observation may be due to a lack of reduced ascorbate, a co-substrate required by DDE, or type-specific differences in the sensitivity of enzyme activation in *Symbiodinium*. Similar observations have been reported for diatoms, where DDE is activated at a thylakoidal pH of between 5.5 and 7.2 (Goss and Jakob 2010).

Compared to other species, *P. heronensis* and its symbionts had a higher baseline concentration of β-carotene relative to chlorophyll *a*. This might contribute to the observed bleaching resistance to both cold and heat stress in this species because in marine organisms β-carotene is one of the major antioxidants responsible for the quenching of singlet oxygen ($^1O_2$). Removal of excessive $^1O_2$ by β-carotene might suppress ROS-mediated inhibition of protein synthesis, as has been proposed for α-tocopherol, and promote the repair of reaction centres (Murata et al. 2012).

2.4.4 Ecological significance

A. yongei was the most susceptible coral to increased temperature in this experiment, exhibiting host mortality without concurrent loss of symbionts, symbiont-specific pigments or photochemical efficiency, demonstrating that in some instances the host can be the more susceptible partner to thermal stress. Among corals that showed no mortality, *P. damicornis* was the most bleaching susceptible at increased temperature, corroborating field observations that showed that Pocilloporidae were among the more bleaching-susceptible corals during the LHI coral bleaching event of March 2010, when seawater temperatures exceeded 27 °C (Harrison et al. 2011). A reduced cover of branching species such as *P. damicornis* in favour of massive species such as *Porites* species has been observed at LHI between 1979 (Veron and Done 1979) and 1995 (Harriott et al. 1995). In light of ongoing climate change, a continuing shift towards sub-massive and massive coral communities has been projected by Dalton and Carroll (2011) for high latitude coral reefs based on coral bleaching monitoring, and the present experimental data (high mortality in *A. yongei* and high bleaching susceptibility in *P. damicornis*, and low bleaching susceptibility in *P. heronensis*) corroborate this prediction. Elucidating the mechanisms in and between the host and symbiont partners that underlie this trend is clearly an area of importance and should be the focus of future work.

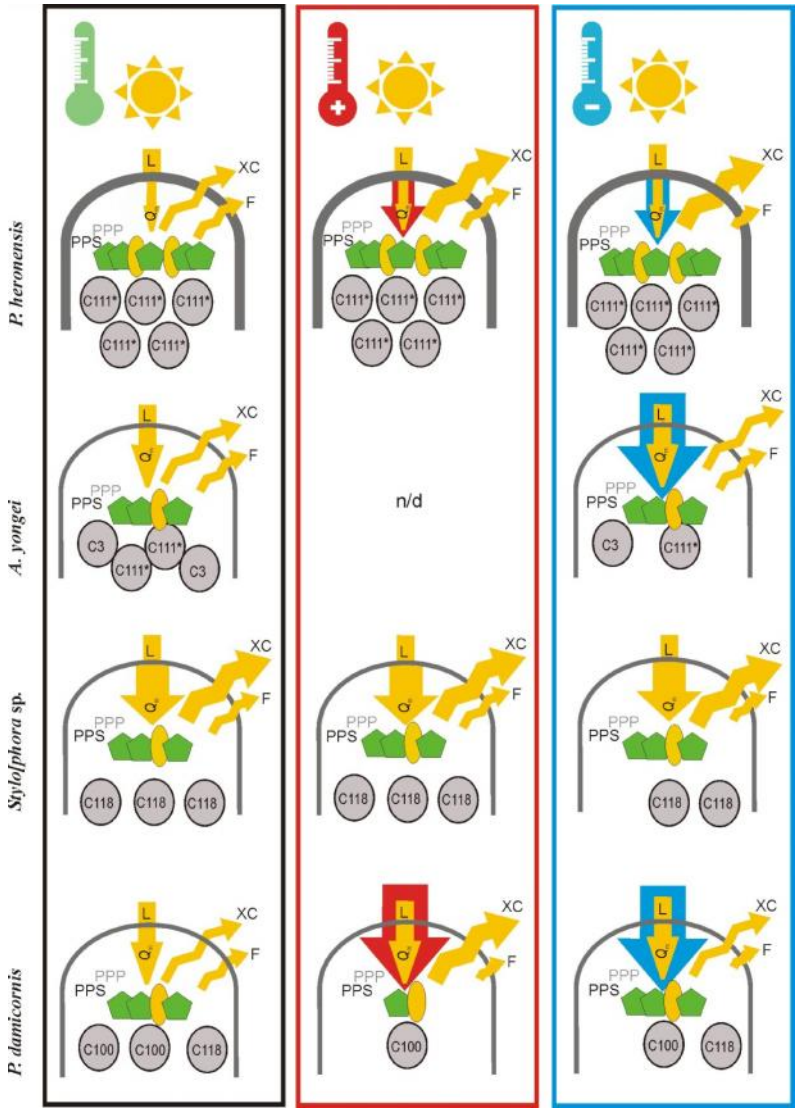

Figure 2.6: Schematic model of cellular properties of the four studied coral-*Symbiodinium* associations at ambient temperature (left panel), and their responses to elevated temperature (middle panel) and decreased temperature (right panel) under conditions of high light illumination. Shown is the estimated relative thickness of the host tissue (dome), density of *Symbiodinium* cells (ovals with denoted ITS2 types), light-harvesting pigments (pentagons, PPS) and photoprotective pigments including β-carotene (ovals, PPP). The size of the straight arrows indicates the intensity of light (L) and the hypothetical electron pressure over the photosystem (Q_m). In general, excessively high or low temperatures increase the electron pressure (indicated by yellow arrows) and the demand for photoprotection, e.g. the dissipation of excess energy as heat via xanthophyll de-epoxidation (indicated by zigzag backscattering arrows, XDE). Size of the zigzag arrows corresponds to degree of de-epoxidation of the xanthophyll pool.

Chapter 3:
Thylakoid fatty acid composition and response to short-term cold and heat stress differs in high latitude *Symbiodinium* spp.

3.1 Introduction

Fatty acids (FAs) are basic constituents of biological membranes. In the thylakoids of higher plants and algae, the FA quality of their membranes affects numerous cellular processes, such as membrane fluidity, light harvesting, electron transport, ion barrier function and the function or turnover of thylakoid membrane-associated proteins (Mullineaux and Kirchhoff 2010). As such, FA composition is expected to influence light-driven processes of photosynthesis. Higher plants and photosynthetic microorganisms have the capability to adjust membrane lipid composition in response to environmental changes (Iba 2002; Morgan-Kiss et al. 2006). These adjustments can be complex and include the level of FA unsaturation, chain length or branching (Iba 2002; Morgan-Kiss et al. 2006). Responses to thermal stress may primarily modulate the fluidity of the thylakoid lipid bilayer, which is necessary to maintain the performance of all membrane-associated processes. In dinoflagellates of the genus *Symbiodinium* (Freudenthal), which are associated with a number of ecologically important marine organisms such as reef corals and sea anemones, acclimation to high temperatures seems to be associated with adjustments in the thermal stability of photosynthetic membranes (Hill et al. 2009). Furthermore, robustness or sensitivity of photosynthetic membranes to high temperatures, as defined by thylakoid integrity, photochemical function, and production of reactive oxygen species (ROS) in the chloroplast, has been linked to the level of FA unsaturation in the microalgae (Tchernov et al. 2004). However, it is controversial whether FA composition could be generally diagnostic of thermally-robust *Symbiodinium* cells (Díaz-Almeyda et al. 2011). Baseline studies of FA composition exist for a few *Symbiodinium* types (Bishop and Kenrick 1980; Mansour et al. 1999; Zhukova and Titlyanov 2003; Awai et al. 2012). Changes in total FA composition have been

monitored in the coral *Montipora digitata* and its dinoflagellate symbionts in response to elevated temperatures (Papina et al. 2007) and the composition of photosynthetic membranes has been studied in *Symbiodinium* cultures grown at different temperatures (Díaz-Almeyda et al. 2011). Yet, the ability of thylakoid membrane FAs to adjust to sub- and super-optimal temperatures has not been investigated in *Symbiodinium* spp. *in hospite* (i.e. inside the host) across a range of hosts.

The mutualistic association of *Symbiodinium* spp. and their animal hosts is widespread and important in marine habitats, but the symbiosis is very sensitive to environmental perturbations (Brown 1997; Muller-Parker and D'Elia 1997). It is well recognized that changes in temperature, often associated with high light intensities, can lead to cellular changes in both symbiosis partners that can include losses of *Symbiodinium* cells or losses of pigments from within the symbionts (Falkowski and Dubinsky 1981; Hoegh-Guldberg 1999). This response is known as coral bleaching and has gained notoriety during the last few decades because of an increased frequency of episodes of mass coral bleaching. Mass bleaching and mortality of reef-building (scleractinian) corals and other symbiotic associations on vast geographic scales are largely driven by thermal anomalies associated with global warming, which result in significant declines of the important coral reef ecosystem (Hoegh-Guldberg and Bruno 2010). Although the emphasis has been placed on the adverse effects of high temperature anomalies, cold temperature anomalies and associated coral bleaching and mortality have been reported from numerous reef systems (Hoegh-Guldberg and Fine 2004; LaJeunesse et al. 2010; Kemp et al. 2011).

The effects of temperature on biochemical, cellular and physiological processes in algal and animal cells are manifold and complex, and the initiation or sequence of mechanisms underlying coral bleaching is poorly understood. Frequently, bleaching is associated with a decline of photosynthetic function and carbon fixation in *Symbiodinium* (Porter et al. 1989; Iglesias-Prieto et al. 1992; Jones et al. 1998). The uncoupling of light harvesting and photochemistry resulting from changes in thylakoid membrane fluidity might result in suppressed NADPH and ATP synthesis and concomitant increased production of ROS (Tchernov et al. 2004) which are thought to play a central role in

coral bleaching (Smith et al. 2005; Suggett et al. 2008; Lesser 2011). ROS are cytotoxic compounds (Lesser 2006), which have been shown to inhibit protein translation and are involved in cell signalling processes that can induce mortality or expulsion of *Symbiodinium* cells (reviewed in Weis 2008).

The genus *Symbiodinium* is highly diverse with 9 distinct clades (A – I) currently recognized (Pochon and Gates 2010), each of which is represented by a number of genetically distinct types (Baker 2003) that can be distinguished using the fast evolving internal transcribed spacer 2 (ITS2) region of the ribosomal DNA (LaJeunesse 2001). Genetic differences in *Symbiodinium* types are reflected by differences in cellular constitution and physiological capabilities (Hennige et al. 2009; Takahashi et al. 2009; Ragni et al. 2010) which have been linked to differential bleaching responses of the coral-*Symbiodinium* association (Berkelmans and van Oppen 2006; Sampayo et al. 2008). *Symbiodinium* ITS2 types C111* and C100/C118 seem to be endemic to the high latitude coral reef of Lord Howe Island (LHI; 31°33′S, 159°05′E), New South Wales, Australia. They have been found to associate with the corals *Porites heronensis* (C111*) and *Pocillopora damicornis* (C100/C118), respectively (Chapter 2; Wicks et al. 2010a; Wicks et al. 2010b). These high latitude coral-*Symbiodinium* associations are ideal models to study the effects of both low- and high-temperature stress because sea surface temperature minima as low as 14.5 °C and maxima as high as 28 °C have been recorded in the past 10 years (www.data.aims.gov.au) at this high latitude coral reef site.

The primary objective of this study was to compare the composition of thylakoid fatty acids in *Symbiodinium* cells C100/C118 (bleaching susceptible, see Chapter 2) and C111* (bleaching tolerant, see Chapter 2) harbored in the two coral species *P. damicornis* and *P. heronensis*, respectively, before and after exposure to short-term heat and cold stress, and thereby determine the link between thylakoid fatty acid composition and physiological performance, estimated as chlorophyll fluorescence of PSII, under thermal stress.

3.2 Materials and methods

3.2.1 Sampling and experimental procedure

In March 2011, three coral fragments with a size of approximately 10 cm (branching coral) or 10 cm^2 (massive coral) each, were sampled from each of four colonies of *Pocillopora damicornis* and *Porites heronensis* from the lagoon site of Sylphs Hole, and from each of four colonies of *P. damicornis* from the lagoon site of Stephens Hole (Table 3.1). Sylphs Hole differs from Stephens Hole in that turbidity is approximately 1.8 fold higher (Wicks et al. 2010a). *P. damicornis* was chosen from these two locations to analyze if different environmental parameters have an effect on thylakoid lipid composition in this species. All fragments were taken from a depth of 0.5 – 3 m at low tide from the top of the colony to ensure that coral fragments had experienced the same light history. Immediately after sampling, fragments from each coral colony were divided to get a total of 16 coral explants of ~ 2 cm length each. One of the explants was preserved in NaCl-saturated 20% dimethyl sulfoxide (DMSO) buffer for subsequent genotyping. The remaining 15 explants (per coral colony) were maintained in aerated 50-L tanks which were supplied with unfiltered seawater from the lagoon, with a temperature of ~ 24 °C, at a flow rate of ~ 80 L per hour. Tanks were covered with shade cloth to reduce sunlight by ~ 50%. Corals were acclimatized to these conditions for four days. After acclimation, a third of the explants were each exposed to decreased temperature averaging 16 °C ± 0.1 (mean ± S.E.), control temperature averaging 24 °C ± 0.1, or elevated temperature averaging 28 °C ± 0.1, for a duration of 4 days. Light intensities peaked at ~ 1400, 1350, 1200, 1250, 1000 µmol photons m^{-2} s^{-1} on Days 0, 1, 2, 3, and 4, respectively. Decreased and elevated temperatures corresponded to 2 °C below the annual monthly mean temperature minimum and 4 °C above the annual monthly mean temperature maximum (MMM), respectively. Temperature and irradiance were monitored using a submersible HOBO pendant logger which was calibrated with a Li-Cor LI-189 photometer (Li-Cor, USA). Chilling/heating to the desired treatment temperature was begun at 06:00 h in the morning of Day 1. Treatment temperatures were attained on Day 1 at 16:40 h (16 °C) and 12:00 h (28 °C). The experiment was terminated at 19:00 h on Day 4. Between 14:00 h and 15:00 h on Days 0 and 4, two explants of each

coral colony were frozen in liquid nitrogen. Frozen coral explants were stored at -80 °C until analysis.

3.2.2 *Symbiodinium* genotyping

A subsample of preserved coral tissue was scraped off the coral skeleton using a sterile scalpel blade. The DMSO buffer was replaced with Tris buffer (0.01 M, pH 8.0) and ~ 50 mg of 710 – 1180 µm glass beads (Sigma, Australia) were added to the sample. *Symbiodinium* cells were lysed with a Tissue Lyser LT (Qiagen, Australia) bead mill for 10 min at 50 Hz at 4 °C. The cell debris was pelleted for 10 min at 16000 × g at 4 °C. A subsample of the cell lysate was mixed with an equal volume of isopropanol, inverted and spun for 30 min at 16000 × g at 4 °C. The DNA pellet was washed twice with 500 µL 70% ethanol, dried and re-suspended in 30 µL sterile water. *Symbiodinium* ITS2 was PCR-amplified using the primers itsD (Pochon et al. 2007) and ITS2CLAMP (LaJeunesse 2002) in a 12.5 µL PCR reaction using MyTaq^{TM} HS DNA Polymerase (Bioline, Australia) and the following conditions: an initial denaturation at 95 °C for 1 min, followed by 32 cycles at 95 °C for 15 s, 55 °C for 15 s, 72 °C for 15 s, and a final elongation at 72 °C for 7 min. Amplicons were separated using denaturing gradient gel electrophoresis (DGGE, Biorad DCode system) as described in detail in Chapter 2. The resulting DGGE fingerprints were compared to those from Chapter 2 and one – two dominant bands per coral-*Symbiodinium* association were re-amplified and sequenced in forward and reverse directions at Macrogen, South Korea, with the primer set ITSD and ITS2REVint (5′-CCATATGCTTAAGTTCAGCGGG-3′) to confirm the ITS2 identity.

3.2.3 Sample preparation

Frozen coral explants were airbrushed in TB buffer (100 mM Tris–HCl pH 8.0, 2 mM $MgCl_2$, 2 mM EDTA dissodium, 1 mM phenylmethyl sulfonyl fluoride) and the homogenates of two explants per colony and time-point were pooled for analysis. The combined homogenate was centrifuged at 800 × g for 5 min, and the algal pellet then re-suspended in TB buffer and centrifuged a further four times (same speed and duration) to clean the *Symbiodinium* cells of coral tissue. After the last step, pelleted *Symbiodinium* cells were re-suspended in 16 mL TB buffer. From this re-suspension, 11 mL were used

for cell lysis and enrichment of photosynthetic membranes, and the remainder of the homogenate was stored at -80 °C in five aliquots of 1 mL each.

3.2.4 Cell fractionation of photosynthetic membranes

Cell lysis and fractionation followed the protocol of Díaz-Almeyda et al. (2011), with the following modifications. Cells were broken by two repeated passes through a pressurized French Press Cell Disruptor (Thermo Electron Corporation) at 6.9 kPa. Preliminary experiments showed that less than 5% of cells remained unbroken after two passes, as determined by *Symbiodinium* cell counts using a haemocytometer. After low-speed centrifugation at 500 × g for 10 min to remove unbroken cells, the supernatant was pelleted by ultra-centrifugation at 50000 × g for 60 min at 4 °C in a Beckman Ultracentrifuge using a fixed 75 Ti Rotor. The cell pellet was re-suspended in 1 mL TB buffer, loaded onto a discontinuous sucrose gradient (5, 10, 15, 20%) and centrifuged at 50000 × g for 3 h at 4 °C to separate photosynthetic membranes. The pellet, containing the membranes, was re-suspended in 1 mL TB buffer and stored at -80 °C. Because thylakoids represent the large part of membranes in photosynthetic cells, the fraction is referred to as membranes enriched in thylakoids.

3.2.5 Lipid extraction and derivatization

Lipids of membranes enriched in thylakoids were extracted using the modified method of Folch et al. (1957). All solvents contained butylated hydroxytoluene (2, 6-Di-*tert*-butyl-4-methylphenol, BHT) in a final concentration of 0.002% to suppress autoxidation of unsaturated fatty acids (Díaz-Almeyda et al. 2011). At all times, crude extracts, lipid extracts and FAs were processed and stored under oxygen-free nitrogen.

Membranes enriched in thylakoids were freeze-dried under vacuum at -60 °C overnight. Lipids were extracted twice in a total volume of 4 mL dichloromethane (DCM, methylene chloride): methanol (2 : 1, v/v) for 18 h at 4 °C with gentle agitation of 25 rpm, in the presence of the internal standard C19:0 methyl ester (methyl nonadecanoate). Proteins were precipitated by addition of 800 µL 0.9% sodium chloride, resulting in phase separation. The organic phase containing the lipid fraction was

recovered and transferred to a glass tube. Solvents were evaporated in a 40 °C water bath under a stream of nitrogen. Fatty acid methyl esters (FAMEs) were synthesized by transesterification with 2% concentrated H_2SO_4 (sulfuric acid) in methanol : toluene (20 : 1, v/v) for 2 hours at 90 °C as described by Díaz-Almeyda et al. (2011). FAMEs were extracted with hexane : sodium chloride (5%) (2 : 1, v/v) for 15 h at -80 °C. Extracted FAMEs were stored under nitrogen at -20 °C before processing on a gas chromatography – mass spectrometer (GC–MS). Fatty acid methyl esters were analyzed on a gas chromatograph (Shimadzu, QP2010–Plus) fitted with a RTX – 5SilMS column (30 m x 0.25 mm i.d. x 0.25 µm film thickness) and attached to an electron impact mass spectrometer (operating at 70 eV in positive ion mode, scanning from *m/z* 40-600 every 0.3 s). Samples were introduced (1 µL) using an auto-sampler (AOC – 20i) with a split injection (20:1) at an injector temperature of 260 °C using He as the carrier gas at a linear velocity of 45.6 cm s^{-1} (1.58 mL min^{-1}) at constant flow. Each sample was injected with an initial oven temperature of 50 °C for 2 min, followed by a ramp at 4 °C min^{-1} to 190 °C, held for 10 min, followed by a second gradient of 3 °C min^{-1} to 240 °C. FAMEs were identified by comparison of both retention time and mass spectra with mixtures of known standards and were quantified by comparing the respective peak areas to the peak area of the internal standard (Díaz-Almeyda et al. 2011). The total lipid (TL) concentration was calculated from the sum of total FAMEs resolved, with the FAMEs presented as relative percentages of TL.

3.2.6 *Symbiodinium* cell density and chlorophyll concentration

Symbiodinium cell density was determined by six replicate counts with a haemocytometer and standardized to cells cm^{-2} coral surface area as determined using the paraffin wax method (Stimson and Kinzie 1991). Chlorophyll concentration was determined in 90% acetone. A cell suspension of 1 mL was pelleted at 16000 × g and 4 °C for 10 min, resuspended in 1 mL acetone and extracted for 24 h in the dark at 4 °C. Absorbance was measured in triplicates of 300 µL at A_{630} and A_{664} in 96 well plates (Greiner Bio-one, Germany) on an EnSpire™ 2300 Multilabel Reader (Perkin Elmer Inc., USA). Concentrations for chlorophyll *a* and chlorophyll c_2 were calculated using the

equation by Jeffrey and Humphrey (1975) using the corrected coefficient for dinoflagellates (Ritchie 2006), and the corrected path-length of 0.8679.

3.2.7 Chlorophyll fluorescence

Chlorophyll fluorescence was measured using an imaging pulse amplitude modulated (IPAM) fluorometer (Walz, Germany). Maximum photochemical quantum yield (F_v/F_m) was measured daily at 19:00 h. Light-acclimated quantum yield ($\Delta F_v/F_m'$) and NPQ were measured daily at noon. Corals were dark-acclimated for 20 min prior to measurement and determination of F_m. After this first saturation pulse, corals were exposed to actinic light with the intensity of 186 µmol photons m^{-2} s^{-1} for 180 s, after which a second saturation pulse was applied to determine F_m' and light-acclimated $\Delta F_v/F_m'$. The IPAM settings were: measuring intensity: 3; saturation intensity: 8; saturation width: 0.8; gain: 1 (F_v/F_m at night-time) or 3 ($\Delta F_v/F_m'$ and NPQ at noon).

NPQ was calculated as:

$$NPQ = (F_m - F_m')/F_m'$$

Excitation pressure over PSII (Q_m) (Iglesias-Prieto et al. 2004) was calculated as in Fisher et al. (2012):

$$Q_m = 1 - [(\Delta F/F_m') \text{ at noon}/(F_v/F_m) \text{ at dawn of Day 0}]$$

3.2.8 Statistical analyzes

Data were analyzed using the IBM SPSS statistics 20.0 software. Repeated measures analysis of variance (rmANOVA) and *post hoc* pairwise comparison with Bonferroni adjustment was used to test significant changes ($p \leq 0.05$) of photophysiological parameters F_v/F_m, Q_m, and NPQ. Data were arcsine transformed (F_v/F_m) or log transformed (Q_m) to meet assumptions of normality. When assumptions of equality of the variances were violated, the Greenhouse-Geisser correction is reported. rmANOVA with Bonferroni adjusted *post hoc* pairwise comparisons or univariate ANOVA with *post hoc* Tukey HSD test were used to test the effects on symbiont density, pigment concentration and arcsine-transformed FA parameters. When assumptions of normality were violated,

statistical results were confirmed using the non-parametric Kruskal-Wallis test and *post hoc* pairwise comparisons with Bonferroni-Dunn adjustments.

3.3 Results

3.3.1 *Symbiodinium* genotyping

Pocillopora damicornis from both sampling locations, Stephens Hole and Sylphs Hole, hosted a mixed *Symbiodinium* ITS2 assemblage of C100 and C118. *Porites heronensis* sampled from Sylphs Hole harboured *Symbiodinium* ITS2 type C111* (Table 3.1). For sequence identity refer to Chapter 2, Section 2.3.1 on page 68 as well as Appendix A.3, on pages 258 – 259.

Table 3.1: Coral species, sampling location at Lord Howe Island, latitude and longitude of sampling location, and *Symbiodinium* type identified by denaturing gel gradient electrophoresis (DGGE) of the internal transcribed spacer 2 (ITS2) region.

Coral species (n = 4)	**Sampling location** (latitude/longitude)	***Symbiodinium* ITS2 type**
Pocillopora damicornis	Stephens Hole (S31°31′937′′, E159°03′251′′)	C100/C118
Pocillopora damicornis	Sylphs Hole (S31°31′249′′, E159°03′261′′)	C100/C118
Porites heronensis	Sylphs Hole (S31°31′249′′, E159°03′261′′)	C111*

3.3.2 Bleaching descriptors

On Day 0, *Symbiodinium* cell density and chlorophyll concentrations (both, *Symbiodinium* cell-specific and coral surface area-specific) were approximately two-fold higher in *P. heronensis* than *P. damicornis* from both sampling locations (Tables 3.2,

3.3). Both *Symbiodinium* cell density and chlorophyll concentration were stable over time in all temperature treatments (Table 3.2), and the response of these parameters was similar between species (Table 3.4) and between temperature treatments within species (Table 3.2). On Day 0, the ratio of chlorophyll c_2 to chlorophyll *a* was lower in *P. heronensis* than *P. damicornis* from both sampling locations (3.2, 3.3). The ratio remained constant over time at all temperatures and in all coral-*Symbiodinium* associations (Tables 3.2, 3.4).

Table 3.2: *Symbiodinium* density, cell-specific and coral surface area-specific chlorophyll parameters (mean ± S.E.), and corresponding rmANOVA results testing for an effect of Time × Temperature in *Pocillopora damicornis* and in *Porites heronensis*. Non-significant effects ($p > 0.05$) are presented in grey. df = degrees of freedom; T = temperature.

Species	**T (°C)**	**Day 0**	**Day 4**	**rmANOVA results**		**Day 0**	**Day 4**	**rmANOVA results**	
		***Symbiodinium* density** (10^6 cells cm^{-2} coral surface area)				**ratio chl c_2 : chl *a***			
P. damicornis	**16**	0.8 ± 0.12	0.8 ± 0.15	***F***	0.8	0.38 ± 0.021	0.59 ± 0.117	***F***	0.5
Stephens	**24**	1.1 ± 0.28	1.3 ± 0.21	***df***	2, 9	0.41 ± 0.010	0.53 ± 0.051	***df***	2, 9
	28	1.0 ± 0.16	0.7 ± 0.18	***p***	0.485	0.39 ±0.013	0.50 ± 0.075	***p***	0.648
P. damicornis	**16**	0.7 ± 0.09	0.6 ± 0.07	***F***	1.1	0.41 ± 0.034	0.52 ± 0.042	***F***	0.1
Sylphs	**24**	0.9 ± 0.08	0.9 ± 0.13	***df***	2, 9	0.40 ±0.029	0.49 ± 0.020	***df***	2, 9
	28	0.6 ± 0.09	0.8 ± 0.18	***p***	0.377	0.39 ± 0.035	0.47 ±0.087	***p***	0.938
P. heronensis	**16**	1.3 ± 0.29	0.9 ± 0.24	***F***	0.3	0.36 ± 0.015	0.36 ± 0.012	***F***	0.2
Sylphs	**24**	1.9 ± 0.16	1.5 ± 0.14	***df***	2, 9	0.36 ± 0.031	0.5 ±0.159	***df***	2, 9
	28	1.2 ± 0.17	1.1 ± 0.10	***p***	0.767	0.32 ±0.016	0.35 ±0.02	***p***	0.819
		chl *a* (pg $cell^{-1}$)				**chl c_2** (pg $cell^{-1}$)			
P. damicornis	**16**	3.1 ± 0.63	0.9 ± 0.17	***F***	2.1	1.2 ± 0.27	0.5 ± 0.05	***F***	1.9
Stephens	**24**	1.9 ± 0.37	1.3 ± 0.34	***df***	2, 9	0.8 ± 1.14	0.6 ± 0.11	***df***	2, 27
	28	2.1 ± 0.23	1.8 ± 0.66	***p***	0.179	0.8 ± 0.08	0.8 ± 0.20	***p***	0.207
P. damicornis	**16**	2.7 ± 0.28	1.6 ± 0.16	***F***	0.1	1.1 ± 0.14	0.8 ±0.07	***F***	0.3
Sylphs	**24**	2.9 ± 0.17	1.8 ± 0.21	***df***	2, 9	1.1 ± 0.06	0.9 ± 0.09	***df***	2, 27
	28	3.4 ± 0.21	2.1 ± 0.36	***p***	0.889	1.3 ± 0.20	0.9 ± 0.04	***p***	0.721
P. heronensis	**16**	7.8 ± 1.82	6.3 ± 1.15	***F***	1.0	2.6 ± 0.72	2.2 ± 0.36	***F***	1.6
Sylphs	**24**	3.5 ± 0.61	4.9 ± 2.40	***df***	2, 9	1.2 ± 0.15	2.4 ± 0.76	***df***	2, 27
	28	5.5 ± 0.66	4.4 ± 0.27	***p***	0.394	1.8 ± 0.31	1.5 ± 0.09	***p***	0.254
		chl *a* (µg cm^{-2} coral surface area)				**chl *a* and c_2** (µg cm^{-2} coral surface area)			
P. damicornis	**16**	2.2 ± 0.13	0.7 ± 0.23	***F***	1.6	3.0 ± 0.17	1.1 ± 0.30	***F***	1.7
Stephens	**24**	2.0 ± 0.43	1.7 ± 0.54	***df***	2, 9	2.9 ± 0.60	2.5 ± 0.70	***df***	2, 9
	28	2.1 ± 0.37	1.1 ±0.4	***p***	0.259	2.9 ± 0.97	1.6 ±0.52	***p***	0.230
P. damicornis	**16**	1.7 ± 0.12	1.0 ± 0.08	***F***	1.2	2.5 ±0.15	1.5 ± 0.12	***F***	1.0
Sylphs	**24**	2.7 ± 0.33	1.7 ± 0.39	***df***	2, 9	3.7 ± 0.44	2.5 ±0.55	***df***	2, 9
	28	2.1 ±0.27	1.8 ± 0.55	***p***	0.355	3.0 ± 0.44	2.6 ±0.44	***p***	0.422
P. heronensis	**16**	8.4 ± 1.10	5.2 ± 1.5	***F***	2.0	11.1 ± 1.45	7.0 ± 1.95	***F***	2.5
Sylphs	**24**	6.5 ± 1.16	7.2 ± 0.65	***df***	2, 9	8.7 ± 1.52	10.6 ± 0.96	***df***	2, 9
	28	6.7 ± 0.77	4.9 ± 0.52	***p***	0.195	8.8 ±1.10	6.7 ±0.75	***p***	0.133

Table 3.3: Results of univariate ANOVA with *post hoc* Tukey HSD, testing parameters on Day 0 for species-specific differences in *Pocillopora damicornis* Stephens (**PdSt**), *Pocillopora damicornis* Sylphs (**PdSy**) and *Porites heronensis* Sylphs (**PhSy**). The parameters are: symbiont density; cell-specific chlorophyll (**chl**) *a*; cell-specific chl c_2; coral surface area (**CSA**) -specific chl *a*; CSA-specific chl *a* and chl c_2; ratio of chl *a* to chl c_2; relative content of saturated fatty acids (**SFA**); relative content of mono-unsaturated fatty acids (**MUFA**); relative content of poly-unsaturated fatty acids (**PUFA**); ratio of unsaturated fatty acids (**UFA**) to saturated fatty acids (**SFA**); ratio of **C18:1cis** to **C18:4**; sum of FAs with 14 carbons (**Σ C14**), 16 carbons (**Σ C16**), 18 carbons (**Σ C18**), 20 carbons (**Σ C20**), and 22 carbons (**Σ C22**). Significant differences ($p \leq 0.05$) are highlighted in bold and non-significant result ($p > 0.05$) is presented in grey. **NN** Results of univariate ANOVA were confirmed with the non-parametric Kruskal-Wallis test and *post hoc* Dunn-Bonferroni corrected pairwise comparison because assumption of normality was not met.

Parameter	**Species**		**Tukey HSD**	
Symbiont density	$F_{2,33} = 11.4$	$\mathbf{p < 0.001}$	(PdSt = PdSy) ≠ Ph	$\mathbf{p \leq 0.008}$
chl *a* (pg cell $^{-1}$)	$F_{2,33} = 11.9$	$\mathbf{p < 0.001}$	(PdSt = PdSy) ≠ Ph	$\mathbf{p \leq 0.002}$
chl c_2 (pg cell $^{-1}$)	$F_{2,33} = 6.6$	$\mathbf{p = 0.004}$	(PdSt = PdSy) ≠ Ph	$\mathbf{p \leq 0.043}$
chl *a* (µg cm $^{-2}$ CSA)	$F_{2,33} = 61.9$	$\mathbf{p < 0.001}$	(PdSt = PdSy) ≠ Ph	$\mathbf{p < 0.001}$
chl *a* and c_2 (µg cm $^{-2}$ CSA)	$F_{2,33} = 61.3$	$\mathbf{p < 0.001}$	(PdSt = PdSy) ≠ Ph	$\mathbf{p < 0.001}$
chl c_2 : chl *a*	$F_{2,33} = 7.2$	$\mathbf{p = 0.003}$	(PdSt = PdSy) ≠ Ph	$\mathbf{p \leq 0.009}$
SFA	$F_{2,33} = 6.4$	$\mathbf{p = 0.004}$	(PdSt = PdSy) ≠ Ph	$\mathbf{p \leq 0.019}$
MUFA^{NN}	$F_{2,33} = 6.4$	$\mathbf{p = 0.005}$	(PdSt = PdSy) ≠ Ph	$\mathbf{p \leq 0.019}$
PUFA	$F_{2,33} = 11.3$	$\mathbf{p < 0.001}$	(PdSt = PdSy) ≠ Ph	$\mathbf{p = 0.001}$
UFA:SFA	$F_{2,33} = 12.1$	$\mathbf{p < 0.001}$	(PdSt = PdSy) ≠ Ph	$\mathbf{p < 0.001}$
C18:1cis/C18:4	$F_{2,33} = 21.5$	$\mathbf{p < 0.001}$	(PdSt = PdSy) ≠ Ph	$\mathbf{p < 0.001}$
Σ C14	$F_{2,33} = 29.7$	$\mathbf{p < 0.001}$	(PdSt = PdSy) ≠ Ph	$\mathbf{p < 0.001}$
Σ C16	$F_{2,33} = 12.9$	$\mathbf{p < 0.001}$	(PdSt = PdSy) ≠ Ph	$\mathbf{p < 0.001}$
Σ C18	$F_{2,33} = 2.2$	$p = 0.124$		
ΣC20	$F_{2,33} = 15.4$	$\mathbf{p < 0.001}$	(PdSt = PdSy) ≠ Ph	$\mathbf{p < 0.001}$
ΣC22	$F_{2,33} = 4.8$	$\mathbf{p = 0.015}$	(PdSt = PdSy) ≠ Ph	$\mathbf{p \leq 0.033}$

Table 3.4: Results of rmANOVA testing the effects of Temperature, Species and the interaction of these variables. Significant effects ($p \leq 0.05$) are highlighted in bold and non-significant effects ($p > 0.05$) are presented in grey. For description of parameters and abbreviations refer to Table 3.3.

Parameter		**Temperature**	**Species**	**Temperature × Species**
Symbiont density	*F*	0.1	1.7	0.7
	df	2, 27	2, 27	4, 27
	p	0.931	0.205	0.569
Chl *a* (pg cell^{-1})	*F*	1.6	0.4	1.0
	df	2, 27	2, 27	4, 27
	p	0.226	0.652	0.447
Chl c_2 (pg cell^{-1})	*F*	2.1	1.2	1.3
	df	2, 27	2, 27	4, 27
	p	0.145	0.314	0.279
Chl *a* and c_2 (µg cm^{-2}coral surface area)	*F*	3.2	0.2	2.0
	df	2, 27	2, 27	4, 27
	p	0.058	0.792	0.120
Chl *a* (µg cm^{-2} coral surface area)	*F*	2.5	0.6	1.6
	df	2, 27	2, 27	4, 27
	p	0.099	0.547	0.205
Chl c_2 : chl *a*	*F*	0.2	0.9	0.3
	df	2, 27	2, 27	4, 27
	p	0.809	0.424	0.877
Σ SFA (Saturates)	*F*	**5.1**	0.9	**7.2**
	df	**2, 27**	2, 27	**4, 27**
	p	**0.013**	0.439	**< 0.001**
Σ MUFA (Monounsaturates)	*F*	0.8	2.1	1.6
	df	2, 27	2, 27	4, 27
	p	0.474	0.142	0.210
Σ PUFA (Polyunsaturates)	*F*	**13.2**	1.1	**8.0**
	df	**1, 27**	2, 27	**2, 27**
	p	**< 0.001**	0.338	**< 0.001**
UFA:SFA (Unsaturates:Saturates)	*F*	**16.2**	0.8	**13.8**
	df	**2, 27**	2, 27	**4, 27**
	p	**< 0.001**	0.451	**< 0.001**
C18:1(cis)/C18:4	*F*	5.1	**3.7**	**3.5**
	df	2, 27	**2, 27**	**4, 27**
	p	0.13	**0.037**	**0.019**
Σ C14	*F*	2.2	0.6	1.8
	df	2, 27	2, 27	4, 27
	p	0.127	0.542	0.167
Σ C16	*F*	1.3	**7.8**	1.6
	df	2, 27	**2, 27**	4, 27
	p	0.280	**0.002**	0.196
Σ C18	*F*	**4.0**	2.2	1.0
	df	**2, 27**	2, 27	4, 27
	p	**0.031**	0.131	0.439
Σ C20	*F*	2.0	**21.3**	**11.0**
	df	2, 27	**2, 27**	**4, 27**
	p	0.160	**< 0.001**	**< 0.001**
Σ C22	*F*	0.1	**7.0**	1.6
	df	2, 27	**2, 27**	4, 27
	P	0.881	**0.003**	0.203

3.3.3 Chlorophyll fluorescence

On Day 0, photochemical maximum quantum yield (F_v/F_m) averaged 0.610 ± 0.006 (mean ± S.E.) in *P. damicornis* Stephens, 0.589 ± 0.008 in *P. damicornis* Sylphs and 0.615 ± 0.007 in *P. heronensis* Sylphs. F_v/F_m decreased markedly under cold stress, but not under heat stress or the control temperature (Figure 3.1 A – C), in all corals. The response to cold stress differed significantly in *P. damicornis* Sylphs from the other two coral-*Symbiodinium* associations, in that the decline from Day 1 onwards was stronger (Figure 3.1 A – C, Tables 3.5, 3.6). This resulted in the greatest overall reduction in F_v/F_m of 68%, compared to 54% in *P. damicornis* Stephens and 59% in *P. heronensis* Sylphs (Day 4 *versus* Day 0).

On Day 0, excitation pressure over PSII (Q_m) averaged 0.493 ± 0.023 (mean ± S.E.) in *P. damicornis* Stephens, 0.475 ± 0.020 in *P. damicornis* Sylphs and 0.571 ± 0.031 in *P. heronensis* Sylphs. Cold stress, but not heat stress or the control temperature, caused significant increases in Q_m in all corals (Figure 3.1 D – F). The dynamics of Q_m at 16 °C were similar between species with increases of 79%, 85%, and 65%, in *P. damicornis* Stephens, *P. damicornis* Sylphs and *P. heronensis* Sylphs, respectively (Table 3.5).

On Day 0, non-photochemical quenching (NPQ) under 186 µmol photons m^{-2} s^{-1} averaged 0.911 ± 0.059 (mean ± S.E.) in *P. damicornis* Stephens, 0.808 ± 0.066 in *P. damicornis* Sylphs and 1.092 ± 0.045 in *P. heronensis* Sylphs. NPQ was not affected by temperature in *P. damicornis* Stephens or *P. heronensis* Sylphs (Figure 3.1 G, I, Table 3.6). However, *P. damicornis* Sylphs showed an adverse effect of cold stress on NPQ (Figure 3.1 H, Tables 3.5, 3.6). Here, NPQ was suppressed compared to the control on Days 3 and 4 by 35% and 40%, respectively.

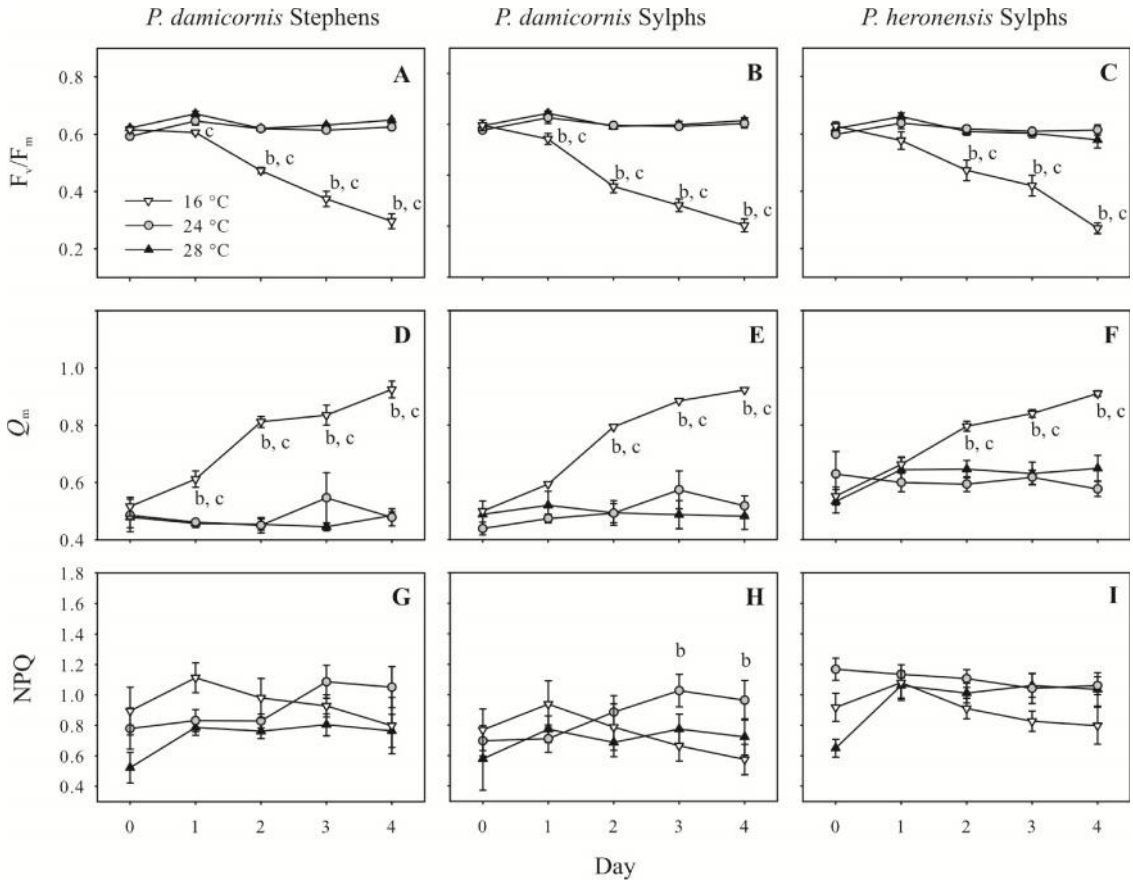

Figure 3.1: Effect of temperature over a 4-day period on maximum quantum yield of PSII (F_v/F_m; **A – C**), excitation pressure over PSII (Q_m; **D – F**) and non-photochemical quenching (NPQ; **G – I**) in *Pocillopora damicornis* sampled from Stephens Hole (left panels) or from Sylphs Hole (middle panels) and in *Porites heronensis* sampled from Sylphs Hole (right panels). Presented are mean values ± S.E., n = 4. Significant differences are reported for (b) 24 °C and 16 °C, and (c) 16 °C and 28 °C ($p \leq 0.05$; rmANOVA and pairwise comparison with Bonferroni correction) b and c are used for consistency with other figures.

Table 3.5: Results of rmANOVA for the photophysiological parameters: maximum quantum yield (F_v/F_m); excitation pressure over PSII (Q_m); and non-photochemical quenching (NPQ). Significant effects on the level of $p \leq 0.05$ are highlighted in bold and non-significant effects ($p > 0.05$) are presented in grey. df = degrees of freedom; Temp = temperature; † indicates that Greenhaus-Geisser correction is presented.

Parameter		**Time**	**Time × Temp**	**Time × Species**	**Time × Temp × Species**	**Temp**	**Species**	**Temp × Species**
F_v/F_m†	*F*	**166.0**	**135.9**	**2.6**	**2.0**	**159.7**	**8.9**	2.7
	df	**2.5, 108**	**5.0, 108**	**5.0, 108**	**10.1, 108**	**2, 27**	**2, 27**	4, 27
	p	**< 0.001**	**< 0.001**	**0.035**	**0.046**	**< 0.001**	**0.001**	0.055
Q_m†	*F*	**34.6**	**21.5**	0.8	1.3	**48.5**	**11.8**	2.2
	df	**2, 54.4**	**4, 54.4**	4, 54.4	8, 54.4	**2, 27**	**2, 27**	4, 27
	p	**< 0.001**	**< 0.001**	0.520	0.261	**< 0.001**	**< 0.001**	0.097
NPQ	*F*	**4.4**	**8.2**	1.2	1.6	2.5	**4.8**	0.7
	df	**4, 24**	**8, 48**	8, 48	16, 74	2, 27	**2, 27**	4, 27
	p	**0.008**	**< 0.001**	0.320	0.092	0.105	**0.017**	0.601

Table 3.6: Results of rmANOVA for the suite of parameters when each coral-*Symbiodinium* association is analyzed separately. Significant effects on the level of $p \leq 0.05$ are highlighted in bold and non-significant effects ($p > 0.05$) are presented in grey. For explanation of parameters and abbreviations refer to Tables 3.3 and 3.5.

		***Pocillopora damicornis* Stephens**			***Pocillopora damicornis* Sylphs**			***Porites heronensis* Sylphs**		
Parameter		Time	Temp	Time × Temp	Time	Temp	Time × Temp	Time	Temp	Time × Temp
F_v/F_m[†]	*F*	**96.8**[†]	**80.9**	**92.2**[†]	**83.3**	**64.5**	**14.6**	**33.5**[†]	**31.9**	**20.4**[†]
	df	**1.9, 17.5**[†]	**2, 9**	**3.9, 17.5**[†]	**4, 6**	**2, 9**	**8, 12**	**1.7, 15.6**[†]	**2, 9**	**3.5, 15.6**[†]
	p	**< 0.001**[†]	**< 0.001**	**< 0.001**[†]	**< 0.001**	**< 0.001**	**< 0.001**	**< 0.001**[†]	**< 0.001**	**< 0.001**[†]
Q_m	*F*	**7.7**[†]	**36.5**	**7.112**[†]	**6.8**	**15.2**	**3.8**	**17.4**	**6.4**	**10.6**
	df	**1.8, 16.6**[†]	**2, 9**	**3.7, 16.6**[†]	**4, 6**	**2, 9**	**8, 12**	**1.5, 13.6**	**2, 9**	**3, 13.6**
	p	**0.005**[†]	**< 0.001**	**0.002**[†]	**0.020**	**0.001**	**0.020**	**< 0.001**	**0.019**	**0.001**
NPQ	*F*	2.5	1.7	2.3	1.5	0.5	**3.2**	2.7	2.7	2.6
	df	4, 6	2, 9	8, 12	4, 6	2, 9	**8, 12**	4, 6	2, 9	8, 12
	p	0.150	0.230	0.097	0.303	0.612	**0.035**	0.133	0.122	0.063
C18:1(cis)/C18:4	*F*	**19.0**	0.4	3.3	**16.5**	**7.5**	**7.3**	**21.9**	2.7	1.6
	df	**1, 9**	2, 9	2, 9	**1, 9**	**2, 9**	**2, 9**	**1, 9**	2, 9	2, 9
	p	**0.002**	0.664	0.082	**0.003**	**0.012**	**0.013**	**0.001**	0.118	0.259
Σ C14	*F*	1.0	0.3	2.4	0.01	1.9	0.6	0.03	1.0	3.2
	df	1, 9	2, 9	2, 9	1, 9	2, 9	2, 9	1, 9	2, 9	2, 9
	p	0.343	0.759	0.148	0.993	0.209	0.570	0.875	0.389	0.089
Σ C16	*F*	1.5	**19.6**	1.1	4.6	0.1	1.1	2.3	**4.3**	**27.6**
	df	1, 9	**2, 9**	2, 9	1, 9	2, 9	2, 9	1, 9	**2, 9**	**2, 9**
	p	0.253	**0.001**	0.361	0.060	0.919	0.387	0.166	**0.049**	**< 0.001**
Σ C18	*F*	**8.3**	1.6	0.1	**10.2**	1.2	2.0	0.02	3.9	3.4
	df	1, 9	2, 9	2, 9	**1, 9**	2, 9	2, 9	1, 9	2, 9	2, 9
	p	**0.018**	0.235	0.895	**0.011**	0.337	0.198	0.898	0.060	0.081
Σ C20	*F*	4.4	1.1	1.1	0.1	0.6	1.5	0.6	**7.4**	**45.5**
	df	1, 9	2, 9	2, 9	1, 9	2, 9	2, 9	1, 9	**2, 9**	**2, 9**
	p	0.066	0.374	0.387	0.711	0.576	0.275	0.302	**0.012**	**< 0.001**
Σ C22	*F*	0.4	0.8	0.02	0.09	**4.7**	**6.2**	0.8	**14.7**	**25.0**
	df	1, 9	2, 9	2, 9	1, 9	**2, 9**	**2, 9**	1, 9	**2, 9**	**2, 9**
	p	0.546	0.494	0.979	0.775	**0.040**	**0.021**	0.387	**0.001**	**< 0.001**

3.3.4 Thylakoid fatty acids

The cell-specific concentration of thylakoid fatty acids (FAs) was similar between species and averaged 22.75 ± 5.3 pg cell^{-1} (mean ± S.E.) in *P. damicornis* Stephens, 25.6 ± 4.25 pg cell^{-1} in *P. damicornis* Sylphs and 20.8 ± 4.5 pg cell^{-1} in *P. heronensis* Sylphs. The baseline composition of membranes enriched in thylakoids in *Symbiodinium* C111* harboured by *P. heronensis* Sylphs differed significantly from that of *Symbiodinium* C100/C118 harboured by *P. damicornis* from both locations. On Day 0, the relative proportion of saturated FAs (Σ SFA) in C111* was lower (relative percentage of 43.5 ± 2.0% of total FAs; mean ± S.E.) compared to C100/C118 in *P. damicornis* Stephens (58.8 ± 4.8%) and *P. damicornis* Sylphs (55.9 ± 2.3%). In contrast, the relative proportions of monounsaturated FAs (Σ MUFA) and polyunsaturated FAs (Σ PUFA) were higher in C111* (Σ MUFA: 15.0 ± 0.6%; Σ PUFA: 38.1 ± 1.7%) than in C100/C118 in *P. damicornis* Stephens (Σ MUFA: 11.6 ± 1.0%; Σ PUFA: 25.7 ± 3.4%) and *P. damicornis* Sylphs (Σ MUFA: 13.1 ± 0.5%; Σ PUFA: 26.1 ± 1.8%). This resulted in a higher baseline ratio of unsaturated FAs to saturated FAs (UFA:SFA) in *P. heronensis* (1.3 ± 0.10; Figure 3.2 C, Table 3.3) compared to *P. damicornis* Stephens and *P. damicornis* Sylphs (0.7 ± 0.10 and 0.7 ± 0.06, respectively; Figure 3.2 A – B). Species-specific significant effects of these parameters are presented in Table 3.3.

On Day 0, the baseline FA ratio of C18:1(cis) to C18:4 was higher in *Symbiodinium* C111* (1.4 ± 0.12, mean ± S.E.) compared to C100/C118 in *P. damicornis* Stephens (0.6 ± 0.10) and *P. damicornis* Sylphs (0.5 ± 0.06; Figure 3.2 D – F, Table 3.3).

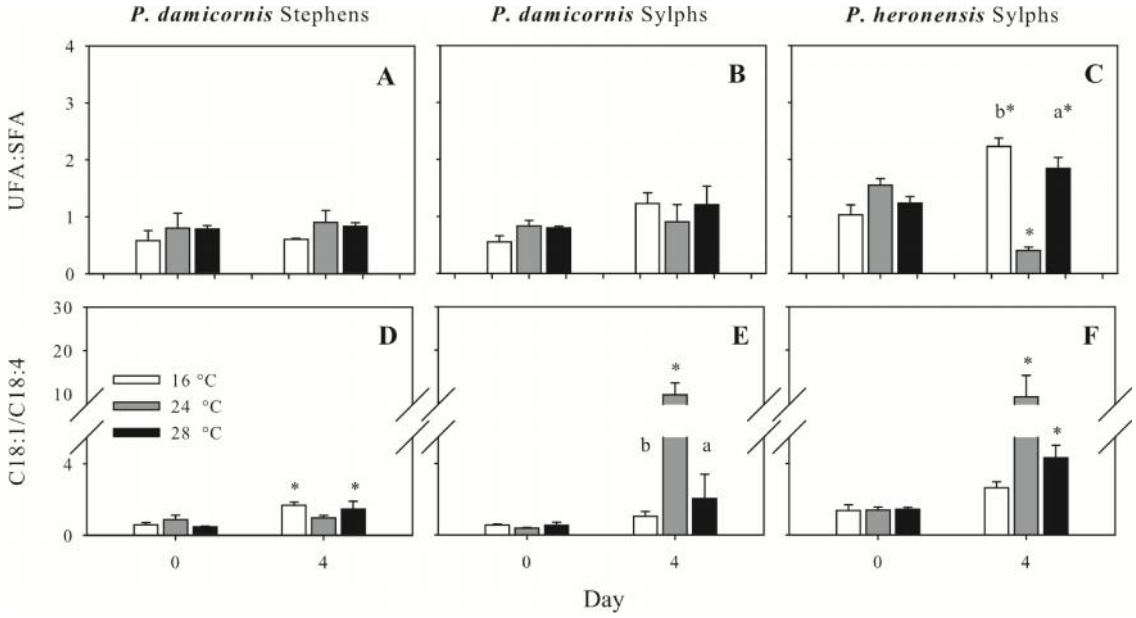

Figure 3.2: Effect of temperature over a 4-day period on the ratio of unsaturated fatty acids (UFAs) to saturated fatty acids (SFAs) (**A – C**) and ratio of C18:1(cis) to C18:4 (**D – F**) in *Pocillopora damicornis* sampled from Stephens Hole (left panels) or from Sylphs Hole (middle panels) and in *Porites heronensis* sampled from Sylphs Hole. Presented are mean values ± S.E., n = 4. Significant differences are reported for (a) 24 °C and 28 °C, (b) 24 °C and 16 °C, (c) 16 °C and 28 °C, and (*) Day 0 and Day 4 at the level of $p \leq 0.05$ (rmANOVA and pairwise comparison with Bonferroni correction). For overall effects of rmANOVA refer to Tables 3.4 and 3.6.

Likewise, the baseline FA composition according to carbon chain-length differed significantly in *Symbiodinium* C111* from that in C100/C118 from both locations. Membranes enriched in thylakoids in *Symbiodinium* C111* had a significantly lower relative content of the short chain FAs C14 and C16 and a higher content of the long chain FAs C18, C20 and C22 than did *Symbiodinium* C100/C118 on Day 0 of the experiment (Figure 3.3 A – C, Table 3.3).

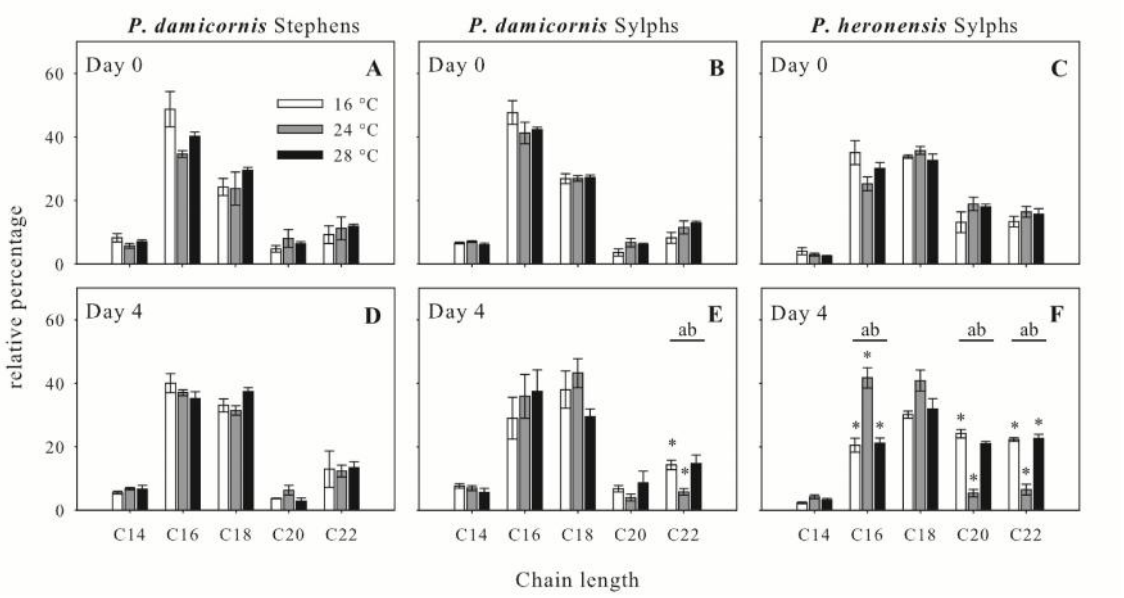

Figure 3.3: Fatty acid composition by chain length on Day 0 (**A – C**) and Day 4 (**D – F**) of temperature treatment in *Pocillopora damicornis* sampled from Stephens Hole (left panels) or from Sylphs Hole (middle panels) and in *Porites heronensis* sampled from Sylphs Hole. Presented are mean values ± S.E., n = 4. Significant differences are reported for (a) 24 °C and 28 °C, (b) 24 °C and 16 °C, and (*) Day 0 and Day 4 at the level of $p \leq 0.05$ (rmANOVA and pairwise comparison with Bonferroni correction). For overall effects of rmANOVA refer to Tables 3.4 and 3.6.

Overall, the cell-specific content of thylakoid fatty acids was not affected by temperature over time. Also, *Symbiodinium* C100/C118 in *P. damicornis* Stephens maintained a stable thylakoid lipid composition over time under all temperature treatments. In contrast, *Symbiodinium* C100/C118 in *P. damicornis* Sylphs adjusted the quality of photosynthetic membranes in response to exposure to 16 °C and 24 °C, but not 28 °C. *Symbiodinium* C111* in *P. heronensis* Sylphs extensively remodelled FAs in membranes enriched in thylakoids at all temperature treatments, with the modifications detailed below.

3.3.4.1 Ratio of UFA : SFA and C18:1(cis) to C18:4

The ratio of UFA : SFA increased in *P. heronensis* at 16 °C and 28 °C, with 2.2 fold and 1.5 fold increases, respectively, and decreased 3.9 fold at 24 °C. The ratio of UFA : SFA did not change in any of the other corals.

There was a trend to increase the ratio of C18:1(cis)/C18:4 in all *Symbiodinium* types over time, independent of the temperature (Figure 3.2 D – F). The strongest increases were observed in *Symbiodinium* C100/C118 Sylphs and C111* Sylphs at 24 °C, with 26 fold and 7 fold increases, respectively.

3.3.4.2 Carbon chain length

When FAs are pooled by chain length, i.e. according to the number of carbons, *Symbiodinium* C100/C118 Sylphs maintained its composition over time at all temperatures (Figure 3.3 A, D, Table 3.6). In membranes enriched in thylakoids of *Symbiodinium* C100/C118 Sylphs, C22 FAs increased in relative content under cold stress, decreased at 24 °C, and remained unchanged under heat stress. Shorter-chain FAs (C14, C16, C18 and C20) remained constant with respect to their relative content over time (Figure 3.3 B, E, and Table 3.6). In *Symbiodinium* C111*, C20 and C22 FAs increased at 16 °C and 28 °C at the expense of C16. In contrast, at 24 °C, C20 and C22 FAs decreased over time with a concomitant increase of C16. The relative concentrations of C14 and C18 FAs were relatively stable over time at all temperatures (Figure 3.3 C, F, and Table 3.6).

3.3.4.3 Saturates

In membranes enriched in thylakoids of *Symbiodinium* C100/C118, Σ SFA was constant under thermal stress (Tables 3.7, 3.8, 3.9). In *Symbiodinium* C111*, cold and heat stresses were associated with decreased Σ SFA, which was largely driven by a decrease in the relative percentage of C16:0. In contrast, exposure to 24 °C caused an increase in Σ SFA due to increases of C16:0 and C18:0 (Tables 3.7, 3.10).

3.3.4.4 Monounsaturates

Overall, Σ MUFA was constant over time in all *Symbiodinium* types and temperatures (Table 3.7). However, Table 3.10 highlights fine-scale differences under thermal treatment in *Symbiodinium* C111* hosted by *P. heronensis*. Under cold and heat stress, C18:1(n-9)cis increased, whereas at 24 °C, C18:1(n-9)trans increased over time. Further, heat stress and 24 °C caused a decrease of the short chain MUFA C14:1(n-5).

3.3.4.5 Polyunsaturates

In membranes enriched in thylakoids *of Symbiodinium* C100/C118 Stephens, Σ PUFA was constant over time at all temperatures (Table 3.7). In *Symbiodinium* C100/C118 in *P. damicornis* Sylphs, cold stress was related to an increased Σ PUFA (Table 3.7) which was driven by increased levels of C22:6(n-3) (Table 3.9). In contrast, exposure to 24 °C caused decreased levels of the PUFAs C22:6(n-3) and C18:4(n-3) (Table 3.9), resulting in an overall lower Σ PUFA on Day 4 compared to Day 0 (Table 3.7). In *Symbiodinium* C111*, cold stress was associated with an increased Σ PUFA (Table 3.7). Table 3.10 shows that this effect was due to increased levels of C20:4(n-6), C20:5(n-3), C22:4(n-6) and C22:5(n-3). Similarly, heat stress caused an increase in C20:4(n-6), C22:4(n-6) and C22:5(n-3), but did not result in an overall increase in Σ PUFA, perhaps because levels of C18:4(n-3) decreased significantly (Tables 3.7, 3.10). Exposure to 24 °C caused reduced levels of all PUFAs identified, except for C18:3 (n-3) (Table 3.10).

Table 3.7: Relative percentage of saturated fatty acids (Σ SFA), monounsaturated fatty acids (Σ MUFA) and polyunsaturated fatty acids (Σ PUFA). Presented are mean ± S.E., n = 4. Statistical results of rmANOVA are reported for (a) 24 °C and 28 °C, (b) 24 °C and 16 °C, (c) 16 °C and 28 °C, and (*) Day 0 and Day 4 and significant results at the level of $p \leq 0.05$ (rmANOVA and *post hoc* pairwise comparison with Bonferroni correction) are highlighted in bold and non-significant effects ($p > 0.05$) are presented in grey. [NN] Data not normally distributed and statistical results verified using the nonparametric Kruskal-Wallis test.

C100/C118 in *Pocillopora damicornis* Stephens							
	16 °C	**24 °C**	**28 °C**	**16 °C**	**24 °C**	**28 °C**	
		Day 0			**Day 4**		**Temperature × Time**
Σ SFA[NN]	64.3 ± 9.61	58.6 ± 11.7	53.6 ± 1.80	61.1 ± 0.61	52.0 ± 4.85	53.1 ± 1.66	$F_{(2,9)} = 2$; $p = 0.190$
Σ MUFA[NN]	10.6 ± 2.17	11.7 ± 2.19	12.4 ±0.65	17.2 ± 0.81	15.1 ± 1.95	17.5 ± 2.03	$F_{(2,9)} = 0.02$; $p = 0.978$
Σ PUFA[NN]	21.5 ± 6.70	26.0 ± 8.38	29.4 ±1.16	20.0 ± 0.41	28.7 ± 3.74	26.4 ± 2.17	$F_{(2,9)} = 1.1$; $p = 0.386$
C100/C118 in *Pocillopora damicornis* Sylphs							
		Day 0			**Day 4**		**Temperature × Time**
Σ SFA	62.8 ± 5.03	52.0 ± 3.11	53.0 ± 1.26	44.4 ± 3.32	56.6 ± 10.06	47.2 ± 8.77	$F_{(2,9)} = 1.5$; $p = 0.267$
Σ MUFA	12.0 ± 0.67	12.7 ± 0.34	14.5 ± 1.01	21.5 ± 4.65	27.9 ± 5.80	16.3 ± 2.88	$F_{(2,9)} = 2.0$; $p = 0.190$
Σ PUFA	21.1 ± 3.77	29.6 ± 2.48	27.7 ± 1.84	31.0 ± 1.22	**14.5 ± 4.65***	32.0 ± 6.35	**$F_{(2,9)} = 4.4$; $p = 0.048$**
C111* in *Porites heronensis* Sylphs							
		Day 0			**Day 4**		**Temperature × Time**
Σ SFA	48.9 ± 4.21	38.0 ± 2.36	43.7 ± 2.22	**29.5 ± 1.5 [b]***	**71.5 ± 3.16 [a, b]***	**34.15 ± 2.00 [a]***	**$F_{(2,9)} = 78.7$; $p < 0.001$**
Σ MUFA	14.4 ± 1.46	16.2 ± 1.13	14.4 ± 0.39	17.4 ± 0.31	19.0 ± 1.7	18.5 ±1.85	$F_{(2,9)} = 0.2$; $p = 0.822$
Σ PUFA	33.5 ± 3.24	42.1 ± 3.19	38.7 ± 2.18	**47.7 ± 1.02 [b]***	**9.1 ± 3.14 [a, b]***	43.3 ± 2.27 [a]	**$F_{(2,9)} = 65.2$; $p < 0.001$**

Table 3.8: Fatty acid composition of *Symbiodinium* C100/C118 hosted by *Pocillopora damicornis* sampled from Stephens Hole, before and after exposure to 16 °C, 24 °C and 28 °C (percentage of total fatty acids). n = 4. Significant differences are indicated testing the null hypothesis that the responses to 28 °C and 24 °C ([a]), 16 °C and 24 °C ([b]), and 16 °C and 28 °C ([c]) are the same, and that the means of Day 0 and Day 4 are the same (*****), using rmANOVA with *post hoc* Bonferroni-corrected pairwise comparison. [NN] Data not normally distributed and statistical results verified using the nonparametric Kruskal-Wallis test.

C100/C118 in *Pocillopora damicornis* Stephens

	Day 0			**Day 4**			**Temperature × Time**
Saturates	**16 °C**	**24 °C**	**28 °C**	**16 °C**	**24 °C**	**28 °C**	
C12:0	0.7 ± 0.24	0.5 ± 0.04	0.5 ± 0.03	0.7 ± 0.08	0.4 ± 0.14	0.8 ± 0.13	$F_{(2,9)} = 1.5$; $p = 0.271$
C13:0	0.3 ± 0.16	0.1 ± 0.05	0.1 ± 0.03	–	–	–	–
C14:0	8.0 ± 1.37	6.7 ± 1.51	6.8 ± 0.56	5.4 ± 0.43	6.4 ± 0.35	6.2 ± 1.30	$F_{(2,9)} = 0.02$; $p = 0.979$
C15:0	0.3 ± 0.16	0.1 ± 0.04	0.1 ± 0.06	–	1.8 ± 1.04	0.9 ± 0.87	$F_{(2,9)} = 1.7$; $p = 0.240$
C16:0	43.7 ± 6.56	38.9 ± 9.49	34.9 ± 1.38	36.9 ± 2.66	33.8 ± 1.56	31.6 ± 1.77	$F_{(2,9)} = 0.04$; $p = 0.963$
C17:0	0.3 ± 0.18	0.2 ± 0.04	0.1 ± 0.02	–	–	–	–
C18:0	10.2 ± 1.30	11.3 ± 1.55	10.1 ± 0.83	13.2 ± 0.53	8.9 ± 3.16	11.9 ± 1.73	$F_{(2,9)} = 1.1$; $p = 0.360$
C20:0	0.6 ± 0.11	0.6 ± 0.20	0.8 ± 0.15	0.5 ± 0.19	0.6 ± 0.16	0.5 ± 0.19	$F_{(2,9)} = 0.2$; $p = 0.846$
C22:0	0.4 ± 0.16	0.2 ± 0.09	0.3 ± 0.11	4.3 ± 4.02	0.2 ± 0.08	1.2 ± 0.98	$F_{(2,9)} = 0.5$; $p = 0.641$
Σ SFA[NN]	64.3 ± 9.61	58.6 ± 11.7	53.6 ± 1.80	61.1 ± 0.61	52.0 ± 4.85	53.1 ± 1.66	$F_{(2,9)} = 2$; $p = 0.190$
Monounsaturates	**16 °C**	**24 °C**	**28 °C**	**16 °C**	**24 °C**	**28 °C**	
C14:1(n-5)	0.2 ± 0.07	0.3 ± 0.13	0.3 ± 0.03	0.2 ± 0.09	0.4 ± 0.10	0.4 ± 0.31	$F_{(2,9)} = 0.02$; $p = 0.979$
C16:1(n-7)	4.4 ± 1.50	4.1 ± 1.38	5.0 ± 0.51	4.0 ± 0.54	2.9 ± 0.99	3.6 ± 0.55	$F_{(2,9)} = 0.02$; $p = 0.799$

C16:1(n-5)	0.6 ± 0.48	0.4 ± 0.37	0.3 ± 0.26	–	0.3 ± 0.19	–	–
C18:1(n-9)cis	3.5 ± 1.10	4.6 ± 1.73	4.8 ± 0.49	11.6 ± 1.00	9.0 ± 1.10	10.1 ± 1.05	$F_{(2,9)} = 2.4$; $p = 0.146$
C18:1(n-9)trans	0.9 ± 0.22	0.9 ± 0.09	1.1 ± 0.24	0.2 ± 0.14	0.9 ± 0.16	0.4 ± 0.15	$F_{(2,9)} = 3.1$; $p = 0.093$
C20:1(n-9)	0.3 ± 0.14	0.4 ± 0.18	0.4 ± 0.06	0.1 ± 0.07	0.2 ± 0.18	0.2 ± 0.12	$F_{(2,9)} = 0.02$; $p = 0.984$
C22:1(n-9)	0.7 ± 0.08	1.0 ± 0.21	0.6 ± 0.26	1.2 ± 0.74	1.3 ± 0.71	2.8 ± 1.71	$F_{(2,9)} = 0.8$; $p = 0.498$
Σ MUFA^{NN}	10.6 ± 2.17	11.7 ± 2.19	12.4 ±0.65	17.2 ± 0.81	15.1 ± 1.95	17.5 ± 2.03	$F_{(2,9)} = 0.02$; $p = 0.978$
Polyunsaturates	**16 °C**	**24 °C**	**28 °C**	**16 °C**	**24 °C**	**28 °C**	
C18:3(n-3)	2.1 ± 0.69	1.8 ± 0.64	2.9 ± 0.14	1.5 ± 0.5	2.8 ± 0.32	3.7 ± 0.61	$F_{(2,9)} = 0.9$; $p = 0.436$
C18:4(n-3)	7.5 ± 2.44	7.2 ± 2.43	10.5 ± 0.87	7.2 ± 1.14	9.8 ± 1.27	8.1 ± 1.41	$F_{(2,9)} = 1.3$; $p = 0.322$
C20:2(n-6)	0.2 ± 0.08	0.2 ± 0.09	0.2 ± 0.04	–	0.0 ± 0.04	–	–
C20:4(n-6)	0.8 ± 0.30	1.3 ± 0.63	1.3 ± 0.34	0.7 ± 0.27	1.0 ± 0.28	0.5 ± 0.27	$F_{(2,9)} = 0.6$; $p = 0.574$
C20:4(n-3)	0.3 ± 0.07	1.0 ± 0.54	0.3 ± 0.13	–	–	–	–
C20:5(n-3)	2.5 ± 0.52	4.5 ± 2.02	3.1 ± 0.16	2.4 ± 0.52	4.3 ± 0.98	1.6 ± 0.57	$F_{(2,9)} = 1.3$; $p = 0.310$
C22:3(n-6)	0.1 ± 0.07	0.1 ± 0.04	0.1 ± 0.03	–	–	–	–
C22:4(n-6)	1.9 ± 0.70	2.6 ± 0.82	2.8 ± 0.34	1.7 ± 0.56	2.3 ± 0.50	1.8 ± 0.22	$F_{(2,9)} = 0.2$; $p = 0.816$
C22:5(n-3)	0.5 ± 0.15	0.8 ± 0.42	0.6 ± 0.07	–	0.3 ± 0.32	–	–
C22:6(n-3)	5.7 ± 2.06	6.6 ± 2.30	7.5 ± 0.27	6.0 ± 1.22	8.2 ± 1.13	7.6 ± 0.88	$F_{(2,9)} = 0.1$; $p = 0.867$
Σ PUFA^{NN}	21.5 ± 6.70	26.0 ± 8.38	29.4 ±1.16	20.0 ± 0.41	28.7 ± 3.74	26.4 ± 2.17	$F_{(2,9)} = 1.1$; $p = 0.386$
Unidentified	3.6 ± 1.05	3.6 ± 1.40	4.6 ± 0.37	1.6 ± 0.16	4.2 ± 0.53	3.0 ± 0.18	–

Table 3.9: Fatty acid composition of *Symbiodinium* C100/C118 hosted *in Pocillopora damicornis* sampled from Sylphs Hole, before and after exposure to 16 °C, 24 °C and 28 °C (percentage of total fatty acids). n = 4. Significant differences are indicated in bold, testing the null hypothesis that the responses to 28 °C and 24 °C (^{a}), 16 °C and 24 °C (^{b}), and 16 °C and 28 °C (^{c}) are the same, and that the means of Day 0 and Day 4 are the same (*****), using rmANOVA with *post hoc* Bonferroni-corrected pairwise comparison. ^{NN} Data not normally distributed and statistical results verified using the nonparametric Kruskal-Wallis test. Font colour highlights an increase (red) or decrease (green) of the relative content of the respective fatty acid.

C100/C118 in *Pocillopora damicornis* Sylphs

	Day 0			**Day 4**			**Temperature × Time**
Saturates	**16 °C**	**24 °C**	**28 °C**	**16 °C**	**24 °C**	**28 °C**	
C12:0	0.6 ± 0.04	0.5 ± 0.08	0.5 ± 0.07	1.3 ± 0.21	0.9 ± 0.67	0.4 ± 0.17	$F_{(2,9)} = 0.9$; $p = 0.434$
C13:0	0.4 ± 0.09	0.1 ± 0.04	0.0 ± 0.03	–	–	–	
C14:0	6.3 ± 0.27	6.6 ± 0.27	5.7 ± 0.49	7.1 ± 0.67	6.1 ± 1.15	5.4 ± 1.31	$F_{(2,9)} = 0.3$; $p = 0.730$
C15:0^{NN}	1.9 ± 1.13	0.1 ± 0.02	0.0 ± 0.02	0.0 ± 0.03	1.0 ± 0.49	0.1 ± 0.05	$F_{(2,9)} = 4.1$; $p = 0.053$
C16:0	41.9 ± 4.02	34.7 ± 3.16	36.2 ± 1.12	22.4 ± 7.46	30.9 ± 7.38	32.7 ± 6.74	$F_{(2,9)} = 1.4$; $p = 0.299$
C17:0	0.1 ± 0.05	0.1 ± 0.03	0.0 ± 0.03	–	–	–	
C18:0	10.8 ± 0.24	9.1 ± 0.96	9.3 ± 0.42	12.0 ± 2.73	14.5 ± 3.08	8.1 ± 2.74	$F_{(2,9)} = 1.2$; $p = 0.353$
C20:0	0.5 ± 0.08	0.6 ± 0.17	0.8 ± 0.18	1.1 ± 0.58	1.6 ± 0.57	0.4 ± 0.15	$F_{(2,9)} = 1.8$; $p = 0.227$
C22:0	0.3 ± 0.15	0.2 ± 0.10	0.5 ± 0.17	0.6 ± 0.25	1.7 ± 0.94	0.1 ± 0.09	$F_{(2,9)} = 2.1$; $p = 0.174$
Σ SFA	62.8 ± 5.03	52.0 ± 3.11	53.0 ± 1.26	44.4 ± 3.32	56.6 ± 10.06	47.2 ± 8.77	$F_{(2,9)} = 1.5$; $p = 0.267$
Monounsaturates	**16 °C**	**24 °C**	**28 °C**	**16 °C**	**24 °C**	**28 °C**	
C14:1(n-5)	0.2 ± 0.08	0.4 ± 0.04	0.4 ± 0.04	0.6 ± 0.04	0.8 ± 0.39	0.2 ± 0.08	$F_{(2,9)} = 1.9$; $p = 0.207$

C16:1(n-7)	5.7 ± 0.30	6.5 ± 0.25	6.1 ± 0.50	6.6 ± 1.41	4.5 ± 1.03	4.7 ± 0.77	$F_{(2,9)}$ = 1.5; p = 0.266
C16:1(n-5)	–	–	–	–	0.6 ± 0.21	0.0 ± 0.04	–
C18:1(n-9)cis	4.8 ± 0.16	4.1 ± 0.19	4.7 ± 0.87	11.7 ± 2.98	16.5 ± 3.97	8.0 ± 1.85	$F_{(2,9)}$ = 1.9; p = 0.212
C18:1(n-9)trans	0.4 ± 0.21	0.8 ± 0.16	1.2 ± 0.24	0.9 ± 0.43	3.3 ± 1.16	2.4 ± 1.82	$F_{(2,9)}$ = 0.6; p = 0.581
C20:1(n-9)	0.4 ± 0.25	0.4 ± 0.18	0.6 ± 0.40	0.4 ± 0.27	1.1 ± 0.63	0.1 ± 0.08	$F_{(2,9)}$ = 1.2; p = 0.347
C22:1(n-9)	0.5 ± 0.34	0.5 ± 0.22	1.4 ± 0.19	1.2 ± 0.50	1.1 ± 0.65	0.9 ± 0.52	$F_{(2,9)}$ = 2.8; p = 0.112
Σ MUFA	12.0 ± 0.67	12.7 ± 0.34	14.5 ± 1.01	21.5 ± 4.65	27.9 ± 5.80	16.3 ± 2.88	$F_{(2,9)}$ = 2.0; p = 0.190
Polyunsaturates	**16 °C**	**24 °C**	**28 °C**	**16 °C**	**24 °C**	**28 °C**	
C18:3(n-3)[NN]	1.8 ± 0.61	2.4 ± 0.61	2.2 ± 0.11	2.1 ± 0.37	6.0 ± 2.95	2.9 ± 0.84	$F_{(2,9)}$ = 0.4; p = 0.656
C18:4(n-3)	9.1 ± 0.84	11.2 ± 0.82	9.8 ± 1.06	11.3 ± 0.49 [b]	2.8 ± 1.46[b]*	8.1 ± 2.43	**$F_{(2,9)}$ = 5.8; p = 0.024**
C20:2(n-6)	0.0 ± 0.02	0.1 ± 0.08	0.2 ± 0.18	0.1 ± 0.04	–	0.2 ± 0.12	–
C20:4(n-6)	0.7 ± 0.27	1.1 ± 0.45	1.0 ± 0.09	1.1 ± 0.36	0.1 ± 0.07	1.3 ± 0.45	$F_{(2,9)}$ = 2.1; p = 0.183
C20:4(n-3)	–	0.2 ± 0.13	0.2 ± 0.11	–	–	–	–
C20:5(n-3)	2.0 ± 0.70	3.9 ± 0.47	3.3 ± 0.34	4.0 ± 0.51	1.2 ± 0.65	5.9 ± 2.44	$F_{(2,9)}$ = 3.5; p = 0.077
C22:3(n-6)	0.0 ± 0.03	0.1 ± 0.05	0.0 ± 0.02	–	–	–	–
C22:4(n-6)	1.7 ± 0.34	2.5 ± 0.69	2.4 ± 0.19	1.6 ± 0.24	0.7 ± 0.33	2.8 ± 0.98	$F_{(2,9)}$ = 2.5; p = 0.139
C22:5(n-3)	0.1 ± 0.10	0.2 ± 0.17	0.6 ± 0.32	0.1 ± 0.14	–	1.0 ± 0.88	–
C22:6(n-3)	5.5 ± 1.04	7.9 ± 1.06	8.0 ± 0.27	10.7 ±1.23 [b]*	2.3 ± 0.73[ab]*	9.7 ± 1.77[a]	**$F_{(2,9)}$ = 12.1; p = 0.003**
Σ PUFA	21.1 ± 3.77	29.6 ± 2.48	27.7 ± 1.84	31.0 ± 1.22	14.5 ± 4.65*	32.0 ± 6.35	**$F_{(2,9)}$ = 4.4; p = 0.048**
Unidentified	4.1 ± 0.65	5.7 ± 0.34	4.9 ± 0.46	3.2 ± 0.48	1.0 ± 0.50	4.5 ± 1.20	–

Table 3.10: Fatty acid composition of *Symbiodinium* C111* before and after exposure to 16 °C, 24 °C and 28 °C (percentage of total fatty acids). n = 4. Significant differences ($p \leq 0.05$) are indicated in bold, testing the null hypothesis that the responses to 28 °C and 24 °C ([a]), 16 °C and 24 °C ([b]), and 16 °C and 28 °C ([c]) are the same, and that the means of Day 0 and Day 4 are the same (*****), using rmANOVA with *post hoc* Bonferroni-corrected pairwise comparison. Font colour highlights an increase (red) or decrease (green) of the relative content of the respective fatty acid.

C111* in *Porites heronensis* Sylphs

	Day 0			**Day 4**			**Temperature × Time**
Saturates	**16 °C**	**24 °C**	**28 °C**	**16 °C**	**24 °C**	**28 °C**	
C12:0	0.4 ± 0.15	0.4 ± 0.22	0.3 ± 0.06	0.2 ± 0.03	0.3 ± 0.04	0.2 ± 0.09	$F_{(2,9)} = 0.4$; $p = 0.714$
C13:0	0.1 ± 0.04	0.1 ± 0.07	0.1 ± 0.04	–	–	–	–
C14:0	3.6 ± 1.18	2.4 ± 0.43	2.0 ± 0.18	2.0 ± 0.28	4.1 ± 0.62	2.9 ± 0.54	$F_{(2,9)} = 3.8$; $p = 0.064$
C15:0	0.1 ± 0.04	0.1 ± 0.07	0.5 ± 0.47	0.5 ± 0.35	1.1 ± 0.95	0.1 ± 0.04	$F_{(2,9)} = 1.1$; $p = 0.373$
C16:0	32.3 ± 3.20	23.3 ± 2.43	28.3 ± 1.86	19.1 ± 2.26 [b]*	40.5 ± 2.93 [a, b]*	20.0 ± 1.71 [a]*	**$F_{(2,9)} = 46.5$; $p < 0.001$**
C17:0	0.1 ± 0.04	0.2 ± 0.07	0.1 07	–	0.03 ± 0.03	–	–
C18:0	11.7 ± 1.51	11.0 ± 0.64	11.6 ± 0.62	6.9 ± 2.34 [b]	23.6 ± 1.29 [b]*	9.9 ± 3.38	**$F_{(2,9)} = 5.1$; $p = 0.034$**
C20:0	0.3 ± 0.07	0.3 ± 0.08	0.3 ± 0.06	0.5 ± 0.23	0.9 ± 0.53	0.6 ± 0.18	$F_{(2,9)} = 0.3$; $p = 0.779$
C22:0	0.2 ± 0.11	0.2 ± 0.09	0.5 ± 0.13	0.3 ± 0.29	1.0 ± 0.61	0.5 ± 0.32	$F_{(2,9)} = 1.0$; $p = 0.403$
Σ SFA	48.9 ± 4.21	38.0 ± 2.36	43.7 ± 2.22	29.5 ± 1.5 [b]*	71.5 ± 3.16 [a, b]*	34.15 ± 2.00 [a]*	**$F_{(2,9)} = 78.7$; $p < 0.001$**
Monounsaturates	**16 °C**	**24 °C**	**28 °C**	**16 °C**	**24 °C**	**28 °C**	
C14:1(n-5)	0.4 ± 0.09	0.5 ± 0.09	0.5 ± 0.04	0.3 ± 0.03 [b]	0.1 ± 0.05 [b]*	0.2 ± 0.05*	**$F_{(2,9)} = 5.8$; $p = 0.024$**
C16:1(n-7)	2.6 ± 0.94	1.8 ± 0.18	1.8 ± 0.13	1.3 ± 0.14	1.0 ± 0.16	1.1 ± 0.22	$F_{(2,9)} = 0.01$; $p = 0.992$

C16:1(n-5)	0.1 ± 0.07	0.1 ± 0.09	–	–	0.2 ± 0.13	0.02 ± 0.02	–
C18:1(n-9)cis	8.6 ± 1.49	11.0 ± 0.70	9.6 ± 0.66	13.7 ± 0.70 [b]*	8.4 ± 0.48 [a, b]	14.4 ± 1.46 [a]*	**$F_{(2,9)}$ = 9.4; p = 0.006**
C18:1(n-9)trans	1.4 ± 0.50	1.0 ± 0.18	0.8 ± 0.42	0.3 ± 0.12 [b]	7.1 ± 1.40 [a, b]*	0.9 ± 0.22 [a]	**$F_{(2,9)}$ = 19.3; p = 0.001**
C20:1(n-9)	0.3 ± 0.07	0.4 ± 0.07	0.5 ± 0.06	0.7 ± 0.19	0.1 ± 0.13 [a]	0.9 ± 0.13 [a]	**$F_{(2,9)}$ = 5.5; p = 0.028**
C22:1(n-9)	1.0 ± 0.55	1.3 ± 0.38	1.2 ± 0.18	1.0 ± 0.16	1.9 ± 0.14	1.0 ± 0.27	$F_{(2,9)}$ = 0.9; p = 0.442
Σ MUFA	14.4 ± 1.46	16.2 ± 1.13	14.4 ± 0.39	17.4 ± 0.31	19.0 ± 1.7	18.5 ±1.85	$F_{(2,9)}$ = 0.2; p = 0.822
Polyunsaturates	**16 °C**	**24 °C**	**28 °C**	**16 °C**	**24 °C**	**28 °C**	
C18:3(n-3)	1.2 ± 0.50	1.0 ± 0.16	0.8 ± 0.08	1.1 ± 0.09	0.2 ± 0.08	1.4 ± 0.60	$F_{(2,9)}$ = 2.6; p = 0.127
C18:4(n-3)	7.0 ± 0.99	8.3 ± 1.38	6.9 ± 0.99	5.5 ± 0.88 [b]	1.0 ± 0.51 [a, b]*	3.5 ± 0.48 [a]*	**$F_{(2,9)}$ = 5.3; p = 0.030**
C20:2(n-6)	0.3 ± 0.07	0.5 ± 0.14	0.4 ± 0.08	0.6 ± 0.10	–	0.7 ± 0.10	$F_{(1,6)}$ = 0.002; p = 0.963
C20:4(n-6)	1.2 ± 0.17	1.9 ± 0.40	1.5 ± 0.21	3.0 ± 0.68 [b]*	0.7 ± 0.26 [a, b]*	2.4 ± 0.14 [a]*	**$F_{(2,9)}$ = 20.5; p < 0.001**
C20:4(n-3)	1.1 ± 0.45	1.5 ± 0.29	1.8 ± 0.13	–	–	–	–
C20:5(n-3)	9.8 ± 2.66	14.0 ± 1.69	13.4 ± 0.56	16.4 ± 0.94 [b]*	3.7 ± 1.09 [a, b]*	13.7 ± 1.02 [a]	**$F_{(2,9)}$ = 22.3; p < 0.001**
C22:3(n-6)	–	0.1 ± 0.07	0.2 ± 0.14	–	–	–	–
C22:4(n-6)	3.2 ± 0.36	3.7 ± 0.40	3.6 ± 0.40	6.4 ± 0.39 [b]*	1.0 ± 0.56 [a, b]*	5.5 ± 0.40 [a]*	**$F_{(2,9)}$ = 31.6; p < 0.001**
C22:5(n-3)	1.6 ± 0.35	2.3 ± 0.65	2.2 ± 0.09	4.6 ± 0.31 [b]*	0.5 ± 0.49 [a, b]*	4.1 ± 0.47 [a]*	**$F_{(2,9)}$ = 19.6; p = 0.001**
C22:6(n-3)	7.3 ± 0.72	8.8 ± 1.16	7.9 ± 1.28	10.0 ± 0.42[b]	2.0 ± 1.18[a, b]*	11.5 ± 1.13 [a]	**$F_{(2,9)}$ = 16.9; p = 0.001**
Σ PUFA	33.5 ± 3.24	42.1 ± 3.19	38.7 ± 2.18	47.7 ± 1.02 [b]*	9.1 ± 3.14 [a, b]*	43.3 ± 2.27 [a]	**$F_{(2,9)}$ = 65.2; p < 0.001**
Unidentified	3.2 ± 0.61	3.7 ± 0.22	3.2 ± 0.42	0.38 ± 0.14	5.5 ± 0.62	4.1 ± 0.21	–

3.4 Discussion

It is not known whether the composition of thylakoid fatty acids (FAs) is a primary determinant of the thermal robustness or sensitivity of PSII in *Symbiodinium* cells (Tchernov et al. 2004; Díaz-Almeyda et al. 2011), and hence whether it is central to the loss of photosynthetic efficiency that often accompanies thermal bleaching (Takahashi et al. 2013). The present study showed that distinct *Symbiodinium* types in symbiosis with different coral species vary in their baseline FA composition of membranes enriched in thylakoids. This agrees with earlier findings, which demonstrated species-specific differences in the composition of total cellular FAs (Bishop and Kenrick 1980; Mansour et al. 1999; Zhukova and Titlyanov 2003) and FAs of photosynthetic membranes (Díaz-Almeyda et al. 2011) in this genus. Furthermore, *Symbiodinium* types or consortia in the current study varied in their flexibility to modulate thylakoid FA quality under short-term cold and heat stress, but this flexibility was neither a sole function of *Symbiodinium* type nor dependent on the species of coral host. Modulations under thermal (both heat and cold) stress included an increase in the relative content of long-chain polyunsaturated fatty acids (LC-PUFAs), i.e. PUFAs with a chain length of 20 or 22 carbons. However, these modifications were not related to benefits or impairment of PSII fluorescence at a certain temperature. These results indicate that, in thermally stressed *Symbiodinium* cells, the maintenance or limits of photosynthetic performance, estimated as chlorophyll fluorescence of PSII, are not dependent on the relative degree of thylakoid FA unsaturation and the related physiochemical properties of the thylakoid membrane, but rather raise questions about alternative roles of LC-PUFAs during cold and heat stress. These observations are discussed further below.

3.4.1 Response to short-term cold stress

In *Symbiodinium* spp., cold stress is linked to a decline in photosynthesis (Steen and Muscatine 1987) which can be estimated by a down-regulation of maximum photochemical quantum yield (F_v/F_m) measured as chlorophyll fluorescence (Saxby et al. 2003; Thornhill et al. 2008; Roth et al. 2012). Declines in F_v/F_m at low temperatures have been linked to decreased activities of enzymes involved in carbon fixation (Saxby et al. 2003; Roth et al. 2012) and/or reduced photosynthetic membrane fluidity (Thornhill et al. 2008). Membrane fluidity is

determined by properties of the FA chain constituents of thylakoid lipids and other membrane-stabilizing components (Guschina and Harwood 2006a). In general, membranes with a higher content of unsaturated, shorter, and/or branched FA chains have a lower melting point and are more fluid at a given temperature than are membranes with a higher content of saturated, longer and/or un-branched FA chains (Iba 2002; Morgan-Kiss et al. 2006). Although a variety of responses to cooler temperatures can be observed, increasing the level of FA unsaturation is the most common acclimatory mechanism among organisms such as poikilothermic animals, vascular plants, algae and microbes (Guschina and Harwood 2006b). The universally conserved response mechanism is believed to counterbalance the increasing rigidity of membranes under cold stress, although the roles of highly unsaturated FAs may be more complex (Guschina and Harwood 2006b). In cyanobacteria, FA unsaturation is a rapid response since the enzymes catalyzing the introduction of double bonds into membrane-integrated FAs, the acyl-lipid desaturases, are bound to the thylakoid membrane (Murata and Wada 1995).

In this study, short-term cold stress caused substantial reductions in F_v/F_m, and increased excitation pressure over PSII (Q_m) in all coral-*Symbiodinium* associations. The down-regulation of F_v/F_m may be considered as photoprotective because no adverse effects of cold stress on pigment concentration or *Symbiodinium* cell density were observed. Coral species differed in their PSII capacity under cold stress, but the differences were not reflected in the composition of photosynthetic-membrane FAs or their adjustment under cold stress. For example, cold stress caused severe reductions in F_v/F_m and suppressed non-photochemical quenching (NPQ) in *P. damicornis* sampled from Sylphs Hole. Its symbionts of the ITS2 type C100/C118 adjusted thylakoid FAs in response to cold stress by increasing the relative content of the polyunsaturated FA C22:6(n-3), which in turn contributed to an increase in the relative content of long-chain C22 FAs. While increased unsaturation is expected to lower the melting point and increase the fluidity of the thylakoid membrane, the concomitant increase of very long chain FAs relative to shorter carbon chains may counteract this effect. Changes in FA unsaturation may further cause changes in the mobility of plastoquinone, membrane transporters and channels (reviewed in Bienert et al. 2006). On the other hand, the same *Symbiodinium* consortium (C100/C118) in the same coral species sampled from a different location at Lord Howe Island (Stephens Hole), with highly similar thylakoid FA baseline compositions, showed no adjustment response to chilling temperatures and maintained slightly, but significantly higher, F_v/F_m values after 4 days of cold

stress. Similarly, *Symbiodinium* C111* had a considerably higher relative content of baseline MUFAs and PUFAs compared to *Symbiodinium* C100/C118 from both sampling locations. However, although in response to cold stress, the level of unsaturation increased, F_v/F_m was not enhanced over that of C100/C118 from Stephens Hole. Perhaps, the simultaneous, relative increase in long-chain FAs at the expense of short-chain FAs counterbalanced the effect of MUFAs and PUFAs, and prevented an overall lowering of the melting point. Interestingly, F_v/F_m was slightly but significantly higher in *Symbiodinium* C111* than C100/C118 from the same location. Because Sylphs Hole is characterized by higher turbidity (Wicks et al. 2010a) than Stephens Hole, it is intriguing to speculate that different capabilities to increase thylakoid membrane fatty acid unsaturation under thermal stress depend on the nutritional status/availability of energy reserves in the respective coral host. Certainly, biosynthesis of FAs or enzymes necessary for the modulation of FAs depends on the allocation of carbon, either through photosynthesis by the algae (Papina et al. 2007) or heterotrophic feeding by the coral host (Houlbreque and Ferrier-Pagès 2009; Tolosa et al. 2011).

Taken together, the data indicate that cold susceptibility of PSII is not associated with the overall membrane fluidity determined by FA unsaturation or chain length of the thylakoid FAs.

3.4.2 Response to short-term heat stress

F_v/F_m, NPQ, Q_m, *Symbiodinium* cell density, and *Symbiodinium* pigment profile, were not affected in any of the corals by short-term exposure to ~ 3 °C above the bleaching threshold (www.coralreefwatch.noaa.gov). Furthermore, thylakoid FA composition in *Symbiodinium* C100/C118 from both locations was not affected by heat stress. However, quite unexpectedly, under high temperature *Symbiodinium* C111* showed very similar dynamics of thylakoid membrane FA elongation and desaturation to those seen under cold stress. These modifications included alterations that would be expected to lower the melting point of the membranes: an overall reduction in the relative content of SFAs, mainly C16:0, and an increase in the relative content of C20 and C22 PUFAs. Moreover, the relative content of the branched FA C18:1(n-9)cis increased; this is believed to enhance the 'free volume' of the thylakoid bilayer and hence fluidity of the membrane (Heipieper et al. 2003). Simultaneously, C18:4(n-3) decreased, resulting in a substantially higher ratio of C18:1 to C18:4 than at the beginning of the experiment. Tchernov et al. (2004) used this ratio to differentiate between thermally robust and

sensitive *Symbiodinium* strains. In their study, *Symbiodinium* strains exhibiting losses of thylakoid integrity and photochemical efficiency, and increased ROS concentrations had a lower ratio of C18:1 to C18:4 compared to those *Symbiodinium* types that showed the opposite cellular and molecular responses. In contrast, Díaz-Almeyda et al. (2011) could not find a correlation between the ratio of C18:1 to C18:4 and the melting point of the respective thylakoid membranes in *Symbiodinium*. In the present study, exposure to 24 °C resulted in a similar decrease in the relative content of C18:4 compared to C18:1, indicating that temperature-independent factors might be responsible for this adjustment.

Taken together, heat stress resulted in a change of FA composition in C111*, yet whether this response helped the *Symbiodinium* cell to tolerate heat stress needs further exploration.

3.4.3 Thylakoid fatty acid adjustments independent from thermal stress

In the present study, thylakoid FAs were also remodeled when exposed to 24 °C, which corresponded to the actual sea temperature in the lagoon at the time of the experiment. The adjustments were evident in *Symbiodinium* types C100/C118 and C111* hosted in *P. damicornis* and *P. heronensis* sampled from Sylphs Hole, but not in C100/C118 hosted in *P. damicornis* sampled from Stephens Hole. *Symbiodinium* C100/C118 reduced the relative content of the PUFAs C18:4(n-3) and C22-6(n-3), while *Symbiodinium* C111* reduced the relative content of all PUFAs and simultaneously increased the relative content of the SFAs C16:0 and C18:0. The reduced PUFA levels and increased SFA levels could be a response to nutrient limitation in these species. Originating from Sylphs Hole, a reef site with potentially higher nutrient load compared to Stephens Hole due to a 1.8 fold increase in turbidity (Wicks et al. 2010a), *Symbiodinium* cells might have responded to the comparable lower nutrient availability in the flow-through seawater from the lagoon. A similar reduction in the relative content of the major PUFAs C18:4(n-3), C20:5(n-3) and C22:6(n-3), and an increase in the relative content of C16:0 has been observed before in the total lipids of the dinoflagellate *Gymnodinium* sp, in response to nutrient limitation (probably phosphorus) (Reitan et al. 1994).

3.4.4 Conclusion

It can be concluded that the capability to adjust FA unsaturation/elongation in photosynthetic membranes, in response to changes in temperature, seems to be dependent on *Symbiodinium* type and environmental conditions/history. Furthermore, this study demonstrates that in *Symbiodinium* C111* the responses of thylakoid FAs to short-term cold and heat stress are highly similar, suggesting a common trigger of the enzymes that catalyze these modifications. Increased levels of unsaturation did not enhance PSII capability under cold stress, nor impair PSII efficiency under heat stress. The absence of such a correlation suggests that the photosynthetic transport of electrons is unaffected by the overall degree of thylakoid FA unsaturation and hence thylakoid membrane fluidity, as has also been reported for cyanobacteria (Gombos et al. 1994; Wada et al. 1994; Nanjo et al. 2010). In cyanobacteria, it has been hypothesized that FA unsaturation might actually stabilize the thylakoid membranes against heat stress (Gombos et al. 1994). Perhaps biosynthesis of certain FAs is needed for the binding of membrane-stabilizing proteins (Takahashi et al. 2013). Alternatively, it has been suggested that FA unsaturation could provide protection from oxidative stress in single-celled eukaryotes (Guerzoni et al. 1997; Guerzoni et al. 2001). All acyl-lipid desaturases need molecular oxygen (Sayanova et al. 1997), and in plant cells and cyanobacteria these enzymes use ferredoxin as an electron donor (Murata and Wada 1995). Hence, the unsaturation of membrane bound FAs consumes oxygen and provides a sink for electrons that could reduce the generation of ROS in the chloroplast. This mechanism disagrees with the traditional idea that PUFAs are apparently very susceptible to ROS (Halliwell 1987). However, an increasing body of evidence suggests that PUFAs, especially C22:6(n-3) and C20:5(n-3), are relatively unaffected by oxidative damage when they are *in vivo* (Yazu et al. 1998; Araseki et al. 2005; Okuyama et al. 2008) and that they could indeed have an antioxidant function. Okuyama et al. (2008) demonstrated that the biosynthesis of C20:5(n-3) is associated with an antioxidant function that protects *Escherichia coli* and the marine bacterium *Shewanella marinitestina* from exogeneous H_2O_2 (Okuyama et al. 2008). In the present study, in *Symbiodinium* C111*, C20:5(n-3) (alongside other PUFAs), increased in response to both cold and heat stress. If the synthesis of C20:5(n-3) is photoprotective, via the utilization of excess electrons, then one would expect a lower pressure over the photosystem which was not evident in this study. Hence, direct or indirect evidence for an antioxidant function for C20:5(n-3) in dinoflagellates is not provided. It would be instructive

to combine FA analysis with the analysis of intracellular ROS concentrations or the quantification of lipid peroxidation, to assess the importance of PUFAs in controlling oxidative stress in *Symbiodinium* cells.

4 Chapter 4:
PSII activity and antioxidant capacity in high latitude *Symbiodinium* spp. exposed to short-term cold and heat stress

4.1 Introduction

Reef-building corals associate with eukaryotic microalgae within the genus *Symbiodinium*. This symbiosis is particularly important in the oligotrophic waters of the tropics due to the translocation of photosynthate from algal cells to animal tissue (Falkowski et al. 1984; Muscatine et al. 1984) and the recycling of inorganic nutrients (Trench 1979), but also extends to sub-tropical and temperate waters at higher latitudes. The survivorship of reef-building corals is determined by thresholds of minimum aragonite saturation, light availability and sea water temperature (Kleypas et al. 1999). Sea water temperature in particular has been identified as a primary determinant of coral health (Hoegh-Guldberg 1999). At high latitudes, sea water temperatures are generally lower and can show more significant annual fluctuations than tropical sites (Kleypas et al. 1999). While corals at low latitudes usually experience seasonal temperature fluctuations of as little as 2 - 3°C, corals at high latitudes can cope with annual temperature fluctuations of more than 13 °C (reviewed in Brown and Cossins 2011). For example, at Lord Howe Island (LHI; 31°33′S, 159°05′E), the world's southernmost coral reef located in New South Wales, Australia, maximum monthly mean temperatures range between 18 °C and 24 °C, with a temperature minimum of 14.5 °C and maximum of 28 °C recorded in the past 10 years (www.data.aims.gov.au). Temperature increases of as little as 1 – 2 °C for extended periods may result in a break-down of the coral-*Symbiodinium* partnership (Hoegh-Guldberg 1999). A similar stress reaction can be observed when temperatures fall below the minimum requirements (Steen and Muscatine 1987; Saxby et al. 2003; Hoegh-Guldberg and Fine 2004). The break–down of the symbiosis is mainly associated with bleaching. i.e. the loss of *Symbiodinium* cells and/or their pigments (Falkowski and Dubinsky 1981; Hoegh-Guldberg 1999), which can lead to a decline in coral health and increased coral mortality (Goreau and Macfarlane 1990; Jones 2008).

It is widely acknowledged that, besides thermal history, the particular combination of coral host and dinoflagellate symbiont, commonly distinguished by the ITS2 region of its ribosomal DNA (LaJeunesse 2001), determines the susceptibility to thermal bleaching and coral mortality (Sampayo et al. 2008; Fitt et al. 2009; Fisher et al. 2012). As demonstrated in Chapter 2, it appears that most coral-*Symbiodinium* associations at the high latitude reef of LHI are better adapted to short-term cold stress (5-day exposure to a mean temperature of 15 °C) than to short-term heat stress (5-day exposure to a mean temperature of 29 °C). Yet, the ability to withstand cold temperatures was not consistently associated with enhanced use of xanthophyll-mediated heat dissipation, a major photoprotective mechanism in *Symbiodinium* cells. Likewise, differential susceptibility of various coral-*Symbiodinium* combinations to short-term heat stress could not be explained by differential use of xanthophyll-mediated heat dissipation alone, suggesting that a different cellular mechanism, or suite of cellular mechanisms, might determine thermal susceptibility.

Various studies have pointed towards reactive oxygen species (ROS) as being central to the cellular mechanism of bleaching (Lesser and Shick 1989; Smith et al. 2005; Suggett et al. 2008; Lesser 2011). Aerobic life is fuelled by redox reactions where reductive processes (gain of an electron) store energy and oxidative processes (loss of an electron) release it. These processes take place in chloroplasts and mitochondria, and continuously generate ROS as by-products when a small proportion of electrons leak from the electron transport chain directly onto oxygen, even under normal metabolic and photosynthetic conditions (Foyer et al. 1994; Møller 2001). Thus, the highly reactive superoxide anion (O_2^-), and in subsequent reduction processes numerous other ROS including hydrogen peroxide (H_2O_2) and the hydroxyl radical (•OH) are generated. Additionally, singlet oxygen ($^1O_2$) can be produced in chloroplasts by photoexcitation of chlorophyll, triplet chlorophyll formation and its reaction with oxygen (Halliwell 2006; Nishiyama et al. 2006). In small doses ROS are important messenger and signalling molecules (Apel and Hirt 2004; Foyer and Noctor 2005), and ROS formation in chloroplasts may be photoprotective because it may effectively dissipate excess excitation energy (Asada 2000). However, in excess concentrations, ROS may be cytotoxic (Halliwell 2006), inhibit the protein translation machinery (Nishiyama et al. 2006; Takahashi and Murata 2008) and/or induce apoptotic programmed cell death (Franklin et al. 2004; Tchernov et al. 2011).

To maintain the protective and signalling properties of ROS while preventing any adverse effects, it is a requirement that their concentrations are tightly controlled. In chloroplasts, ROS generation can be minimized either through effective dissipation of excess energy at the light-harvesting antennae, effective utilization of electrons in downstream processes, or effective scavenging of ROS by antioxidant enzymes or compounds (Halliwell 2006; Murata et al. 2012). Antioxidant enzymes in the chloroplast include superoxide dismutase (SOD), which catalyzes the conversion of O_2^- to H_2O_2, and ascorbate peroxidase (APX), which catalyzes the conversion of H_2O_2 to water in the so-called water-water-cycle (Asada 1999). These enzymes act in concert with other enzymes such as catalase and small antioxidant compounds including tocopherols, ascorbate, carotenoids and glutathione to control the intracellular concentration of ROS (Halliwell 2006).

The balance between production and scavenging of ROS can be disturbed by stressors including high or low temperatures (Apel and Hirt 2004). The resulting imbalance of production and scavenging of ROS in favour of the former, results in oxidative stress (Sies 1991). Oxidative stress and the antioxidant capacity have been linked to thermal bleaching susceptibility of the symbiotic coral (Downs et al. 2000; 2002). Indeed, in heat-stressed cultured *Symbiodinium* cells, accumulation of ROS has been observed (Tchernov et al. 2004; Suggett et al. 2008; McGinty et al. 2012) as it also has in heat-stressed cnidarian host tissue (Nii and Muscatine 1997; Dunn et al. 2012). Similarly, oxidative degradation of DNA, proteins and/or lipids has been reported under bleaching conditions in *Symbiodinium* cells and/or cnidarian host tissue (Downs et al. 2000; Flores-Ramírez and Liñán-Cabello 2007; Richier et al. 2008; Fitt et al. 2009; Yakovleva et al. 2009). ROS generation in symbionts is influenced by the intensity of photosynthetically active radiation (PAR) or ultraviolet radiation (UVR), as has been demonstrated by irradiance-dependent production of SOD and other ROS-scavenging enzymes (Lesser and Shick 1989; Shick et al. 1995; Lesser 1996). Furthermore, it has been demonstrated that H_2O_2 production (Suggett et al. 2008) and antioxidant capacity (McGinty et al. 2012) differ between different cultured *Symbiodinium* types. These results suggest that in *Symbiodinium*, a greater pool of ROS-scavenging enzymes or the capability to adjust their pool sizes might be important factors influencing the tolerance of the holobiont, i.e. the coral and its associated symbionts, to changing temperatures.

This study tested the hypothesis that high latitude corals at Lord Howe Island are able to deal with temperature fluctuations, and in particular cooler temperatures, because they adjust their SOD and APX activity to changing temperature. To address this question, the thermal sensitivity (expressed as mortality or sub-lethal bleaching), PSII activity (estimated by chlorophyll fluorescence), and SOD and APX capacities in a variety of *Symbiodinium* types and consortia (C3, C100/C118 and C117) harboured by the coral species *Acropora solitariensis*, *Isopora palifera*, *Pocillopora damicornis* and *Porites heronensis* were analyzed in response to short-term cold and heat stress.

4.2 Materials and methods

4.2.1 Sampling and experimental procedure

The experiment was performed at Lord Howe Island (31°33′S, 159°05′E), New South Wales, Australia, which is the world's southernmost coral reef (Harriott et al. 1995). In September 2011, three coral fragments, with a size of approximately 10 cm (branching corals) or 10 cm^2 (massive corals) each, from each of four replicate colonies of *Acropora solitariensis*, *Isopora palifera*, *Pocillopora damicornis* and *Porites heronensis* (Table 4.1) were sampled in the western lagoon (S31°31′937″, E159°03′251″) at a depth of 0.5 – 3 m at low tide. All coral species were identified based on the morphological characteristics described in Veron and Stafford-Smith (2000). Immediately after sampling, the fragments of each replicate coral were split into a total of 22 explants (*A. solitariensis* and *P. damicornis*) or 13 explants (*I. palifera* and *P. heronensis*), with each explant being 1 – 2 cm in size. One explant of each replicate coral colony was stored in NaCl-saturated 20% dimethyl sulfoxide (DMSO) buffer for subsequent *Symbiodinium* genotyping. The remaining explants were split in three groups of equal size and acclimatized in three aerated 50-L tanks which were supplied with unfiltered seawater from the lagoon at a flow rate of ~ 80 L per hour for four days. On Day 1 of the experiment, at 6:00 h, the temperature in one of the tanks was lowered to 15 °C ± 0.1 (mean ± S.E.) (corresponding to 3 °C below the monthly temperature minimum), increased to 29 ± 0.1 °C (corresponding to 5 °C above the monthly temperature maximum), or maintained at the ambient lagoon temperature of 19 ± 0.1 °C. The adjusted temperatures were attained by 6:30 h (15 °C) and 9:00 h (29 °C). Tanks were shaded (approximately 50% sunlight) during both acclimation and the experiment.

Irradiation and temperature were monitored using a HOBO pendant logger which was calibrated with a Li-Cor LI-189 photometer (Li-Cor, USA). Light intensities peaked at 1242, 1133, 614, 1060, and 1302 µmol photons m^{-2} s^{-1} on Days 0, 1, 2, 3, and 4, respectively. Between 14:00 h and 15:00 h on Days 0 and 4, one explant (*I. palifera* and *P. heronensis*) or two explants (*A. solitariensis* and *P. damicornis*) from each coral colony were frozen in liquid nitrogen, stored at -20 °C for the remainder of the experiment, transported on dry ice and stored at -80 °C until analysis. For *A. solitariensis* and *P. damicornis*, two explants per coral colony were frozen at each time-point and pooled for downstream analysis, to compensate for their lower biomass compared to the other two coral species (Loya et al. 2001).

4.2.2 Chlorophyll fluorescence

Chlorophyll fluorescence of PSII was measured using a diving pulse amplitude modulated (PAM) fluorometer (Walz, Germany), with these settings: measuring intensity 5; saturation intensity 8; saturation width 0.8; and gain 2 – 3. Maximum quantum yield of PSII (F_v/F_m) was recorded each day after sunset (18:00 h) and before dawn (06:00 h). Effective quantum yield of PSII ($\Delta F/F_m'$) was measured between 12:00 h and 12:45 h. Excitation pressure over PSII (Q_m) (Iglesias-Prieto et al. 2004) was calculated as in Fisher et al. (2012):

Q_m = 1 - [($\Delta F/F_m'$) at noon/(F_v/F_m) at dawn of Day 0]

4.2.3 Sample preparation

All steps were performed at 4 °C. Coral fragments were airbrushed in a defined volume of phosphate buffer (50 mM $NaPO_4$, 0.1 mM EDTA, pH 7.8) and the homogenate centrifuged for 5 min at 800 × g at 4 °C. The algal pellet was then re-suspended in phosphate buffer and centrifuged a further four times, as previously described, to clean the *Symbiodinium* cells of coral tissue. The *Symbiodinium* cell pellet was re-suspended in 10 mL phosphate buffer, from which 2 mL were removed for chlorophyll (chl) determination, and 500 µL were removed for cell counts. Cell counts were performed in six replicate counts using a haemocytometer and cells were standardized to cm^2 coral surface area (Stimson and Kinzie 1991). The remaining 7.5 mL were centrifuged (4000 × g for 5 min at 4 °C) and re-suspended in 500 µL phosphate buffer for cell lysis. *Symbiodinium* cells were ruptured using 710 – 1180 µm glass beads (Sigma, Australia)

at 50 Hz for 3 min at 4 °C in a Tissue Lyser LT, Qiagen (Australia). The cell lysate was centrifuged immediately at 16000 × g for 10 min at 4 °C. The cell lysate was frozen in four aliquots of 80 µL each at -80 °C for subsequent determination of protein content, and APX and SOD activity. All assays were performed within 10 days of cell lysis.

4.2.4 *Symbiodinium* genotyping

Symbiodinium ITS2 identity was determined as described in Chapter 3, Section 3.2.2 (see page 91) using denaturing gradient gel electrophoresis (DGGE). Briefly, to isolate genomic DNA (gDNA), preserved *Symbiodinium* cells were broken in a Tissue Lyser LT (Qiagen, Australia) bead mill for 10 min at 50 Hz at 4 °C in Tris buffer (0.01 M, pH 8.0). Next, gDNA was precipitated in isopropanol. Precipitated gDNA was washed in 70% ethanol and then eluted and stored in sterile water, using the volumes given in Chapter 3. The ribosomal ITS2 region was PCR-amplified using the primers itsD (Pochon et al. 2007) and ITS2CLAMP (LaJeunesse 2002), using the protocol outlined in Chapter 3. Amplicons were separated using DGGE (Biorad DCode system) as described in detail in Chapter 2. DGGE fingerprints were compared to fingerprints of known *Symbiodinium* ITS2 populations. DGGE bands that could not be identified were removed, eluted in water, re-amplified by PCR, and sequenced in forward and reverse directions at Macrogen, South Korea, with the primer set ITSD and ITS2REVint (5′-CCATATGCTTAAGTTCAGCGGG-3′) as described in detail in Chapter 2.

4.2.5 Chlorophyll determination

Chlorophyll concentration was determined in 90% acetone. A cell suspension of 1.5 mL was pelleted at 16000 × g and 4 °C for 10 min, re-suspended in 1.5 mL acetone and extracted for 36 h in the dark at 4 °C. Absorbance was measured in triplicates for each sample (300 µL) at A_{630} and A_{664} in 96-well plates (Greiner Bio-one, Germany) on an EnSpire^{TM} 2300 Multilabel Reader (Perkin Elmer Inc., USA). Concentrations for chlorophyll *a* and chlorophyll c_2 were calculated using the equation by Jeffrey and Humphrey (1975) using the corrected coefficient for dinoflagellates (Ritchie 2006), and the corrected path-length of 0.8679.

4.2.6 Ascorbate peroxidase (APX) assay

APX activity in *Symbiodinium* fractions was estimated following the technique of Nakano and Asada (1981). The method is based on the capacity of APX to scavenge H_2O_2 (Sigma, Australia) using L-ascorbate (Sigma, Australia) as an electron donor. The assay was performed at 25 °C in a reaction volume of 1 mL in a UV-proof cuvette (Global Science, New Zealand) on a Shimadzu UV-2550 spectrophotometer. The reaction contained 350 µM L-ascorbate and 100 µM H_2O_2 in 50 mM sodium phosphate buffer, 0.1 mM EDTA, pH 7.8. The reaction was started by addition of H_2O_2, and the subsequent decrease of absorbance at 290 nm was measured spectrophotometrically every 10 s for 200 s. The activity of APX in samples was calculated by the equation of Lambert-Beer, using the absorbance coefficient of 2.8 mM^{-1} cm^{-1} (Nakano and Asada 1981). The activity of APX is presented as the amount of enzyme that is required to convert 1 µmol of H_2O_2 per minute (unit) per mg total soluble protein, as determined using the method of Bradford (1976) in triplicates for each sample (20 µL) in 96-well plates (Greiner Bio-one, Germany).

4.2.7 Superoxide dismutase (SOD) assay

SOD activity in *Symbiodinium* fractions was estimated following a spectrophotometric Riboflavin/NitroBlue Tetrazolium (RF/NBT) assay (Beauchamp and Fridovich 1971; Beyer Jr and Fridovich 1987). Here, under illumination and in aerobic conditions, riboflavin is reduced by L-methionine and generates O_2^-. NBT is reduced by O_2^- and changes colour from yellow to blue upon reduction, which can be monitored spectrophotometrically. This change in colour is influenced by SOD present in the reaction because it scavenges O_2^- and consequently inhibits the photoreduction of NBT. The reaction was performed in technical triplicates in 96-well microtiter plates, using 20 µL cell lysate or SOD standard (Sigma, Australia) in a final volume of 300 µL 50 mM sodium phosphate buffer pH 7.8, 0.1 mM EDTA, 1.3 µM riboflavin, 10 mM L-methionine, 57 µM NBT and 0.025% Triton-X100. Absorbance was measured at 560 nm immediately prior to and after 10 min of exposure to light (130 µmol photons m^{-2} s^{-1}). Bovine SOD was used as a standard and a sigmoidal 5-parameter semi-logarithmic standard curve was fitted to determine SOD activity in samples. The activity of SOD is presented as units, which is

the amount of SOD inhibiting 50% of the reduction of O_2^- by NBT, expressed per mg *Symbiodinium* soluble protein quantified using the technique of Bradford (1976).

4.2.8 Statistical analysis

Data were analyzed using the IBM SPSS statistics 20.0 software (SPSS Inc, Chicago). Repeated measures analysis of variance (rmANOVA) and *post hoc* pairwise comparison with Bonferroni adjustment were used to test parameters. If necessary, parameters were transformed to meet assumptions of normality. When assumptions of equality of the variances (Mauchly's test) were violated, the Greenhouse-Geisser correction is reported. Univariate ANOVA with *post hoc* Tukey HSD was used to test for differences of baseline parameters (on Day 0).

4.3 Results

4.3.1 *Symbiodinium* genotyping

Both *Acropora solitariensis* and *Isopora palifera* pre-dominantly harboured identical *Symbiodinium* ITS2 types with high similarity to C3 (280/283 basepairs; Table 4.1). Alignments showed that these ITS2 sequences are identical to *Symbiodinium* sequences HM031101 and HM031102 derived from symbionts harboured by *Acropora millepora* at Heron Island, Australia (Fisher et al. 2012), but differs by three basepairs to *Symbiodinium* C3 available on GeoSymbio (Franklin et al. 2012). Therefore, this type is hereafter referred to as sequence C3*. *Pocillopora damicornis* explants harboured *Symbiodinium* ITS2 types C100/C118 (Table 4.1). *Porites heronensis* pre-dominantly harboured *Symbiodinium* ITS2 type C117. For sequences refer to Appendix A.3 on pages 258 – 259).

Table 4.1: Coral species and *Symbiodinium* type identified by denaturing gel gradient electrophoresis (DGGE) of the internal transcribed spacer 2 (ITS2) region.

Coral species (n = 4)	***Symbiodinium* ITS2 type**
Acropora solitariensis	C3*
Isopora palifera	C3*
Pocillopora damicornis	C100/C118
Porites heronensis	C117

4.3.2 Mortality and bleaching

At both 15 °C and 29 °C, 37.5% of *I. palifera* coral explants had died by 18:00 h of Day 3 in each of the low-temperature and high-temperature treatments. In this species, 12.5% of coral explants had died by the same time-point in the control treatment. Mortality was not observed in any of the other corals. In all coral species, bleaching was more severe under elevated than decreased temperature (Figure 4.1). *Symbiodinium* cell densities *in A. solitariensis* were reduced to 45.8% of initial values at 15 °C and to 22.8% at 29 °C. In *I. palifera*, *Symbiodinium* cell densities declined to 51.5% of initial values at 15 °C (Tables 4.2, 4.3; Bonferroni: $p = 0.001$), and to 21.2% at 29 °C ($p < 0.001$). In *P. damicornis*, *Symbiodinium* cell densities declined to 53.5% of initial values at 15 °C ($p = 0.015$) and to 11.3% at 29 °C ($p = 0.002$). In *P. heronensis* cell densities declined to 14.1% of initial values at 29 °C ($p = 0.001$), but remained stable over the 4-day period at 15 °C. The concentration of cellular chlorophyll *a* reflected the response of cell density (Figure 4.1, Table 4.2, 4.3), except in *P. heronensis*, which lost cells but not chlorophyll *a* at 29 °C. The concentration of chlorophyll c_2 was stable over time in all coral species (Figure 4.1 A – L, Table 4.2, 4.3).

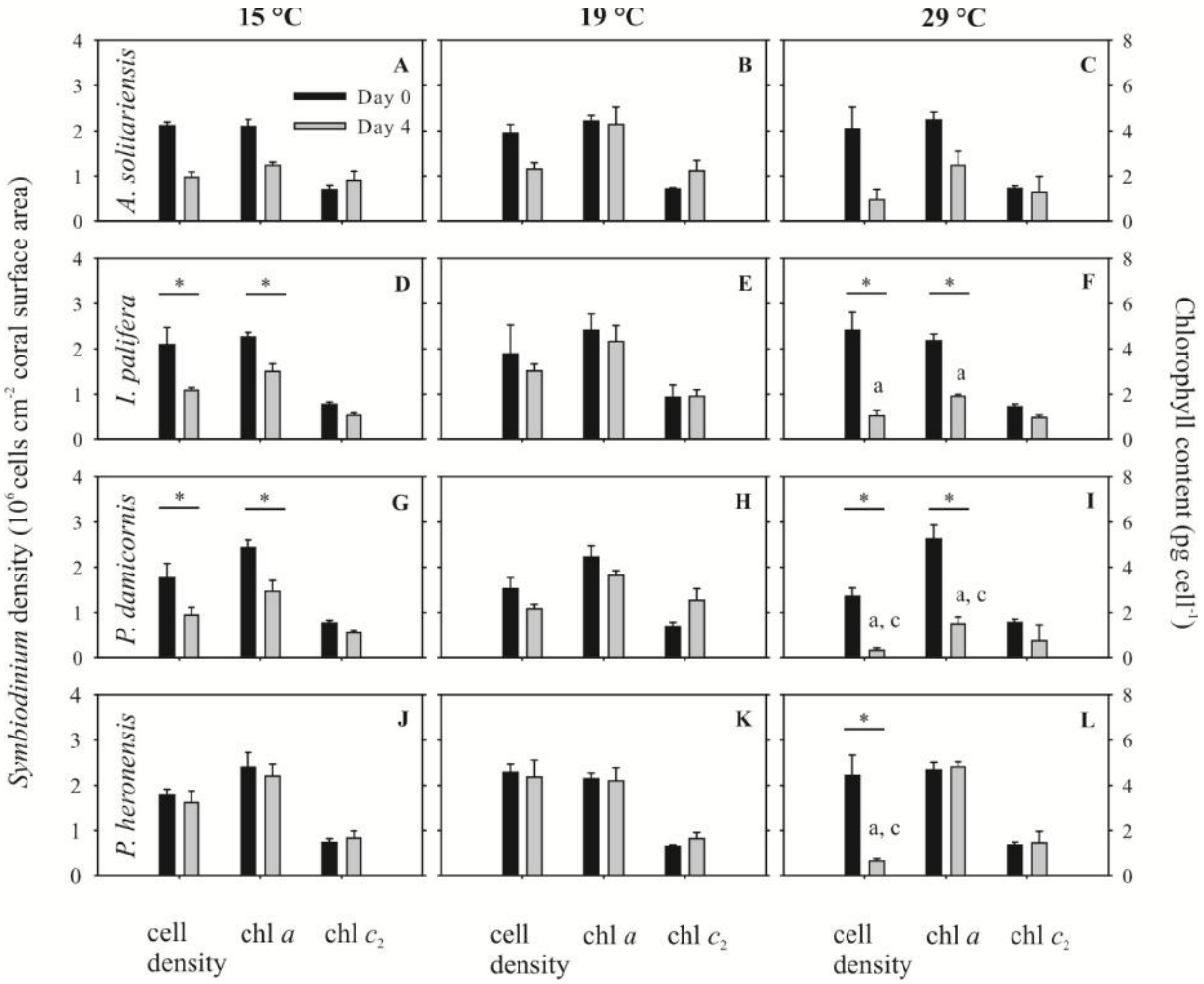

Figure 4.1: *Symbiodinium* density in 10^6 cells cm^{-2} coral surface area (left y-axis) as well as chlorophyll *a* and c_2 content in pg $cell^{-1}$ (right y-axis) for Day 0 (black bars) and Day 4 (grey bars) at the temperatures 15 °C (left vertical lane), 19 °C (middle vertical lane) and 29 °C (right vertical lane) in the coral species *Acropora solitariensis* (first horizontal lane), *Isopora palifera* (second horizontal lane), *Pocillopora damicornis* (third horizontal lane) and. *Porites heronensis* (forth horizontal lane). Legend in A is valid for all graphs. Asterisks indicate significant differences between days 0 and 4 ($p \leq 0.05$). Letters indicate significant differences between 29 °C and 19 °C (a), 15 °C and 19 °C (b) and 15 °C and 29 °C (c) as revealed by rmANOVA and *post hoc* Bonferroni.

Table 4.2: Results of rmANOVA for the parameters: *Symbiodinium* density (SD); chlorophyll (chl) *a* concentration (pg cell^{-1}); chl c_2 concentration (pg cell^{-1}); maximum quantum yield (F_v/F_m); excitation pressure (Q_m); superoxide dismutase (SOD) and ascorbate peroxidase (APX). Significant effects on the level of $p \leq 0.05$ are highlighted in bold, non-significant effects ($p > 0.05$) are presented in grey. df = degrees of freedom; Temp = temperature †; indicates that Greenhaus-Geisser correction is reported.

Parameter		Time	Time × Temp	Time × Species	Time × Temp × Species	Temp	Species	Temp × Species
SD	*F*	**81.5**	**18.8**	0.7	1.8	**7.4**	**6.4**	2.1
	df	**1, 34**	**2, 34**	3, 34	6, 34	**2, 34**	**3, 34**	6, 34
	p	**< 0.001**	**< 0.001**	0.583	0.120	**0.002**	**0.001**	0.079
Chl *a*	*F*	**64.5**	**12.1**	**7.5**	2.4	**5.3**	**3.9**	1.6
	df	**1, 34**	**2, 34**	**3, 34**	6, 34	**2, 34**	**3, 34**	6, 34
	p	**< 0.001**	**< 0.001**	**0.001**	0.051	**0.010**	**0.017**	0.175
Chl c_2	*F*	0.1	**3.9**	1.0	0.7	**4.1**	0.2	0.6
	df	1, 34	**2, 34**	3, 34	6, 34	**2, 34**	3, 34	6, 34
	p	0.739	**0.030**	0.425	0.618	**0.024**	0.899	0.723
F_v/F_m †	*F*	**135.3**	**41.1**	**2.8**	**2.5**	**47.3**	**13.4**	1.2
	df	**2.4, 80.9**	**4.8. 80.9**	**7.1, 80.9**	**14.3, 80.9**	**2, 34**	**3, 34**	6, 34
	p	**< 0.001**	**< 0.001**	**0.011**	**0.006**	**< 0.001**	**< 0.001**	0.345
Q_m	*F*	**131.9**	**10.0**	**2.1**	**2.0**	**47.5**	**19.6**	**3,4**
	df	**4, 31**	**8, 62**	**12, 82.3**	**24, 109.4**	**47.5**	**19.6**	**3.4**
	p	**< 0.001**	**< 0.001**	**0.027**	**0.009**	**< 0.001**	**< 0.001**	**0.009**
SOD	*F*	**16.5**	0.01	**3.4**	1.60.256	1.4	**35.7**	1.2
	df	**1, 32**	2, 32	**3, 32**	6, 32	2, 32	**3, 32**	6, 32
	p	**< 0.001**	0.992	**0.031**	0.188	0.256	**< 0.001**	0.314
APX	*F*	**12.2**	0.3	**4.1**	0.7	0.1	**19.4**	1.7
	df	**1, 34**	2, 34	**3, 34**	6, 34	2, 34	**3, 34**	6, 34
	p	**0.001**	0.762	**0.014**	0.624	0.931	**< 0.001**	0.141

Table 4.3: Results of rmANOVA testing the interactive effect of Time × Temperature within each coral-*Symbiodinium* association for the parameters: *Symbiodinium* density (SD); chlorophyll (chl) *a* concentration (pg cell^{-1}); chl c_2 concentration (pg cell^{-1}); maximum quantum yield (F_v/F_m); excitation pressure over PSII (Q_m); superoxide dismutase (SOD) and ascorbate peroxidase (APX). Significant effects ($p \leq 0.05$) are highlighted in bold and non-significant effects ($p > 0.05$) are presented in grey. df = degrees of freedom.

		SD	**chl *a***	**chl c_2**	**F_v/F_m**	**Q_m**	**SOD**	**APX**
Acropora solitariensis	*F*	1.7	2.2	0.7	**4.9**	1.8	0.4	0.04
C3*	df	2, 9	2, 9	2, 9	**3.1, 13.9**	8, 12	2, 8	2, 9
	P	0.244	0.171	0.491	**0.032**	0.166	0.663	0.966
Isopora palifera	*F*	**24.3**	**10.8**	0.6	**28.7**	**9.9**	0.2	0.7
C3*	df	**2, 7**	**2, 7**	2, 7	**5.7, 19.9**	**8, 8**	2, 7	2, 7
	P	**0.001**	**0.007**	0.568	**< 0.001**	**0.002**	0.800	0.537
Pocillopora damicornis	*F*	**5.4**	**19.8**	3.7	**20.7**	**2.9**	**5.5**	0.1
C100/C118	df	**2, 9**	**2, 9**	2, 9	**4.3, 19.5**	**8, 12**	**2, 8**	2, 9
	P	**0.006**	**0.001**	0.067	**< 0.001**	**0.046**	**0.031**	0.912
Porites heronensis	*F*	**7.1**	0.1	0.1	**9.8**	**12.7**	1.1	2.4
C117	df	**2, 9**	2, 9	2, 9	**2.8, 12.5**	**8, 12**	2, 9	2, 9
	P	**0.014**	0.887	0.909	**0.002**	**< 0.001**	0.378	0.147

4.3.3 Chlorophyll fluorescence

On Day 0, maximum quantum yield (F_v/F_m) averaged 0.599 ± 0.006 (mean ± S.E.) in *A. solitariensis*, 0.617 ± 0.010 in *I. palifera*, 0.585 ± 0.014 in *P. damicornis*, and 0.663 ± 0.007 in *P. heronensis*. At this time-point, F_v/F_m in *P. heronensis* was significantly higher than in all other species (Tukey HSD: $p \leq 0.005$; Table 4.4).

Over the 4-day period, coral species responded differently to a given temperature (significant Time × Temperature × Species interaction, Table 4.2). In all coral species, the decline in F_v/F_m was more severe under elevated than decreased temperature (Figures 4.2 A, C, E, G). At elevated temperatures, *I. palifera* showed the strongest response, with a decline in F_v/F_m by 88% by Day 3 and 100% by Day4 (the dark-acclimated baseline fluorescence F_0 was > 130). *A. solitariensis* and *P. damicornis* at first showed a similar response to each other, with reductions in F_v/F_m to 33.4% (Bonferroni: $p = 0.047$) and 30.2% ($p < 0.001$) of initial values at Day 3, respectively. By Day 4,F_v/F_m in *P. damicornis* was only 2.1% of the initial value ($p < 0.001$). In comparison, F_v/F_m in *P. heronensis* declined less rapid, to 25.2% of its initial value by Day 4 ($p = 0.001$). At decreased temperature, all coral species showed a slight reduction in F_v/F_m, with values during the latter stages of the experiment being significantly lower in *P. damicornis* (Days 3, 4 versus Day 0: $p = 0.004$ and 0.021, respectively) and *P. heronensis* (Day 3 versus Day 0: $p = 0.001$) than at the start, but not in the other two species. F_v/F_m was also significantly lower in *P. damicornis* after 3 days at reduced temperature than in the corresponding control ($p = 0.029$); this trend was not seen in any of the other species.

On Day 0, excitation pressure over PSII (Q_m) was highly similar between species (Table 4.4) and averaged 0.3 ± 0.03 (mean ± S.E.) in *A. solitariensis*, 0.3 ± 0.04 in *I. palifera*, 0.4 ± 0.03 in *P. damicornis*, and 0.3 ± 0.03 in *P. heronensis*. By the end of the experiment, the increase of Q_m was stronger in heat-treated corals than cold-treated corals (Figure 4.2 B, D, F, H). However, cold-induced an earlier increase in Q_m that was driven by a light-dependent decrease in quantum yield at noon on Day 1 (Figure 4.2 B, D, F, H). Heat resulted in increased Q_m values compared to the control on Day 3 (Bonferroni: $p < 0.019$) and Day 4 ($p \leq 0.001$) in both *I. palifera* and *P. damicornis*, and on Day 4 in *P. heronensis* ($p < 0.001$).

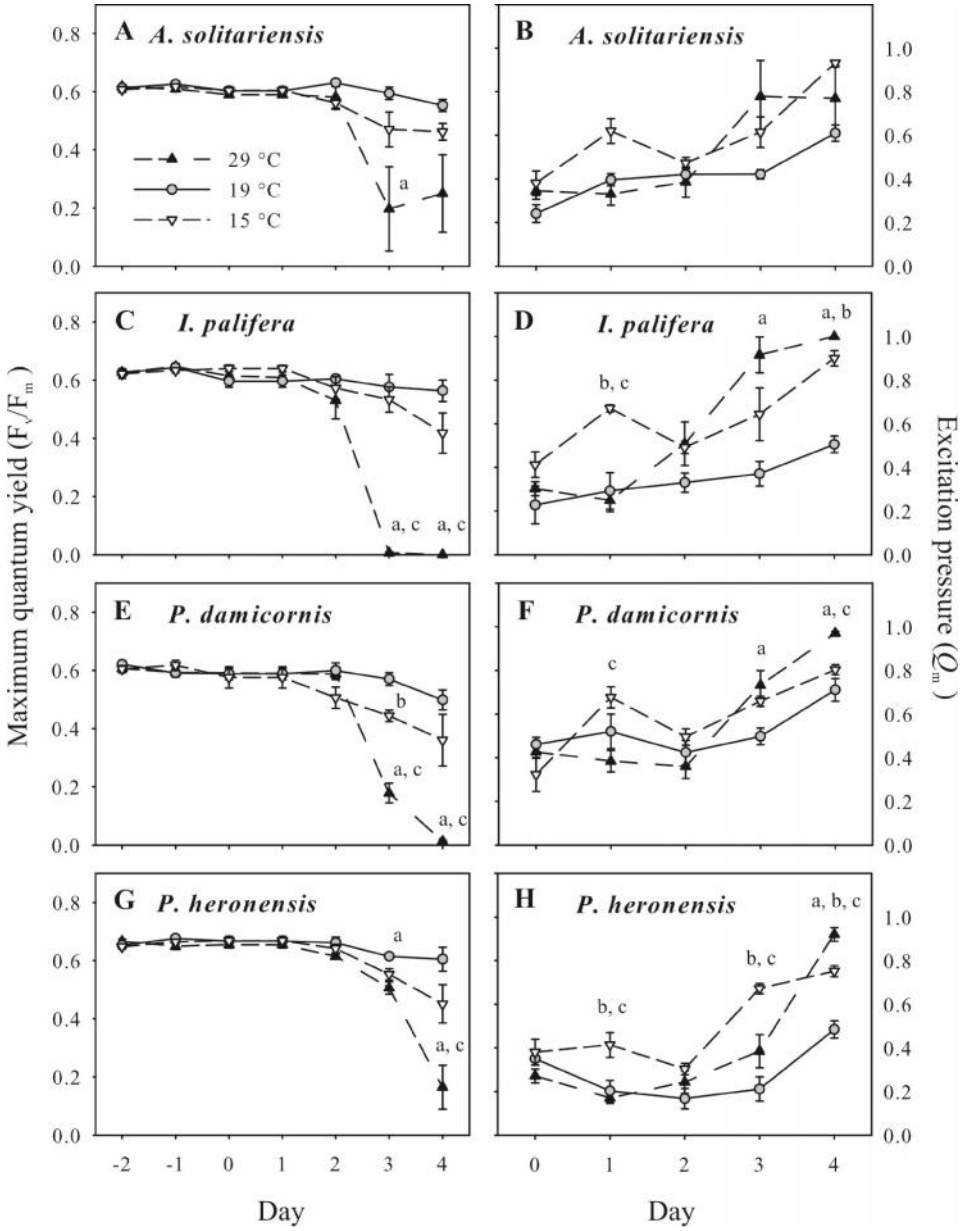

Figure 4.2: Effect of temperature over a 7-day period on maximum quantum yield of PSII (F_v/F_m; **A**, **C**, **E**, **G**) and excitation pressure over PSII (Q_m; **B**, **D**, **F**, **H**) in the four coral species A*cropora solitariensis*, *Isopora palifera*, *Pocillopora damicornis* and *Porites heronensis*. Treatment temperatures as denoted in graph A were attained in the morning of Day 1. Presented are mean values ± S.E., n = 4. Significant differences are reported for (a) 19 °C and 28 °C, (b) 19 °C and 15 °C, and (c) 15 °C and 29 °C at the level of $p \leq 0.05$ (rmANOVA and pairwise comparison with Bonferroni correction). For overall effects of rmANOVA refer to supplementary Tables 4.2 and 4.3.

Table 4.4: Results of univariate ANOVA testing the null-hypothesis that the tested parameter is equal across corals at the beginning of the experiment. The parameters are: *Symbiodinium* density (SD); chlorophyll (chl) *a* concentration (pg cell^{-1}); chl c_2 concentration (pg cell^{-1}); maximum quantum yield (F_v/F_m); excitation pressure (Q_m); superoxide dismutase (SOD) and ascorbate peroxidase (APX). Significant effects on the level of $p \leq 0.05$ are highlighted in bold and non-significant effects are presented in grey. df = degrees of freedom.

		SD	**chl *a***	**chl c_2**	**F_v/F_m**	**Q_m**	**SOD**	**APX**
Day 0	*F*	2.1	0.7	0.8	**13.0**	1.7	**13.1**	**17.0**
	df	3, 44	3, 44	3, 44	**3, 44**	3, 44	**3, 44**	**3, 44**
	P	0.100	0.550	0.491	**< 0.001**	0.184	**< 0.001**	**< 0.001**

4.3.4 *Symbiodinium* antioxidant enzymes

On Day 0, the initial activity of *Symbiodinium* SOD was 69.2 ± 5.6 units mg^{-1} (mean ± S.E.) in *A. solitariensis*, 39.3 ± 6.3 units mg^{-1} in *I. palifera*, 143.2 ± 7.9 units mg^{-1} in *P. damicornis*, and 169.9 ± 31.8 units mg^{-1} in *P. heronensis*. At this time-point, SOD activity in *P. damicornis* and *P. heronensis* was significantly higher than in the other two species (Tukey HSD: $p \leq 0.018$; Table 4.4). Over the 4-day period, *P. damicornis* was the only coral species that changed its SOD activity in response to elevated temperature (Figure 4.3, Tables 4.2, 4.3). Here, SOD activities on Day 4 were about two-fold lower than in either the control (Bonferroni: $p = 0.036$) or cold treatment ($p = 0.018$). In contrast, the response to cold stress was similar to that of control temperature in all coral species (Figure 4.3, Tables 4.2, 4.3).

On Day 0, the initial activity of *Symbiodinium* APX was 0.15 ± 0.03 units mg^{-1} (mean ± S.E.) in *A. solitariensis*, 0.20 ± 0.05 units mg^{-1} in *I. palifera*, 0.51 ± 0.1 units mg^{-1} in *P. damicornis*, and 0.72 ± 0.1 units mg^{-1} in *P. heronensis*. At this time-point, APX activity in *P. damicornis* and *P. heronensis* was significantly higher than in the other two species (Tukey HSD: $p \leq 0.002$; Table 4.4). Over the 4-day period, APX activity was stable in all coral species at all temperatures.

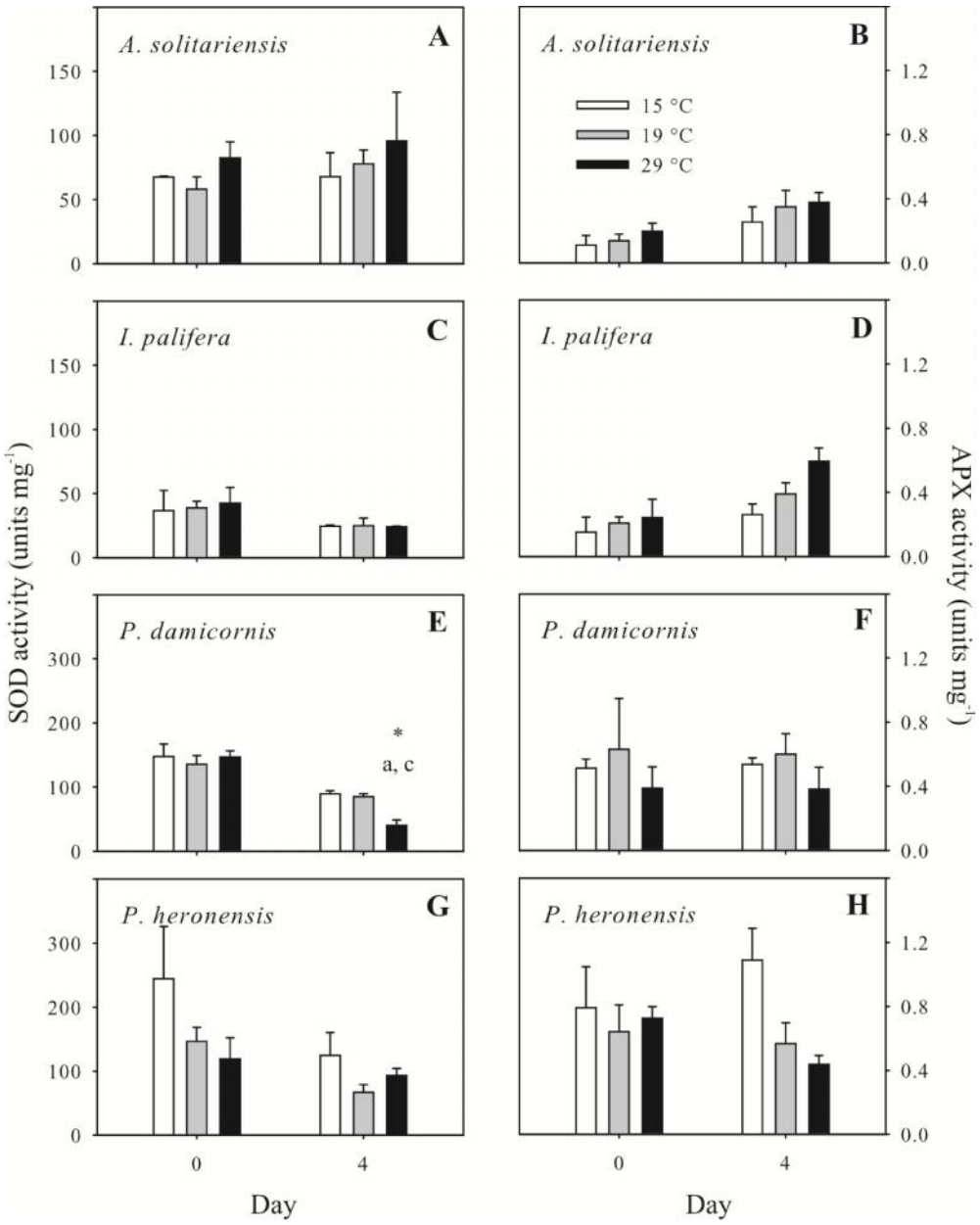

Figure 4.3: Activity of superoxide dismutase (SOD; **A**, **C**, **E**, **G**) and ascorbate peroxidase (APX; **B**, **D**, **F**, **H**) in symbionts hosted by the four coral species *Acropora solitariensis*, *Isopora palifera*, *Pocillopora damicornis* and *Porites heronensis* on days 0 and 4 of the experiment. Figure legend denoted in B is valid for all graphs. Note that scale is different in A and C from that in E and G. Presented are mean values ± S.E., n = 4. Significant differences are reported for (a) 19 °C and 28 °C, (b) 19 °C and 15 °C, and (c) 15 °C and 29 °C ($p \leq 0.05$; (rmANOVA and *post hoc* pairwise comparison with Bonferroni correction). For overall effects of rmANOVA refer to supplementary Tables 4.2 and 4.3.

4.4 Discussion

Reactive oxygen species (ROS) are thought to be key molecules involved in coral bleaching (Lesser and Shick 1989; Downs et al. 2000; Smith et al. 2005; Suggett et al. 2008; Lesser 2011), which occurs when there is a breakdown in the coral-*Symbiodinium* association in response to thermal perturbation (Hoegh-Guldberg 1999). Corals at high latitude reefs, such as the southernmost coral reef of Lord Howe Island (LHI; Harriott et al. 1995), are able to deal with a relatively broad range of temperatures. In particular, they have to cope with generally cooler sea water temperatures compared to their tropical relatives. The present study demonstrates that the LHI corals *Acropora solitariensis*, *Isopora palifera*, *Pocillopora damicornis* and *Porites heronensis* are better able to cope with short-term cold stress (4-day period of 15 °C, corresponding to – 3 °C below the annual monthly mean temperature minimum) than short-term heat stress (4-day period of 29 °C, corresponding to + 5 °C above the annual monthly mean temperature maximum) and further reveals differential susceptibility to mortality, bleaching and PSII activity in heat-stressed corals. The results of this study confirm previous studies that showed *Symbiodinium* type-specific differences in superoxide dismutase (SOD) and ascorbate peroxidase (APX) activity (Lesser 2011; McGinty et al. 2012). However, the results do not provide evidence that tolerance to cold temperatures is associated with enhanced use of these two major antioxidant enzymes *Symbiodinium*. Also, there is no direct relationship between SOD and APX activity and thermal susceptibility described as mortality, bleaching susceptibility, or PSII efficiency at high temperatures.

4.4.1 Mode of bleaching and PSII activity

I. palifera hosting *Symbiodinium* ITS2 type C3* was the most susceptible coral to both, short-term cold and heat stress: at both temperature extremes, more than a third of the coral explants died after three days of exposure. Surviving *I. palifera* explants lost substantially more *Symbiodinium* cells and chlorophyll *a* pigment at 29 °C than at 15 °C. Further, in heat-stressed explants F_v/F_m equalled zero on Days 3 and 4. Similarly, *A. solitariensis* (hosting *Symbiodinium* C3*) and *P. damicornis* (hosting *Symbiodinium* C100/C118) lost substantially more *Symbiodinium* cells and chlorophyll *a* per *Symbiodinium* cell when exposed to 29 °C than 15 °C. In these two corals, F_v/F_m dropped significantly at 29 °C but not at 15 °C by Day 4. A similar

response was described in *P. damicornis* in Chapter 2, and by Wicks et al. (2010b). *P. heronensis* hosting C117 was the only coral species that maintained stable *Symbiodinium* populations and chlorophyll concentrations at 15 °C. Further, although symbiont density in this species was substantially reduced at 29 °C, chlorophyll concentrations per symbiont cell did not change at this temperature. F_v/F_m at 15 °C in *P. heronensis* was comparable to that of the other corals while at 29 °C it dropped to a similar extent to that of the other corals but with a delay of one day. Similarly, excitation pressure over PSII increased to a similar extent as in the other corals, again with a delay of one day.

4.4.2 SOD and APX baseline activities in *Symbiodinium* are type-specific but not related to thermal susceptibility

It is well established that *Symbiodinium* ITS2 types have different physiological, cellular and biochemical properties (Hennige et al. 2009; Ragni et al. 2010; McGinty et al. 2012). Likewise, type-specific differences in the baseline activities of SOD and APX were detected here for *Symbiodinium* C3*, C117 and C100/C118. In *Symbiodinium* C3* (*A. solitariensis* and *I. palifera*), initial SOD activity was about two – four fold lower and APX activity was about three – five fold lower than in *Symbiodinium* C100/C118 (*P. damicornis*) and C117 (*P. heronensis*). It is especially noteworthy that these differences were apparent even though these cells had been isolated from corals at identical depths, and acclimated to identical temperature and light regimes. Host species also seemed to have little influence, with *Symbiodinium* C3* isolated from *A. solitariensis* or *I. palifera* having similar (low) constitutive SOD and APX activities in both species. In contrast, the probably endemic *Symbiodinium* types C100/C118 and C117 (Wicks et al. 2010a) had similar (high) concentrations of both enzymes. However, different baseline SOD and APX activities in *Symbiodinium* did not influence the thermal susceptibility of the coral, corroborating findings by McGinty et al. (2012). These authors showed that baseline activity of SOD was 2-fold higher in thermal sensitive C1 compared to thermally tolerant A1 and F2 in cultures. In the present study, both SOD activity and APX activity were similarly low in the two coral species hosting *Symbiodinium* C3*, yet mortality was observed under both short-term cold stress and heat stress in *I. palifera* but not in *A. solitariensis*. Likewise, both SOD and APX activity were similarly high in *Symbiodinium* C100/C118 and C117, yet cold-water bleaching was observed in *P. damicornis* C100/C118 but

not in *P. heronensis* C117. Furthermore, chlorophyll *a* concentration was reduced in *P. damicornis* C100/C118 but not in *P. heronensis* C117 under elevated temperature. In conclusion, a clear and consistent correlation between SOD and APX concentration and thermally-induced mortality or bleaching (both loss of cell or reduction of pigments) is not apparent in these high latitude host-symbiont combinations.

4.4.3 SOD and APX activity did not increase in thermally challenged *Symbiodinium* cells

Despite mortality in *I. palifera*, and significant reductions in symbiont cell density, chlorophyll *a* concentration and F_v/F_m in most coral species, my results revealed stable SOD and APX activities in all *Symbiodinium* types at both decreased and elevated temperatures, with the exception of symbionts in *P. damicornis* that showed reduced SOD activity under heat stress. A reduction of SOD activity can be explained by inhibition through the accumulation of H_2O_2 (Cheng and Song 2006), or perhaps oxidative damage to the enzyme itself. Depletion of antioxidant activity has been described in hyperoxic aposymbiotic anemones (Richier et al. 2005) as well as in stressed plants (de Carvalho 2008) and may constitute a toxicity response. The maintenance of SOD and APX activity in all other symbionts was unexpected, since enhanced SOD and/or APX activities have been reported in heat-stressed *Symbiodinium* in previous studies, after 6 hours (Yakovleva et al. 2004), 3 – 5 days (Richier et al. 2005; Higuchi et al. 2008), or 10 – 17 days (Lesser 1996) of exposure. Enhanced SOD and APX activities have also been demonstrated in cold-stressed plants (Lee and Lee 2000). From my observation it could be argued that the abovementioned mortality observed in cold-stressed and heat-stressed *I. palifera,* and the loss of *Symbiodinium* cells in all heat-stressed and most cold-stressed corals could be a host-driven response. Clearly, *Symbiodinium* cells were stressed under treatment conditions, demonstrated by concomitant substantial reductions of cellular chlorophyll *a* concentrations and F_v/F_m, as well as increases in Q_m. Therefore, the unresponsiveness of the important, first-in-line antioxidant enzymes SOD and APX in all *Symbiodinium* types studied here indicates that they might have a different mode of stress response that does not include up-regulation of SOD and APX. A parallel measurement of O_2^- or H_2O_2 concentrations would have been hugely insightful with respect to revealing the exact level of cellular oxidative stress and the need for enhanced ROS-scavenging in both *Symbiodinium* and the host tissue.

In previous studies, coral bleaching has been tightly linked to the over-production of ROS in the coral and its symbionts in several ways. Firstly, programmed cell death (apoptosis) and uncontrolled cell death (necrosis) are associated with signalling pathways that may be triggered by ROS (Lesser 2011); yet there is no consensus whether apoptotic pathways are primarily induced by excess ROS in *Symbiodinium* cells (Franklin et al. 2004; Tchernov et al. 2011) or whether apoptotic pathways in host cells might precede mortality in *Symbiodinium* (Dunn et al. 2012; Paxton et al. 2013). Secondly, the reduction of pigments (photobleaching; Takahashi et al. 2008) in *Symbiodinium* chloroplasts is linked to ROS. However, it is not resolved whether photobleaching is primarily a result of ROS-mediated oxidative damage to pigments and pigment-associated proteins or thylakoids (Niyogi 1999), or the inhibition of their replacement by *de novo* synthesis (Takahashi et al. 2008). Traditionally these adverse effects have been associated with excess concentrations of ROS. However, in plants it has been shown that at low (not cytotoxic) concentrations, $^1O_2$ can activate genetic networks, i.e. the up-regulation of approximately 300 nuclear genes, including transcription factors and genes involved in signal-transduction pathways and the mediation of cell death (Wagner et al. 2004; Kim et al. 2008). This example shows that, in plants, complex genetic stress programmes can be activated at ROS concentrations that are far from cytotoxic levels. This highlights the complexity of stress responses in photosynthetic organisms in general, and particularly stresses the need for a more subtle and integrative understanding of ROS and antioxidant capacity in a complex cellular network.

4.4.4 Alternative energy dissipating and ROS-scavenging mechanisms

In high latitude *Symbiodinium*, alternative energy dissipating or ROS-scavenging mechanisms might be more important than SOD or APX. Dissipating mechanisms, such as xanthophyll-dependent heat dissipation and alternative electron transport pathways such as photorespiration, minimize the electron pressure and therefore mitigate generation of excess ROS. Xanthophyll de-epoxidation may account for the high Q_m values observed in *P. heronensis* and other coral species at both decreased and elevated temperatures. However, Q_m is not necessarily correlated with xanthophyll de-epoxidation (see Chapter 2); it also depends on the utilization of reducing equivalents downstream of PSII (Smith et al. 2005). Photorespiration uses ATP and reducing equivalents to oxygenate ribulose-1,5-bisphosphate (RuBP) by RuBP

carboxylase-oxygenase (rubisco), in a series of reactions in the chloroplast, peroxisomes and mitochondria (Wingler et al. 2000). In this process, H_2O_2 is generated as a by-product, and importantly its production is shifted from chloroplasts to peroxisomes, where H_2O_2 is readily detoxified by catalase (Wingler et al. 2000). In this process, the oxidizing and/or inhibitory risk of H_2O_2 is lowered at the site where photosynthetic processes take place (Cruz de Carvalho 2008). Furthermore, the photorespiratory cycle generates glycine, a precursor molecule for the small antioxidant glutathione, thereby adding to the overall antioxidant capacity (Wingler et al. 2000). In fact, an important functional role of the photorespiratory cycle has recently been demonstrated in the coral *Acropora formosa* (Crawley et al. 2010), and enhanced activity of catalase has been shown in thermally-stressed corals and their symbionts (Yakovleva et al. 2004; Higuchi et al. 2008).

Due to different affinity properties of the carbon assimilating enzyme rubisco, the affinity for O_2 decreases at low temperatures and photorespiration is probably of lesser importance under cold stress (Ort and Baker 2002). Tolerance to cold temperatures could be attributed to a number of *Symbiodinium*- or host-related reasons; including the use or recruitment of a greater pool of carbon-assimilating enzymes to compensate for temperature-dependent deceleration of enzyme activity. Furthermore, green fluorescent proteins (GFPs) that can be present in high concentrations in coral tissues quench $^1O_2$ (Bou-Abdhallah 2006) and H_2O_2 (Palmer 2009). GFPs are relatively stable compounds (Bou-Abdhallah 2006) and are therefore suitable candidates for ROS-scavenging over a range of temperatures. Dinoflagellates also produce dimethylsulfide (DMS) from dimethylsulphoniopropionate (DMSP) (Broadbent 2002), which have the ability to quench the hydroxyl radical •OH and singlet oxygen $^1O_2$, respectively (Sunda 2002), and might act in concert with other antioxidants such as carotenoids, ascorbate or glutathione to control cellular ROS concentrations (Halliwell 2006).

4.4.5 Conclusion

In conclusion, the present study did not show that the survivorship or bleaching tolerance of LHI corals to short-term cold stress is linked to SOD or APX activity in their symbionts. Likewise, susceptibility to short-term heat stress was not associated with the activity of these two major ROS-scavenging enzymes. Much more needs to be learned about the relationship between coral

bleaching and oxidative stress, oxidative signalling and oxidative damage in *Symbiodinium* and their hosts in general, and in high latitude symbioses in particular.

Chapter 5:
Differential rates of photoinhibition, photorepair and photoprotection in high latitude *Symbiodinium* spp. from Lord Howe Island

5.1 Introduction

Coral reefs are among the most productive and diverse ecosystems on Earth (Connell 1978). Worldwide, function and diversity of coral reefs are adversely affected by coral bleaching (Hoegh-Guldberg and Bruno 2010), which is defined by losses of dinoflagellate endosymbionts (genus *Symbiodinium*) and/or their pigments from the cnidarian host (Falkowski and Dubinsky 1981; Hoegh-Guldberg 1999), and often involves alterations of sub-cellular structures, protein translation and cell signalling pathways in both symbiotic partners (Ainsworth et al. 2008; Dunn et al. 2012; Paxton et al. 2013). Bleaching susceptibility and post-bleaching mortality of the host varies between and within species (Edmunds 1994; Loya et al. 2001; Fisher et al. 2012) and is influenced by the combination of host *and* its endosymbionts (i.e. the holobiont) (Sampayo et al. 2008; Fitt et al. 2009; Fisher et al. 2012). However, the exact mechanisms underlying bleaching and post-bleaching mortality remain elusive.

High solar radiation can trigger bleaching (Hoegh-Guldberg and Smith 1989; Lesser and Shick 1989) and often acts synergistically with elevated sea surface temperature (SST) to elicit the bleaching response (Bhagooli and Hidaka 2004b; Lesser and Farrell 2004). Indeed, thermal stress associated with high SST is the principle cause for episodes of mass coral bleaching worldwide (Hoegh-Guldberg and Bruno 2010). Temperatures exceeding 28 °C (~ 4 °C above the normal summer maximum mean temperature), in combination with calm seas and high light penetration, resulted in a severe bleaching event at the world's southernmost coral reef at Lord Howe Island (LHI), New South Wales, Australia, in March 2010 (Harrison et al. 2011). Here, Pocilloporidae bleached more extensively than other corals, including Poritidae (Harrison et al. 2011). Previous experiments have shown that *Pocillopora damicornis* bleaches more readily under experimentally elevated temperature (increase of ~ 5 °C above maximum monthly mean temperature for a 5-day period), than either *Stylophora pistillata* or *Porites heronensis*

(Chapters 2, 4). This differential bleaching susceptibility was not correlated with enhanced use of xanthophyll de-epoxidation (Chapter 2), or enhanced scavenging of reactive oxygen species (ROS) by superoxide dismutase (SOD) and ascorbate peroxidase (APX; Chapter 4) in the corals' symbiotic dinoflagellates. Therefore, a different mechanism, or suite of mechanisms, must determine bleaching susceptibility of corals at this high latitude site.

Bleaching conditions often result in photoinactivation of PSII reaction centres in chloroplasts of *Symbiodinium* cells (Warner et al. 1999; Smith et al. 2005; Hill and Ralph 2006). Photoinactivation is correlated with super-saturating light intensities, but can also occur under optimal or sub-saturating light conditions when thermal stress reduces the capability to process light energy (Iglesias-Prieto et al. 1992). Photoinactivated PSII reaction centres are incapable of transferring electrons from water to the plastoquinone pool, more specifically from the primary electron acceptor Q_A to the secondary electron acceptor Q_B, and can therefore result in declines in photosynthetic electron transport (Smith et al. 2005; Hill and Ralph 2006). PSII reaction centre inactivation can further result in enhanced enzymatic degradation of D1, the core protein of PSII reaction centres (often referred to as photodamage), and subsequent *de novo* synthesis of the D1 protein and re-integration into thylakoids in the photoinhibition-repair cycle (Smith et al. 2005). As such, photoinactivation describes the primary photon-induced event that can cause photoinhibition, while photoinhibition describes "a reaction in which the electron transport activity of PSII is lost in such a manner that synthesis of the D1 protein is required before the activity returns" (Tyystjärvi 2008). D1 has the highest metabolic turnover rate of all thylakoid proteins (Mattoo et al. 1984). Under optimal conditions, the rate of D1 repair equals the rate of D1 damage, but if the rate of D1 damage exceeds the rate of repair then the content of functional PSII reaction centres declines (Hill et al. 2011). A reduction of functional PSII reaction centres results in reduced electron generation and may constitute a photoprotective mechanism to avoid electron accumulation when downstream acceptors and sinks are limited (Dunn et al. 2012). However, a sustained reduction of functional PSII reaction centres can eventually lead to depletions in photosynthetic productivity and translocation of photosynthetic products to the coral host, and hence may affect holobiont health and survival (Takahashi et al. 2008).

The exact mechanisms underlying D1 damage in *Symbiodinium* are not yet resolved. It is thought that photoinactivation promotes the generation of ROS such as singlet oxygen ($^1O_2$),

hydroxyl radicals (•OH), superoxide anion (O_2^-) and hydrogen peroxide (H_2O_2) in chloroplasts of oxygenic organisms (Asada 1999; 2000). In particular, $^1O_2$ might be responsible for oxidative damage of D1, although the PSII reaction centre chlorophyll radical (P_{680}^+) might also be involved (Nishiyama et al. 2006). Takahashi et al. (2009) suggested that thermal stress accelerates photoinhibition in *Symbiodinium* because ROS, particularly H_2O_2, might inhibit D1 protein translation and hence the repair cycle of PSII reaction centres. It has been further hypothesized that *Symbiodinium* cells might have unique PSII protein repair systems which might be different from those of plants or cyanobacteria (Hennige et al. 2011; Takahashi et al. 2013).

Elevated temperatures accelerate photoinhibition in cultured *Symbiodinium* cells (Takahashi et al. 2009) and in *Symbiodinium* cells *in hospite* in *Acropora digitifera* (Takahashi et al. 2004) and *Pocillopora damicornis* (Hill et al. 2011). Distinct *Symbiodinium* phyloptypes differ in their susceptibility to photoinhibition in culture (Takahashi et al. 2009) and *in hospite* (Hennige et al. 2011). It has therefore been proposed that differential sensitivities to photoinhibition underlie differential bleaching susceptibilities of corals (Hoegh-Guldberg 1999; Smith et al. 2005). Furthermore, several studies proposed that *Symbiodinium* type-specific differences in the repair capacity of PSII may underlie distinct bleaching susceptibilities of corals (Warner et al. 1999; Takahashi et al. 2004; Takahashi et al. 2009; Ragni et al. 2010; Hennige et al. 2011).

Photoinhibition correlates with PSII quantum yield which can be measured using chlorophyll fluorescence (Warner et al. 1996; Hill and Ralph 2006). Temperature-dependent loss of PSII activity and a parallel decrease in the D1 protein concentration have been shown to occur in corals (Warner et al. 1999; Takahashi et al. 2004; Robison and Warner 2006; Hill et al. 2011). However, while it is it easy to estimate PSII efficiency by chlorophyll fluorescence i.e. by the ratio of variable chlorophyll *a* fluorescence (F_v) to maximum fluorescence (F_m), which equates to the maximum quantum yield of PSII (F_v/F_m), it is difficult to relate F_v/F_m to photoinhibition. Indeed, while F_v/F_m drops when electrons cannot be transported past PSII reaction centres (Campbell and Tyystjärvi 2012), a number of other processes contribute to the reduction of quantum yield (Smith et al. 2005). Importantly, non-photochemical quenching (NPQ) mechanisms lower the quantum yield of PSII photochemistry. The use of chloroplast protein

synthesis inhibitors, such as lincomycin, allows the analysis of D1 damage in the absence of its repair and in the absence of NPQ (Campbell and Tyystjärvi 2012). Lincomycin has been shown to specifically inhibit D1 synthesis in cultured *Symbiodinium* cells (Ragni et al. 2010) and in *Symbiodinium* cells *in hospite* (Hill et al. 2011; Krämer et al. 2013).

In dinoflagellates, the major component of NPQ is xanthophyll de-epoxidation-mediated heat dissipation (Goss and Jakob 2010), though light-induced dissociation of antenna complexes from PSII may be involved in NPQ in *Symbiodinium* cells (Reynolds et al. 2008; Hill et al. 2012). Xanthophyll de-epoxidation dissipates excess energy, reduces the electron pressure over PSII, and reduces the risk of photoinactivation and photoinhibition under high light (e.g. Ambarsari et al. 1997; Krämer et al. 2012) or elevated temperature (Dove et al. 2006; Abrego et al. 2008; Middlebrook et al. 2008), and has also been shown to maintain this protective function in the dark (Middlebrook et al. 2010). Therefore, PSII activity has been described as a function of the net rates of photoprotection, photodamage and photorepair (Ragni et al. 2010).

The objectives of this study were to explore the rates of photodamage, photorepair and NPQ as major components of photoprotection under ambient (23.4 °C) and elevated (27.2 °C) temperature in LHI coral-*Symbiodinium* associations with differing bleaching susceptibilities. In particular, the study focused on two bleaching susceptible (*Pocillopora damicornis* hosting a mixed *Symbiodinium* ITS2 assemblage of C100 and C118, *Porites heronensis* hosting C117) and two bleaching tolerant corals (*Stylophora pistillata* hosting C118 and *P. heronensis* hosting C111*). I hypothesized that the bleaching tolerant corals would have a more rapid D1 repair mechanism, and that enhanced D1 turnover and efficient D1 repair could be a key-mechanism by which high latitude corals deal with the relatively variable temperature and irradiance regime that is characteristic of high latitude sites.

5.2 Materials and methods

5.2.1 Sampling and experimental procedure

In March 2012, three coral fragments with a size of approximately 10 cm (branching corals) or 10 cm^2 (massive corals) each, were sampled from each of four colonies of *Pocillopora damicornis* and *Porites heronensis*, and each of three colonies of *Stylophora* sp. from the lagoon site of Sylphs Hole (S31°31′249″, E159°03′261″). A further three coral fragments were sampled from each of four colonies of *P. heronensis* from the lagoon reef site Stephens Hole (S31°31′937″, E159°03′251″). *P. heronensis* was chosen from these two locations because it has been shown to host different *Symbiodinium* ITS2 types (Chapters 2, 4). Furthermore, *P. heronensis* fragments from Sylphs Hole have been observed as bleaching tolerant at ~ 29 °C over five days (Chapter 2), whereas those from Stephens Hole bleached after four days at ~ 29 °C (Chapter 4). All fragments were taken from a depth of 0.5 – 3 m at low tide from the top of the colony to ensure that they had experienced similar light histories. Immediately after sampling, the three fragments from each coral colony were divided equally to obtain a total of 15 coral explants of ~ 1 – 2 cm length each. One of these explants was preserved in NaCl-saturated 20% dimethyl sulfoxide (DMSO) buffer for subsequent genotyping. The remaining 14 explants (per coral colony) were maintained in two 500-L tanks (seven replicates per coral colony per tank) which were supplied with unfiltered seawater from the lagoon and covered with shade cloth to reduce sunlight by ~ 50%. Temperature and light were monitored using a HOBO pendant data logger (ENVCO, New Zealand), which was calibrated with a Li-Cor LI-189 photometer (Li-Cor, USA). Explants were acclimatized for four days to a temperature averaging 23.8 °C ± 0.01 (mean ± S.E.). At 6:00 h on Day 1 of the experiment, the temperature in one of the tanks was raised to 27 °C, which was attained by 10:30 h. Over the 9-day experimental period, treatment temperatures averaged 23.4 °C ± 0.03 in the control temperature treatment (referred to as C), corresponding to the ambient seawater temperature in the lagoon at the time of the experiment, and 27.2 °C ± 0.03 in the high temperature treatment (referred to as H), corresponding to + 3 °C above the maximum summer monthly mean temperature, and + 2 °C above the bleaching threshold for corals at this site as estimated on www.coralreefwatch.noaa.gov. Natural light intensities, which were reduced using shade cloth, peaked at 523, 432, 273, 455, 364, 205, 637, 364, and 409 µmol photons m^{-2} s^{-1} on Days 1 - 9.

5.2.2 *Symbiodinium* genotyping

Symbiodinium phylotypes were identified according to their ITS2 identity as described in Chapters 3 and 4. Briefly, preserved *Symbiodinium* cells were broken in a Tissue Lyser LT (Qiagen, Australia) bead mill for 10 min at 50 Hz at 4 °C in Tris buffer (0.01 M, pH 8.0). Genomic DNA (gDNA) was precipitated in isopropanol. Precipitated gDNA was washed in 70% ethanol and then eluted and stored in sterile water, using the volumes given in Chapter 3. The ribosomal ITS2 region was PCR-amplified using the primers itsD (Pochon et al. 2007) and ITS2CLAMP (LaJeunesse 2002), using the protocol outlined in Chapter 3. Amplicons were separated using denaturing gradient gel electrophoresis (DGGE, Biorad DCode system) as described in detail in Chapter 2. DGGE fingerprints were compared to fingerprints of known *Symbiodinium* ITS2 populations. DGGE bands that could not be identified were picked, eluted in water, re-amplified by PCR, and sequenced in forward and reverse directions at Macrogen, South Korea, with the primer set ITSD and ITS2REVint (5′-CCATATGCTTAAGTTCAGCGGG-3′).

5.2.3 Chlorophyll fluorescence

Chlorophyll fluorescence was measured using a diving pulse amplitude modulated (PAM) fluorometer (Walz, Germany) with the following settings: measuring intensity 8; saturation intensity 8; saturation width 0.8; and gain 2 – 4. Maximum photosynthetic quantum yield (F_v/F_m) was measured daily at 18:00 h. On Day 9, an induction curve was performed for three replicates of each coral colony. Corals were dark-acclimated for 30 min. After assessment of F_0 and F_m and subsequent calculation of F_v/F_m [maximum quantum yield of PSII; $(F_m - F_0)/F_m$], corals were exposed to 600 µmol photons m^{-2} s^{-1} until F_0 and F_m' stabilized. F and F_m' were assessed every 100 seconds and stabilized in all coral species within 13 – 20 min of exposure. The last F_m' measurement was used for the calculation of NPQ $(F_m - F_m')/F_m'$. An irradiance of 600 µmol photons m^{-2} s^{-1} was chosen because it reflected maximum light intensities (averaged over the 30 min exposure period) experienced during the lincomycin treatment. For this induction curve and NPQ calculation the following PAM settings were used: measuring intensity 8; saturation intensity 8; saturation width 0.8; and gain 4.

5.2.4 Lincomycin treatment

On Day 8 at 11:30 h, two replicate explants of each coral colony from each of the two temperature treatment tanks were removed and one of them was placed haphazardly in one of four 600-mL plastic beakers (15 explants per beaker). Two beakers were placed in each of two 50-L water baths, set to (i) the control temperature or (ii) high temperature. The water from the holding tanks was exchanged approximately every 20 – 30 min with control or heated water from the 500-L temperature treatment tanks. Hence, each of the 50-L water baths contained two beakers; one of each pair was then treated with lincomycin (+ Lin) and one was treated as a control (– Lin). Lincomycin-treated corals were exposed to a final concentration of 0.930 mM (378 µg mL^{-1}) lincomycin in 0.825% ethanol, while the control corals were exposed to a final concentration of 0.825% ethanol. [Note: exposure to ethanol was necessary because lincomycin must be dissolved in 99% ethanol; with a stock dilution of 111.7 mM in 99% ethanol]. Lincomycin concentrations were in the range of those used in *Symbiodinium* cultures (Ragni et al. 2010) and corals before (Hill et al. 2011; Krämer et al. 2013). Furthermore, the efficiency of lincomycin and the effect of ethanol at these concentrations were assessed in a preliminary experiment with explants of *P. damicornis* and *P. heronensis*. These preliminary experiments showed no effect of ethanol on the control corals. However, in lincomycin-treated corals a significant decline of effective quantum yield ($\Delta F_v/F_m'$) and F_v/F_m was monitored over a period of 6 hours.

Before addition of the inhibitor, corals were dark-acclimated for 30 min. At 12:00 h, the dark-acclimated quantum yield of PSII (F_v/F_m) was determined. Next, the inhibitor with ethanol or ethanol control were added to + Lin and – Lin treatment beakers, respectively. Corals were exposed to natural sunlight for 30 min, after which the light-acclimated quantum yield of PSII ($\Delta F_v/F_m'$) was determined. Corals were then dark-acclimated for further 30 min, followed by the measurement of F_v/F_m. The cycle of 30 min dark acclimation and 30 min light acclimation was repeated until the experiment was terminated at 16:00 h, after the last dark-acclimated reading. This period of time was chosen because it included daily maximum irradiation. At 16:00 h, after the last measurement of F_v/F_m, corals were frozen rapidly on dry ice, stored at -20 °C for three days, and then transferred to -80 °C for long-term storage. Intensities of natural sunlight during this procedure are outlined in Figure 5.2.

5.2.5 Calculation of gross photoinhibition, net photoinhibition and repair rate of D1

Using the values of F_v/F_m for lincomycin-treated and untreated corals, gross photoinhibition (GPiR; Table 5.1, Equation 5.1), net photoinhibition (NGPiR; Table 5.1, Equation 5.2) and repair rate (RR; Table 5.1, Equation 5.3) were calculated according to Ragni et al. (2008). These equations have also been applied to *Symbiodinium* cells in culture (Ragni et al. 2010) and *in hospite* (Hennige et al. 2011), and assume that the decline of F_v/F_m occurs at a constant rate (Ragni et al. 2010).

Equation 5.1: Gross photoinhibition $= \mathrm{GPiR(E)} = -\frac{Ln\frac{Fv/FmLIN(E)}{Fv/Fm(DA)}}{\Delta T}$

Equation 5.2: Net photoinhibition $= \mathrm{NPiR(E)} = -\frac{Ln\frac{Fv/Fm(E)}{Fv/Fm(DA)}}{\Delta T}$

Equation 5.3: Repair rate of D1 $= RR = GPiR - NPiR$

E refers to the light level to which the corals were exposed and F_v/F_mLIN(E) is the quantum yield measured after 4 h of treatment for the dark-acclimated lincomycin-treated corals (+ LIN). F_v/F_m(E) is the same value measured for dark-acclimated untreated corals. F_v/F_m(DA) is the dark-acclimated quantum yield measured before sunrise (05:30 h) on the same day, and corresponds to the maximum quantum yield of PSII. ΔT is the duration of the light incubation time in minutes (120 min).

5.2.6 Statistical analysis

Data were analyzed using the IBM SPSS statistics 20.0 software. Repeated measures analysis of variance (rmANOVA) and *post hoc* pairwise comparison with Bonferroni adjustment was used to test F_v/F_m over the 9-day period in the temperature tanks, and $\Delta F_v/F_m'$ over the 4-h period of lincomycin treatment. Data were arcsine transformed to meet assumptions of normality. When assumptions of equality of the variances were violated, the Greenhouse-Geisser correction is reported. Univariate ANOVA with *post hoc* Tukey HSD was used to analyze if there are differences in any of the parameters GPiR, NPiR, and RR, between species or treatments. Within species, an independent sample t-test was used to analyze for differences

between lincomycin-treated and untreated corals at each temperature. NPQ was tested using the Mann-Whitney U test, because assumptions of normality could not be met.

Table 5.1: Definition of photophysiological terminology used in this study.

Photoinactivation	Primary photon-induced event that can lead to photoinhibition; electrons are generated at PSII reaction centres but cannot be transported past PSII; electrons may accumulate and generate highly reactive compounds such as P_{680}^{+} or $^{1}O_{2}$.
Photoinhibition	Secondary event initiated by photoinactivation: loss of functional PSII reaction centres due to losses of the primary protein D1; in contrast to photoinactivation, photoinhibition involves enzymatic processes such as the degradation of D1.
Gross photoinhibition	Rate of photoinhibition in the presence of a chloroplast protein synthesis inhibitor equating to photoinhibition that occurs when D1 synthesis, re-assembly of functional PSII reaction centres (and NPQ) is blocked.
Net photoinhibition	Rate of photoinhibition in the absence of a chloroplast protein synthesis inhibitor equating to photoinhibition that occurs when D1 synthesis, re-assembly of functional PSII reaction centres (and NPQ) is possible.
Repair rate	Rate of PSII reaction centre protein degradation, synthesis and replacement, which primarily refers to the turnover rate of D1

5.3 Results

5.3.1 Genetic identification of *Symbiodinium*

All coral species hosted distinct, dominant *Symbiodinium* types, as identified by their ribosomal ITS2 region (Table 5.2). *Pocillopora damicornis* hosted a mixed assemblage of C100 and C118, while *Stylophora* sp. hosted *Symbiodinium* C118. All P*orites heronensis* sampled at Sylphs Hole hosted C111*, while three out of four replicates of this species sampled at Stephens Hole hosted C117 and the other hosted a variant of C131, with 99% identity (282 out of 283 basepairs) to C131 (NCBI accession number JF320826). The coral fragment hosting the *Symbiodinium* ITS2 variant of C131 was excluded from further analysis. For sequences refer to Appendix A.3 on pages 258 – 259.

Table 5.2: Coral species, replication, sampling location and *Symbiodinium* type identified by denaturing gel gradient electrophoresis (DGGE) of their internal transcribed spacer 2 (ITS2) regions.

Coral species	**Replication (n)**	**Sampling location**	***Symbiodinium* ITS2 type**
Pocillopora damicornis	4	Sylphs Hole	C100, C118
Porites heronensis	4	Sylphs Hole	C111*
Porites heronensis	3	Stephens Hole	C117
Porites heronensis	1	Stephens Hole	C131 variant
Stylophora pistillata	3	Sylphs Hole	C118

5.3.2 Maximum quantum yield

Maximum quantum yield (F_v/F_m) measured on Days 0 – 8 was very similar between species and treatments (Figure 5.1; Table 5.3). When species were analyzed separately, F_v/F_m was again similar between temperature treatments in all cases (Table 5.4).

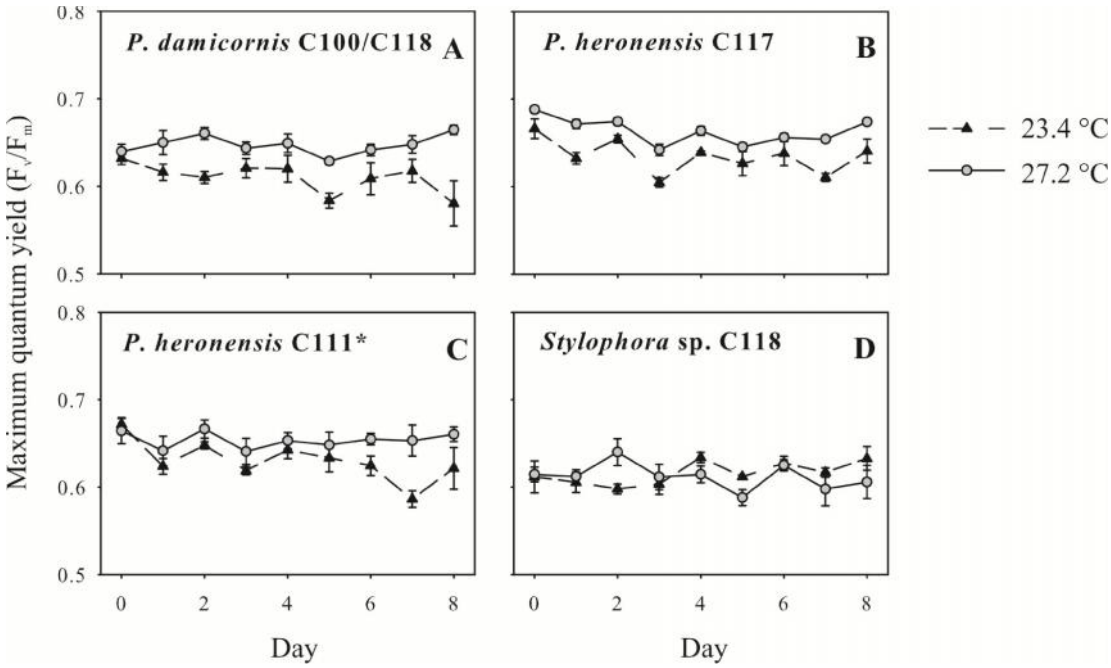

Figure 5.1: Maximum quantum yield of PSII (F_v/F_m) monitored over an 8-day period in the four coral associations: *Pocillopora damicornis* hosting *Symbiodinium* C100/C118 (**A**); *Porites heronensis* hosting C111* (**B**); *Porites heronensis* hosting C117 (**C**); and *Stylophora* sp. hosting C118 (**D**). Presented are mean values ± S.E., n = 3 – 4.

5.3.3 Photoinhibition and photorepair

At the control temperature, effective quantum yield ($\Delta F_v/F_m'$) of control fragments (- Lin) and lincomycin-treated fragments (+ Lin) was similar in all coral species (Figure 5.2 A, C, E, G). In contrast, at the high temperature, $\Delta F_v/F_m'$ of lincomycin-treated *P. damicornis* dropped significantly (Bonferroni: p = 0.040) below that of untreated corals after 4 h of treatment (Figure 5.2 B, Tables 5.3, 5.4). The other coral-*Symbiodinium* associations did not show this effect (Figure 5.2 D, F, H).

Table 5.3: Results of rmANOVA for the parameters: maximum quantum yield (F_v/F_m) measured on Days 0 – 8 (Figure 5.1); and effective quantum yield ($\Delta F_v/F_m'$) measured on Day 8 between 12:00 h and 16:00 h during the lincomycin treatment (Figure 5.2). Significant effects ($p \leq 0.05$) are highlighted in bold, and non-significant effects ($p > 0.05$) are presented in grey. df = degrees of freedom; Temp = temperature; Treat = treatment; † indicates that Greenhaus-Geisser correction is reported.

Parameter		**Time**	**Time × Temp**	**Time × Species**	**Time × Temp × Species**	**Temp**	**Species**	**Temp × Species**
F_v/F_m†	*F*	**6.7**	1.3	1.5	1.5	< 0.1	**5**	0.1
	df	**3.9, 77.9**	3.9, 77.9	11.7, 77.9	11.7, 77.9	1, 20	**3, 20**	3, 20
	p	**< 0.001**	0.279	0.152	0.513	0.989	**0.010**	0.931
Parameter		**Time**	**Time × Treat**	**Time × Species**	**Time × Treat × Species**	**Treat**	**Species**	**Treat × Species**
$\Delta F_v/F_m'$†	*F*	1.9	**3.7**	1.1	1.0	2.3	**34.1**	0.6
	df	3, 38	**9, 92.6**	9, 92.6	27, 111.6	3, 40	**3, 40**	9, 40
	p	0.142	**< 0.001**	0.387	0.444	0.093	**< 0.001**	0.819

Table 5.4: Results of rmANOVA when coral species are analyzed separately. The parameters are: maximum quantum yield (F_v/F_m) measured on Days 0 – 8 (Figure 5.1); and effective quantum yield ($\Delta F_v/F_m'$) measured on Day 8 between 12:00 h and 16:00 h during the lincomycin treatment (Figure 5.2). Bold numbers highlight significant differences at $p \leq 0.05$. df = degrees of freedom; Pd = *Pocillopora damicornis*; Ph = *Porites heronensis*; S = *Stylophora* sp.; † indicates that Greenhaus-Geisser correction is reported.

Parameter		**Time × Temperature**			
Species		**Pd/C100/C118**	**Ph/C111***	**Ph/C117**	**S/C118**
F_v/F_m†	*F*	0.6	1.5	0.7	1
	df	3.1, 18.8	2.3, 13.8	2.2, 8.7	2.3, 9.3
	p	0.645	0.254	0.557	0.424
Parameter		**Time × Treatment**			
Species		**Pd/C100/C118**	**Ph/C111***	**Ph/C117**	**S/C118**
$\Delta F_v/F_m'$	*F*	**2.9**	1.3	1.4	0.8
	df	**9, 24.5**	9, 24.5	9, 14.8	9, 14.8
	p	**0.018**	0.298	0.272	0.615

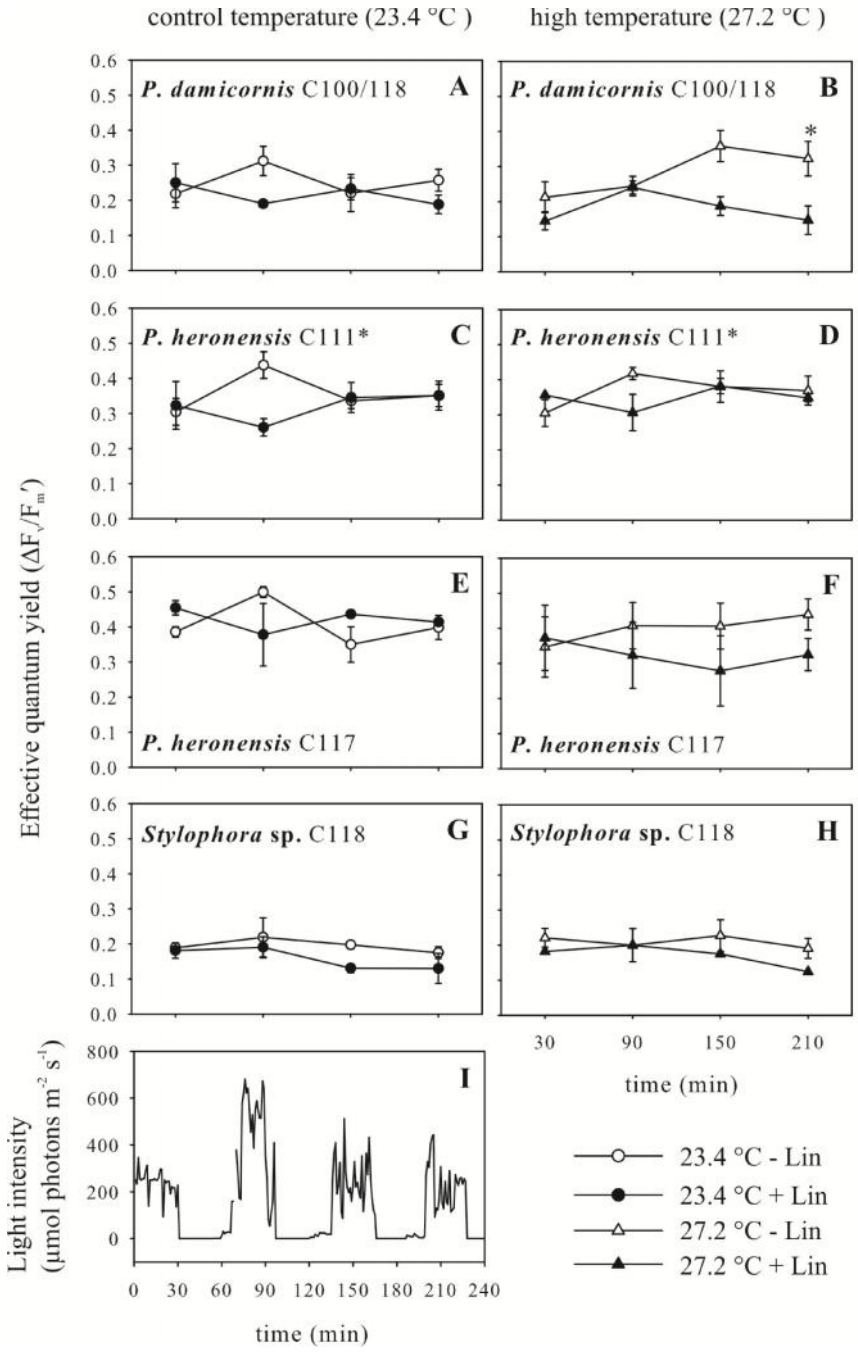

Figure 5.2: Effective quantum yield (ΔFv/Fm') measured on Day 8 between 12:30 h and 15:30 h in four coral associations exposed (+ Lin) or not exposed (– Lin) to lincomycin. Associations were *Pocillopora damicornis* hosting *Symbiodinium* C100/C118 (**A, B**); *Porites heronensis* hosting C111* (**C, D**) or C117 (**E, F**); and *Stylophora* sp. hosting C118 (**G, H**). Presented are mean values ± S.E., n = 3 – 4. Corals were light-acclimated for 30 min before each measurement, to light intensities peaking at 347, 918, 512, and 442 µmol photons m^{-2} s^{-1}, respectively (**I**). Asterisk indicates a significant difference ($p \leq 0.05$) between lincomycin-treated and untreated corals, as revealed by rmANOVA and *post hoc* Bonferroni corrected pairwise comparisons.

The rate of gross photoinhibition (GPiR) was similar at the control and high temperatures in all species (Figure 5.3 A, Table 5.5). However, the rate of GPiR at both temperatures was significantly higher in *P. damicornis* C100/C118 than in both *P. heronensis* associations (Tukey HSD: $p < 0.030$ for all comparisons). Likewise, GPiR was higher in *Stylophora* sp. than in *P. heronensis* hosting C111* (Tukey HSD: $p = 0.043$).

The rate of net photoinhibition (NPiR) was not significantly different at the control and high temperatures in any coral species, though they all tended to decrease NPiR in response to elevated temperature (Figure 5.3 B, Table 5.5, significant effect of treatment). When species were pooled for analysis, the rate of NPiR was significantly lower at elevated temperature (Table 5.5). NPiR at both the control and elevated temperatures was significantly higher in *Stylophora* sp. C118 than in both of the *P. heronensis* associations (Tukey HSD: $p = 0.027$ for both comparisons).

Lower net photoinhibition at elevated temperature translated to significantly higher repair rates of D1 in *P. damicornis* and *P. heronensis* C117, with 3.1 fold and 3.7 fold increments, respectively (Figure 5.3 C, Table 5.5). In contrast, *Stylophora* sp. and *P. heronensis* C111* did not change their repair rates in response to elevated temperature.

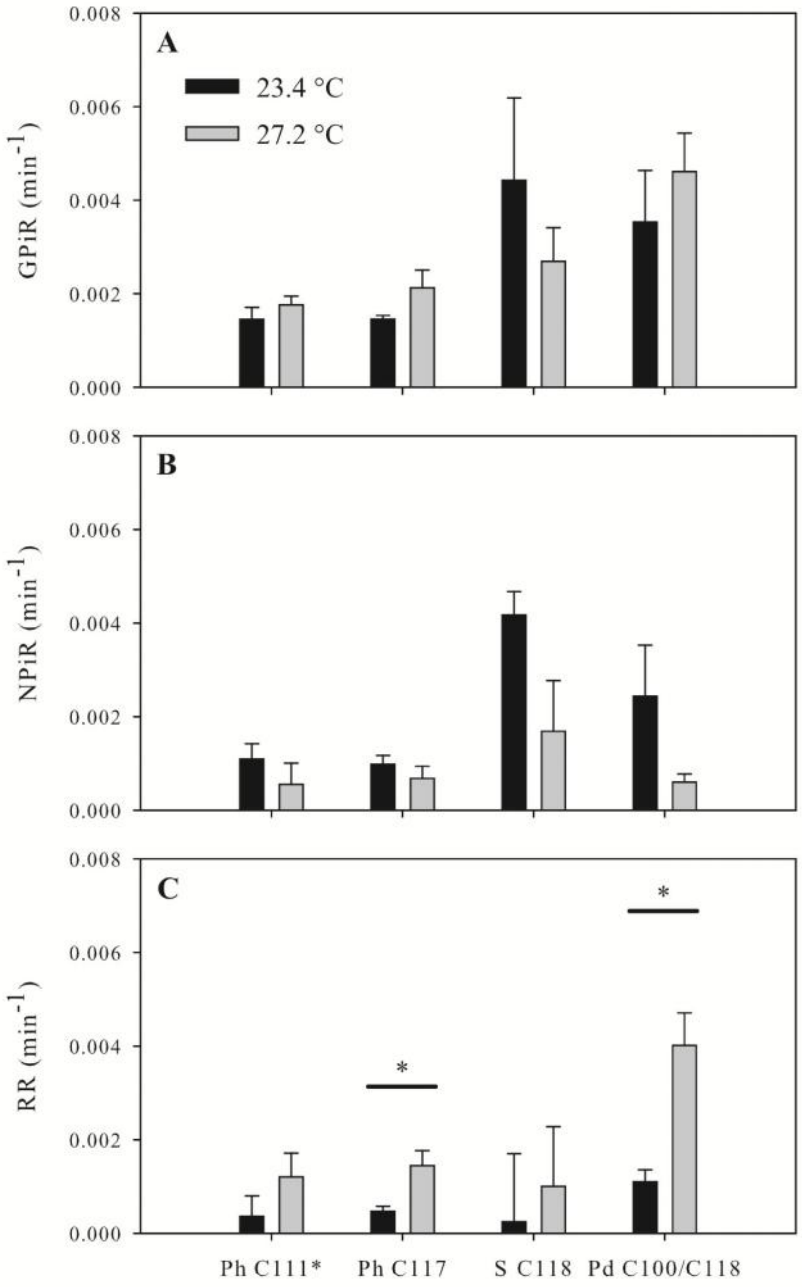

Figure 5.3: Gross photoinhibition (GPiR; **A**), net photoinhibition (NPiR; **B**) and repair rates (RR; **C**) (min^{-1}) in *Porites heronensis* (Ph) hosting *Symbiodinium* C111* or C117, *Stylophora* sp. (S) hosting C118, and *Pocillopora damicornis* (Pd) hosting a mixed assemblage of C100 and C118 under control temperature (23.4 °C) or elevated temperature (27.2 °C). Presented are mean values ± S.E., n = 3 – 4. Asterisks indicate significant differences between control and high temperature ($p \leq 0.05$) as revealed by an independent sample t-test (Table 5.4).

Table 5.5: Results of univariate ANOVA and independent sample t-test analyzing the effect of treatment on gross photoinhibition (GPiR), net photoinhibition (NPiR) and repair rate (RR). Treatment is grouped as C + Lin (lincomycin-treated at control temperature), C – Lin (lincomycin-untreated at control temperature, H + Lin (lincomycin-treated at high temperature), and H – Lin (lincomycin-untreated at high temperature). Significant effects ($p \leq 0.05$) are highlighted in bold and non-significant effects ($p > 0.05$) are presented in grey. df = degrees of freedom; Pd = *Pocillopora damicornis*; Ph = *Porites heronensis*; S = *Stylophora* sp.

		All species			**Pd/C100/C118**	**Ph/C111***	**Ph/C117**	**S/C118**
Parameter		Treatment	Species	Treatment × Species	Treatment	Treatment	Treatment	Treatment
GPiR (min^{-1})	*F*	0.6	**6.5**	1.1	1.0	1.0	3.5	0.8
	df	1, 20	**3, 20**	3, 20	6	6	4	4
	p	0.434	**0.003**	0.366	0.367	0.365	0.134	0.411
NPiR (min^{-1})	*F*	**8.3**	**4.5**	1.3	1.9	1.1	1.8	0.7
	df	**1, 20**	**3, 20**	3, 20	6	6	4	4
	p	**0.009**	**0.014**	0.304	0.367	0.365	0.134	0.465
RR (min^{-1})	*F*	**7.4**	**3.5**	1.2	**6.9**	0.1	**5.8**	0.2
	df	**1, 20**	**3, 20**	3, 20	**3.8**	6	**4**	4
	p	**0.013**	**0.036**	0.351	**0.019**	0.255	**0.044**	0.716

5.3.4 Photoprotection – Non-photochemical quenching (NPQ)

High temperatures resulted in higher NPQ at 600 µmol photons m^{-2} s^{-1} in *P. heronensis* when hosting C117 (Mann-Whitney U: $p = 0.05$), but not when hosting C111* (Figure 5.4). *Stylophora* sp. did not change NPQ with increasing temperature. *P. damicornis* showed a drop in NPQ to about 56% of initial values (Mann-Whitney U: $p = 0.05$).

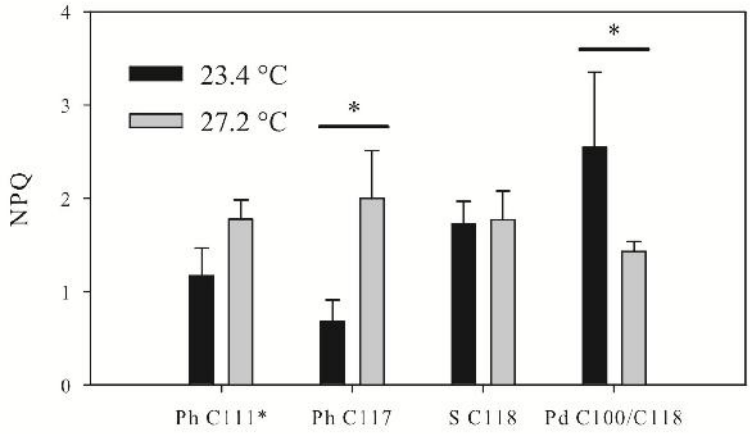

Figure 5.4: Non-photochemical quenching in *Porites heronensis* (Ph) hosting *Symbiodinium* C111* or C117, *Stylophora* sp. (S) hosting C118, and *Pocillopora damicornis* (Pd) hosting a mixed assemblage of C100 and C118 under control temperature (23.4 °C) or elevated temperature (27.2 °C) at 600 µmol photons m^{-2} s^{-1}. Presented are mean values ± S.E., n = 3 – 4. Asterisks indicate significant differences between control and high temperature ($p \leq 0.05$) as revealed by the non-parametric Mann-Whitney U test.

5.4 Discussion

Previous experiments have demonstrated that at Lord Howe Island *Pocillopora damicornis* is more susceptible to increases in seawater temperature than *Stylophora* sp. or *Porites heronensis* (Chapters 2, 4). Differential bleaching susceptibility of corals was not correlated with enhanced use of xanthophyll de-epoxidation (Chapter 2) or enhanced activity of ROS-scavenging enzymes, such as superoxide dismutase (SOD) and ascorbate peroxidase (APX; Chapter 4), in their endosymbionts. It was therefore hypothesized that the capacity for photorepair might contribute to the differential bleaching susceptibilities of corals at the high latitude coral reef of Lord Howe Island (LHI).

In this study, chlorophyll fluorescence in combination with the chloroplast specific protein synthesis inhibitor lincomycin was used to estimate photorepair of PSII (in the following referred to as photorepair) as outlined in Ragni et al. 2008. Because lincomycin inhibits the *de novo* synthesis of the PSII core protein D1 (for example shown in Hill et al. 2001), photorepair is closely linked to D1 turnover within the PSII complex. In the following the terminology photorepair and photoinhibition is used according to Ragni et al. and Hennige et al. 2011. The latter authors found that symbionts within bleaching tolerant *Porites asteroids* had higher photorepair rates under increased light availability, resulting in lower net photoinhibition relative to symbionts within bleaching sensitive *Montastrea faveolata*. The present study clearly shows that the four coral-*Symbiodinium* associations (with different bleaching susceptibilities) also differ in their thermal response with respect to photorepair. Symbionts of *P. damicornis* (*Symbiodinium* ITS2 types C100 and C118) and *P. heronensis* (C117), though not the other symbiont types, increased photorepair 3.7 and 3.1 fold, respectively, when exposed to temperatures that exceeded the maximum monthly mean temperature by ~ 3 °C, and the bleaching threshold for corals at this site estimated on www.coralreefwatch.noaa.gov by ~ 2 °C, for a period of eight days. This increased photorepair was sufficient for recovery of PSII reaction centre functionality at night in both associations; they therefore avoided long-term photoinhibition over the course of the experiment. However, under persistent conditions of high temperature, elevated metabolic needs associated with photorepair might become exhausted and result in sustained loss of functional PSII reaction centres and long-term photoinhibition. Increased dependency on photorepair, together with a reduction of NPQ at high temperature, might be key mechanisms that explain the greater bleaching susceptibility of *P. damicornis* at LHI. Furthermore, differences in photorepair and photoprotection in two symbiont types (C111* and C117) associated with the same coral species (*P. heronensis*) at elevated temperature, highlights *Symbiodinium* type-specific differences in PSII functionality. Whether these differences are associated with differential bleaching susceptibilities of their *Porites* hosts needs further investigation.

5.4.1 Rates of photoinhibition and photorepair at ambient temperature differ between distinct *Symbiodinium* types

Under control conditions, the two branching corals *P. damicornis* and *Stylophora* sp. had significantly higher rates of gross photoinhibition than the massive species *P. heronensis* (whether harbouring *Symbiodinium* C111* or C117). Because gross photoinhibition describes the rate of photoinhibition in the presence of the chloroplast protein synthesis inhibitor lincomycin, this result implies that the symbionts of the two branching species experience higher rates of photodamage than the symbionts of *P. heronensis*. There are two possible explanations for the observed difference in gross photoinhibition. (1) Previous studies have shown that gross photoinhibition positively correlates with light intensity (Takahashi et al. 2009; Ragni et al. 2010; Hennige et al. 2011). It is therefore possible that symbionts within the two branching and the massive species experience different light regimes. For instance, this could be due to different light-scattering properties of the skeletons (Enríquez et al. 2005), different quantities or organization of *Symbiodinium* pigments (Hennige et al. 2009), different host tissue thicknesses (Loya et al. 2001), or other mechanisms that screen and/or dissipate light in *Symbiodinium* or host cells, including fluorescent proteins (Salih et al. 2000) and mycosporine-like amino acids (Shick and Dunlap 2002). (2) Gross photoinhibition depends on the availability of ATP and NADPH (Smith et al. 2005). If the consumption of ATP and NADPH in photosynthesis or alternative pathways is restricted, e.g. because of limitations of the activities of ribulose 1,5-bisphosphate carboxylase/oxygenase or carbonic anhydrase, then the electron transport will be restricted and the risk of photoinhibition increases because electron acceptors become increasingly reduced, i.e. unavailable (Smith et al. 2005). It is therefore possible that *P. heronensis* had the capability to maintain ATP and NADPH consumption under conditions in which sinks for reduction equivalents downstream of PSII were saturated in *P. damicornis* and *Stylophora* sp., and that these differences account for distinct rates of gross photoinhibition.

Net photoinhibition, i.e. the rate of inhibition in the presence of repair systems, was highest in *Stylophora* sp. under control conditions. In general, net photoinhibition does not solely depend on D1 synthesis and re-assembly into functional PSII reaction centres (i.e. the rate of repair), but also on the extent of NPQ. [In contrast, gross photoinhibition is not influenced by NPQ because lincomycin relaxes NPQ mechanisms (Campbell and Tyystjärvi 2012)]. However,

in this study NPQ was similar between species under control conditions, suggesting that the high rate of net photoinhibition in *Stylophora* sp. was probably due to the high rate of photodamage and a concomitant low rate of photorepair. In comparison to *Stylophora* sp., *P. heronensis* (containing both C111* and C117) exhibited significantly less photodamage, although the rates of photorepair were similarly low in all species.

5.4.2 Elevated temperatures can stimulate photorepair in *Symbiodinium* C100/C118 and C117

Excess light can cause photoinactivation and photoinhibition, i.e. the loss of functional PSII reaction centres that involves losses of D1 and its recovery, which involves replacement by D1 (Powles 1984; Aro et al. 1993; 2005). Although high light alone can result in coral bleaching (Hoegh-Guldberg and Smith 1989; Lesser and Shick 1989), natural bleaching events often involve temperatures that exceed the physiological thresholds of corals and their endosymbionts (Harrison et al. 2011). It has been proposed that high temperatures accelerate photoinhibition due to the inhibition of *de novo* synthesis of photodamaged proteins, particularly D1 (Takahashi and Murata 2008). It has been further hypothesized that ROS, particularly hydrogen peroxide (H_2O_2) inhibit protein translation. On the contrary, Hill et al. (2011) demonstrated that, in *P. damicornis*, increased thermal stress leads to accelerated photorepair. Similarly, Hennige et al. (2011) found that increased light availability does not inhibit, but rather accelerate photorepair in the corals *Porites astreoides* and *Montastraea faveolata*. In corroboration with the results of Hill et al. (2011), the present study suggested, based on chlorophyll fluorescence measurements, that elevated temperature can result in accelerated rates of photorepair in some species, in particular in *P. damicornis* C100/C118 and in *P. heronensis* C117. In these two host-symbiont combinations, net photoinhibition was not affected by increased temperature, indicating that higher photorepair rates were necessary to maintain similar (low) rates of net photoinhibition. In summary, the chlorophyll fluorescence measurements combined with the use of lincomycin suggest that temperatures exceeding the predicted bleaching threshold increased rather than blocked photorepair of PSII in *P. damicornis* and *P. heronensis* C117.

5.4.3 Implications for coral bleaching

Previous studies have suggested that *Symbiodinium* cells with higher initial and/or stress-stimulated D1 repair rates are more stress resistant both in culture (Ragni et al. 2010) and *in hospite* (Hennige et al. 2011). Although corals did not bleach in the present study (see Appendix B on page 262) it was previously shown (Chapter 2) that, at temperatures exceeding the summer monthly mean temperature maximum by ~ 5 °C for five days, *P. damicornis* is more thermally sensitive than *Stylophora* sp. or *P. heronensis* hosting C111* at LHI. This was evident from substantially higher losses/reductions of *Symbiodinium* cells, *Symbiodinium* pigments and maximum quantum yield of PSII. In the current study, bleaching-susceptible *P. damicornis* associated with *Symbiodinium* cells that exhibited the strongest increases in photorepair, estimated from chlorophyll fluorescence. Similarly, *P. heronensis* colonies hosting C111* and C117 have different thermal thresholds, with those hosting C117 bleaching more rapidly (Chapters 2, 4). In the current experiment, *P. heronensis* hosting C117 accelerated photorepair under bleaching conditions, while *P. heronensis* hosting C111* did not. As such, bleaching susceptibility, rather than tolerance, seems to be associated with accelerated photorepair in these corals. Accelerated turnover of PSII reaction centre proteins facilitates maintenance and recovery of PSII function, and therefore reduces the formation of ROS (Hennige et al. 2011), particularly singlet oxygen ($^1O_2$) by excited chlorophyll molecules that pass their excitation energy to oxygen (Nishiyama et al. 2006). However, while the bleaching response might be mitigated initially (Hennige et al. 2011), the findings presented here suggest that, when stress conditions persist, the repair system might not be able to maintain its function at an appropriate rate. This ultimately could lead to the PSII reaction centres not being replaced, disintegration of light-harvesting pigment antennae, and the initiation of bleaching cascades. In conclusion, rapid repair rates at high temperatures are probably not sufficient to counteract sustained losses of PSII reaction centres and are unlikely to prevent the bleaching response.

Chapter 6:
Symbiodinium diversity in the sea anemone *Entacmaea quadricolor* on the east Australian coast

6.1 Introduction

Numerous cnidarians host symbiotic dinoflagellates of the genus *Symbiodinium*. There is considerable diversity within this genus, with at least nine distinct clades (A – I) (Pochon et al. 2010) each containing several sub-clades or types (Baker 2003). This diversity has important ecological consequences as *Symbiodinium* type may influence the physiological response of the holobiont (i.e., host cnidarian and its associated symbionts) to environmental change (Berkelmans and van Oppen 2006; Fisher et al. 2012). High *Symbiodinium* diversity at both the cladal and sub-cladal levels occurs at high latitudes in corals and sea anemones (Savage et al. 2002; Wicks et al. 2010a), and understanding patterns of this diversity can provide important insights into the ability of symbioses to withstand different stressors across their geographic range.

Sea anemones that host obligate ectosymbiotic anemonefishes also harbour *Symbiodinium* as an obligate endosymbiotic partner (Dunn 1981). *Entacmaea quadricolor* is the most common species of host sea anemone being found in the Indo-west Pacific and the Red Sea (Fautin and Allen 1992), in both shallow-water and mesophotic reef environment (Bridge et al. 2012). Although the number of study locations is limited, this species has been shown to associate with clade C (Roopin et al. 2008; Chang et al. 2011; Hill and Scott 2012). At the sub-cladal level, ITS1 type C1/3 has been recorded on the southern coasts of Japan and South Korea (Chang et al. 2011) and ITS2 type C1 has been recorded in the northern Red Sea (Roopin et al. 2008).

The combination of host and symbiont type plays a significant role in determining bleaching sensitivity during periods of elevated temperature and high irradiance (Baird et al. 2009a), with many studies identifying oxidative stress in the photosynthetic apparatus of the algal symbionts as the underlying mechanism responsible for the breakdown in the symbiosis

(Lesser 2011). In *E. quadricolor* from North Solitary Island (New South Wales, Australia), bleaching and host mortality occurred when temperatures exceeded the summer maximum of 26 °C (Hill and Scott 2012). Knowledge of these associations is therefore essential for understanding how the endosymbiotic relationship of *E. quadricolor* will respond to rising ocean temperatures. This study provides the first information on the diversity of *Symbiodinium* found in *E. quadricolor* on the east coast of Australia.

6.2 Materials and methods

6.2.1 Sample collection

Entacmaea quadricolor samples (n = 62) were collected from five locations along the east coast of Australia from 0.3 – 18.4 m depth (Fig. 6.1, Table 6.1) between 29 June 2012 and 11 February 2013. One or two tentacles from each individual were preserved in 60 – 100% ethanol. The diluted ethanol was replaced with 100% ethanol after transportation.

6.2.2 DNA extraction and amplification of the ITS2 region

Subsamples of the tentacles were homogenized in Tris buffer (0.01 M, pH 8.0) using micro-pestles. Then samples were homogenized further in ~ 50 mg of 710 – 1180 µm glass beads with a Tissue Lyser LT (Qiagen, Australia) bead mill for 10 min at 50 Hz at 4 °C. The cell lysate was spun for 10 min at 16000 × g at 4 °C. A subsample of the supernatant was mixed with an equal volume of isopropanol, inverted and immediately spun for 30 min at 16000 × g at 4 °C. The DNA pellet was washed twice with 500 µL 70% ethanol, dried and re-suspended in 30 µL sterile water.

Dinoflagellate nuclear nucleotide sequences, consisting of partial 5.8S rDNA (5′), full length internal transcribed spacer 2 (ITS2) and partial 28S rDNA (3′) were amplified using the *Symbiodinium*-specific forward primer ItsD (Pochon et al. 2007), and reverse primer ITS2CLAMP (LaJeunesse 2002). These amplicons are from hereon referred to as ITS2 sequences. Sequences were separated using denaturing gradient gel electrophoresis (DGGE) following Wicks et al. (2010a), except that gels were run at 100 V for 16 h and DNA was stained with ethidium bromide (0.5 µg/mL). Representative and dominant bands were dissolved in 30

µL sterile water, and re-amplified using the primer set ITSD and ITS2CLAMP. Re-amplified products were sequenced in forward and reverse directions at Macrogen, South Korea, with the primer set ITSD and ITS2REVint (5′-CCATATGCTTAAGTTCAGCGGG-3′). To reveal low-abundance ITS2 variants that were below the detection limits of the DGGE method (Thornhill et al. 2006) one representative sample of each characteristic DGGE pattern except for C1 was ligated with TOPO-TA vector and transformed using One Shot ® Mach1^{TM}-T1^{R} chemically competent cells following the manufacturer's recommendations. Plasmids from 9 – 10 positive clones per sample were isolated using the PureLinkTM Quick Plasmid Miniprep Kit (Invitrogen, New Zealand) and sequenced as described above. Cloning generated predominantly unique sequences, as has been described for *Symbiodinium* ITS2 clone libraries before and can be explained by PCR bias or errors, cloning artefacts, and/or high intragenomic variability (e.g. Sampayo et al. 2009). All clone singletons were used for alignment and phylogenetic tree construction without modification, since it could not differentiated between rare intragenomic variants and PCR bias or errors (Stat et al. 2011).

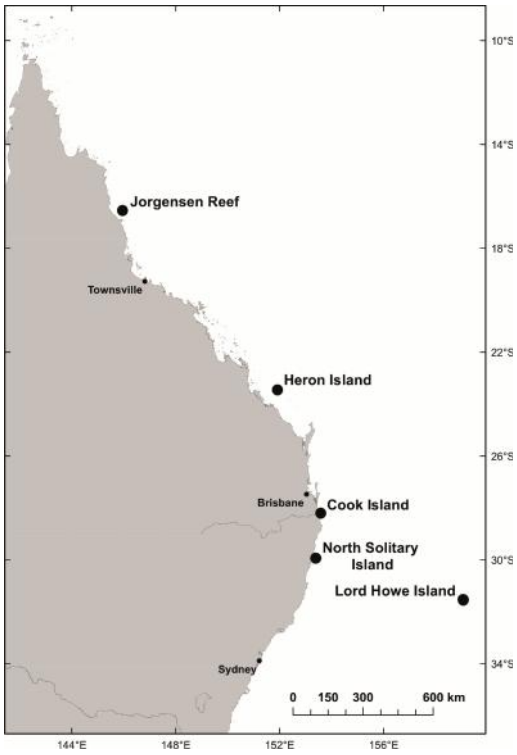

Figure 6.1: Map of the east Australian coast showing the sample collection locations, which are represented by large filled circles. Map was produced by Thomas Bridge.

Table 6.1: Sample collection information and ITS2 type(s) identified by DGGE and sequencing.

Location	Latitude, longitude	Sample collection date	Depth at low tide (m)	*n*	ITS2 type
Jorgensen Reef	16°32'28"S, 145°57'12"E	27.10.2012	5	1	C1
		27.10.2012		3	C42(type2).2
		11.02.2013		3	C42(type2).2
Heron Island lagoon	23°26'41"S, 151°54'50"E	29.06.2012 – 02.07.2012	0.3	7	C25, C3.25
				3	C42(type2).1
Cook Island	28°11'44"S, 153°34'41"E	20.08.2012	4 – 8.2	7	C25, C3.25
North Solitary Island					
Anemone Bay	29°55'24.87"S, 153°23'16.11"E	04.10.2012	3.3 – 4.5	6	C25, C3.25
Canyons	29°55'30.29"S, 153°23'11.98"E	09.08.2012	17.3	12	C25, C3.25
Elbow Cave	29°55'53.85"S, 153°23'26.75"E	09.08.2012	17.9	5	C25, C3.25
Lord Howe Island					
Neds Beach	31°31'00.78"S, 159°03'57.03"E	22.09.2012	0.3 – 1	4	C25, C3.25
Sylphs Hole	31°31'13.16"S, 159°03'16.50"E	29.09.2012	0.3	2	C25, C3.25
				3	C25.1
Comets Hole	31°32'26.36"S, 159°03'51.70"E	26./27.09.2012	4 – 5.1	6	C25, C3.25

6.2.3 DNA sequence alignment and phylogenetic tree construction

ITS2 secondary structures were predicted as described in Stat et al. (2009) and Pochon and Gates (2010). If ITS2 sequences did not correctly fold into functional secondary structures, they were not included in downstream analysis. All sequences were analyzed by BLAST on Genbank and compared to sequences available on Geosymbio (Franklin et al. 2012). Alignments were created using Clustal W and a maximum likelihood tree was calculated using MrBayes (Huelsenbeck and Ronquist 2001) or Geneious Basic 5.5.7 (Biomatters Ltd, New Zealand) and the PhyML plug-in (Guindon and Gascuel 2003). MrBayes phylograms were estimated by calculation of 1000000 trees, a sampling frequency of 50 and a burn-in of the initial 25% trees sampled. PhyML phylograms were estimated using the GTR substitution model and 1000 bootstraps.

6.3 Results and Discussion

Five distinct DGGE gel fingerprints were identified (Figure 6.2 A) along a ~ 2100 km distance ranging from the northern GBR to the world's southernmost barrier reef on Lord Howe Island, revealing six different ITS2 types of *Symbiodinium* clade C (Table 6.1). C1 and C25 have been described previously (e.g. LaJeunesse et al. 2003), but four sequences represent previously undescribed ITS2 types. These novel types are variants of C3, C25, and C42(type2), as defined by the closest reported sequence on GenBank and supported by phylogenetic tree construction (Figures 6.3, 6.4). These are named C3.25 (two basepair insertions; GenBank Accession Number: KF134175), C25.1 (two basepair mismatches; GenBank Accession Number: KF134174), C42(type2).1 (three basepair mismatches; GenBank Accession Number: KF134172) and C42(type2).2 (four basepair mismatches and three basepair insertions; GenBank Accession Number: KF134173), respectively (*sensu* Stat et al. 2009). For sequence identity refer to Appendix A.4 on page 261. The reconstruction of the ITS2 secondary structure yielded highly stable molecules, indicating that these novel ITS2 sequences are structurally conserved and, as such, functional.

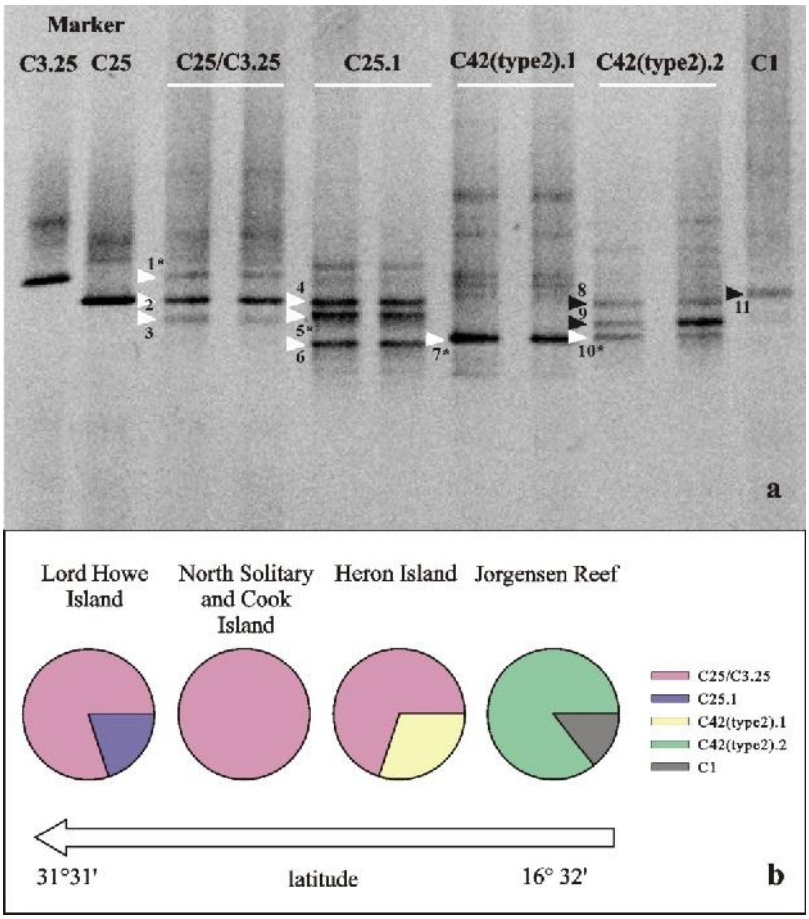

Figure 6.2: A Five distinct DGGE profiles for the *Symbiodinium* ITS2 types detected in this study. Eleven distinct bands were re-amplified and sequenced from at least two replicate samples (white arrows) or one of the samples (black arrows), resulting in a total of 22 sequences. Two were identical and named C3.25 (1), four were identical to C25 (2, 3), eight were identical and named C25.1 (4 – 6), two were identical and named C42(type2).1 (7), four were identical and named C42(type2).2 (8 – 10) and two were identical to C1 (11). One of each of the novel sequences was deposited in GenBank (as denoted by *). **B** Abundance (%) of distinct DGGE profiles in anemones from different collection sites.

A mixed ITS2 assemblage of C25 and C3.25 was found in the majority of anemones (49 of 62 individuals); this was the most prevalent assemblage in *E. quadricolor* on the southern reefs and was also frequent in anemones on the central GBR, but absent at the northernmost sampling location, Jorgensen Reef (Figure 6.2 B, Table 6.1). Additionally, 20% of individuals at Lord Howe Island showed a distinct DGGE profile predominantly encoding for C25.1, which was

absent at the other locations. *Symbiodinium* C42(type2).1 was dominant in 30% of individuals at Heron Island but not found at any of the other locations; C1 variants co-occurred in at least one of these Heron Island individuals, as identified by cloning (Table 6.2, Figure 6.4). At Jorgensen Reef, the majority (86%) of individuals hosted C42(type2).2 (Table 6.1), with C3 variants and E1 present in low abundance in one individual, again identified by cloning (Table 6.2, Figure 6.4). This is the first evidence that *E. quadricolor* may harbour *Symbiodinium* spp. belonging to clade E.

Table 6.2: Cloned ITS2 sequence variants obtained from the rDNA pool from one of each of the DGGE fingerprints encoding for C25/C3.25, C25.1, C42(type2).1 and C42(type2).2. C1 was not cloned. Percentages show abundance within 9 – 10 sequenced clones.

ITS2 type (s), DGGE	**ITS2 sequence variants, bacterial cloning**
C25, C3.25	C25 (55.6%), C3 variants (44.4%)
C25.1	C25 variants (90%), C25 (10%)
C42(type2).1	C42(type2).1 variants (66.7%), C1 variants (33.3%)
C42(type2).2	C42(type2).2 variants (80%), C3 variants (10%), E1 (10%)

The well supported separation of cloned E1, C1 and C3 variants in the phylogenetic tree (Figure 6.4) suggest that they represent symbiont types additional to pre-dominant C42(type2). In contrast, heterogeneous but closely related sequences clustering with C25, C25.1, C42(type2).1 and C42(type2).2 (Figure 6.4) might represent: (i) intragenomic variations of the corresponding "type", indicative of a highly heterogeneous genome as has been observed for C42(type1); (ii) aberrant sequences produced by PCR bias or errors or cloning artefacts; or a combination of the two (Sampayo et al. 2009).

There are several factors that may determine *Symbiodinium* distribution patterns, including changing environments (e.g. temperature, irradiance) associated with depth (e.g. Sampayo et al. 2007; Bongaerts et al. 2011) season (e.g. Chen et al. 2005) or latitude (e.g. LaJeunesse and Trench 2000; Rodriguez-Lanetty et al. 2001; Silverstein et al. 2011). In this study, anemones

sampled from two depths at North Solitary Island harboured identical *Symbiodinium* ITS2 types (Table 6.1). Also, among the remaining individuals (sampled between 0.3 and 8.2 m), no depth-dependent pattern was evident. Temperatures in the study regions range annually between ~ 18 - 26 °C at Lord Howe Island, and ~ 24 – 31 °C at Jorgensen Reef (www.noaa.gov) suggesting that the C42(type2) ITS2 variants found at lower latitudes might be specialized for the warmer temperatures and perhaps higher light conditions associated with these lower latitudes. However, a larger number of sites would need to be surveyed to confirm this hypothesis. Furthermore, C25.1 is found exclusively in anemones from Sylphs Hole at Lord Howe Island. This site differs from other sites at this location in that turbidity is higher and salinity is lower (Wicks et al. 2010a). Therefore, turbidity and/or salinity might be important determinants of symbionts at this site.

Symbiodinium types C25 and C3.25 span a distance of ~ 1100 km and a maximum monthly mean temperature range of ~ 3.5 °C. The summer maximum monthly mean temperature of ~ 27.5 °C at Heron Island would lead to bleaching and host mortality in *E. quadricolor* at North Solitary Island (Hill and Scott 2012) indicating that symbiont-specific (Howells et al. 2011) or host-specific (Baird et al. 2009a) adaptations to a certain thermal regime strongly influence holobiont performance. Although it is evident that *Symbiodinium* type is not the sole determinant of thermal tolerance, the capability to associate with multiple ITS2 types simultaneously might be advantageous in an era of rising sea temperatures, if the ITS2 population could change in favour of a better-suited type that would optimize the performance of the holobiont (Buddemeier and Fautin 1993). Physiological studies are needed to confirm these hypotheses and to understand the possible responses of *E. quadricolor* and its symbionts to future climate changes.

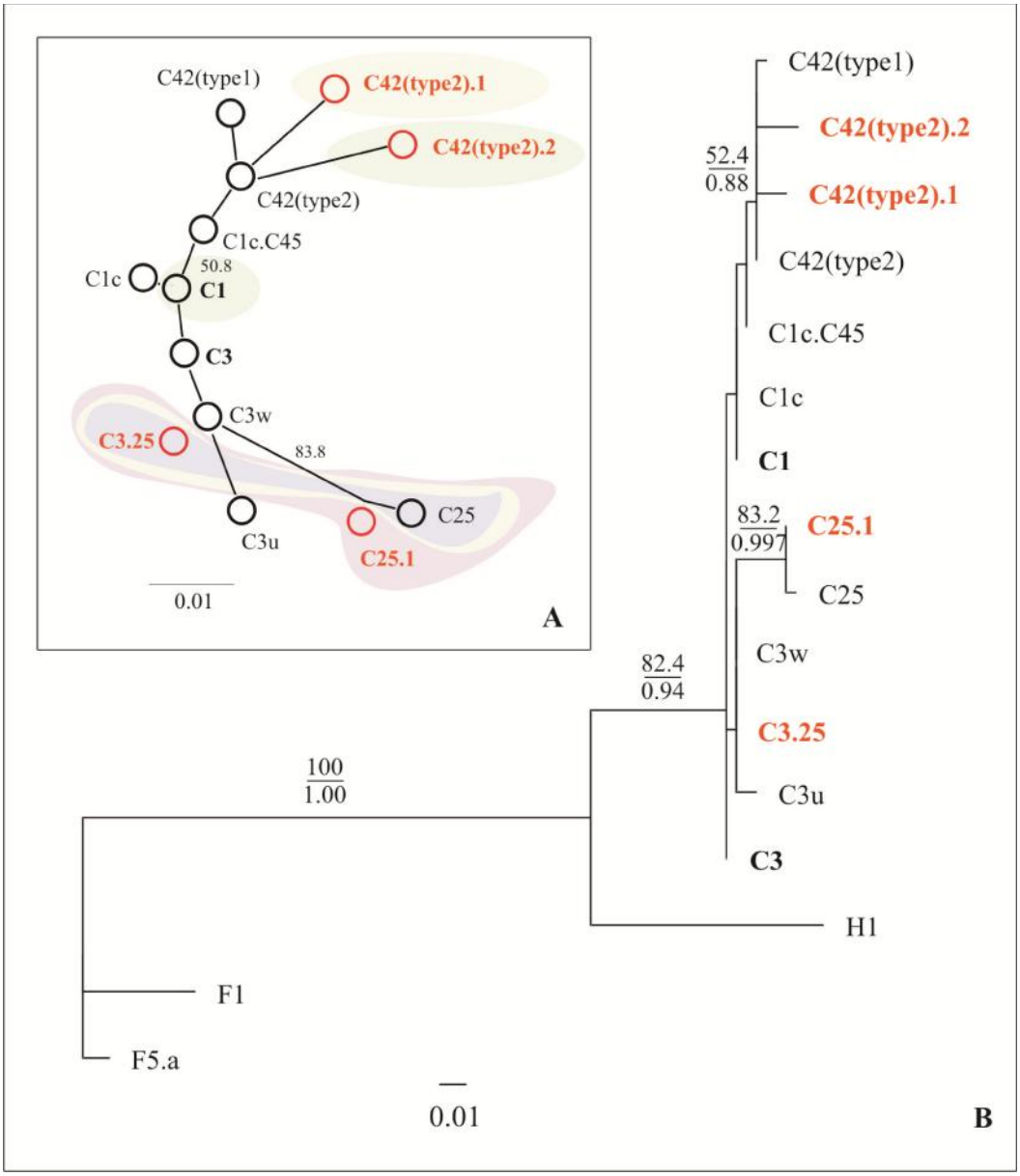

Figure 6.3: Unrooted **(A)** and rooted **(B)** phylograms of novel predominant *Symbiodinium* internal transcribed spacer (ITS) 2 types identified in *Entacmaea quadricolor* (red font) and previously published ITS2 types (black font). Phylograms were estimated using PhyML and Bayesian methods resulting in highly similar results. The trees presented are PhyML estimates. Numbers at nodes show the support of maximum likelyhood (ML) bootstrap analysis (BP, numbers above line) and Bayesian posterior probabilities (BiPP, numbers below line) and are presented when stronger than 50% BP or 0.8 BiPP. Colours highlight ITS2 types predominantly identified in *E. quadricolor* sampled at Jorgensen Reef (green), Heron Island (yellow), Cook Island and North Solitary Island (blue) and Lord Howe Island (purple). Published ITS2 sequences are derived from Geosymbio (Franklin et al. 2012). Bold font highlights ancestral IS2 types.

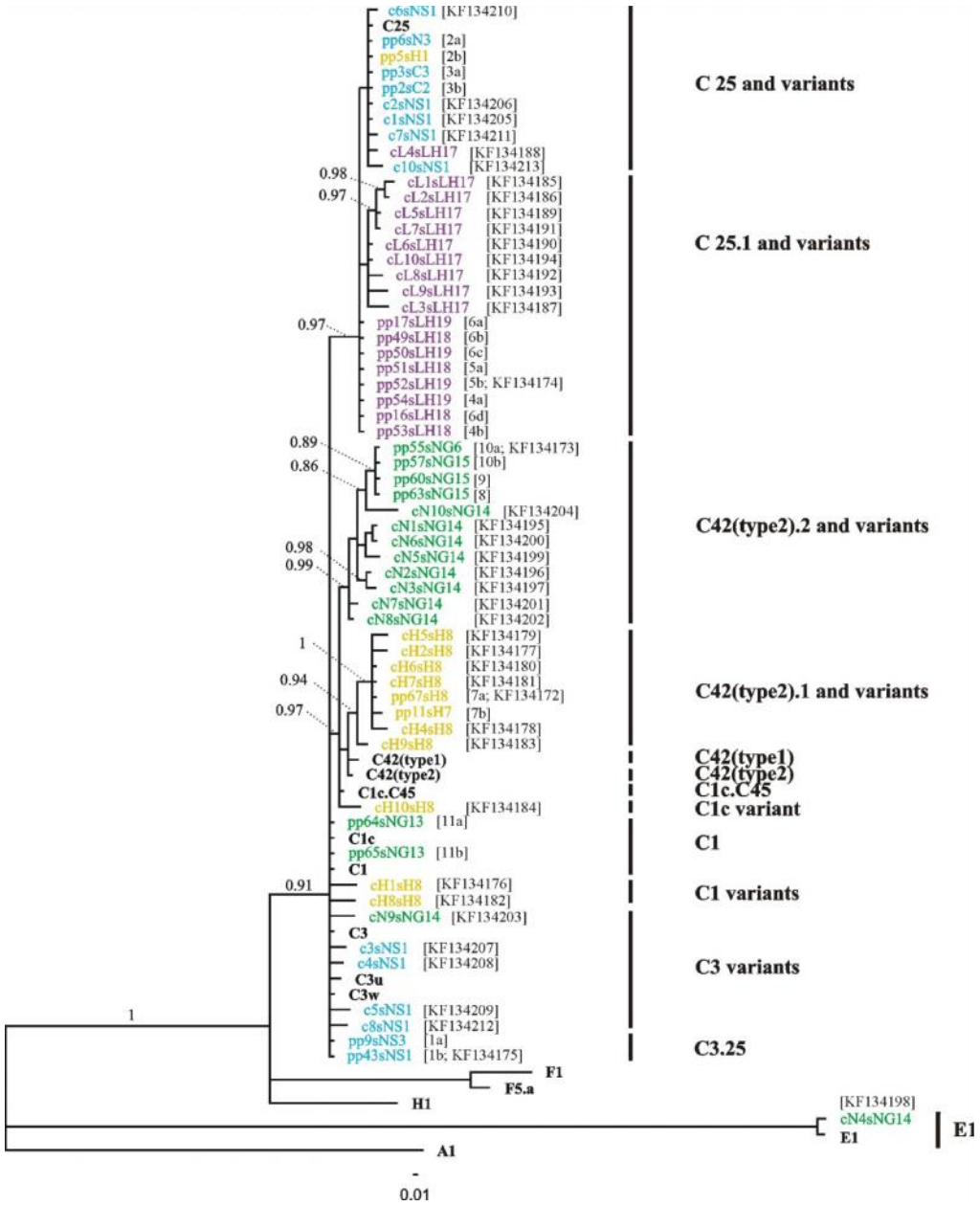

Figure 6.4: Rooted phylogenetic tree of *Symbiodinium* ITS2 sequences identified by denaturing gradient gel electrophoresis (DGGE) (pp; GenBank Accession Numbers KF134172 – KF134175) or bacterial cloning (c; GenBank Accession Numbers KF134176 – KF134213) from samples collected from Lord Howe Island (LH, purple), North Solitary Island (NS, blue), Cook Island (C, blue), Heron Island (H, yellow) and Jorgensen Reef (NG, green). One – two digits coding in brackets refers to DGGE band position as outlined in Figure 2, from which sequences were retrieved. ITS2 types in black font are previously published types obtained from Geosymbio (Franklin et al. 2012). ITS2 types C3.25, C25, C25.1, C42(type2).1 and C42(type2).2 were assigned to sequences identified by DGGE and their variants were assigned to sequences obtained by bacterial cloning. The phylogenetic tree was constructed using the Bayesian method and Bayesian posterior probabilities are shown if stronger than 0.8.

Chapter 7:
Symbiodinium genotypic flexibility and antioxidant capacity during thermal stress in the anemone *Entacmaea quadricolor* are dependent on host pigmentation

7.1 Introduction

The association of heterotrophic animals with intracellular autotrophic algal cells is widespread in the phylum cnidaria, including reef-building corals, jellyfish and sea anemones (Stambler 2010). Dinoflagellates of the genus *Symbiodinium*, commonly identified by their variable ITS2 region of the ribosomal DNA (LaJeunesse 2001), can meet the metabolic demands of their hosts by translocation of photosynthetically fixed carbon (Falkowski et al. 1984; Muscatine et al. 1984). In return, the host contributes to the symbionts' inorganic nutrient demands (Trench 1979; Davy et al. 2012). This association is particularly important in, but not restricted to, oligotrophic shallow tropical waters (Muscatine and Porter 1977). Indeed, cnidarian-*Symbiodinium* associations are abundant over a broad range of latitudes from tropical to temperate zones (Muller-Parker and Davy 2001) and extend into mesophotic regions (Bongaerts et al. 2011; Bridge et al. 2012).

The persistence and health of *Symbiodinium*-associated species worldwide is threatened by rapidly changing environmental conditions, such as anthropogenically driven increases in oceanic temperature and the increasing frequency of thermal anomalies (Hoegh-Guldberg and Bruno 2010). The waters of southeastern Australia in particular are predicted to warm faster than other Australian marine regions, mainly due to an intensification of the East Australian Current (EAC), which transports warm water southwards from tropical regions (Hobday and Lough 2011). By 2050, average water temperatures in southeastern Australia are predicted to be 2 °C higher than the 1990 – 2000 average (Hobday and Lough 2011). High temperature, often in concert with other stressors such as high light intensity, can cause the collapse of the symbiosis and/or death of the host, which is often preceded by cellular changes in both symbiotic partners. Most notable is a decline in photosynthetic capacity of *Symbiodinium*, loss of *Symbiodinium* cells

and/or *Symbiodinium*-specific pigments (i.e. bleaching; Brown 1997; Hoegh-Guldberg 1999; Hill and Scott 2012).

Entacmaea quadricolor (Rüppell and Leuckart 1828) is the most common and widespread species of sea anemone in the Indo-Pacific that hosts *Symbiodinium* and anemonefishes in a three-way symbiosis (Dunn 1981; Fautin and Allen 1992). *E. quadricolor* occurs in a range of distinctly pigmented phenotypes, with varying colouration of column, oral disc or tentacle tips (Dunn 1981). On the east Australian coast, *E. quadricolor* is found on tropical and subtropical reefs, with the highest densities at North Solitary Island, Solitary Island Marine Park, New South Wales (Richardson et al. 1997; Scott et al. 2011). A previous study has shown that *E. quadricolor* at North Solitary Island, where mean daily temperatures range between ~ 18 °C and 26 °C (Dalton and Carroll 2011), lives within 1 °C of its upper physiological threshold (Hill and Scott 2012). Given the projected + 2 °C increase by 2050, rapid acclimatization or adaptation mechanisms are necessary to ensure the survival of *E. quadricolor* at this high latitude site.

As described in Chapter 6, *E. quadricolor* at North Solitary Island harbour two *Symbiodinium* ITS2 types simultaneously: C25 and C3.25. Although somewhat controversial, it has been hypothesized that the potential to associate with multiple symbiont types might be advantageous for the maintenance of the symbiosis and persistence of the holobiont (i.e. the animal host and all associated symbionts) under changeable conditions (Baker 2003; Berkelmans and van Oppen 2006; LaJeunesse et al. 2009; Putnam et al. 2012). The importance of *Symbiodinium* cells in influencing, in part, the response of the holobiont to environmental perturbations has gained much attention over the past few decades (e.g. Sampayo et al. 2008; Fisher et al. 2012), associated with an increasing awareness that distinct *Symbiodinium* clades and/or types have different physiological capabilities (Robison and Warner 2006; Ragni et al. 2010; Krämer et al. 2012). Indeed, shifts in the dominant members of *Symbiodinium* populations have been suggested as a potential acclimatory mechanism to rising sea temperatures (Buddemeier and Fautin 1993; Buddemeier et al. 2004). In the “adaptive bleaching hypothesis” (ABH) it has been hypothesized that shifts in the dominant *Symbiodinium* populations could be achieved by the repopulation of a bleached coral with a new, stress-tolerant *Symbiodinium* partner, or by the shuffling of the relative proportion of pre-existing multiple *Symbiodinium*

partners towards a more stress-tolerant assemblage (Buddemeier and Fautin 1993; Buddemeier et al. 2004). Therefore, shuffling of *Symbiodinium* ITS2 types C25 and C3.25 might be a key mechanism underlying the success of *E. quadricolor* at the high latitude site of North Solitary Island, where temperatures show substantial variations over the year. Furthermore, a capacity to shuffle the type of *Symbiodinium* in this sea anemone towards a more thermally tolerant type might influence holobiont physiology and hence facilitate survivorship in an era of rising seawater temperatures.

Thermal tolerance, i.e. the maintenance of an intact association of *Symbiodinium* cells and their cnidarian partners, has been linked to the capability of the antioxidant defence system of both partners to deal with oxidative stress (Lesser 2011). Oxidative stress refers to the imbalance of reactive oxygen species (ROS) and detoxifying antioxidants (Sies 1991), which can be disturbed in favour of ROS under stressful conditions. In small doses, ROS are important cell signalling molecules (Apel and Hirt 2004) and may be involved in photoprotection (Asada 1999; 2000). However, excessive concentrations can be cytotoxic and adversely affect PSII and the carbon-fixing enzyme ribulose-1,5-biphosphate carboxylase/oxygenase (rubisco) (Nishiyama et al. 2006; Takahashi and Murata 2008; Lesser 2011). Hence, excess ROS generation might affect photosynthetic performance (Lesser 2011) and often accompanies bleaching (Takahashi et al. 2013). Indeed, high levels of ROS have been associated with reduced photosynthesis in thermally susceptible *Symbiodinium* types (Suggett et al. 2008). Furthermore, ROS are involved in apoptosis, the programmed cell death often observed in *Symbiodinium* and host cells exposed to excessively high temperatures (Franklin et al. 2004; Tchernov et al. 2011). Hence, the capability to tightly control levels of ROS under thermal stress seems necessary to guarantee the health and survival of both *Symbiodinium* and the animal host.

ROS, including the superoxide anion (O_2^-), hydrogen peroxide (H_2O_2) and the hydroxyl radical (•OH) are generated during photosynthetic pathways in chloroplasts (Lesser 2006) and also during aerobic pathways in the mitochondria of the animal host and *Symbiodinium* cell (Nii and Muscatine 1997; Dunn et al. 2012). O_2^- is a highly reactive radical, which can undergo a chemical reaction with nitric oxide (NO) to form the toxic products peroxynitrite $ONOO^-$ and •OH (Fattman et al. 2003). To prevent these unwanted processes, the concentration of O_2^- is controlled by a variety of enzymatic and non-enzymatic compounds in both symbiotic partners.

The enzyme superoxide dismutase (SOD) catalyzes the conversion of O_2^- to oxygen (O_2) and H_2O_2, which in turn is detoxified by the enzymes ascorbate peroxidase (APX) or catalase (CAT) (Asada 1999; Halliwell 2006). As such, SOD is the first-in-line ROS-scavenging enzyme. In addition, singlet oxygen ($^1O_2$) can be produced at PSII by excited chlorophyll molecules that pass their excitation energy to oxygen (Lesser 2006). Dimethylsulfide (DMS) and dimethylsulfoniopropionate (DMSP) have been shown to quench $^1O_2$ and •OH, respectively (Sunda et al. 2002). These compounds act in concert with other antioxidants (e.g. ascorbate, carotenoids, tocopherols, glutathione) and antioxidant enzymes to maintain the redox balance of the chloroplast and/or cell (Halliwell 2006).

Considering the above, the objectives of this study were to explore the effects of short-term heat stress on the: (i) dynamics of *Symbiodinium* C25 and C3.25 populations, and (ii) the activity of SOD in *Symbiodinium* cells and *E. quadricolor* tissue. We hypothesized that shuffling symbiont types might relate to their respective SOD capacities and that shuffling and/or the use of antioxidant mechanisms such as enhanced SOD activity, might be key mechanisms facilitating thermal tolerance. These hypotheses were tested by analysing two distinct anemone colour phenotypes.

7.2 Materials and methods

7.2.1 Anemone specimen for temperature experiment

In August 2012, 36 individuals of *Entacmaea quadricolor* were collected at approximately 18 m depth from North Solitary Island, Solitary Island Marine Park, New South Wales, Australia (29°55′S, 153°23′E). 18 individuals had a red column, brown tentacles and green tips (referred to as green phenotype; Figure 7.1 A), and 18 individuals had an orange column and brown tentacles, with white pigmentation below pink tentacle tips (referred to as pink phenotype B; Figure 7.1 B). These two different colour phenotypes were used to assess whether they exhibited similar thermal responses and whether the genetic and biochemical findings could be generalized across anemones with dissimilar pigmentation. Specimens were maintained outdoors in 3000-L tanks supplied with flow-through seawater at a temperature of 19 – 20 °C and irradiance of < 50 µmol photons m^{-2} s^{-1} for 32 d before the experiment and fed

periodically. Four days before the start of the experiment, the anemones were fed to satiation with small pieces of prawn meat.

7.2.2 Set-up of the temperature experiment

On Day 1 of the temperature experiment, anemones with a submerged weight [determined by weighing each anemone while it was submerged in sea water; (Fitt 1982)] of 0.6 – 1.6 g (green phenotype) and 0.3 – 1.9 g (pink phenotype) were placed into individual transparent 15-L tubs supplied with 5 µm filtered seawater (Filtaflo sediment filters, Australia) from three temperature controlled (heat pump, Aquahort) 3000-L header tanks with a flow rate of 600 mL min $^{-1}$.

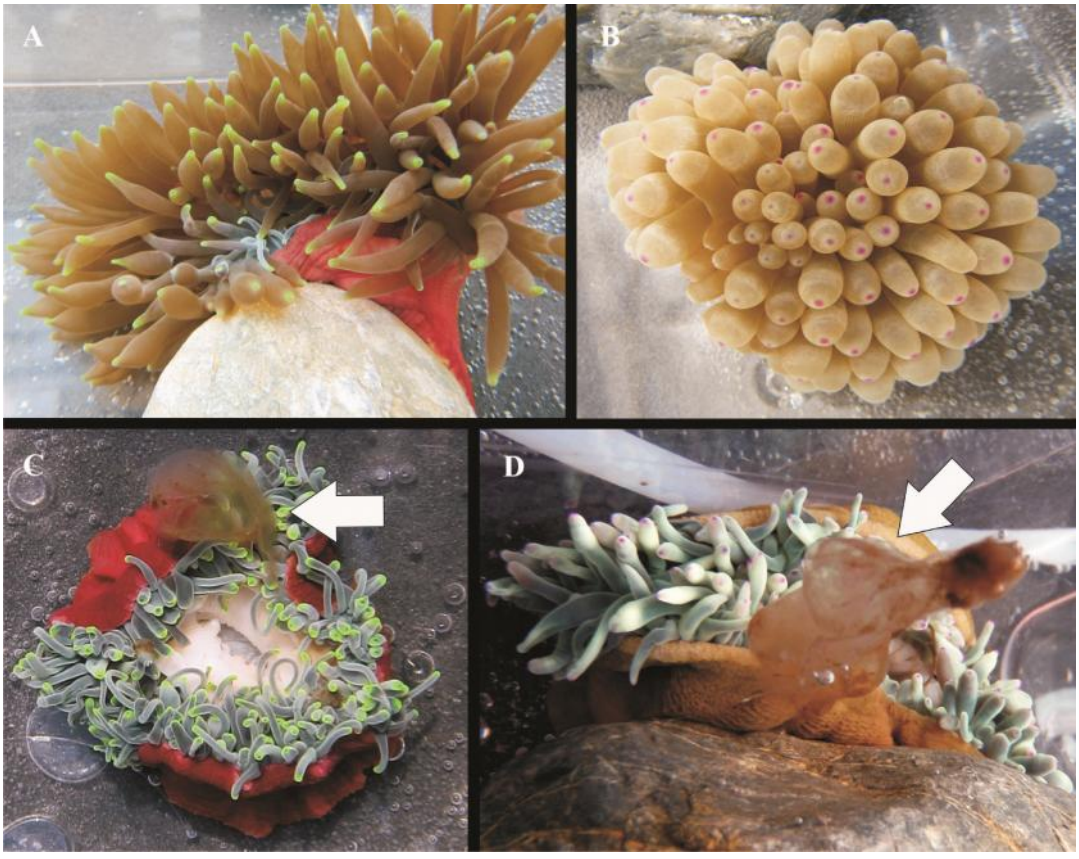

Figure 7.1: Green phenotype (**A**) and pink phenotype (**B**) of *Entacmaea quadricolor* specimens used in the temperature experiment. White arrows indicate expulsion of *Symbiodinium* observed on Day 3 in both anemone phenotypes exposed to the highest temperature (**C**, **D**). Anemones are approximately 15 – 20 cm in diameter. **C** photo courtesy by Ross Hill.

Three 1200-L tanks each contained twelve 15-L tubs, so that in total 36 tubs were used, each containing a single anemone. All 15-L tubs contained flow-through filtered sea water (at a flow rate of 600 mL min^{-1}). Of these, 12 tubs were exposed to control temperature (C) averaging 21.3 °C, 12 tubs were exposed to medium temperature (M) averaging 24.5 °C (1.5 °C below maximum summer temperature), and 12 tubs were exposed to high temperature (H) averaging 27.6 °C (1.6 °C above maximum summer temperature; http://data.aims.gov.au), as shown in Figure 7.2 A. Temperature treatment was allocated haphazardly within each 1200-L tank, so that each tank contained four tubs per temperature treatment. Anemone phenotypes were placed haphazardly within each treatment with a replication of six (two anemones per 1200-L tank). The final temperature was attained by gradually increasing the temperature in small increments over 36 hours starting at 12:00 h on Day 1 (Figure 7.2 A). The desired temperature was attained at 24:00 h in all treatments on Day 2 and was maintained until the end of the experiment (12:00 h on Day 9) (Figure 7.2 A). Temperature was monitored using Thermochron iButton temperature loggers (temperature accuracy ± 0.5 °C; Maxim, USA), calibrated against a high precision mercury thermometer. The tanks were covered with two layers of white shade cloth to reduce the natural light intensity to approximately 25% of incoming solar radiation, to simulate light intensities at depth of collection. The light intensity was monitored using an underwater Odyssey light logger (Dataflow Systems, New Zealand), calibrated against a Li-1400 photometer with a 2π Li-192SA quantum sensor (Lincoln, USA) (Figure 7.2 B).

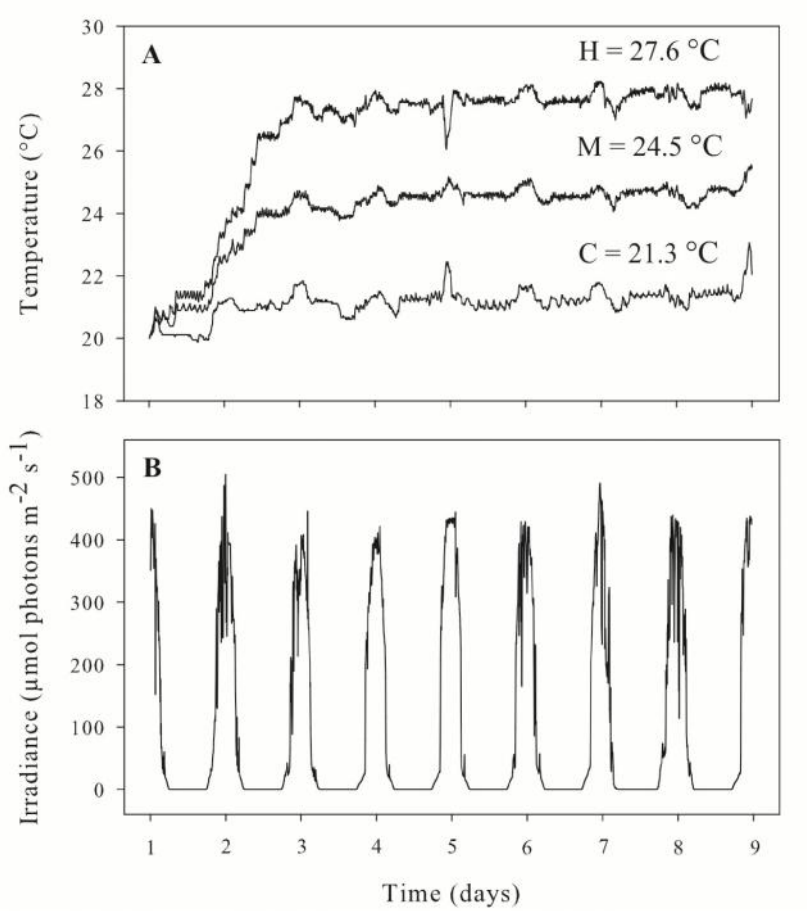

Figure 7.2: Average temperatures for high (H), medium (M) and control (C) temperature treatments (**A**), and average irradiance for all temperature treatment over the 9-day period (**B**).

7.2.3 Quantification of ITS2 copies

At 12:00 h at the beginning (Day 1) and end (Day 9) of the experiment, one tentacle per anemone was removed using scissors and forceps and preserved in 95% ethanol for DNA extraction, amplification of the ITS2 region and absolute quantification of ITS2 copies. DNA was extracted from all 36 individuals, the ITS2 region of the ribosomal DNA was amplified, and the amplicons were separated using denaturing gradient gel electrophoresis (DGGE) as described in Chapter 6, Section 6.2.2 on pages 168 – 169. Furthermore, the ITS2 amplicons obtained with the primerpair ItsD (Pochon et al. 2007) and ITS2CLAMP (LaJeunesse 2002) for each of two *E. quadricolor* individuals were cloned as described in Chapter 6, Section 6.2.2 on page 168. The concentrations of purified plasmids were measured by absorbance at 230, 260, 280 and 320 nm using a Nanophotometer (Implen GmbH, Germany). Plasmid DNA standards were generated by

10 fold serial dilutions ranging from 10.8 ng μL^{-1} to 0.0108 pg μL^{-1} for C3.25 ITS2 plasmid DNA (seven dilutions) and from 11.5 ng μL^{-1} to 0.115 pg μL^{-1} for C25 ITS2 plasmid DNA (six dilutions). The absolute copy number of the corresponding ITS2 sequences within each plasmid DNA standard was calculated as:

$$ITS2\ copy\ number\ (molecules/\mu L) = \frac{DNA\ concentration\left(\frac{g}{\mu L}\right) \times Avogadro's Number\ \left(\frac{molecules}{mole}\right)}{total\ molecular\ weight\ \left(\frac{g}{mole}\right)}$$

Avogadro's Number	6.022 x 10^{23} molecules/mole
Molecular weight of 1 basepair (bp)	660 g/mole
Plasmid length	4000 bp (pCR®4-TOPO® TA) +
	120 bp (ITS2 fragment)
Total molecular weight	660 × plasmid length in base pairs

Accordingly, ITS2 copy numbers in C3.25 plasmid DNA standards ranged from $2.39 \times 10^3 – 2.39 \times 10^9$ copies μL^{-1} and ITS2 copy numbers in C25 plasmid DNA standards ranged from $2.55 \times 10^4 – 2.55 \times 10^9$ copies μL^{-1}. Primers amplifying a 120 bp-long ITS2 fragment specific for C25 and C3.25 were designed for quantitative PCR (Table 7.1).

Quantitative (q) PCR was run on a Step One Real-time PCR system thermal cycler (AB Applied Bioscience, CA, USA) using SYBR® Green Real-Time PCR Master Mix (Invitrogen, New Zealand) containing 10 µL Master Mix, 0.5 µL primer (10 mM) forward, 0.5 µL primer (10 mM) reverse, 1 µL sample DNA and 8 µL water in a total reaction volume of 20 µL. Thermal cycling conditions were specified as: initial start at 95 °C for 10 min followed by 40 cycles at 95 °C for 15 s (denaturation) and T_a (annealing and extension, see Table 7.1) for 60 s. The threshold cycle (C_T; the point when a significant increase in florescence is detectable) was set by default to 0.35, and kept at this level throughout the standard and experimental runs. The efficiency of amplification was 93.7% for C3.25 and 90.5% for C25, and the correlation coefficient (R^2) was 0.997 for both ITS2 types. The potential of cross-amplification (i.e. the amplification of C3.25 ITS2 amplicons using C25 primer-pair and *vice versa*) was tested across the whole range of plasmid DNA dilutions. Here, the C3.25 primer-pair amplified < 0.04% of

C25 copies and the C25 primer-pair amplified < 0.001% of C3.25 copies. Moreover, the specificity of each primer-pair was tested over a range of C3.25/C25 dilutions (0:1, 1:3, 1:1, 3:1, 1:0).

The ratio of ITS2 populations was calculated by dividing the ITS2 copy number (C25) by the ITS copy number (C3.25):

$$\frac{ITS2\ copy\ number\ (C25)}{ITS2\ copy\ number\ (C3.25)}$$

Table 7.1: Sequence and properties of primer pairs specific for the amplification of C25 and C3.25. T_a = annealing temperature.

ITS2 type	primer	primer sequence	T_a
C25	ITS2-C25-FW	5′- TCAATGGCCTCCTGAACGTTC -3′	67 °C
	ITS2-C25-REV	5′- GCAATGACTCATAAGAGCGC -3′	67 °C
C3.25	ITS2-C3-FW	5′- CCAATGGCCTCCTGAACGTGC -3′	68 °C
	ITS2-C3-REV	5′- GGGCAATAGCTCATAAGAACGC -3′	68 °C

7.2.4 Chlorophyll fluorescence

Chlorophyll fluorescence was measured using a Diving Pulse Amplitude Modulated (PAM) fluorometer (Walz, Germany). Maximum (F_v/F_m) and effective ($\Delta F/F_m'$) quantum yield were measured daily. F_v/F_m was measured before removal of the anemones from the holding tanks and placement into treatment tanks, and then daily at 05:00 h (pre-dawn) and 19:00 h (post-dusk). $\Delta F/F_m'$ was measured daily at 09:00 h, 12:00 h, and 16:00 h. The PAM settings were as follows: measuring intensity 3 (< 0.15 µmol photons m^{-2} s^{-1}); saturation intensity 12 (> 4500 µmol photons m^{-2} s^{-1}); saturation width 0.8 s; and gain 1. The light pressure over PSII (Q_m) (Iglesias-Prieto et al. 2004) was calculated using the equation: $Q_m = 1 - [(\Delta F/F_m'$ at noon)/(initial F_v/F_m on Day 1)]. On Days 1, 3, 5 and 9, rapid light curves (RLCs) were conducted on light-acclimated specimens with increasing actinic irradiances (0, 100, 151, 213, 322, 443, 680, 1015

and 1538 µmol photons m^{-2} s^{-1}), where each actinic irradiance was held for 10 s. Relative electron transport rate (rETR) was calculated as PAR × $\Delta F/F_m'$. A double decay exponential function of rETR at increasing actinic irradiances was fitted after Platt et al. (1980), using Sigma Plot 11.0. The initial slope of the rapid light curve (RLC) was described by alpha (α). The maximum relative electron transport rate ($rETR_{max}$), and the saturating light intensity (I_k) were calculated as in Hill et al. (2004b).

7.2.5 Sampling and sample processing

At 12:00 h on Days 1, 3, 5, and 9, three tentacles per anemone were removed using scissors and forceps and snap-frozen in liquid nitrogen for subsequent determination of host and symbiont superoxide dismutase (SOD) activity.

Samples were processed while being held on ice. Frozen tentacles were homogenized in 6 mL of 75 mM sodium phosphate buffer, pH 7.4 for 10 s using an Ultra-Turrax homogenizer (IKA, Germany). Homogenates were centrifuged at 4500 × g for 10 min to separate the algal symbionts from the host. Pelleted algal cells were re-suspended in 6 mL sodium phosphate buffer and the host supernatant was centrifuged two more times at 4500 × g for 5 min to remove any remaining symbiont cells. The anemone host and *Symbiodinium* cell fractions were each split into aliquots of 1 mL and sonicated for 5 min in a chilled sonicating bath, snap frozen in liquid nitrogen and kept at -20 °C for the remainder of the experiment. Samples were then transported on dry ice and stored at -80 °C until analysis. To increase SOD concentrations in the *Symbiodinium* cell fraction (in order to increase the detection signal), one 1-mL aliquot of the algal suspension was centrifuged at 7000 × g for 5 min, the supernatant discarded and the pellet resuspended in 300 µL sodium phosphate buffer, and then sonicated and processed as described above.

7.2.6 Superoxide dismutase (SOD) assay

The activities of SOD in anemone host (SOD_A) and *Symbiodinium* fractions (SOD_S) were measured following the method of Beauchamp and Fridovich (1971) and Beyer and Fridovich (1987). All reagents were obtained from Sigma, Australia. Standards were prepared from bovine SOD and samples were diluted in 75 mM potassium phosphate buffer, pH 7.4. The assay was

conducted in 96-well microtiter plates using 20 µL cell lysate or SOD standard in a final volume of 300 µL potassium phosphate buffer (50 mM, pH 7.8) containing EDTA (0.1 mM), riboflavin (1.3 µM), L-methionine (10 mM), nitro blue tetrazolium chloride (NBT) (57 µM) and 0.025% (v/v) triton X100. The method is based on the ability of SOD to inhibit the reduction of NBT by O_2^- produced by L-methionine and riboflavin. The reduction of NBT was monitored spectrophotometrically at 560 nm at 25 °C. A measurement was taken at the start, and after 10 min incubation at a light intensity of 130 µmol photons m^{-2} s^{-1}. One unit of SOD was defined as the amount of SOD inhibiting 50% of the reduction and was determined by comparison to a sigmoidal 5-parameter semi-logarithmic standard curve. The activity of SOD in samples is expressed per mg host or *Symbiodinium* soluble protein, as quantified using the technique of Bradford (1976).

7.2.7 Statistical analysis

Data were analyzed using the IBM SPSS statistics 20.0 software. Repeated measures (rm) analysis of variance and *post hoc* pairwise comparison with Bonferroni adjustment were used to analyze the effects of temperature. If necessary, data were transformed (arcsine transformation for F_v/F_m and $\Delta F_v/F_m'$; log transformation for all other parameters) to meet assumptions of normality, which were ascertained by the Kolmogorov-Smirnov test. Data were evaluated for assumptions of sphericity using Mauchly's test and, if violated, the Greenhouse-Geisser correction is reported. Univariate ANOVA was used to test the null hypothesis, that a particular photophysiological parameter was equal across phenotypes at the beginning of the experiment. Because symbiont ratio data did not meet assumptions of normality, they were analyzed using a non-parametric Friedman test (the non-parametric alternative to rmANOVA) with *post hoc* Wilcoxon rank comparisons to examine the null hypothesis that symbiont ratios were the same across days at a particular temperature, while the non-parametric Mann-Whitney U test was used to test the null hypothesis that symbiont ratios were equal across phenotypes at the beginning of the experiment.

A discriminant function analysis (DFA) was applied to test if the constitutive set of log-transformed parameters (values on Day 1; except for Q_m on Day 2) could predict (i) colour phenotype or (ii) *Symbiodinium* ratio. For this analysis, symbiont ratios were ranked from 1 – 4,

coding symbiont ratios (C25:C3.25) of < 5, 5.01 – 10, 10.01 – 15 and > 15, respectively. In two separate analyzes, (i) colour phenotype or (ii) ranked symbiont ratio were used as the grouping variables, and all other parameters (symbiont ratio, F_v/F_m, Q_m, $rETR_{max}$, I_k, α, SOD_A and SOD_S) were used as independent variables. DFA was also used to determine the set of parameters that allowed for the best discrimination between the three temperature treatments. For this analysis, values at Day 1 for each of the parameters (except values at Day 2 for Q_m) were subtracted from those at Day 9 (except Day 8 for F_v/F_m). Because DFA is very sensitive to outliers, data were checked for univariate outliers visually by scatter plots and mathematically by conversion to standard Z-scores; outliers were defined as those cases with a standard Z-score ± 3.0 (Shiffler 1988). One – two univariate outliers were identified, removed and replaced with the average of the remaining replicates. Also, data were checked for multivariate outliers using the Mahalanobis D^2 test (calculating a multidimensional version of Z-scores) and no multivariate outliers were identified based on Mahalanobis $D^2 \leq 0.001$ (Hadi 1992). DFA was run separately for both phenotypes using temperature as the grouping variable and all other parameters (symbiont ratio, F_v/F_m, Q_m, $rETR_{max}$, I_k, α, SOD_A and SOD_S) as independent variables. The identification of the most important variables that predicted a dimension was based on significant differences of group means and structure matrix.

7.3 Results

7.3.1 Algal genetic, photobiological and holobiont antioxidant constitution in two anemone phenotypes on Day 1

All anemones used in the study simultaneously hosted the mixed ITS2 assemblage of *Symbiodinium* C25 and C3.25. At the beginning of the experiment (Day 1), the ratio of ITS2 types, defined as the ratio of types C25 to C3.25, was higher in the green phenotype (8.6 ± 1.2, mean ± S.E.) compared to the pink phenotype (5.1 ± 0.6; mean ± S.E.; Table 7.2, Figure 7.3).

F_v/F_m measured as dark-acclimated yield at 19:00, ranged between 0.612 – 0.786 in the green phenotype and between 0.623 – 0.677 in the pink phenotype (Table 7.2, Figure 7.4). Initial excitation pressure over PSII (Q_m) was similar between colour phenotypes, and averaged 0.469 ± 0.039 in the green phenotype and 0.457 ± 0.037 in the pink phenotype (Table 7.2, Figure

7.4). In contrast, maximum relative electron transport rate ($rETR_{max}$) and photosynthetic rate in the light-limited region of the RLC (α) on Day 1 were lower in the green than the pink phenotype (Tables 7.2, 7.3). The initial minimum saturating irradiance (I_k) was similar in the two colour phenotypes (Tables 7.2, 7.3).

Algal and anemone superoxide dismutase (SOD_S and SOD_A) activities were each similar in the green and pink colour phenotypes (Table 7.2, Figure 7.5). In the *Symbiodinium* fraction, constitutive levels of SOD activity were higher than in the anemone host (Figure 7.5). In the green phenotype, SOD activity was 53.2 ± 5.41 units mg^{-1} in the *Symbiodinium* cells and 14.2 ± 2.51 units mg^{-1} in the host (Mann-Whitney-U test: $U_{(36)} = 309$; $p < 0.001$), while in the pink phenotype, SOD activity was 57.2 ± 4.33 units mg^{-1} in the *Symbiodinium* cells and 20.9 ± 3.57 units mg^{-1} in the host (Mann-Whitney-U test: $U_{(36)} = 301$; $p < 0.001$).

Table 7.2: Results of independent sample t-test analyzing the null hypothesis that the parameters are equal between green and pink phenotypes of *Entacmaea quadricolor* on Day 1 (Day 2 for Q_m). Parameters are: symbiont ratio; F_v/F_m (maximum quantum yield at 19:00); Q_m (excitation pressure over PSII); $rETR_{max}$ (maximum relative electron transport rate); α (photosynthetic rate in the light-limited region of the rapid light curve); I_K (minimum saturating irradiance); and superoxide dismutase activity in the anemone host (SOD_A) and in *Symbiodinium* (SOD_S). Significant differences (two-tailed; $p \leq 0.05$) are highlighted in bold. df = degrees of freedom.

parameter	**t**	**df**	***p***	
symbiont ratio	-2.6	34	**0.013**	**Green > Pink**
F_v/F_m	2.7	20.4	**0.015**	**Green > Pink**
Q_m	0.1	34	0.911	
$rETR_{max}$	2.6	34	**0.013**	**Pink > Green**
α	-3.8	34	**0.001**	**Pink > Green**
I_k	0.1	34	0.779	
SOD_A	1.6	34	0.110	
SOD_S	0.6	34	0.568	

A discriminant function analysis (DFA) reliably predicted colour phenotype based on four parameters: F_v/F_m, $rETR_{max}$, α, and symbiont ratio (Wilks' Lambda = 0.427, $\chi^2_{(8)} = 25.5$,

$p = 0.001$). However, the suite of cellular and physiological parameters was not sufficiently distinct between *Symbiodinium* ITS2 ratios to reliably discriminate between them on this basis (DFA: Wilks' Lambda = 0.611, $\chi^2_{(21)} = 14.5$, $p = 0.845$).

7.3.2 Effects of thermal stress on distinct phenotypes

7.3.2.1 Visible signs of symbiont expulsion

At noon on Day 3, all anemones exposed to the highest temperature expelled mucus masses containing *Symbiodinium* cells through their mouths (Figure 7.1 C – D). By Day 5, three of six pink individuals and one of six green individuals exposed to the highest temperature appeared visually pale, and by Day 6 in this treatment all anemones appeared pale. Symbiont expulsion was also sporadically observed in both phenotypes at the middle temperature. By Day 6 one of six pink individuals appeared visually pale.

7.3.2.2 *Symbiodinium* ITS2 shuffling

In individuals of the green phenotype, the symbiont ratio (defined as the ratio of types C25 to C3.25) declined over time at the highest temperature by 47.2% (Figure 7.3 A; Friedman test: $\chi^2_{(1)} = 5.6$, $p = 0.018$; Wilcoxon *post hoc*: $Z = -2.2$, $p = 0.028$) resulting in a symbiont ratio of 5.7 ± 1.3 on Day 9. Although this ratio was significantly lower than at Day 1, it was highly similar to the symbiont ratio of individuals of the pink phenotype under the same treatment (6.4 ± 0.8). In the pink phenotype, the symbiont ratio was stable over time in all temperature treatments (Figure 7.3 B).

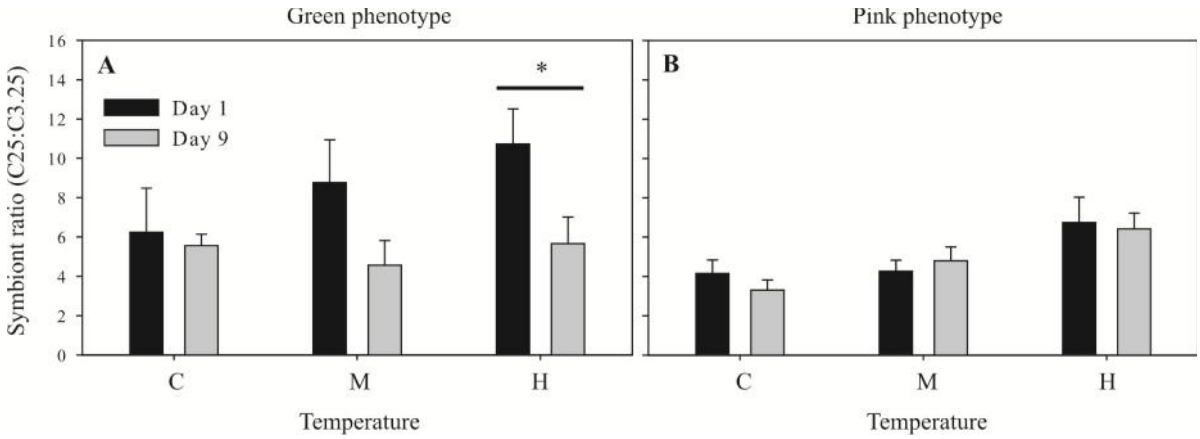

Figure 7.3: Change in symbiont ratio (*Symbiodinium* C25:C3.25) between Day 1 and Day 9, when the sea anemone *Entacmaea quadricolor* was exposed to control (C; 21.3 °C), medium (M; 24.5 °C) and high (H; 27.6 °C) temperatures for 9 days. Values are mean ± S.E. (n = 6) in (**A**) green phenotypes and (**B**) pink phenotypes. Asterisk indicates significant difference at the level of $p \leq 0.05$ (Friedman test with *post hoc* Wilcoxon rank comparison).

Table 7.3: Photosynthetic rate in the light-limited region of the rapid light curve (α), maximum relative electron transport rate ($rETR_{max}$) and minimum saturating irradiance (I_k) for each temperature treatment in the green and pink phenotypes of *Entacmaea quadricolor* over the 9-day period of exposure to control temperature (C; 21.3 °C), medium temperature (M; 24.5 °C) or high temperature (H; 27.6 °C). Values are mean ± S.E., n = 6.

		Green Phenotype				**Pink Phenotype**			
Parameter	**Temp**	**Day 1**	**Day 3**	**Day 5**	**Day 9**	**Day 1**	**Day 3**	**Day 5**	**Day 9**
α	C	0.46 ± 0.03	0.49 ± 0.04	0.39 ± 0.03	0.42 ± 0.03	0.52 ± 0.02	0.48 ± 0.04	0.42 ± 0.05	0.45 ± 0.05
	M	0.48 ± 0.04	0.44 ± 0.04	0.39 ± 0.3	0.37 ± 0.02	0.54 ± 0.03	0.53 ± 0.05	0.38 ± 0.03	0.43 ± 0.05
	H	0.45 ± 0.03	0.52 ± 0.03	0.40 ± 0.04	0.34 ± 0.03	0.55 ± 0.01	0.56 ± 0.02	0.34 ± 0.03	0.36 ± 0.04
$rETR_{max}$	C	117.4 ± 10.1	87.2 ± 4.8	69.4 ± 4.2	73.7 ± 3.5	127.3 ± 8.4	88.2 ± 6.1	88.8 ± 10.8	86.0 ± 9.2
	M	130.8 ± 7.6	92.0 ± 5.1	78.4 ± 7.3	83.8 ± 6.5	143.1 ± 6.1	93.5 ± 5.4	93.3 ± 5.1	110.8 ± 7.7
	H	115.5 ± 9.7	110.9 ± 15.1	77.2 ± 6.4	81.7 ± 4.7	149.8 ± 9.2	105.4 ± 4.9	73.8 ± 4.0	89.3 ± 4.5
I_k	C	259.6 ± 21.6	186.9 ± 25.1	184.1 ± 20.0	177.9 ± 11.5	245.2 ± 18.5	190.2 ± 15.5	223.1 ± 30.0	214.4 ± 50.5
	M	277.2 ± 15.5	219.0 ± 21.7	207.0 ± 25.5	226.7 ± 17.4	268.0 ± 11.3	183.7 ± 18.7	254.6 ± 25.8	277.2 ± 47.3
	H	258.1± 17.2	223.3 ± 40.3	201.4 ± 24.5	250.1 ± 27.1	270.3 ± 15.9	190.7 ± 13.8	221.6 ± 15.4	263.0 ± 331.8

7.3.2.3 Chlorophyll fluorescence

Overall, the responses of chlorophyll fluorescence parameters to thermal stress were similar between the two phenotypes, with no significant three-way interaction of time, temperature and phenotype for any of the parameters measured (i.e. F_v/F_m, Q_m, $rETR_{max}$, I_k, and α; Table 7.4).

Maximum quantum yield (F_v/F_m)

In both colour phenotypes, F_v/F_m differed significantly between temperature treatments (significant interaction of time and temperature; Tables 7.4, 7.5). At the control temperature, F_v/F_m was stable in both phenotypes throughout the experiment (Figure 7.4 A, B). At the medium temperature, F_v/F_m significantly declined from Day 3 onwards in the green phenotype (Bonferroni: $p \leq 0.048$ for Days 3 – 8 compared to Day 1) resulting in an overall decline of 22.3% (mean Day 8 *versus* mean Day 1); in contrast, it was stable in the pink phenotype. In both phenotypes, F_v/F_m declined markedly at the highest temperature, with reductions of 27% and 23% in the green and pink phenotype, respectively. In this treatment, the green phenotypes had significantly lower F_v/F_m values from Day 5 onwards ($p \leq 0.017$ for Days 5 – 8 compared to Day 1), while the pink phenotype had significantly lower F_v/F_m values from Day 4 onwards ($p \leq 0.007$ for Days 4 – 8 compared to Day 1).

In comparison to the control temperature, exposure to the medium temperature resulted in a significantly lower F_v/F_m on Day 5 in the green phenotype (Bonferroni: $p = 0.007$). In contrast, in the pink phenotype, F_v/F_m was not different between the control and medium treatments at any time-point. Furthermore, compared to the control temperature, exposure to the highest temperature resulted in a significantly lower F_v/F_m on all days except for Day 3 in the green phenotype ($p \leq 0.047$ for Days 1, 2, 4 and $p = 0.007$ from Day 5 onwards) and a significantly lower F_v/F_m from Day 5 onwards in the pink phenotype ($p \leq 0.004$ for Days 5 – 8).

Excitation pressure over PSII (Q_m)

In both phenotypes, Q_m differed significantly between temperature treatments (significant interaction of time and temperature; Tables 7.4, 7.5). Over time, at the control temperature, Q_m showed little variation in both phenotypes (Figure 7.4 C, D). Q_m was significantly higher on Day

4 than Day 8 (Bonferroni: $p = 0.036$) in the green phenotype, and significantly higher on Day 4 than days 5, 7 – 9 ($p < 0.042$) in the pink phenotype. At the medium temperature, Q_m increased ~ 1.8 fold (Day 9 *versus* Day 2, $p = 0.016$) in the green phenotype, and ~ 1.6 fold (Day 9 *versus* Day 2, $p = 0.060$) in the pink phenotype. At the highest temperature, Q_m increased ~ 1.4 fold (Day 9 *versus* Day 3, $p = 0.045$) in the pink phenotype and to a similar extent in the green phenotype, though this increase was not significant.

In comparison to the control temperature, exposure to the medium temperature resulted in a significantly higher Q_m from Day 6 onwards in the green phenotype (Days 6, 7: $p < 0.015$; Days 8, 9: $p \leq 0.001$). In contrast, in the pink phenotype Q_m at the medium temperature was significantly higher only on the last day of the experiment ($p = 0.002$). In comparison to the control temperature, exposure to the highest temperature resulted in a significantly higher Q_m from Day 6 onwards in the green phenotype (Days 6 – 9: $p \leq 0.002$) and from Day 5 onwards in the pink phenotype (Day 5: $p = 0.008$, Days 7 – 9: $p < 0.009$).

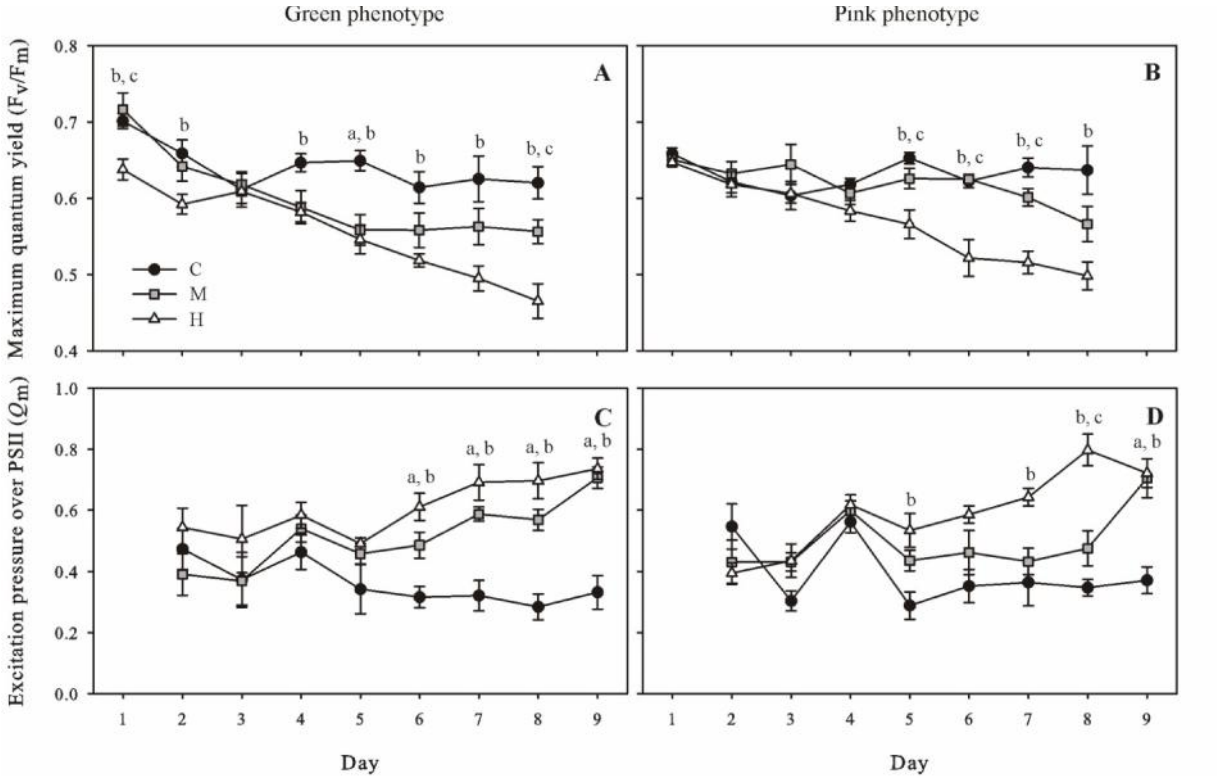

Figure 7.4: Effect of temperature over a 9-day period on maximum quantum yield of PSII (F_v/F_m; **A, B**) and excitation pressure over PSII (Q_m; **C, D**) in the green phenotype (**A, C**) and pink phenotype (**B, D**) of *Entacmaea quadricolor* exposed to control (C; 21.3 °C), medium (M; 24.5 °C) and high (H; 27.6 °C) temperature for 9 days. Values are mean ± S.E., n = 6. Significant differences are reported for (a) C *versus* M, (b) C *versus* H, and (c) M *versus* H at the level of $P \leq 0.05$ (rmANOVA and pairwise comparison with Bonferroni correction). For overall effects of rmANOVA refer to Tables 7.4 and 7.5.

Table 7.4: Results of rmANOVA for the parameters: F_v/F_m (maximum quantum yield at 19:00); Q_m (excitation pressure over PSII), $rETR_{max}$ (maximum relative electron transport rate); α (photosynthetic rate in the light-limited region of the rapid light curve); I_K (minimum saturating irradiance); and superoxide dismutase activity in the anemone host (SOD_A) and in *Symbiodinium* (SOD_S) when both anemone colour phenotypes are included in the analysis. Significant effects ($p \leq 0.05$) are highlighted in bold, non-significant effects ($p > 0.05$) are presented in grey. df = degrees of freedom; Temp = Temperature; † indicates that the Greenhaus-Geisser correction is presented.

Parameter		Time	Time × Temp	Time × Phenotype	Time × Temp × Phenotype	Temp	Phenotype	Temp × Phenotype
F_v/F_m†	*F*	**26.1**	**4.8**	**2.6**	1.1	**56.3**	1.7	2.3
	df	**5.1, 154.2**	**10.3, 154.2**	**5.2, 154.2**	10.3, 154.2	**2, 30**	1, 30	2, 30
	p	**< 0.001**	**< 0.001**	**0.029**	0.362	**< 0.001**	0.205	0.120
Q_m†	*F*	**673.3**	**5.1**	0.38	0.8	**38.8**	0.1	0.7
	df	**4.9, 148**	**9.9, 148**	4.9, 148	9.9, 148	**2, 30**	1, 30	2, 30
	p	**< 0.001**	**< 0.001**	0.857	0.626	**< 0.001**	0.799	0.484
$rETR_{max}$	*F*	**56.8**	1.3	1.3	1.2	**4.2**	**11.3**	0.3
	df	**3, 28**	6, 56	3, 28	6, 56	**2, 30**	**1, 30**	2, 30
	p	**< 0.001**	0.254	0.308	0.323	**0.024**	**0.002**	0.722
α	*F*	**15.2**	0.5	**4.5**	0.5	0.5	**4.7**	1.6
	df	**3, 28**	6, 56	**3, 28**	6, 56	2, 30	**1, 30**	2, 30
	p	**< 0.001**	0.778	**0.011**	0.630	0.592	**0.039**	0.214
I_k	*F*	**8.3**	0.5	2.4	0.3	2.4	0.9	0.1
	df	**3, 28**	6, 56	3, 28	6, 56	2, 30	1, 30	2, 30
	p	**< 0.001**	0.841	0.086	0.925	0.106	0.354	0.891
SOD_A†	*F*	**9.1**	0.8	3.0	4.3	0.9	**25.2**	0.7
	df	**2.1, 64**	4.3, 64	2.1, 64	4.3, 64	2, 30	**1, 30**	2, 30
	p	**< 0.001**	0.533	0.055	0.626	0.401	**< 0.001**	0.524
SOD_S†	*F*	**16.1**	1.0	**4.1**	1.0	0.3	1.4	1.8
	df	**1.8, 54.1**	3.6, 54.1	**1.8, 54.1**	3.6, 54.1	2, 30	1, 30	2, 30
	p	**< 0.001**	0.781	**0.026**	0.407	0.734	0.241	0.186

Table 7.5: Results of rmANOVA for the parameters: F_v/F_m (maximum quantum yield at 19:00); Q_m (excitation pressure over PSII); $rETR_{max}$ (maximum relative electron transport rate); α (photosynthetic rate in the light-limited region of the rapid light curve); I_K (minimum saturating irradiance); and superoxide dismutase activity in the anemone host (SOD_A) and in *Symbiodinium* (SOD_S) when anemone colour phenotypes are analyzed separately. Significant effects ($p \leq 0.05$) are highlighted in bold, non-significant effects ($p > 0.05$) are presented in grey. df = degrees of freedom; Temp = Temperature; † indicates that the Greenhaus-Geisser correction is presented.

		Green phenotype			**Pink phenotype**		
Parameter		**Time**	**Temp**	**Time × Temp**	**Time**	**Temp**	**Time × Temp**
F_v/F_m	*F*	**22.6**	**26.4**	**3.9**	**7.9**†	**35.9**	**3.6**†
	df	**7, 9**	**2, 15**	**14, 18**	**3.5, 52.5**†	**2, 15**	**7, 52.5**†
	P	**< 0.001**	**< 0.001**	**0.004**	**< 0.001**†	**< 0.001**	**0.003**†
Q_m	*F*	**283.4**†	**22.8**	**2.5**†	**414**†	**16.2**	**3.6**†
	df	**3.6, 54.4**†	**2, 15**	**7.2, 54.4**†	**4.2, 62.4**†	**2, 15**	**8.3, 62.4**†
	P	**< 0.001**†	**< 0.001**	**0.024**†	**< 0.001**†	**< 0.001**	**0.002**†
$rETR_{max}$	*F*	**20.8**	2.0	0.4	**35.7**	2.5	**2.9**
	df	**3, 13**	2, 15	6, 26	**3, 13**	2, 15	**6, 26**
	P	**< 0.001**	0.167	0.879	**< 0.001**	0.115	**0.028**
α	*F*	**4.9**	0.6	0.1	**21.5**	2.3	1.3
	df	**3, 13**	2, 15	6, 26	**3, 13**	2, 15	6, 26
	P	**0.018**	0.594	0.991	**< 0.001**	0.133	0.292
I_k	*F*	**8.5**	1.7	0.6	**7.9**	0.9	0.5
	df	**3, 13**	2, 15	6, 26	**3, 13**	2, 15	6, 26
	P	**0.002**	0.223	0.744	**0.003**	0.418	0.854
SOD_A	*F*	**10.1**†	0.1	0.7†	2.3	1.4	1.1
	df	**2, 30.1**†	2, 15	4, 30.1†	3, 13	2, 15	6, 26
	P	**< 0.001**†	0.925	0.623†	0.122	0.274	0.395
SOD_S	*F*	**8.3**†	0.4	0.3†	**19.3**	2.3	1.8
	df	**1.5, 23**†	2, 15	3.1, 23†	**3, 13**	2, 15	6, 26
	P	**0.004**†	0.657	0.847†	**< 0.001**	0.133	0.134

Rapid light curves

The maximum relative electron transport rate ($rETR_{max}$) decreased in both phenotypes at all three temperatures (Table 7.3), with overall response patterns being similar between phenotypes and among temperatures (no significant three-way interaction of time, temperature and phenotype; Table 7.4). The reduction in $rETR_{max}$ differed significantly between temperatures in the pink but not the green phenotype (Table 7.5). In particular, there was a significant decrease in this parameter at the highest temperature between Days 3 and 5 (p = 0.004) that was not apparent at the other two temperatures (Table 7.3).

Overall, a similar pattern was observed for the rate of photosynthesis in the light-limited region (α) under increasing irradiance, and the minimum saturating irradiance (I_k). α decreased in both phenotypes regardless of temperature treatment (Tables 7.3, 7.5). When temperatures were pooled for analyzes, I_k decreased in both colour phenotypes from Day 5 onwards (Days 5, 9 *versus* Day 3, $p < 0.038$), and recovered to initial values on Day 9 in the pink but not the green phenotype (Tables 7.3, 7.5).

7.3.2.4 Superoxide dismutase (SOD)

In the host tissues of the two anemone phenotypes, SOD activities over time were similar among temperature treatments (no significant three-way interaction of time, temperature and phenotype; Figure 7.5 A, B, Table 7.4). However, when temperatures were pooled for statistical analyzes, clear differences between the two phenotypes were revealed (significant effect of phenotype; Figure 7.4). This effect was driven by the green phenotype, which showed changes in SOD activity over time that were independent of temperature (Table 7.5). Here, anemone SOD activity was higher on Day 5 than Day 3 (Bonferroni: p = 0.002), and higher on Day 9 than Days 1 and 3 (p = 0.036 and $p < 0.002$, respectively). In contrast, the pink phenotype showed no changes in host tissue SOD activity over time (Figure 7.5 A, B, Table 7.5). Furthermore, SOD activity over Days 1 – 9 was significantly lower in the host tissue of the green phenotype (14.2 ± 2.51 units mg^{-1}) than the pink phenotype (20.9 ± 3.57 units mg^{-1}; Table 7.4).

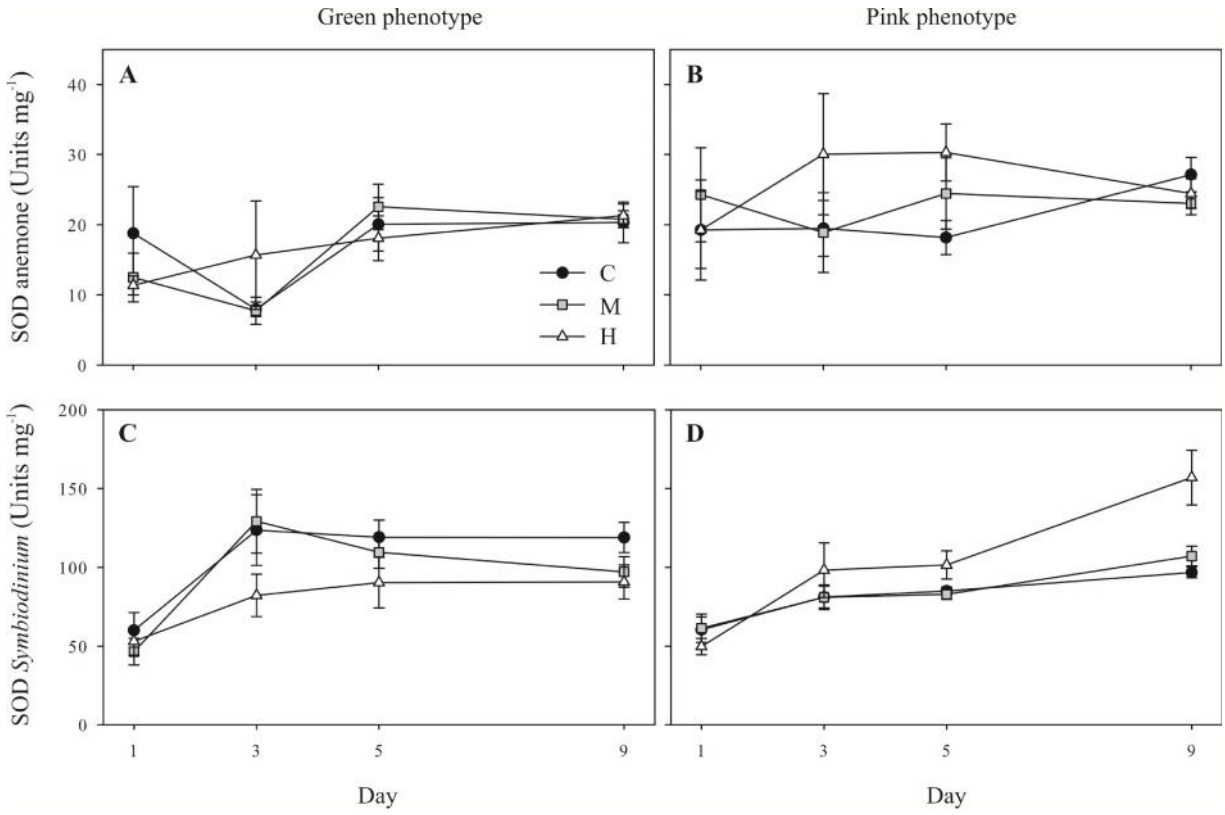

Figure 7.5: Effect of temperature over a 9-day period on superoxide dismutase activity (SOD) in anemone host (**A**, **B**) and *Symbiodinium* fractions (**C**, **D**) of *Entacmaea quadricolor* green phenotype (**A**, **C**) and pink phenotype (**B**, **D**) exposed to control (C; 21.3 °C), medium (M; 24.5 °C) and high (H; 27.6 °C) temperature. Values are mean ± S.E., n = 6.

In the *Symbiodinium* fraction, SOD activity was similar among temperature treatments in both phenotypes (no significant three-way interaction of time, temperature and phenotype; Figure 7.5 C, D, Table 7.5). However, when temperatures were pooled for analyzes, the overall response over time was different between phenotypes (significant two-way interaction of time and phenotype; Table 7.5). Here, symbionts in the green phenotype had significantly increased their SOD activity by Day 3 (Bonferroni: $p = 0.021$) and maintained higher SOD activities for the remainder of the experiment (Bonferroni: $p < 0.001$ for both comparisons, Days 5 and 9 *versus* 1). There was a similar 1.7 – 2.0 fold increment in SOD activity at all temperatures by Day 9 (Day 9 *versus* Day 1, Figure 7.5 C). Symbionts in the pink phenotype had significantly increased their SOD activity by Day 5 (Bonferroni $p < 0.001$) and by Day 9 SOD activity was higher than at Day 1 ($p < 0.001$) and Day 5 ($p = 0.034$). By Day 9, there was a 1.6 – 1.7 fold

increment in SOD activity at the control and medium temperatures, and a 3.2 fold increment at the highest temperature (Day 9 *versus* Day 1, Figure 7.5 C).

On Day 9, SOD activity in *Symbiodinium* (SOD_S) could be accurately predicted using the combination of photobiological and cellular parameters: F_v/F_m, Q_m, $rETR_{max}$, I_k, α, SOD_A, and symbiont ratio (multiple regression: R = 0.446, R^2 = 0.199). However higher resolution bivariate analysis revealed that symbiont ratio alone was sufficient to predict SOD_S and that, in fact, the other photophysiological and cellular parameters contributed little to the prediction (Pearson Correlation, r = 0.357, p = 0.032; Table 7.6). The significant positive correlation translated to higher SOD activities across all temperature treatments in *Symbiodinium* consortia with higher proportions of C25.

Table 7.6: Results for Pearson Correlations on Day 9 (n = 36) for the parameters: F_v/F_m (maximum quantum yield at 19:00); Q_m (excitation pressure over PSII); $rETR_{max}$ (maximum relative electron transport rate); α (photosynthetic rate in the light-limited region of the rapid light curve); I_K (minimum saturating irradiance); and superoxide dismutase activity in the anemone host tissue (SOD_A), SOD activity in the *Symbiodinium* fraction (SOD_S) and symbiont ratio (SR). Significant effects (two-tailed, $p \leq 0.05$) are highlighted in bold and non-significant effects ($p > 0.05$) are presented in grey. PC = Pearson correlation.

		F_v/F_m	**Q_m**	**$rETR_{max}$**	**I_k**	**α**	**SOD_A**	**SOD_S**	**SR**
F_v/F_m	PC		**-.534**	-.045	**-.430**	**.524**	.080	-.016	.033
	P		**.001**	.796	**.009**	**.001**	.644	.926	.849
Q_m	PC			**.336**	**.482**	**-.365**	.076	-.104	.082
	P			**.045**	**.003**	**.029**	.660	.548	.633
$rETR_{max}$	PC				**.632**	-.027	.236	-.036	.013
	P				**.000**	.874	.165	.835	.942
I_k	PC					**-.792**	-.013	-.043	-.058
	P					**.000**	.938	.803	.735
a	PC						.196	.028	.080
	P						.251	.872	.642
SOD_A	PC							.085	-.057
	P							.623	.741
SOD_S	PC								**.357**
	P								**.032**

7.3.2.5 Predictors of thermal response

DFA revealed that, in both phenotypes, the response of the suite of parameters measured, reliably differed between temperature treatments and could be reduced to two dimensions (Functions 1 and 2; Figure 7.6). However, not all of the most important variables explaining the discrimination were identical between phenotypes. In the green phenotype, Discriminant Functions (DF) 1 and 2 explained 96.5% and 3.5% of the variation, respectively (Wilks' Lambda = 0.079, $\chi^2_{(24)} = 31.7$, $p = 0.002$; Figure 7.6 A). Q_m seemed to be the most important predictor for DF 1, and symbiont ratio and F_v/F_m contributed largely for the delineation of DF 2. In the pink phenotype, DF 1 and 2 explained 84.1% and 15.9% of the variation, respectively (Wilks' Lambda = 0.142, $\chi^2_{(24)} = 24.4$, $P = 0.018$; Figure 7.6 B). Here, Q_m and SOD activity in *Symbiodinium* were the most important variables for defining DF 1 and 2, respectively. To a lesser extent, $rETR_{max}$ and symbiont ratio contributed to DF 2.

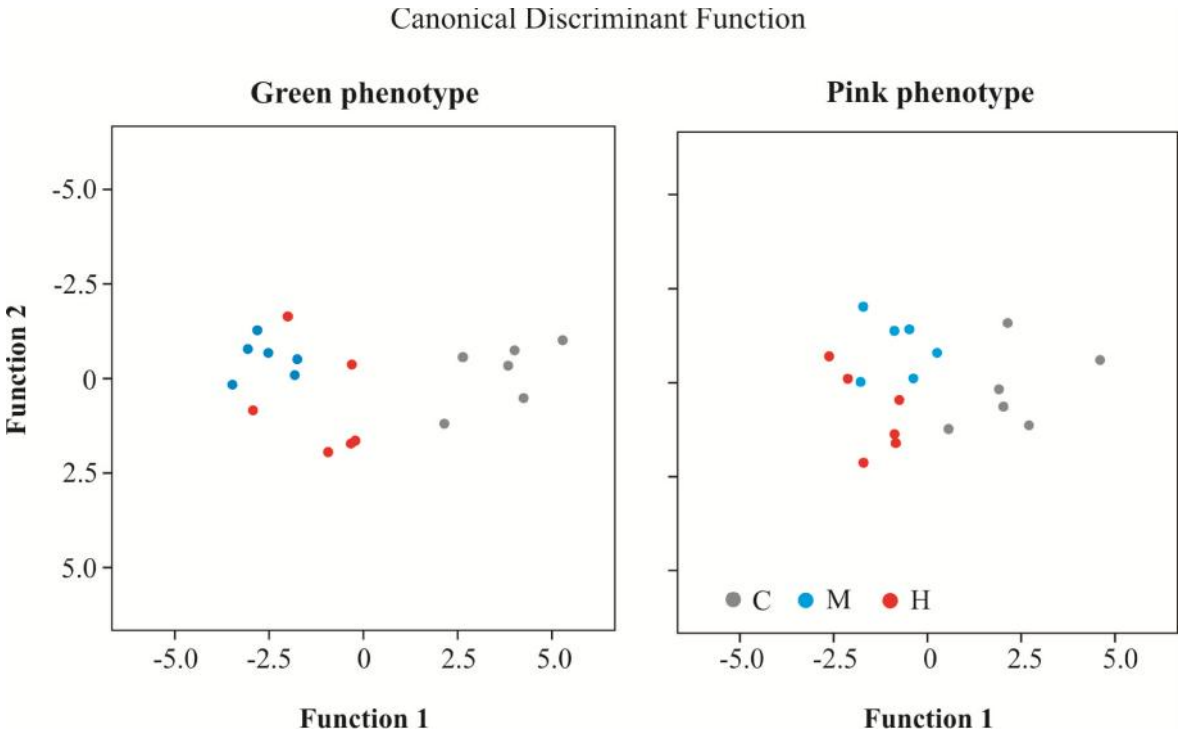

Figure 7.6: Canonical Discriminant Function scatterplot showing the discrimination of temperature effects in the green and pink phenotype of *Entacmaea quadricolor* based on the integration of the parameters F_v/F_m (maximum quantum yield at 19:00), Q_m (excitation pressure over PSII), $rETR_{max}$ (maximum relative electron transport rate), SOD_A (superoxide dismutase activity in the anemone host), SOD_S (superoxide dismutase activity in *Symbiodinium*) and symbiont ratio. C = control temperature (21.3 °C); M = medium temperature (24.5 °C); H = high temperature (27.6 °C).

7.4 Discussion

This study demonstrated that two distinct colour phenotypes of *Entacmaea quadricolor* at North Solitary Island, differed in their baseline ratios of *Symbiodinium* C25:C3.25 and their photobiological properties. Furthermore, the study revealed phenotype-specific responses to short-term heat stress that included *Symbiodinium* type shuffling in the green but not the pink phenotype. In the highest temperature treatment, the green phenotype increased the relative proportion of C3.25 relative to C25. Superoxid dismutase (SOD) activity in the algal symbiont increased over time in both phenotypes, though regardless of the temperature. However, after nine days of heat stress, SOD activity correlated with *Symbiodinium* ratio, with a higher SOD activity in the presence of more *Symbiodinium* C25. This suggests that this *Symbiodinium* type has more superoxide anion (O_2^-) scavenging enzyme SOD. This study set out to investigate whether heat-induced shuffling of *Symbiodinium* ITS2 populations might relate to enhanced use of SOD capacity. I found, that heat indeed induced the shuffling of *Symbiodinium* types, yet, in contrast to my hypothesis, the shuffling of symbionts was not related to enhanced use of algal SOD.

7.4.1 Phenotype-specific variation in baseline *Symbiodinium* ITS2 populations and photobiological characteristics

Significant differences of photobiological characteristics between distinct *Symbiodinium* ITS2 types have been demonstrated repeatedly (e.g. Robison and Warner 2006; Hennige et al. 2009; Ragni et al. 2010; Krämer et al. 2013). In the present study, two distinct colour phenotypes of *E. quadricolor* that were collected from identical depths and acclimated to an identical light regime for 32 days, differed markedly in their baseline *Symbiodinium* ITS2 assemblages. Furthermore, the two phenotypes showed significant variations in baseline maximum quantum yield of PSII (F_v/F_m), an estimator of PSII photochemical efficiency, and the rapid light curve (RLC) parameters: maximum relative electron transport rate ($rETR_{max}$) and photosynthetic rate in the light-limited region of the RLC (α). Compared to the pink phenotype, the green phenotype hosted a higher proportion of C25 relative to C3.25, and exhibited higher F_v/F_m, lower $rETR_{max,}$ and lower α values. The lower $rETR_{max}$ measured in the green phenotype is indicative of lower maximum transport rates of electrons through the photosynthetic chain and indicates acclimation

or adaptation to lower light conditions (Ralph and Gademann 2005). The lower α-values indicate lower photosynthetic rates in the light-limited region of the RLC (Ralph and Gademann 2005). These marked differences suggest that *Symbiodinium* ITS2 types C25 and C3.25 might have distinct genetic photophysiological properties. However, *in hospite* a physiological response is influenced by the confounding effect of host tissue, e.g. the capability of the cnidarian tissue to filter photosynthetically active radiation (PAR; Dove 2004) or ultraviolet radiation (UVR; Shick and Dunlap 2002). In this study, fluorescence or RLC parameters did not predict *Symbiodinium* ITS2 ratio but accurately predicted colour phenotype, corroborating the hypothesis that the photophysiological properties of the colour phenotypes were in part a function of host or host-specific properties.

Several host-derived properties may influence light utilization and photosynthesis in *Symbiodinium*. These include host-related changes in pH or dissolved organic carbon supply, as well as photoprotective mechanisms (Bhagooli et al. 2008; Baird et al. 2009b). PAR-filtering, non-fluorescent chromophors (Dove et al. 2006), fluorescent protein chromophors (FPs; Salih et al. 2000; Dove et al. 2001), and UVR-screening mycosporine like amino acids (MAAs; Dunlap and Chalker 1986) may alter the light environment that impacts upon the endosymbiont. The vast diversity in pigmentation of cnidarians is predominantly due to fluorescent protein chromophors, including the green fluorescent protein (GFP) and its homologues (Dove 2004). In *E. quadricolor*, a far-red fluorescent protein (eqFP611) has been identified which is derived from a green FP (Wiedenmann et al. 2002). The eqFP611 absorbs between approximately 450 and 600 nm, with the maximum at 559 nm (Wiedenmann et al. 2002), and therefore appears red. Whether eqFP611, or other fluorescent or non-fluorescent chromoproteins are involved in the red pigmentation of the green phenotype's column or the pink pigmentation of the pink phenotype's tentacle tips, needs to be investigated. Because FPs absorb, dissipate and scatter light, it seems likely that endosymbionts within the green phenotype might experience a different light environment compared to the endosymbionts within the pink phenotype. Although alternative host-related factors might be equally important, host pigmentation might therefore be a key mechanism influencing the internal light environment and light utilization in *Symbiodinium* cells. Acclimatization to these different light regimes rather than varying genetic photophysiological properties of distinct ITS2 types may explain the observed phenotype-specific variations in baseline photobiological characteristics.

7.4.2 Phenotype-specific variation in thermal stress responses

Shuffling of *Symbiodinium* ITS2 assemblages may be a potential rapid acclimatory mechanism to rising sea temperatures if the new dominant symbiont is better adapted to the new environment and benefits the fitness of the holobiont (Buddemeier and Fautin 1993; Buddemeier et al. 2004). In the present study, both anemone phenotypes hosted a mixed assemblage of *Symbiodinium* C25 and C3.25, with C25 being the dominant symbiont type. Hosting multiple *Symbiodinium* types seems to be more common among cnidarians than initially recognized (Baker and Romanski 2007; Goulet 2007). In particular, the use of real-time PCR as a very sensitive molecular tool has allowed the identification of multiple symbiont populations in numerous cnidarians, and as such discovered considerable potential for shuffling of symbiont assemblages (Mieog et al. 2007; Correa and Baker 2009; Silverstein et al. 2012). In the present experiment, a 9-day exposure to ~ 27.6 °C resulted in an increase in *Symbiodinium* ITS2 type C3.25 relative to C25 in the green phenotype. In contrast, the pink phenotype maintained a stable *Symbiodinium* association over time at all temperatures. This result clearly demonstrates that the *Symbiodinium* association within *E. quadricolor* can be highly flexible (depending on colour phenotype) in response to changing environments, as has been demonstrated for scleractinian corals after natural bleaching events (Berkelmans and van Oppen 2006; Jones et al. 2008; LaJeunesse et al. 2009). The change in *Symbiodinium* assemblages could be a result of selective expulsion or loss of C25, or preferential proliferation of C3.25; this is possible due to short clonal turnover times of *Symbiodinium in hospite* (3 – 16 d; Wilkerson et al. 1988).

Programmed cell death (apoptosis) has been identified as one key mechanism of *Symbiodinium* loss, and reactive oxygen species (ROS) are thought to be involved in the initiation of apoptosis pathways (Franklin et al. 2004). The results showed a positive correlation between *Symbiodinium* C25 abundance and symbiont SOD activity. Although the higher rates of SOD activity in *Symbiodinium* C25 potentially reduced accumulation of superoxide anion (O_2^-) and hence attenuated levels of oxidative stress felt, SOD accumulation may be indicative of higher oxidative stress in C25 than C3.25 at elevated temperature. It is possible that these higher levels of oxidative stress in C25 triggered selective loss of C25 via apoptosis in the green phenotype; alternatively, C3.25 might have proliferated more rapidly and hence outcompeted C25. Although not directly measured in this study, differential use of UV- or PAR-screening

proteins could provide a possible explanation for the shuffling of *Symbiodinium* ITS2 populations in *E. quadricolor*. The maturation of the GFP homologue eqFP611 is sensitive to temperature (Wiedenmann et al. 2002) as is transcription, translation and/or maturation of other FPs (Dove 2004; Smith-Keune and Dove 2008). Exposure to the highest temperature treatment could have therefore reduced the shielding potential in the green phenotype, exposing resident symbionts to higher light levels than at the control temperature, and causing the symbiont population to shuffle in favour of C3.25.

From the above, it seems that the green phenotype of *E. quadricolor* would be more sensitive to elevated temperature than the pink phenotype, and this was supported by the photophysiological data. Hill and Scott (2012) showed that *E. quadricolor* bleaches through symbiont loss when exposed to 25 °C or 27 °C, and through losses of symbionts and pigments (photobleaching; Takahashi et al. 2008) when exposed to 29 °C for five days. They also showed that bleaching is accompanied by reduced maximum photochemical efficiency (F_v/F_m) at 29 °C. In the present study, reduction of F_v/F_m were highly similar between phenotypes at the highest temperature, but exposure to the medium temperature of ~ 24.5 °C caused significant declines in F_v/F_m in the green but not the pink phenotype. Similarly, at this temperature, excitation pressure over PSII at midday (Q_m) was higher in the green phenotype from Day 6 onwards, while in the pink phenotype, Q_m had only increased after nine days of treatment. High excitation pressure over PSII is linked to the saturation of downstream electron sinks and/or acceptors, the inactivation of PSII reaction centres, and the activation of non-photochemical quenching (NPQ) mechanisms such as xanthophyll de-epoxidation. Decreases in F_v/F_m may have resulted from sustained NPQ mechanisms that did not relax with dark-adaptation (Middlebrook et al. 2010), and/or inactivation of functional reaction centres which can be dynamic or sustained (Warner et al. 1996; Warner et al. 1999), and are thought to result from imbalanced damage to PSII reaction centres and their repair (Takahashi and Murata 2008; Takahashi and Badger 2011). The results show that at ~ 24.5 °C, the pink phenotype but not the green phenotype could sustain efficient electron transport past PSII until the last day of the experiment. Moreover, in the green phenotype, NPQ and other photoprotective mechanisms such as ROS-scavenging were not sufficient to enable complete recovery of PSII reaction centres, although xanthophyll de-epoxidation might be sustained in the dark (Middlebrook et al. 2010; Hill et al. 2012). Taken together, these results demonstrate that the PSII efficiencies of the two colour phenotypes have

distinct critical thermal thresholds, of > 24.5 °C in the pink phenotype and < 24.5 °C in the green phenotype.

There is growing evidence that ROS might be associated with the accumulation of non-functional PSII reaction centres because ROS, particularly hydrogen peroxide (H_2O_2), can damage cellular components (Halliwell 2006) and inhibit protein translation (Takahashi and Murata 2008). It is therefore vital to tightly control the intracellular concentrations of ROS to balance photoprotection, e.g. the down-regulation of active PSII reaction centres (Dunn et al. 2012) or utilization of electrons in the water-water-cycle (Asada 2000), and damage, e.g. oxidative damage to cellular components (Halliwell 2006), sustained inhibition of protein translation (Takahashi et al. 2008) and initiation of apoptosis (Franklin et al. 2004). In the present study, the two phenotypes and their symbionts showed different dynamics of SOD activity over time, with increases in SOD activity in the symbionts but not the anemone tissue. In symbionts within both phenotypes, SOD activity increased regardless of the temperature. A positive correlation between light and SOD activity is well described (Shick et al. 1995; Richier et al. 2008), and suggests that the antioxidant defense was primarily induced by experimental light intensities. Interestingly, however, the dynamics differed between the two colour phenotypes: the symbionts of the green phenotype exhibited higher SOD activities across all temperatures by Day 3, while the symbionts of the pink phenotype showed enhanced SOD activities only by Day 5. Moreover, SOD levels stabilized after Day 3 in the green phenotype but continued to increase in the pink phenotype. The methods employed in this study did not reveal whether differential rates of O_2^--scavenging by SOD was indicative of differential levels of oxidative stress at a given time-point or whether adjustments of SOD activity was effective in maintaining pro-oxidant/antioxidant balance, so that the oxidative stress felt was ultimately the same in the two anemone phenotypes. Measurements of ROS concentrations or oxidative damage to lipids, proteins or DNA, would help to elucidate whether increased rates of SOD activity decreased cellular oxidative stress.

In anemone tissue, ROS are produced during aerobic pathways in mitochondria (Dykens et al. 1992; Nii and Muscatine 1997). Furthermore, ROS, particularly H_2O_2, are believed to penetrate cell membranes and walls, and may leak from *Symbiodinium* cells to host tissue (Lesser 2006; Suggett et al. 2008). The tissue of the pink phenotype of *E. quadricolor*

maintained a constant SOD activity over time at all temperatures, suggesting oxidative homeostasis even though SOD activity significantly increased with time in its resident symbionts. In contrast, tissue of the green phenotype increased its SOD activity over time in all of the temperatures. Perhaps the green phenotype needed to compensate for its overall lower SOD activity to maintain efficient scavenging of ROS under prolonged exposure to high light? Notably, it has been demonstrated that FPs have the ability to quench O_2^- and H_2O_2 (Bou-Abdallah et al. 2006; Palmer et al. 2009), and so these compounds might act as functional equivalents to SOD in the green host tissue.

7.4.3 Conclusion

This study analyzed the dynamics of *Symbiodinium* ITS2 populations, chlorophyll fluorescence parameters and SOD activities in two distinct colour phenotypes of the ecologically important sea anemone *E. quadricolor*. The results suggest that baseline parameters and thermal responses are, at least in part, influenced by host-derived factors in this anemone. Although not measured directly, suitable candidates may be fluorescent or non-fluorescent chromophors, that also influence host pigmentation. Other mechanisms, including the differential use of MAAs, also cannot be excluded. The shuffling of *Symbiodinium* C25 and C3.25 in the green phenotype was not associated with enhanced use of algal SOD activity and may have been a secondary effect of elevated temperature on host properties. The differential ability to cope with elevated temperatures might have profound impacts on *E. quadricolor* phenotype abundance in times of changing climates.

Chapter 8:
General discussion

It has been hypothesized that high latitude *Symbiodinium* types might be particularly well adapted to seasonally variable environmental conditions, and this might underlie the success of reef-building corals and other cnidarians (Wicks et al. 2010b) in environmental conditions that are close to their survival thresholds such as water temperature (Kleypas et al. 1999). The overall aim of this study was to investigate the importance of, and possible interactions between, protective mechanisms that underlie both heat and cold tolerance in *Symbiodinium* types common on high latitude coral reefs, such as those of Lord Howe Island (LHI), and in coral communities such as those of North Solitary Island (NSI), both located in New South Wales, Australia. The research focused on a suite of photoprotective mechanisms in the *Symbiodinium* cell, including xanthophyll de-epoxidation-mediated heat dissipation, thylakoid fatty acid composition and plasticity, the antioxidant defense system, and photorepair capacity of photosystem II (PSII), and how these influence PSII efficiency in *Symbiodinium* cells and sub-lethal bleaching susceptibility or survivorship of their cnidarian partner.

The results of this thesis showed that the photoprotective mechanisms analyzed in *Symbiodinium* cells were not necessarily correlated with PSII efficiency, sub-lethal bleaching susceptibility or survivorship under short-term heat and cold stress across a range of *Symbiodinium*-host combinations. It would therefore seem unlikely from the results obtained in this thesis that *Symbiodinium* types or their specific cellular adaptations alone determine thermal tolerance of the holobiont. On the contrary, the results highlight the importance of the host and emphasize the significance of the particular host-symbiont combination in determining the thermal response of the holobiont. Therefore, specific physiological or cellular adaptations of the cnidarian host may act together with a complex protective cellular network in *Symbiodinium* to determine how well the holobiont responds to variable temperatures at high latitude locations, and in particular to temperatures that often fall below 18 °C (i.e. the lower thermal threshold for reef accretion).

The results of the thesis raise two major questions which will be discussed in greater detail here: Firstly, which cellular mechanisms do *Symbiodinium* cells use to deal with the often variable and generally lower seawater temperatures occurring at high latitude locations? Secondly, are high latitude *Symbiodinium* cells well equipped to face a future of rising ocean temperatures, and what might be the fate of high latitude coral reefs and coral communities in the face of climate change?

8.1 What mechanisms do high latitude *Symbiodinium* types use to deal with thermal perturbations?

8.1.1 The role of *Symbiodinium* type

High latitude cnidarian-*Symbiodinium* associations might have an advantage in withstanding variability in their thermal environments because they naturally experience a broad range of temperatures over the course of the year (Cook et al. 1990; Wicks et al. 2010b). The presence of endemic *Symbiodinium* types (i.e. *Symbiodinium* types that so far have not been described from any other location) at the world's southernmost coral reef of LHI prompted the suggestion that these *Symbiodinium* types might be particularly well adapted to the variable environmental conditions and cooler sea temperatures at this high latitude site (Wicks et al. 2010a; 2010b). If the type of *Symbiodinium* primarily determines tolerance of the holobiont to colder or warmer temperatures, then consistency in the stress response across a range of coral species that harbour the same *Symbiodinium* type would be expected.

Contrary to these expectations, the results of this study revealed that coral-*Symbiodinium* associations at the high latitude coral reef of LHI exhibit highly variable thermal responses to short-term heat stress (~ 3 – 5 °C above the maximum monthly mean temperature of 24 °C, ~ 2 – 4 °C above the temperature at which heat stress is predicted by Coral Watch [www.coralreefwatch.noaa.gov]) and short-term cold stress (~2 – 3 °C below the monthly mean temperature minimum of 18 °C), and demonstrated a clear inconsistency in the stress response across a range of coral species that partly harbour the same *Symbiodinium* type at a particular temperature regime. As shown in Chapters 2 and 4, coral-*Symbiodinium* associations were generally more tolerant to cold stress than heat stress, as demonstrated by significantly less or no

losses of PSII activity, significantly less or no losses of *Symbiodinium* cells or *Symbiodinium*-specific pigments, and no mortality, corroborating previous studies in *Pocillopora damicornis* at the same location (Wicks et al. 2010b). Exceptions were *Porites heronensis* hosting *Symbiodinium* ITS2 type C111* which did not bleach at all under cold or heat stress, and *Stylophora* sp. harbouring *Symbiodinium* ITS2 type C118 which bleached under cold stress but not under heat stress. Of note, *P. heronensis* coped much better with increased seawater temperature when associated with *Symbiodinium* ITS2 type C111* (Chapter 2) than when associated with *Symbiodinium* ITS2 type C117 (Chapter 4), although caution should be used when extrapolating this observation as this compares thermal responses between two independent experiments. Also of note, the increased temperature bleaching tolerant *Stylophora* sp. and bleaching susceptible *P. damicornis* (Chapters 2, 4) shared the same symbiont type: C118. Yet, *Stylophora* exclusively hosted C118, while in *P. damicornis Symbiodinium* type C100 was dominant. Finally, *Symbiodinium* C111*, which associated with increased temperature bleaching tolerant *P. heronensis*, did not prevent mortality in *Acropora yongei* under bleaching conditions as demonstrated in Chapter 2, and corals that associated with *Symbiodinium* C3 (*Acropora solitariensis* and *Isopora palifera*) exhibited significantly different bleaching and photophysiological responses to heat stress as shown in Chapter 4. Collectively, these results demonstrate that a consistent correlation between symbiont type and thermal bleaching susceptibility is lacking, and highlight the importance of the host-symbiont combination in determining the physiological response to changing temperatures. These results are congruent with several studies which demonstrated that the response of a coral or anemone, as a holobiont, to thermal perturbation depends on the combination of host species and endosymbiont type, and their respective physiological optima (Abrego et al. 2008; Sampayo et al. 2008; Baird et al. 2009a; Fisher et al. 2012).

The importance of the host in influencing a thermal stress response was corroborated by an experiment analyzing stress responses of two distinct colour morphs of the sea anemone *E. quadricolor* (Chapter 7). In this experiment, colour morph determined the photophysiological responses of the endosymbionts, both in control conditions and in response to thermal stress. Furthermore, distinct colour morphs differed in their relative abundance of endosymbiont ITS2 types, suggesting an overriding importance of host properties in regulating the quality of *Symbiodinium* populations (Chapter 7).

8.1.2 The role of the host

A number of host factors have been linked to the different stress responses of the holobiont (Baird et al. 2009a). These factors primarily influence the quality and quantity of light that impacts on the endosymbionts, and may include UVR screening compounds MAAs (Dunlap and Chalker 1986) PAR screening compounds (fluorescent proteins; Salih et al. 2000; Dove et al. 2001) and host tissue thickness (Loya et al. 2001). In scleractinian corals, fine-scale differences in skeletal corallite structure may alter the within-tissue light intensity (Enríquez et al. 2005). Furthermore, differential use of antioxidants and/or antioxidant enzymes has also been demonstrated in distinct coral species and these act together with the algal antioxidant defence system to minimize oxidative stress in the holobiont (Yakovleva et al. 2004). Similarly, in Chapter 7, I demonstrated colour phenotype-specific differences in the SOD activity of the tissues of the sea anemone *Entacmaea quadricolor* from NSI. Analyzing host mechanisms in high latitude symbiotic cnidarians and how they influence cellular mechanisms in their symbionts would enhance our understanding of why some of the corals studied here were better able to deal with changes in temperature than others; this warrants future study.

8.1.3 The role of cellular mechanisms in *Symbiodinium*

This thesis provides detailed insight into the mechanisms that high latitude *Symbiodinium* cells use when exposed to excessively low or high temperatures. Although the responses of *Symbiodinium* cells were highly variable, and depended on the particular combination with their coral host, certain patterns could be observed across *Symbiodinium* types and holobiont combinations that will be discussed further. Firstly, in thermally tolerant *Symbiodinium* cells, cold and heat stress resulted in similar final cellular modifications, e.g. an increase of xanthophyll de-epoxidation and thylakoid fatty acid unsaturation (Chapters 2, 3), or maintenance of cellular properties, e.g. the maintenance of the activity of SOD or APX and photorepair of PSII (Chapters 4, 5), within the timeframe of the experiments. Secondly, in all corals, cold stress almost always led to an instant increase in the excitation pressure over PSII (Q_m), while heat stress caused a slower increase in Q_m; this latter response was, however, ultimately more deleterious in the majority of hosts and symbionts (Chapter 2, page 79 and Chapter 4, page 101).

These findings suggest that heat and cold may affect similar cellular mechanisms, but at different time-scales as has been suggested before (Roth et al. 2012).

Two hypothetical models are presented that describe cellular responses to cold stress (Figure 8.1) and heat stress (Figure 8.2) in a *Symbiodinium* cell of a bleaching tolerant symbiosis (Figures 8.1 B, 8.2 B) and a bleaching susceptible symbiosis (Figures 8.1 C, 8.2 C). The responses of two particular coral-*Symbiodinium* associations (bleaching tolerant C111* hosted by *P. heronensis*; bleaching sensitive C100/C118 hosted by *P. damicornis*) were chosen as the basis for these models, because they showed distinct responses to heat and cold stress, and because they represent the most extensively analyzed coral-*Symbiodinum* combinations in this study.

In these models, light intensities that reach *Symbiodinium* cells are hypothetically controlled by screening of PAR and UVR by the host tissue. It is hypothesized that the bleaching-tolerant *Symbiodinium* cell is exposed to lower intensities of PAR and/or UVR due to these host screening-factors, although a multitude of other *Symbiodinium* cell and chloroplast factors can also influence the light field that impacts on the light-harvesting antennae (LHC) of PSI and PSII. These are not shown in the model, but include: (i) *Symbiodinium* cell density (*P. heronensis* had substantially higher cell densities than *P. damicornis*; Chapter 2); (ii) organization of *Symbiodinium* cells within the host tissues or cells (as proposed by Santos et al. 2009); (iii) hypothetical chloroplast movement, (as commonly observed in plants, mosses, ferns and green algae as reviewed in Takahashi and Badger 2011); and (iv) chlorophyll concentration (*P. heronensis* had substantially higher concentrations of chlorophyll *a*, c_2, and the accessory pigment peridin than *P. damicornis*; Chapter 2). All these factors potentially influence light availability and absorption efficiency through shading or full exposure. Therefore, these factors may account for the observed differences of excitation pressure over PSII (Q_m) across species reported in Chapter 2. For example, the high concentrations of *Symbiodinium* cells and chlorophyll concentrations in *P. heronensis* hosting C111* would have caused shading and therefore would have minimized light absorption, resulting in reduced levels of electron generation and reduced $Q_{m.}$

Q_m describes the excitation pressure over PSII and is a proxy for the balance of light harvesting at the LHC and light energy utilization in photochemical and non-photochemical

processes (Iglesias-Prieto et al. 2004). High Q_m values indicate that light harvesting exceeds light-energy utilization (Iglesias-Prieto et al. 2004). This situation has been associated with enhanced levels of reactive oxygen species (ROS), including singlet oxygen ($^1O_2$), the superoxide anion(O_2^-), hydrogen peroxide (H_2O_2) and the hydroxyl radical (•OH) (Lesser 2011). An imbalance between light harvesting and light-energy utilization usually occurs during phases of high solar radiation, that are naturally associated with solar noon, and the down-regulation of PSII activity (Gorbunov et al. 2001). There are a number of processes in the chloroplast of *Symbiodinium* that reduce PSII activity and electron transport, including over-reduction of the primary electron acceptor or downstream electron transport components, reduced carbon fixation in the Calvin-Benson cycle, xanthophyll de-epoxidation-mediated heat dissipation, degradation of PSII reaction centres and/or saturation of alternative electron-, reducing equivalent- and ATP-sinks (Smith et al. 2005). Thermal stress, both heat stress and cold stress, may affect these processes, enhancing the adverse effect of light and increasing Q_m.

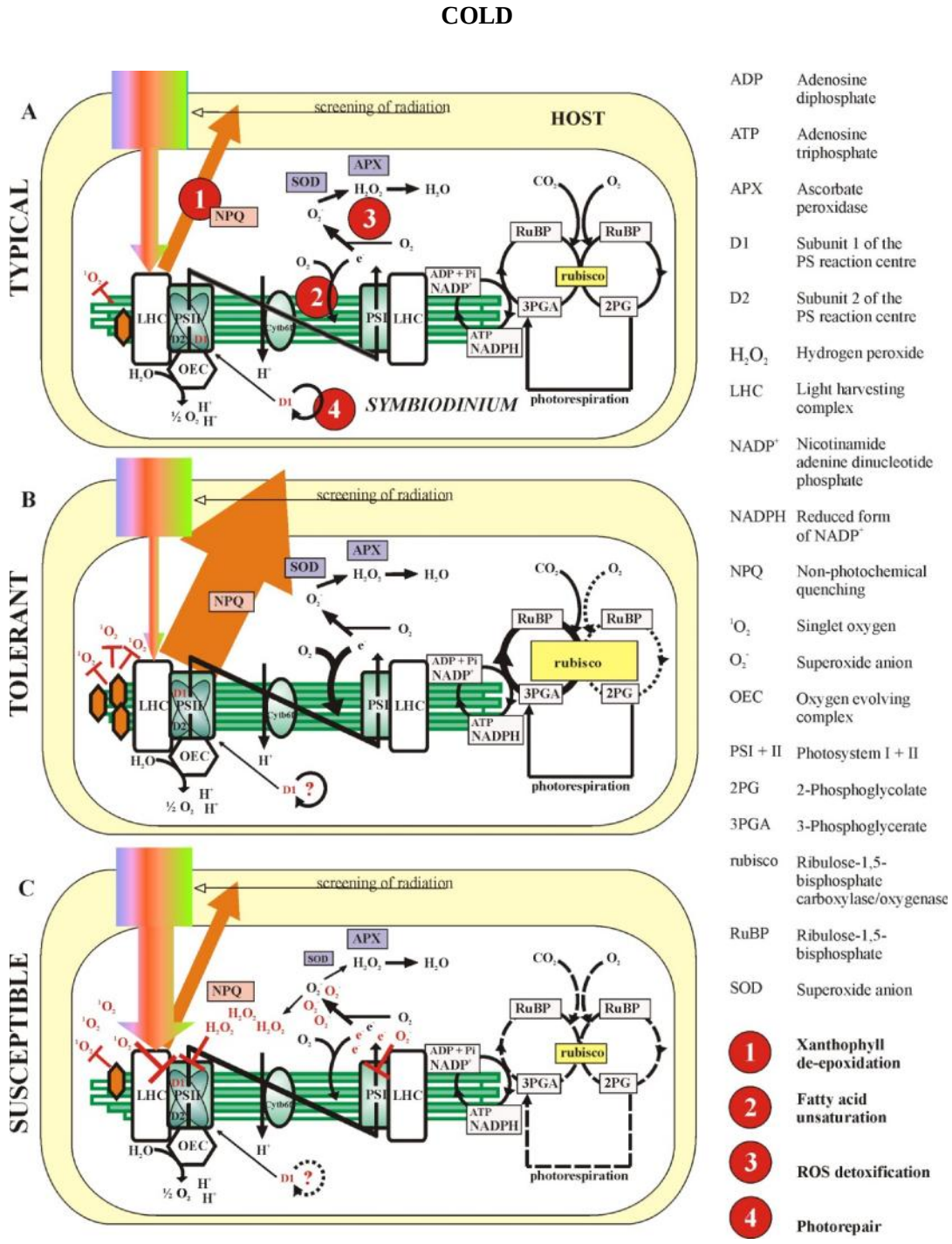

Figure 8.1: Hypothetical model describing typical cellular responses at control temperature (**A**), or under cold conditions in a cold-tolerant *Symbiodinium* type (**B**) and in a cold-susceptible *Symbiodinium* type (**C**), highlighting the mechanisms studied in this thesis (xanthophyll de-epoxidation, fatty acid unsaturation, ROS detoxification and photorepair capacity). Symbols are described in Figure 8.2.

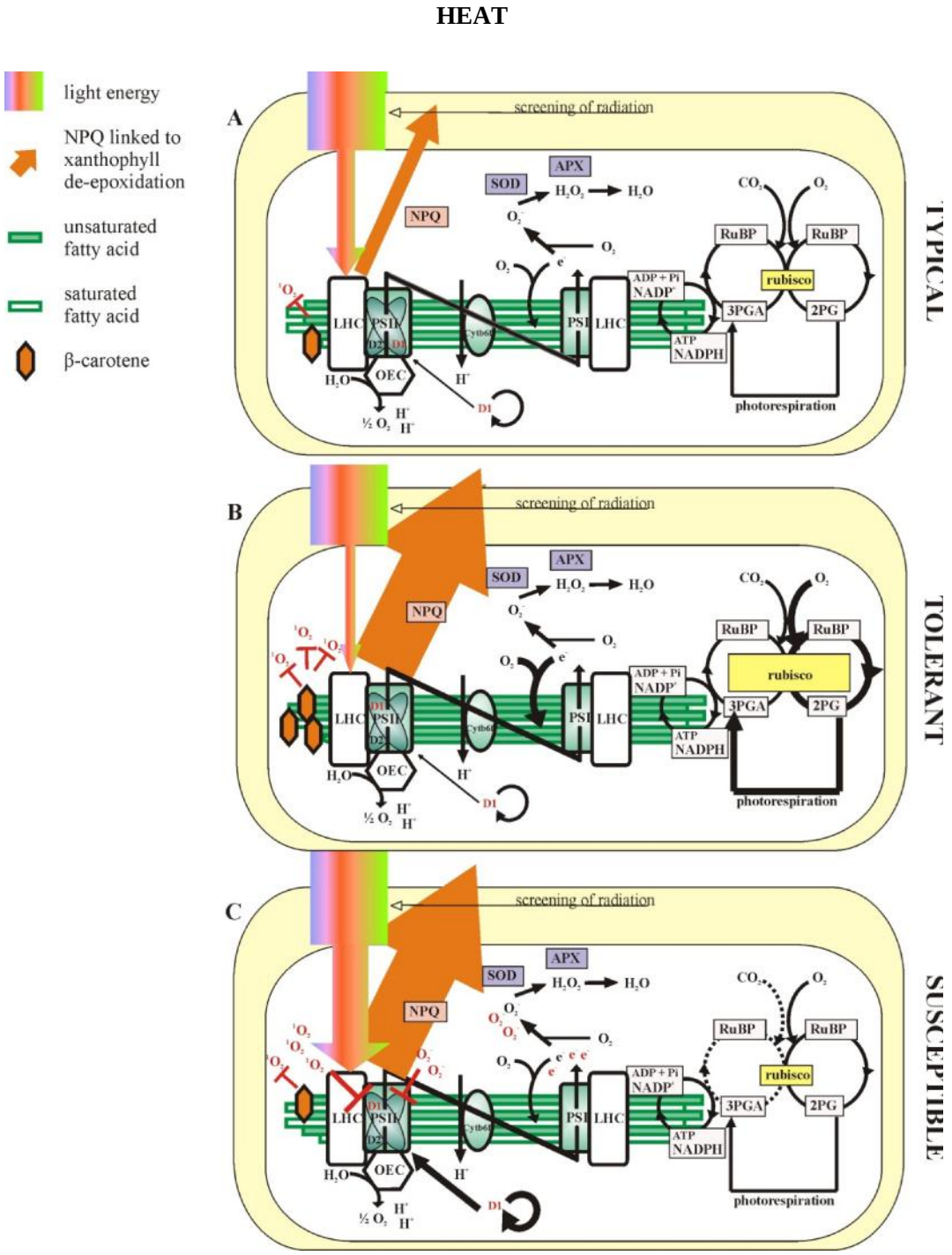

Figure 8.2: Hypothetical model describing typical cellular responses at control temperature (**A**), or under warm conditions in a heat-tolerant *Symbiodinium* type (**B**) and in a heat-susceptible *Symbiodinium* type (**C**). For the description of abbreviations refer to Figure 8.1. Briefly, light energy (arrow) may be screened in the host tissue and be absorbed by the light-harvesting complex (LHC). Excitation energy is transferred to

diatoxanthin and safely dissipated as heat (orange arrow), or transduced to chemical energy at the oxygen-evolving complex (OEC). Electrons derived from water are transported to the primary electron acceptor associated with D1 in photosystem II (PSII), and via $Cytb_6f$ to PSI. The final electron acceptor is $NADP^+$. This linear electron transport generates a trans-thylakoidal proton gradient which drives the generation of ATP. NADPH and ATP enter the Calvin-Benson cycle in which the enzyme rubisco (yellow square) catalyzes the fixation of carbon. Alternatively, rubisco may oxygenate ribulose-1,5-bisphosphate (RuBP), and the product 2-phosphoglycolate (2PG) is recycled to 3-phosphoglycerate (3PGA) via photorespiration. Electrons leak from the electron transport chain and can be transferred onto oxygen, generating the superoxide anion (O_2^-), which is converted to H_2O_2 by superoxide dismutase (SOD, purple) and then to H_2O by ascorbate peroxidase (APX, purple). Further, singlet oxygen ($^1O_2$) can be produced at PSII when excitation energy is transferred onto oxygen. β-carotene (orange hexagon) can scavenge $^1O_2$. The overall degree of saturation/unsaturation of the thylakoid lipid bilayer is indicated by the colour of the stacks: white stacks represent saturated and green stacks represent unsaturated fatty acids. Unsaturation of fatty acids involves the utilization of oxygen and electrons, as indicated by the arrow pointing towards the thylakoid layers. Size of arrows indicates how efficient one mechanism is; intermittent arrows indicate that one mechanism is suppressed. Size of respective squares indicates size of pool of compound (e.g. rubisco, SOD, APX).

In dinoflagellates, heat dissipation is the most important non-photochemical quenching mechanism, in which excess energy is safely dissipated at the light-harvesting antennae (Goss and Jakob 2010). As shown in Chapter 2, *Symbiodinium* type C111* in *P. heronensis* consistently increased xanthophyll de-epoxidation and Q_m under cold stress and heat stress, demonstrating that, at both temperatures, NPQ is efficiently activated through xanthophyll de-epoxidation (indicated by the size of the orange arrows in Figures 8.1 and 8.2). The *Symbiodinium* C100/C118 consortium in *P. damicornis* enhanced xanthophyll de-epoxidation and Q_m when heat-stressed. In contrast, when cold-stressed, Q_m but not xanthophyll de-epoxidation increased. Therefore, under cold stress, xanthophyll de-epoxidation was an effective protective mechanism in C111* but not in C100/C118, although both *Symbiodinium* populations had xanthophyll pools of similar size, indicating: (i) type-specific differences in the sensitivity of diadinoxanthin de-epoxidase (DDE) activation; (ii) a lack of a trans-thylakoidal proton gradient and enhanced activity of diatoxanthin epoxidase (DEP); or (iii) a lack of ascorbate, a co-substrate required for xanthophyll de-epoxidation. The lack of xanthophyll de-epoxidation under cold

stress in C100/C118 suggest an increased need for alternative quenching mechanisms, to avoid over-excitation of the photosynthetic machinery.

As shown in Chapters 2 and 4, cold stress resulted in an almost instant increase in Q_m, while heat stress also caused an increase in Q_m but with a time-delay. The most likely explanation for these different timescales is the temperature dependency of enzyme activity, as has been suggested before (Saxby et al. 2003; Roth et al. 2012). While increased temperatures initially accelerate enzyme activity, decreased temperatures generally decelerate enzyme activity (Somero 1995). The down-regulation of enzyme activity affects all cellular processes. However, the dark reaction of photochemistry, i.e. the Calvin–Benson cycle which is responsible for carbon fixation, is decelerated more than the light reaction of photochemistry, which is responsible for transducing sunlight energy to reducing power and ATP (Wise 1995). As such, the Calvin-Benson cycle might be the initial site of impact under cold stress, as has been suggested previously for *Montipora digitata* (Saxby et al. 2003). Although it was not directly measured in the present study, deceleration of carbon fixation associated with decreased temperatures would result in an accumulation of ATP and NADPH if those compounds were not to be used in alternative pathways, such as photorespiration (Badger et al. 2000; Ort and Baker 2002) or nitrogen metabolism (Smith et al. 2005). Photorespiration describes a number of catalytic reactions which take place in chloroplasts and peroxisomes, and ultimately generate 3-phosphoglycerate (3-PGA) out of 2-phosphoglycolate (2-PG), the product of the oxygenation reaction of ribulose-1,5-bisphospate carboxylase/oxygenase (rubisco; Badger et al. 2000; Ort and Baker 2002). Photorespiration is probably of minor importance under cold stress because chilling temperatures reduce the affinity of rubisco for CO_2, as well as for O_2, as indicated by the intermittent arrows in Figure 8.1 (Ort and Baker 2002). When the availability of $NADP^+$ and ADP is limited but light harvesting and light-energy transduction are intact, components of the photosynthetic electron transport chain would quickly become reduced, resulting in increased excitation pressure over PSII unless electrons are used with greater efficiency elsewhere, such as in the Mehler reaction (Asada 2000; Badger et al. 2000).

As part of the water-water-cycle, SOD catalyzes the conversion of O_2^- to H_2O_2, which in turn is detoxified by APX (Asada 1999; 2000; 2006; Lesser 2006; 2011). O_2^- is largely generated at PSI when the supply of $NADP^+$ is limited, and oxygen instead of $NADP^+$ is reduced (Asada

1999; 2000; 2006). Neither cold nor warm conditions enhanced the activity of SOD or APX in the LHI *Symbiodinium* types analyzed, as shown in Chapter 4. On the contrary, cold stress resulted in reduced activity of SOD in *Symbiodinium* C100/C118 harboured by *P. damicornis*, as indicated by the smaller size of the SOD box in Figure 8.1 C. In vascular plants, inactivation of the water-water-cycle due to chilling has been demonstrated, and the inability to maintain the activity of SOD and APX has been linked with cold temperature bleaching (Wise 1995; Asada 2000). Site-specific oxidative damage at PSI is likely to occur when O_2^- cannot efficiently be detoxified (Nishiyama et al. 2006). Furthermore, O_2^- can convert to H_2O_2 spontaneously (Lesser 2006). H_2O_2 can inhibit the enzymes of the Calvin-Benson cycle through disulfide formation (Asada 1999), and H_2O_2 might also be involved in the inhibition of protein translation (Nishiyama et al. 2006), thereby potentially accelerating the generation of O_2^- in a feedback loop. My results (reduced activity of SOD in cold-stressed *Symbiodinium* C100/C118) combined with these considerations support the hypothesis that, in cold-stressed *Symbiodinium* cells, photodamage to PSI might occur when scavenging by SOD is suppressed, as has been proposed for cold-stressed vascular plants (Asada 2000). Photodamage to PSI might precede or accompany photodamage to PSII, which is primarily caused by excited $P680^+$ and/or $^1O_2$ at PSII (Nishiyama et al. 2006). $^1O_2$ is generated at PSII when excitation energy is transferred from triplet excited chlorophyll onto oxygen (Lesser 2006; Nishiyama et al. 2006). $^1O_2$ can damage components of the PSII reaction centre, such as the D1 protein. Damaged PSII proteins are degraded and replaced in the photorepair-cycle (Aro et al. 1993). Although not shown for cold-stressed C100/C118 cells, heat-stressed cells of this type depended heavily on D1 turnover, as demonstrated in Chapter 5, suggesting that D1 in C100/C118 was more susceptible to degradation than in C111*. The suppression of SOD activity under cold stress could therefore have enhanced the need for increased D1 metabolism in C100/C118. A substantially higher concentration of β-carotene relative to chlorophyll *a* in *Symbiodinium* C111* than in *Symbiodinium* C100/C118, as reported in Chapter 2, could provide one explanation for the lower gross-photoinhibition (i.e. loss of PSII reaction centre activity that involves loss of D1) revealed in Chapter 5. The lipid soluble antioxidant β-carotene scavenges $^1O_2$ and therefore reduces the risk of PSII damage (Asada 2006; Lesser 2006), although the PSII photoinhibition-photorepair cycle is likely to be influenced by the oxidizing power of excited $P680^+$ as well as by alternative ROS, particularly H_2O_2 (Nishiyama et al. 2006). Direct measurements of ROS concentrations,

ROS-mediated damage such as lipid peroxidation, protein oxidation or damage to DNA, and concurrent measurements of multiple antioxidant enzymes and small molecular antioxidant compounds would be needed to elucidate the exact role of oxidative stress and its relationship to inactivation of PSI and/or PSII.

Tylakoid-bound enzymes catalyzing the desaturation of thylakoid fatty acids also use oxygen and electrons (Murata and Wada 1995) and are therefore involved in scavenging electrons. In Chapter 3, it was demonstrated that *Symbiodinium* cells that are considered bleaching tolerant at both low and high temperatures (ITS2 type C111*) enhance their degree of thylakoid fatty acid unsaturation in response to both short-term cold and heat stress. More research is needed to understand whether fatty acid unsaturation may have acted in a photoprotective manner (due to scavenging of electrons), or whether enhanced fatty acid unsaturation at high temperatures would ultimately adversely affect electron transport due to altered thermodynamic and chemical properties. Within the timeframe of the experiment, increased levels of unsaturation did not hinder PSII efficiency under heat stress (nor improve PSII efficiency under cold stress). However, longer-term studies would be needed to confirm whether or not increased levels of unsaturation would increase overall levels of lipid peroxidation, especially as unsaturated fatty acids are considered to be more susceptible to the reactivity of hydroxyl radicals than saturated fatty acids. Presumably, rapid turnover of fatty acids would counteract such a negative impact, however synthesis of fatty acids and their elongation depends on the allocation of carbon, and as such on the maintenance of photosynthesis by the algae (Papina et al. 2007), unless carbon is acquired through heterotrophic feeding by the coral host and transferred to the algae (Houlbreque and Ferrier-Pagès 2009; Tolosa et al. 2011). Therefore, enhancing the unsaturation of thylakoid fatty acids might be adequate for short-term protection but unsuitable for sustained protection under bleaching conditions that are known to reduce photosynthesis.

In my proposed model, adequate catalytic activity at cold temperatures could be achieved by increases in enzyme concentrations (Somero 1995), for example by increases in the pool of the carbon-fixing enzyme rubisco (Figure 8.1 B). In contrast, adjustments of enzyme concentrations would not be of much benefit under heat stress; while metabolic processes would be stimulated initially by high temperatures, sustained and excess temperatures would disrupt

proper protein folding and enzyme activity (Somero 1995). Therefore, under heat stress, heat-shock proteins might become of superior importance for maintaining enzyme activity and carbon fixation (Leggat et al. 2007).

In conclusion, *Symbiodinium* types in bleaching-tolerant corals exhibit different protective pathways from *Symbiodinium* types in bleaching-sensitive corals. *Symbiodinium* C111* in the bleaching-tolerant *P. heronensis* enhanced xanthophyll de-epoxidation and thylakoid fatty acid unsaturation when exposed to short-term cold or heat stress. Simultaneously, scavenging of O_2^- and H_2O_2 by SOD and APX, and D1 turnover were maintained at unchanged rates. In contrast, *Symbiodinium* C100/C118 in the bleaching-susceptible *P. damicornis* enhanced xanthophyll de-epoxidation when exposed to short-term heat stress, however enhanced heat dissipation did not prevent sustained down-regulation of PSII activity. Although a number of mechanisms may account for the loss of PSII activity, it is possible that D1 metabolism, which has been shown to increase under heat stress (Hill et al. 2011) may have exceeded a tipping point. When exposed to short-term cold stress, xanthophyll de-epoxidation, overall thylakoid fatty acid unsaturation, and APX activity did not change, while SOD activity decreased. The inability to adjust these factors in combination with temperature-dependent decelerated enzyme activity may have resulted in excess ROS accumulation and hence triggered cold water bleaching. The effects of cold water on photoprotective mechanisms in *Symbiodinium* cells are summarized in Figure 8.3.

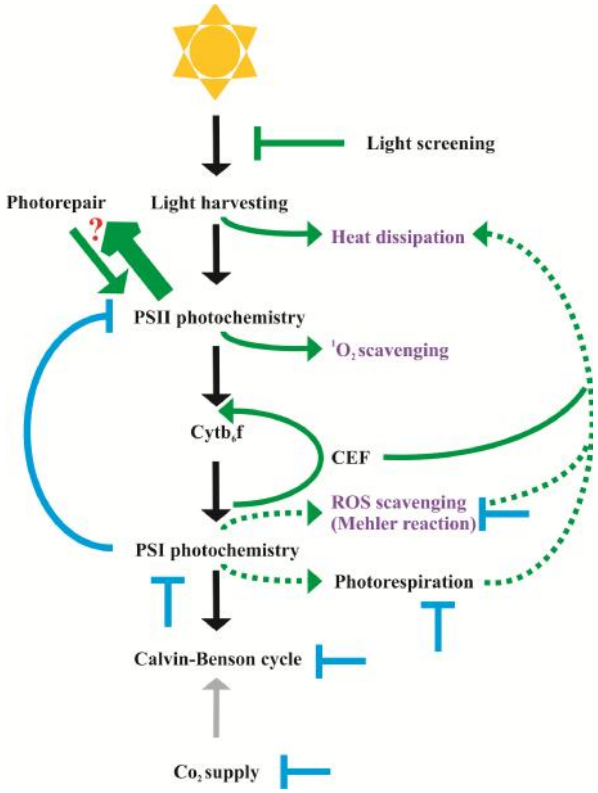

Figure 8.3: Schematic diagram of the putative effects of cold stress on protective mechanisms in *Symbiodinium* C100/C118 chloroplasts. Black arrows indicate the flow of energy and electrons along the photosynthetic electron transport chain, green arrows indicate protective mechanisms, green dotted arrows indicate inhibition of a protective mechanism, blue symbols indicate suppression by cold stress, and purple font highlights mechanisms that have been analyzed in this thesis. Briefly, cold temperatures likely inhibit CO_2 supply and suppress photorespiration due to decreased affinity of rubisco for CO_2 and O_2 (Badger et al. 2000; Ort and Baker 2002). Further, cold temperatures likely decelerate the enzyme activity of the Calvin-Benson cycle (Somero 1995) and directly or indirectly suppress SOD activity in bleaching susceptible *Symbiodinium* cells (Chapter 4). Suppressed SOD activity and limitation of $NADP^+$ availability might result in the accumulation of O_2^- which is likely to oxidize PSI components and/or thylakoid lipids. Further, O_2^- could spontaneously be converted to H_2O_2, which is believed to inhibit protein translation and seems to be involved in programmed and necrotic cell death. The inhibition of PSI could precede or parallel inhibition of PSII, which is characterized by losses of functional PSII reaction centres, and might be a result of direct damage by $^1O_2$ and or $P680^+$, or inhibition of D1 metabolism (Nishiyama et al. 2006; Takahashi and Badger 2011; Murata et al. 2012). Suppressed activity of SOD and the photorespiratory pathway suppress the formation of a trans-thylakoidal pH-gradient, which is necessary to maintain the xanthophyll pool in its de-epoxidized (i.e. photoprotective) conformation. Thus, heat dissipation might be limited by the lack of a trans-thylakoidal pH-gradient (Chapter 2), although cyclic electron flow (CEF) might also be involved in the formation in the gradient.

8.2 The future of high latitude coral reefs and communities

Anthropogenic climate change adversely affects ocean ecosystems worldwide and there is growing concern about the future function and viability of coral reef ecosystems under rising sea temperatures and acidification (Hoegh-Guldberg and Bruno 2010; Caldeira 2013; Van Hooidonk et al. 2013). This thesis set out to explore how well corals at high latitudes would be able to cope with future temperature shifts, in particular with episodes of short-term temperature anomalies. However, based on the results of this thesis, a detailed prediction cannot be made. Predictions are limited because the present study tested the effect of *short-term* thermal stress and did not take into account how corals would respond to long-term thermal stress or recovery. Equally, the potential to acquire tolerance through repeated exposure to stress is not evaluated. These factors will significantly influence eventual survivorship of a coral-symbiont association.

For the south-east Australian region, including Lord Howe Island and the Solitary Islands Marine Reserve (SIMP) which covers North Solitary Island, sea surface temperature (SST) is projected to rise by 2 °C between 2000 and 2050 (Hobday and Lough 2011). It appears that warming in south-east Australia will be more significant compared to other locations due to a predicted intensification of the East Australian current (EAC), which transports warm waters from the Equator southwards (Hobday and Lough 2011). The projected rise of 2 °C translates to a predicted maximum monthly mean (MMM) temperature of 26.3 °C at LHI and 27.1 °C at SIMP by 2050, while the summer bleaching threshold is currently estimated at 26.5 °C and 26.8 °C, respectively, for these two sites (Dalton and Carroll 2011). Not taking into account other biotic or abiotic factors that may influence the bleaching response, it is clear that by 2050, corals and other *Symbiodinium*-hosting organisms at LHI and SIMP (as well as at other reefs and reef communities) will be very close to (LHI) or exceed (NSI) their upper bleaching thresholds. A prediction that can be tentatively made is, that in the future we might see a shift from branching to massive or sub-massive coral species, as has been predicted before by Dalton and Carroll (2011). Harriott et al. (1995) observed a decline in the abundance of branching corals in favour of massive corals at LHI and our experimental data suggest that this trend might continue if bleaching thresholds are exceeded regularly.

There is some speculation that warming could improve the current temperature conditions of high latitude sites and extend the distribution of many tropical coral species into higher latitudes as their habitats at lower latitudes are progressively degraded (Precht and Aronson 2004; Yamano et al. 2011). While tropical coral species might shift towards higher latitudes, this does not imply a future increase of coral diversity at high latitude sites, because those species adapted to higher latitudes and cooler conditions may become extinct. Importantly, there is evidence in the fossil record that reef growth and persistence do not solely depend on species diversity (Johnson et al. 2008), raising hopes for the development of reefs in a species-poor environment.

The likelihood of this scenario will have to be assessed site-by-site, because a potential shift in species composition is influenced by biotic (e.g. the tolerance or resilience of corals and associated symbionts) and abiotic (e.g. other local stressors and reef connectivity) factors. For instance, at NSI, the recruitment of tropical coral larvae is low, probably because the East Australian Current (EAC) is very strong in this area and suitable reef substrate is relatively small (Harriott and Banks 1995). Furthermore, the EAC often moves offshore at NSI, limiting the probability of southward extension of corals from this location (Harriott and Banks 1995). My study revealed a high diversity of *Symbiodinium* ITS2 types in *E. quadricolor* on the east coast of Australia and found two novel variants of ITS2 type C42(type2) at two locations from the Northern and Central Great Barrier Reef that were absent on southern reefs and in southern coral communities (Chapter 6). If these variants are adapted to higher temperatures, then we might see their shift towards higher latitudes as the climate warms. However, a potential shift depends on reef connectivity. Given current projections, that the EAC will intensify with warming oceans (Hobday and Lough 2011), the probability for successful settlement of tropical larvae at NSI is even smaller. At LHI, the situation is similar: LHI is very isolated, located over 1000 km south of the GBR, and the recruitment rate of tropical corals is low (Harriott 1992). Low long-distance dispersal of tropical coral larvae argues against the successful settlement of many tropical species at these high latitude sites. What is more, new generation models project that all reef locations will experience annual bleaching events by 2056 – 2075, deeming high latitude refuges as temporary at most (Caldeira 2013; Van Hooidonk et al. 2013).

The suitability of habitats at higher latitudes is further complicated by the extent of ocean acidification and the associated reduction of the aragonite saturation state. From pre-industrial times to 2007, atmospheric carbon dioxide (CO_2) levels have increased by 40% from 280 ppmv (parts per million volume) to nearly 400 ppmv (www.co2now.org). Oceanic uptake of CO_2 is increasing at the same rate, resulting in a reduction in seawater pH, imbalances in oceanic chemistry, and reduced aragonite availability (Doney et al. 2009). Reduced aragonite saturation levels hinder reef accretion and may restrict reef development, particularly at higher latitudes (Doney et al. 2009) where oceanic waters are predicted to be under-saturated with respect to aragonite by 2050 (Orr et al. 2005). In contrast to these expectations, a recent study revealed that the combined effects of elevated SST and ocean acidification are not likely to degrade habitat suitability at sites currently considered as marginal for tropical coral reefs (Couce et al. 2013). Much more needs to be learnt about the combined effects of warming and ocean acidification on coral survivorship and coral reef function, including for high latitude coral reefs and communities.

Whether symbiotic corals and anemones will survive the perturbations associated with anthropogenic climate change will not only depend on the magnitude of warming and the intensity of other local and global stressors, but also on the ecological, morphological, physiological, and genetic traits of the host cnidarians and their associated symbionts, which determine the overall sensitivity to environmental change (Tewksbury et al. 2008; Williams et al. 2008). Furthermore, vulnerability depends on the resilience or ability to recover from perturbations and the capacity of the holobiont to adapt to changes, including phenotypic adaptation (i.e. acclimatization or physiological plasticity) and genotypic adaptation (i.e. the genomic manifestation of beneficial phenotypic traits) (Tewksbury et al. 2008; Williams et al. 2008). The scientific coral reef literature is pessimistic with regards to the coral holobiont's capability to acclimatize or adapt, with concerns that the rate of environmental change, coral mortality and reef degradation is faster than the rate of acclimatization or evolutionary change (Hoegh-Guldberg et al. 2007; Edmunds and Gates 2008; Brown and Cossins 2011). However, there is now evidence that climate change has led to genotypic adaptation (heritable changes of genetic information) in various animals (in squirrels, birds and mosquitoes) over a relatively short time-span, resulting in adaptations in the timing of seasonal events (Bradshaw and Holzapfel 2006). As shorter generation time fosters evolution, these results give hope that

Symbiodinium spp, with a generation time of about 4-16 days *in hospite* (Wilkerson et al. 1988), might be able to adapt to changing temperatures within the projected timeframe. However, it is unlikely that *Symbiodinium* alone determines tolerance or resilience to perturbations, which partly depend on the host and host-specific properties. Given that generation times and genetic diversity of reef-building corals are generally low (Potts 1984), concern about the timely adaptation of the holobiont persists (Csaszar et al. 2010).

References

Abram NJ, Gagan MK, Cole JE, Hantoro WS and Mudelsee M (2008) Recent intensification of tropical climate variability in the Indian Ocean. Nature Geosci **1**(12):849-853

Abrego D, Ulstrup KE, Willis BL and van Oppen MJH (2008) Species-specific interactions between algal endosymbionts and coral hosts define their bleaching response to heat and light stress. Proc R Soc Lond B Biol Sci **275**(1648):2273-2282

Ainsworth T, Hoegh-Guldberg O, Heron S, Skirving W and Leggat W (2008) Early cellular changes are indicators of pre-bleaching thermal stress in the coral host. J Exp Mar Biol Ecol **364**(2):63-71

Altschul SF, Gish W, Miller W, Myers EW and Lipman DJ (1990) Basic local alignment search tool. J Mol Biol **215**(3):403-410

Ambarsari I, Brown B, Barlow R, Britton G and Cummings D (1997) Fluctuations in algal chlorophyll and carotenoid pigments during solar bleaching in the coral *Goniastrea aspera* at Phuket, Thailand. Mar Ecol Prog Ser **159**:303-307

Anthony K, Hoogenboom M and Connolly S (2005) Adaptive variation in coral geometry and the optimization of internal colony light climates. Funct Ecol **19**(1):17-26

Anthony K, Kline D, Diaz-Pulido G, Dove S and Hoegh-Guldberg O (2008) Ocean acidification causes bleaching and productivity loss in coral reef builders. Proc Natl Acad Sci USA **105**(45):17442-17446

Apel K and Hirt H (2004) Reactive oxygen species: metabolism, oxidative stress, and signal transduction. Annu Rev Plant Biol **55**:373-399

Araseki M, Kobayashi H, Hosokawa M and Miyashita K (2005) Lipid peroxidation of a human hepatoma cell line (HepG2) after incorporation of linoleic acid, arachidonic acid, and docosahexaenoic acid. Biosci, Biotechnol, Biochem **69**(3):483-490

Aro EM, Virgin I and Andersson B (1993) Photoinhibition of photosystem II. Inactivation, protein damage and turnover. Biochim Biophys Acta - Bioenergetics **1143**(2):113-134

Aro EM, Suorsa M, Rokka A, Allahverdiyeva Y, Paakkarinen V, Saleem A, Battchikova N and Rintamaki E (2005) Dynamics of photosystem II: a proteomic approach to thylakoid protein complexes. J Exp Bot **56**(411):347-356

Asada K (1999) The water-water cycle in chloroplasts: Scavenging of active oxygens and dissipation of excess photons. Annu Rev Plant Physiol Plant Mol Biol **50**:601-639

Asada K (2000) The water-water cycle as alternative photon and electron sinks. Phil Trans R Soc B **355**:1419-1431

References

Asada K (2006) Production and scavenging of reactive oxygen species in chloroplasts and their functions. Plant Physiol **141**(2):391-396

Awai K, Matsuoka R and Shioi Y (2012) Lipid and fatty acid compositions of *Symbiodinium* strains. Proceedings of the 12th International Coral Reef Symposium, Cairns, Australia

Badger MR, von Caemmerer S, Ruuska S and Nakano H (2000) Electron flow to oxygen in higher plants and algae: rates and control of direct photoreduction (Mehler reaction) and rubisco oxygenase. Phil Trans R Soc B **355**(1402):1433-1446

Baird AH, Bhagooli R, Ralph PJ and Takahashi S (2009a) Coral bleaching: the role of the host. Trends Ecol Evol **24**(1):16-20

Baird AH, Guest JR and Willis BL (2009b) Systematic and biogeographical patterns in the reproductive biology of scleractinian corals. Annu Rev Ecol Evol Syst **40**:551-571

Baker AC (2001) Reef corals bleach to survive change. Nature **411**(6839):765-766

Baker AC (2003) Flexibility and specificity in coral-algal symbiosis: Diversity, ecology, and biogeography of *Symbiodinium*. Annu Rev Ecol Evol Syst **34**:661-689

Baker AC (2004) Corals' adaptive response to climate change. Nature **430**:741

Baker AC and Romanski AM (2007) Multiple symbiotic partnerships are common in scleractinian corals, but not in octocorals: comment on Goulet (2006). Mar Ecol Prog Ser **335**:237-242

Banaszak AT and Trench RK (1995) Effects of ultraviolet (UV) radiation on marine microalgal-invertebrate symbioses. II. The synthesis of mycosporine-like amino acids in response to exposure to UV in *Anthopleura elegantissima* and *Cassiopeia xamachana*. J Exp Mar Biol Ecol **194**(2):233-250

Banaszak AT, LaJeunesse TC and Trench RK (2000) The synthesis of mycosporine-like amino acids (MAAs) by cultured, symbiotic dinoflagellates. J Exp Mar Biol Ecol **249**(2):219-233

Banaszak AT and Trench RK (2001) Ultraviolet sunscreens in dinoflagellates. Protist **152**(2):93-101

Banaszak AT (2003) Photoprotective physiological and biochemical responses of aquatic organisms. UV effects in aquatic organisms and ecosystems **1**:329-356

Banaszak AT, Barba Santos MG, LaJeunesse TC and Lesser MP (2006) The distribution of mycosporine-like amino acids (MAAs) and the phylogenetic identity of symbiotic dinoflagellates in cnidarian hosts from the Mexican Caribbean. J Exp Mar Biol Ecol **337**(2):131-146

Banaszak AT and Lesser MP (2009) Effects of solar ultraviolet radiation on coral reef organisms. Photochem Photobiol Sci **8**(9):1276-1294

References

Barbier EB, Hacker SD, Kennedy C, Koch EW, Stier AC and Silliman BR (2011) The value of estuarine and coastal ecosystem services. Ecol Monogr **81**(2):169-193

Barnes DD and Chalker BB (1990) Calcification and photosynthesis in reef-building corals and algae. In: Coral Reefs Ecosystems of the World. Amsterdam, Elsevier. **25:**109-131

Beauchamp C and Fridovich I (1971) Superoxide dismutase: improved assays and an assay applicable to acrylamide gels. Anal Biochem **44**(1):276-287

Ben-Amotz A, Shaish A and Avron M (1989) Mode of action of the massively accumulated β-carotene of *Dunaliella bardawil* in protecting the alga against damage by excess irradiation. Plant Physiol **91**(3):1040

Berkelmans R and van Oppen MJH (2006) The role of zooxanthellae in the thermal tolerance of corals: a 'nugget of hope' for coral reefs in an era of climate change. Proc R Soc Lond B Biol Sci **273**(1599):2305-2312

Beyer Jr WF and Fridovich I (1987) Assaying for superoxide dismutase activity: some large consequences of minor changes in conditions. Anal Biochem **161**(2):559-566

Bhagooli R and Hidaka M (2004a) Release of zooxanthellae with intact photosynthetic activity by the coral *Galaxea fascicularis* in response to high temperature stress. Mar Biol **145**(2):329-337

Bhagooli R and Hidaka M (2004b) Photoinhibition, bleaching susceptibility and mortality in two scleractinian corals, *Platygyra ryukyuensis* and *Stylophora pistillata*, in response to thermal and light stresses. Comp Biochem Physiol A Mol Integr Physiol **137**(3):547-555

Bhagooli R, Baird A and Ralph P (2008) Does the coral host protect its algal symbionts from heat and light stresses. Proceedings of the 11th International Coral Reef Symposium, Ft Lauderdale, Florida

Bienert GP, Schjoerring JK, Jahn TP (2006) Membrane transport of hydrogen peoxide. Biochim Biophys Acta – Biomembranes: **1758**(8): 994-1003

Bishop DG and Kenrick JR (1980) Fatty acid composition of symbiotic zooxanthellae in relation to their hosts. Lipids **15**(10):799-804

Bongaerts P, Sampayo EM, Bridge TC, Ridgway T, Vermeulen F, Englebert N, Webster JM and Hoegh-Guldberg O (2011) *Symbiodinium* diversity in mesophotic coral communities on the Great Barrier Reef: a first assessment. Mar Ecol Prog Ser **439**:117-126

Bou-Abdallah F, Chasteen ND and Lesser MP (2006) Quenching of superoxide radicals by green fluorescent protein. Biochim Biophys Acta **1760**:1690-1695

Boucher DH, James S and Keeler KH (1982) The ecology of mutualism. Annu Rev Ecol Syst **13**:315-347

Bradford MM (1976) A rapid and sensitive method for the quantitation of microgram quantities of protein utilizing the principle of protein-dye binding. Anal Biochem **72**(1):248-254

References

Bradshaw WE and Holzapfel CM (2006) Evolutionary response to rapid climate change. Science **312**(5779):1477-1478

Brandt ME and McManus JW (2009) Disease incidence is related to bleaching extent in reef-building corals. Ecology **90**(10):2859-2867

Bridge T, Scott A and Steinberg D (2012) Abundance and diversity of anemonefishes and their host sea anemones at two mesophotic sites on the Great Barrier Reef, Australia. Coral Reefs **31**(4):1057-1062

Brown B, Ambarsari I, Warner M, Fitt W, Dunne R, Gibb S and Cummings D (1999) Diurnal changes in photochemical efficiency and xanthophyll concentrations in shallow water reef corals: evidence for photoinhibition and photoprotection. Coral Reefs **18**(2):99-105

Brown B, Downs C, Dunne R and Gibb S (2002) Preliminary evidence for tissue retraction as a factor in photoprotection of corals incapable of xanthophyll cycling. J Exp Mar Biol Ecol **277**(2):129-144

Brown BE (1997) Coral bleaching: causes and consequences. Coral Reefs **16**:129-138

Brown BE and Cossins AE (2011) The potential for temperature acclimatisation of reef corals in the face of climate change. In: Coral Reefs: An Ecosystem in Transition. New York, Springer**:**421-434

Buddemeier RW and Fautin DG (1993) Coral bleaching as an adaptive mechanism. Bioscience **43**(5):320-326

Buddemeier RW, Baker AC, Fautin DG and Jacobs JR (2004) The Adaptive Hypothesis of Bleaching. In: Coral Health and Disease. Berlin, Springer**:**427-444

Burriesci MS, Raab TK and Pringle JR (2012) Evidence that glucose is the major transferred metabolite in dinoflagellate–cnidarian symbiosis. The Journal of experimental biology **215**(19):3467-3477

Caldeira K (2013) Coral Bleaching: Coral 'refugia' amid heating seas. Nature Clim Change **3**(5):444-445

Campbell DA and Tyystjärvi E (2012) Parameterization of photosystem II photoinactivation and repair. Biochim et Biophys Acta - Bioenergetics **1817**(1):258-265

Carlos AA, Baillie BK, Kawachi M and Maruyama T (1999) Phylogenetic position of *Symbiodinium* (Dinophyceae) isolates from tridacnids (Bivalvia), cardiids (Bivalvia), a sponge (Porifera), a soft coral (Anthozoa), and a free-living strain. J Phycol **35**:1054-1062

Chang S-J, Rodriguez-Lanetty M, Yanagi K, Nojima S and Song J-I (2011) Two anthozoans, *Entacmaea quadricolo*r (order Actiniaria) and *Alveopora japonica* (order Scleractinia), host consistent genotypes of *Symbiodinium* spp. across geographic ranges in the northwestern Pacific Ocean. Animal Cells Syst **15**(4):315-324

References

Chang SS, Prezelin BB and Trench RK (1983) Mechanisms of photoadaptation in 3 strains of the symbiotic dinoflagellate *Symbiodinium microadriaticum*. Mar Biol **76**(3):219-229

Chen CA, Wang J-T, Fang L-S and Yang Y-W (2005) Fluctuating algal symbiont communities in *Acropora palifera* (Scleractinia: Acroporidae) from Taiwan. Mar Ecol Prog Ser **295**:113-121

Cheng HY and Song SQ (2006) Species and organ diversity in the effects of hydrogen peroxide on superoxide dismutase activity in vitro. J Integr Plant Biol **48**(6):672-678

Coffroth MA and Santos SR (2005) Genetic diversity of symbiotic dinoflagellates in the genus *Symbiodinium*. Protist **156**(1):19-34

Coffroth MA, Poland DM, Petrou EL, Brazeau DA and Holmberg JC (2010) Environmental symbiont acquisition may not be the solution to warming seas for reef-building corals. PLoS ONE **5**(10):e13258

Coles SL and Fadlallah YH (1991) Reef coral survival and mortality at low temperatures in the Arabian Gulf: new species-specific lower temperature limits. Coral Reefs **9**(4):231-237

Connell JH (1978) Diversity in tropical rain forests and coral reefs. Science **199**(4335):1302-1310

Cook CB, Logan A, Ward J, Luckhurst B and Jr. BCR (1990) Elevated temperatures and bleaching on a high latitude coral reef: the 1988 Bermuda event. Coral Reefs **9**:45-49

Correa A and Baker A (2009) Understanding diversity in coral-algal symbiosis: a cluster-based approach to interpreting fine-scale genetic variation in the genus *Symbiodinium*. Coral Reefs **28**(1):81-93

Couce E, Ridgwell A and Hendy EJ (2013) Future habitat suitability for coral reef ecosystems under global warming and ocean acidification. Glob Change Biol DOI:10.1111/geb.12335

Crawley A, Kline DI, Dunn S, Anthony K and Dove S (2010) The effect of ocean acidification on symbiont photorespiration and productivity in *Acropora formosa*. Glob Change Biol **16**(2):851-863

Crossland C (1984) Seasonal variations in the rates of calcification and productivity in the coral *Acropora formosa* on a high-latitude reef. Mar Ecol Prog Ser **15**(1):135-140

Cruz de Carvalho M (2008) Drought stress and reactive oxygen species: production, scavenging and signaling. Plant signaling & behavior **3**(3):156-165

Csaszar NB, Ralph PJ, Frankham R, Berkelmans R and van Oppen MJ (2010) Estimating the potential for adaptation of corals to climate warming. PLoS ONE **5**(3):e9751

Dalton SJ and Carroll AG (2011) Monitoring coral health to determine coral bleaching response at high latitude eastern Australian reefs: an applied model for a changing climate. Diversity **3**(4):592-610

References

Davies PS (1991) Effect of daylight variations on the energy budgets of shallow-water corals. Mar Biol **108**(1):137-144

Davy SK, Allemand D and Weis VM (2012) Cell biology of cnidarian-dinoflagellate symbiosis. Microbiol Mol Biol Rev **76**(2):229-261

de Carvalho MHC (2008) Drought stress and reactive oxygen species: production, scavenging and signaling. Plant Signal Behav **3**(3):156-165

Denis V, Mezaki T, Tanaka K, Kuo C-Y, De Palmas S, Keshavmurthy S and Chen CA (2013) Coverage, Diversity, and Functionality of a High-Latitude Coral Community (Tatsukushi, Shikoku Island, Japan). PLoS ONE **8**(1):e54330

Díaz-Almeyda E, Thomé P, El Hafidi M and Iglesias-Prieto R (2011) Differential stability of photosynthetic membranes and fatty acid composition at elevated temperature in *Symbiodinium*. Coral Reefs **30**(1):217-225

Doney SC, Fabry VJ, Feely RA and Kleypas JA (2009) Ocean acidification: the other CO_2 problem. Ann Rev Mar Sci **1**:169-192

Dove S, Hoegh-Guldberg O and Ranganathan S (2001) Major colour patterns of reef-building corals are due to a family of GFP-like proteins. Coral Reefs **19**(3):197-204

Dove S (2004) Scleractinian corals with photoprotective host pigments are hypersensitive to thermal bleaching. Mar Ecol Prog Ser **272**:99-116

Dove S, Ortiz JC, Enriquez S, Fine M, Fisher P, Iglesias-Prieto R, Thornhill D and Hoegh-Guldberg O (2006) Response of holosymbiont pigments from the scleractinian coral *Montipora monasteriata* to short-term heat stress. Limnol Oceanogr **51**(2):1149-1158

Downs C and Downs A (2007) Preliminary examination of short-term cellular toxicological responses of the coral *Madracis mirabilis* to acute Irgarol 1051 exposure. Arch Environ Contam Toxicol **52**(1):47-57

Downs CA, Mueller E, Phillips S, Fauth JE and Woodley CM (2000) A molecular biomarker system for assessing the health of coral (*Montastraea faveolata*) during heat stress. Mar Biotechnol **2**(6):533-544

Downs CA, Fauth JE, Halas JC, Dustan P, Bemiss J and Woodley CM (2002) Oxidative stress and seasonal coral bleaching. Free Radical Biol Med **33**(4):533-543

Downs CA, Fauth JE, Robinson CE, Curry R, Lanzendorf B, Halas JC, Halas J and Woodley CM (2005) Cellular diagnostics and coral health: Declining coral health in the Florida Keys. Mar Pollut Bull **51**:558-569

Dunlap W and Chalker B (1986) Identification and quantitation of near-UV absorbing compounds (S-320) in a hermatypic scleractinian. Coral Reefs **5**(3):155-159

References

Dunlap WC and Shick JM (1998) Ultraviolet radiation-absorbing mycosporine-like amino acids in coral reef organisms: A biochemical and environmental perspective. J Phycol **34**(3):418-430

Dunn DF (1981) The clownfish sea anemones: Stichodactylidae (Coelenterata: Actiniaria) and other sea anemones symbiotic with pomacentrid fishes. Trans Am Philos Soc **71**(1):3-115

Dunn SR, Bythell JC, le Tissier MDA, Burnett WJ and Thomason JC (2002) Programmed cell death and cell necrosis activity during hyperthermic stress-induced bleaching of the symbiotic sea anemone *Aiptasia* sp. J Exp Mar Biol Ecol **272**:29-53

Dunn SR, Thomason JC, le Tissier MDA and Bythell JC (2004) Heat stress induces different forms of cell death in sea anemones and their endosymbiotic algae depending on temperature and duration. Cell Death Differ **11**:1213-1222

Dunn SR, Phillips WS, Green DR and Weis VM (2007a) Knockdown of actin and caspase gene expression by RNA interference in the symbiotic anemone *Aiptasia pallida*. Biol Bull **212**(3):250-258

Dunn SR, Schnitzler CE and Weis VM (2007b) Apoptosis and autophagy as mechanisms of dinoflagellate symbiont release during cnidarian bleaching: every which way you lose. Proc R Soc Lond B Biol Sci **274**(1629):3079-3085

Dunn SR and Weis VM (2009) Apoptosis as a post-phagocytic winnowing mechanism in a coral-dinoflagellate mutualism. Environ Microbiol **11**(1):268-276

Dunn SR, Pernice M, Green K, Hoegh-Guldberg O and Dove SG (2012) Thermal stress promotes host mitochondrial degradation in symbiotic cnidarians: are the batteries of the reef going to run out? PLoS ONE **7**(7):e39024

Dykens JA and Shick JM (1984) Photobiology of the symbiotic sea anemone, *Anthopleura elegantissima*: defenses against photodynamic effects, and seasonal photoacclimatization. Biol Bull **167**(3):683-697

Dykens JA, Shick JM, Benoit C, Buettner GR and Winston GW (1992) Oxygen radical production in the sea anemone *Anthopleura elegantissima* and its endosymbiotic algae. J Exp Biol **168**(1):219-241

Edmunds P (1994) Evidence that reef-wide patterns of coral bleaching may be the result of the distribution of bleaching-susceptible clones. Mar Biol **121**(1):137-142

Edmunds PJ and Gates RD (2008) Acclimatization in tropical reef corals. Mar Ecol Prog Ser **361**:307-310

Enríquez S, Méndez ER and Iglesias-Prieto R (2005) Multiple scattering on coral skeletons enhances light absorption by symbiotic algae. Limnol Oceanogr **50**(4):1025-1032

Eskling M, Arvidsson PO and Akerlund HE (1997) The xanthophyll cycle, its regulation and components. Physiol Plant **100**(4):806-816

References

Falkowski PG and Dubinsky Z (1981) Light-shade adaptation of *Stylophora pistillata*, a hermatypic coral from the Gulf of Eilat. Nature **289**(5794):172-174

Falkowski PG, Dubinsky Z, Muscatine L and Porter JW (1984) Light and the bioenergetics of a symbiotic coral. Bioscience **34**(11):705-709

Fattman CL, Schaefer LM and Oury TD (2003) Extracellular superoxide dismutase in biology and medicine. Free Radical Biol Med **35**(3):236-256

Fautin DG and Allen GR (1992) Field guide to anemonefishes and their host sea anemones. Perth, Australia, Western Australian Museum

Ferrier-Pagès C, Hoogenboom M and Houlbrèque F (2011) The role of plankton in coral trophodynamics. In: Coral Reefs: An Ecosystem in Transition. New York, Springer**:**215-229

Fisher P, Malme M and Dove S (2012) The effect of temperature stress on coral–*Symbiodinium* associations containing distinct symbiont types. Coral Reefs **31**(2):473-485

Fitt W and Warner M (1995) Bleaching patterns of four species of Caribbean reef corals. Biol Bull **189**(3):298-307

Fitt W, Gates R, Hoegh-Guldberg O, Bythell J, Jatkar A, Grottoli A, Gomez M, Fisher P, Lajuenesse T and Pantos O (2009) Response of two species of Indo-Pacific corals, *Porites cylindrica* and *Stylophora pistillata*, to short-term thermal stress: The host does matter in determining the tolerance of corals to bleaching. J Exp Mar Biol Ecol **373**(2):102-110

Fitt WK (1982) Photosynthesis, respiration, and contribution to community productivity of the symbiotic sea anemone *Anthopleura elegantissima* (Brandt, 1835). J Exp Mar Biol Ecol **61**(3):213-232

Fitt WK, Brown BE, Warner ME and Dunne RP (2001) Coral bleaching: interpretation of thermal tolerance limits and thermal thresholds in tropical corals. Coral Reefs **20**:51-65

Flores-Ramírez LA and Liñán-Cabello MA (2007) Relationships among thermal stress, bleaching and oxidative damage in the hermatypic coral *Pocillopora capitata*. Comp Biochem Physiol C **146**(1):194-202

Flot JF, Magalon H, Cruaud C, Couloux A and Tillier S (2008) Patterns of genetic structure among Hawaiian corals of the genus *Pocillopora* yield clusters of individuals that are compatible with morphology. C R Biol **331**(3):239-247

Folch J, Lees M and Sloane-Stanley G (1957) A simple method for the isolation and purification of total lipids from animal tissues. J Biol Chem **226**(1):497-509

Folmer O, Black, M., Hoeh, W., Lutz, R., Vrijenhoek, R. (1994) DNA primers for amplification of mitochondrial cytochrome c oxidase subunit I from diverse metazoan invertebrates. Mol Mar Biol Biotechnol **3**(5):294-299

References

Foyer CH, Lelandais M and Kunert KJ (1994) Photooxidative stress in plants. Physiol Plant **92**(4):696-717

Foyer CH and Noctor G (2005) Oxidant and antioxidant signalling in plants: a re-evaluation of the concept of oxidative stress in a physiological context. Plant, Cell Environ **28**(8):1056-1071

Foyer CH, Neukermans J, Queval G, Noctor G and Harbinson J (2012) Photosynthetic control of electron transport and the regulation of gene expression. J Exp Bot **63**(4):1637-1661

Franklin DJ, Hoegh-Guldberg O, Jones R and Berges JA (2004) Cell death and degeneration in the symbiotic dinoflagellates of the coral *Stylophora pistillata* during bleaching. Mar Ecol Prog Ser **272**:117-130

Franklin EC, Stat M, Pochon X, Putnam HM and Gates RD (2012) GeoSymbio: a hybrid, cloud-based web application of global geospatial bioinformatics and ecoinformatics for *Symbiodinium*–host symbioses. Mol Ecol Resour **12**(2):369-373

Freudenthal HD (1962) *Symbiodinium* gen. nov. and *Symbiodinium microadriaticum* sp. nov., a Zooxanthella: Taxonomy, Life Cycle, and Morphology. J Eukaryot Microbiol **9**(1):45-52

Furla P, Richier, S., Allemand, D. (2011) Physiological adaptation to symbiosis in cnidarians. In: Coral Reefs: An Ecosystem in Transition. New York, Springer**:**187-198

Gates RD, Baghdasarian G and Muscatine L (1992) Temperature stress causes host cell detachment in symbiotic cnidarians:implications for coral bleaching. Biol Bull **182**:324-332

Glynn PW (1984) Widespread coral mortality and the 1982–83 El Niño warming event. Environ Conserv **11**(02):133-146

Gombos Z, Wada H, Hideg E and Murata N (1994) The unsaturation of membrane lipids stabilizes photosynthesis against heat stress. Plant Physiol **104**(2):563-567

Gorbunov MY, Kolber ZS, Lesser MP and Falkowski PG (2001) Photosynthesis and photoprotection in symbiotic corals. Limnol Oceanogr **46**(1):75-85

Goreau T and Macfarlane A (1990) Reduced growth rate of *Montastrea annularis* following the 1987–1988 coral-bleaching event. Coral Reefs **8**(4):211-215

Goss R and Jakob T (2010) Regulation and function of xanthophyll cycle-dependent photoprotection in algae. Photosynth Res **106**(1-2):103-122

Goujon M, McWilliam H, Li W, Valentin F, Squizzato S, Paern J and Lopez R (2010) A new bioinformatics analysis tools framework at EMBL–EBI. Nucleic Acids Res **38**(suppl 2):W695-W699

Goulet TL (2007) Most scleractinian corals and octocorals host a single symbiotic zooxanthella clade. Mar Ecol Prog Ser **335**:243-248

Greenstein BJ and Pandolfi JM (2008) Escaping the heat: range shifts of reef coral taxa in coastal Western Australia. Glob Change Biol **14**(3):513-528

Grottoli AG, Rodrigues LJ and Palardy JE (2006) Heterotrophic plasticity and resilience in bleached corals. Nature **440**(7088):1186-1189

Guerzoni ME, Ferruzzi M, Sinigaglia M and Criscuoli GC (1997) Increased cellular fatty acid desaturation as a possible key factor in thermotolerance in *Saccharomyces cerevisiae*. Can J Microbiol **43**(6):569-576

Guerzoni ME, Lanciotti R and Cocconcelli PS (2001) Alteration in cellular fatty acid composition as a response to salt, acid, oxidative and thermal stresses in *Lactobacillus helveticus*. Microbiology **147**(8):2255-2264

Guindon S and Gascuel O (2003) A simple, fast and accurate algorithm to estimate large phylogenies by maximum likelihood. Syst Biol **52**(5):696-704

Guschina IA and Harwood JL (2006a) Lipids and lipid metabolism in eukaryotic algae. Prog Lipid Res **45**(2):160-186

Guschina IA and Harwood JL (2006b) Mechanisms of temperature adaptation in poikilotherms. FEBS Lett **580**(23):5477-5483

Hadi AS (1992) Identifying multiple outliers in multivariate data. J R Stat Soc Series B Stat Methodol:761-771

Halliwell B (1987) Oxidative Damage, Lipid Peroxidation and Antioxidant Protection in Chloroplasts. Chem Phys Lipids **44**:327-340

Halliwell B (2006) Reactive species and antioxidants. Redox biology is a fundamental theme of aerobic life. Plant Physiol **141**(2):312-322

Harriott V (1992) Recruitment patterns of scleractinian corals in an isolated sub-tropical reef system. Coral Reefs **11**(4):215-219

Harriott V, Smith S and Harrison P (1994) Patterns of coral community structure of subtropical reefs in the Solitary Islands Marine Reserve, Eastern Australia. Mar Ecol Prog Ser **109**:67-67

Harriott V and Banks S (1995) Recruitment of scleractinian corals in the Solitary Islands Marine Reserve, a high latitude coral-dominated community in eastern Australia. Mar Ecol Prog Ser **123**(1):155-161

Harriott V and Banks S (2002) Latitudinal variation in coral communities in eastern Australia: a qualitative biophysical model of factors regulating coral reefs. Coral Reefs **21**(1):83-94

Harriott VJ, Harrison PL and Banks SA (1995) The coral communities of Lord Howe Island. Mar Freshw Res **46**(2):457-465

Harrison P (2008) Coral spawn slicks at Lord Howe Island, Tasman Sea, Australia; the world's most southerly coral reef. Coral Reefs **27**(1):35-35

References

Harrison PL, Dalton SJ and Carroll AG (2011) Extensive coral bleaching on the world's southernmost coral reef at Lord Howe Island, Australia. Coral Reefs **30**(3):775-775

Hawkins TD and Davy SK (2013) Nitric oxide and coral bleaching: is peroxynitrite generation required for symbiosis collapse? J Exp Biol DOI:10.1242/jeb.087510

Heipieper HJ, Meinhardt F and Segura A (2003) The cis–trans isomerase of unsaturated fatty acids in *Pseudomonas* and *Vibrio*: biochemistry, molecular biology and physiological function of a unique stress adaptive mechanism. FEMS Microbiol Lett **229**(1):1-7

Hennige SJ, Suggett DJ, Warner ME, McDougall KE and Smith DJ (2009) Photobiology of *Symbiodinium* revisited: bio-physical and bio-optical signatures. Coral Reefs **28**(1):179-195

Hennige SJ, McGinley MP, Grottoli AG and Warner ME (2011) Photoinhibition of *Symbiodinium* spp. within the reef corals *Montastraea faveolata* and *Porites astreoides*: implications for coral bleaching. Mar Biol **158**(11):2515-2526

Higuchi T, Fujimura H, Arakaki T and Oomori T (2008) Activities of antioxidant enzymes (SOD and CAT) in the coral *Galaxea fascicularis* against increased hydrogen peroxide concentrations in seawater. Proceeding of the 11th International Coral Reef Symposium, Fort Lauderale, Florida, USA

Hill R, Larkum AW, Frankart C, Kühl M and Ralph PJ (2004a) Loss of functional Photosystem II reaction centres in zooxanthellae of corals exposed to bleaching conditions: using fluorescence rise kinetics. Photosynth Res **82**(1):59-72

Hill R, Schreiber U, Gademann R, Larkum AW, Kühl M and Ralph PJ (2004b) Spatial heterogeneity of photosynthesis and the effect of temperature-induced bleaching conditions in three species of corals. Mar Biol **144**(4):633-640

Hill R, Frankart C and Ralph PJ (2005) Impact of bleaching conditions on the components of non-photochemical quenching in the zooxanthellae of a coral. J Exp Mar Biol Ecol **322**(1):83-92

Hill R and Ralph PJ (2005) Diel and seasonal changes in fluorescence rise kinetics of three scleractinian corals. Funct Plant Biol **32**(6):549-559

Hill R and Ralph PJ (2006) Photosystem II heterogeneity of in hospite zooxanthellae in scleractinian corals exposed to bleaching conditions. Photochem Photobiol **82**(6):1577-1585

Hill R and Ralph PJ (2007) Post-bleaching viability of expelled zooxanthellae from the scleractinian coral *Pocillopora damicornis*. Mar Ecol Prog Ser **352**:137

Hill R and Ralph PJ (2008) Impact of bleaching stress on the function of the oxygen evolving complex of zooxanthellae from scleractinian corals. J Phycol **44**(2):299-310

References

Hill R, Ulstrup KE and Ralph PJ (2009) Temperature induced changes in thylakoid membrane thermostability of cultured, freshly isolated, and expelled zooxanthellae from scleractinian corals. Bull Mar Sci **85**(3):223-244

Hill R, Brown CM, DeZeeuw K, Campbell DA and Ralph PJ (2011) Increased rate of D1 repair in coral symbionts during bleaching is insufficient to counter accelerated photo-inactivation. Limnol Oceanogr **56**(1):139

Hill R, Larkum A, Prášil O, Kramer D, Szabó M, Kumar V and Ralph P (2012) Light-induced dissociation of antenna complexes in the symbionts of scleractinian corals correlates with sensitivity to coral bleaching. Coral Reefs **31**(4):963-975

Hill R and Scott A (2012) The influence of irradiance on the severity of thermal bleaching in sea anemones that host anemonefish. Coral Reefs **31**(1):273-284

Hill RW, Dacey JWH and Krupp DA (1995) Dimethylsulfoniopropionate in Reef Corals. Bull Mar Sci **57**(2):489-494

Hobday AJ and Lough JM (2011) Projected climate change in Australian marine and freshwater environments. Mar Freshw Res **62**(9):1000-1014

Hoegh-Guldberg O and Smith GJ (1989) The effect of sudden changes in temperature, light and salinity on the population density and export of zooxanthellae from the reef corals *Stylophora pistillata* Esper and *Seriatopora hystrix* Dana. J Exp Mar Biol Ecol **129**(3):279-303

Hoegh-Guldberg O (1999) Climate change, coral bleaching and the future of the world's coral reefs. Mar Freshw Res **50**(8):839-866

Hoegh-Guldberg O and Fine M (2004) Low temperatures cause coral bleaching. Coral Reefs **23**(3):444-444

Hoegh-Guldberg O, Fine M, Skirving W, Johnstone R, Dove S and Strong A (2005) Coral bleaching following wintry weather. Limnol Oceanogr **50**(1):265-271

Hoegh-Guldberg O, Mumby PJ, Hooten AJ, Steneck RS, Greenfield P, Gomez E, Harvell CD, Sale PF, Edwards AJ, Caldeira K, Knowlton N, Eakin CM, Iglesias-Prieto R, Muthiga N, Bradbury RH, Dubi A and Hatziolos ME (2007) Coral reefs under rapid climate change and ocean acidification. Science **318**(5857):1737-1742

Hoegh-Guldberg O and Bruno JF (2010) The impact of climate change on the world's marine ecosystems. Science **328**(5985):1523-1528

Hoey AS, Pratchett MS and Cvitanovic C (2011) High macroalgal cover and low coral recruitment undermines the potential resilience of the world's southernmost coral reef assemblages. PLoS ONE **6**(10):e25824

Houlbreque F and Ferrier-Pagès C (2009) Heterotrophy in tropical scleractinian corals. Biol Rev **84**(1):1-17

References

Howells E, Beltran V, Larsen N, Bay L, Willis B and Van Oppen M (2011) Coral thermal tolerance shaped by local adaptation of photosymbionts. Nature Clim Change **2**(2):116-120

Huelsenbeck JP and Ronquist F (2001) MRBAYES: Bayesian inference of phylogenetic trees. Bioinformatics **17**(8):754-755

Hughes TP (1994) Catastrophes, phase-shifts, and large-scale degradation of a caribbean coral reef. Science **265**(5178):1547-1551

Hughes TP, Baird AH, Bellwood DR, Card M, Connolly SR, Folke C, Grosberg R, Hoegh-Guldberg O, Jackson JBC, Kleypas J, Lough JM, Marshall P, Nystrom M, Palumbi SR, Pandolfi JM, Rosen B and Roughgarden J (2003) Climate change, human impacts, and the resilience of coral reefs. Science **301**(5635):929-933

Iba K (2002) Acclimative response to temperature stress in higher plants: approaches of gene engineering for temperature tolerance. Annu Rev Plant Biol **53**(1):225-245

Iglesias-Prieto R, Govind N and Trench R (1991) Apoprotein composition and spectroscopic characterization of the water-soluble peridinin-chlorophyll *a*-proteins from three symbiotic dinoflagellates. Proc R Soc Lond B Biol Sci **246**(1317):275-283

Iglesias-Prieto R, Matta JL, Robins WA and Trench RK (1992) Photosynthetic response to elevated temperature in the symbiotic dinoflagellate *Symbiodinium microadriaticum* in culture. Proc Natl Acad Sci USA **89**(21):10302-10305

Iglesias-Prieto R, Govind NS and Trench RK (1993) Isolation and characterization of 3 membrane-bound chlorphyll-protein complexes from 4 dinoflagellate species. Philos Trans R Soc Lond B Biol Sci **340**(1294):381-392

Iglesias-Prieto R (1997) Temperature-dependent inactivation of photosystem II in symbiotic dinoflagellates. Proceedings of the 8th International Coral Reef Symposium Vol 2 Smithsonian Tropical Research Institute, Panama

Iglesias-Prieto R, Beltran VH, LaJeunesse TC, Reyes-Bonilla H and Thome PE (2004) Different algal symbionts explain the vertical distribution of dominant reef corals in the eastern Pacific. Proc R Soc Lond B Biol Sci **271**(1549):1757-1763

Jackson JBC, Kirby MX, Berger WH, Bjorndal KA, Botsford LW, Bourque BJ, Bradbury RH, Cooke R, Erlandson J, Estes JA, Hughes TP, Kidwell S, Lange CB, Lenihan HS, Pandolfi JM, Peterson CH, Steneck RS, Tegner MJ and Warner RR (2001) Historical overfishing and the recent collapse of coastal ecosystems. Science **293**(5530):629-638

Jeffrey S and Humphrey G (1975) New spectrophotometric equations for determining chlorophylls *a*, *b*, c_1 and c_2 in higher plants, algae and natural phytoplankton. Biochem Physiol Pflanz (BPP) **167**(19):191-194

References

Jeong HJ, Du Yoo Y, Kang NS, Lim AS, Seong KA, Lee SY, Lee MJ, Lee KH, Kim HS and Shin W (2012) Heterotrophic feeding as a newly identified survival strategy of the dinoflagellate *Symbiodinium*. Proc Natl Acad Sci USA **109**(31):12604-12609

Johannes R, Wiebe W, Crossland C, Rimmer D and Smith S (1983) Latitudinal limits of coral reef growth. Mar Ecol Prog Ser **11**(2):105-111

Johnson KG, Jackson JB and Budd AF (2008) Caribbean reef development was independent of coral diversity over 28 million years. Science **319**(5869):1521-1523

Jokiel P and Coles S (1977) Effects of temperature on the mortality and growth of Hawaiian reef corals. Mar Biol **43**(3):201-208

Jones AM, Berkelmans R, van Oppen MJ, Mieog JC and Sinclair W (2008) A community change in the algal endosymbionts of a scleractinian coral following a natural bleaching event: field evidence of acclimatization. Proc R Soc Lond B Biol Sci **275**(1641):1359-1365

Jones RJ, Hoegh-Guldberg O, Larkum AWD and Schreiber U (1998) Temperature-induced bleaching of corals begins with impairment of the CO_2 fixation mechanism in zooxanthellae. Plant Cell and Environment **21**(12):1219-1230

Jones RJ (2008) Coral bleaching, bleaching-induced mortality, and the adaptive significance of the bleaching response. Mar Biol **154**(1):65-80

Kemp DW, Oakley CA, Thornhill DJ, Newcomb LA, Schmidt GW and Fitt WK (2011) Catastrophic mortality on inshore coral reefs of the Florida Keys due to severe low-temperature stress. Glob Change Biol **17**(11):3468-3477

Kim C, Meskauskiene R, Apel K and Laloi C (2008) No single way to understand singlet oxygen signalling in plants. EMBO Rep **9**(5):435-439

Kleppel G, Dodge R and Reese C (1989) Changes in pigmentation associated with the bleaching of stony corals. Limnol Oceanogr **34**(7):1331-1335

Kleypas JA, McManus JW and Meñez LAB (1999) Environmental limits to coral reef development: Where do we draw the line? Am Zool **39**(1):146-159

Krämer WE, Caamaño-Ricken I, Richter C and Bischof K (2012) Dynamic regulation of photoprotection determines thermal tolerance of two phylotypes of *Symbiodinium* clade A at two photon fluence rates. Photochem Photobiol **88**(2):398-413

Krämer WE, Schrameyer V, Hill R, Ralph PJ and Bischof K (2013) PSII activity and pigment dynamics of *Symbiodinium* in two Indo-Pacific corals exposed to short-term high-light stress. Mar Biol **160**(3):563-577

LaJeunesse T (2002) Diversity and community structure of symbiotic dinoflagellates from Caribbean coral reefs. Mar Biol **141**(2):387-400

References

LaJeunesse TC and Trench RK (2000) Biogeography of two species of *Symbiodinium* (Freudenthal) inhabiting the intertidal sea anemone *Anthopleura elegantissima* (Brandt). Biol Bull **199**(2):126-134

LaJeunesse TC (2001) Investigating the biodiversity, ecology, and phylogeny of endosymbiotic dinoflagellates in the genus *Symbiodinium* using the ITS region: in search of a "species" level marker. J Phycol **37**(5):866-880

LaJeunesse TC, Loh WKW, van Woesik R, Hoegh-Guldberg O, Schmidt GW and Fitt WK (2003) Low symbiont diversity in southern Great Barrier Reef corals, relative to those of the Caribbean. Limnol Oceanogr **48**(5):2046-2054

LaJeunesse TC, Bonilla HR, Warner ME, Wills M, Schmidt GW and Fitt WK (2008) Specificity and stability in high latitude eastern Pacific coral-algal symbioses. Limnol Oceanogr **53**(2):719-727

LaJeunesse TC, Smith RT, Finney J and Oxenford H (2009) Outbreak and persistence of opportunistic symbiotic dinoflagellates during the 2005 Caribbean mass coral 'bleaching'event. Proc R Soc Lond B Biol Sci **276**(1676):4139-4148

LaJeunesse TC, Smith R, Walther M, Pinzón J, Pettay DT, McGinley M, Aschaffenburg M, Medina-Rosas P, Cupul-Magaña AL and Pérez AL (2010) Host–symbiont recombination versus natural selection in the response of coral–dinoflagellate symbioses to environmental disturbance. Proc R Soc Lond B Biol Sci **277**(1696):2925-2934

Lee DH and Lee CB (2000) Chilling stress-induced changes of antioxidant enzymes in the leaves of cucumber: in gel enzyme activity assays. Plant Sci **159**(1):75-85

Leggat W, Badger MR and Yellowlees D (1999) Evidence for an inorganic carbon-concentrating mechanism in the symbiotic dinoflagellate *Symbiodinium* sp. Plant Physiol **121**(4):1247-1255

Leggat W, Marendy EM, Baillie B, Whitney SM, Ludwig M, Badger MR and Yellowlees D (2002) Dinoflagellate symbioses: strategies and adaptations for the acquisition and fixation of inorganic carbon. Funct Plant Biol **29**(3):309-322

Leggat W, Whitney S and Yellowlees D (2004) Is coral bleaching due to the instability of the zooxanthellae dark reactions? Symbiosis **37**(1-3):137-153

Leggat W, Hoegh-Guldberg O, Dove S and Yellowlees D (2007) Analysis of an EST library from the dinoflagellate (*Symbiodinium* sp.) symbiont of reef-building corals. J Phycol **43**(5):1010-1021

Lesser MP and Shick JM (1989) Effects of irradiance and ultraviolet radiation on photoadaptation in the zooxanthellae of *Aiptasia pallida*: primary production, photoinhibition, and enzymic defenses against oxygen toxicity. Mar Biol **102**:243-255

Lesser MP (1996) Elevated temperatures and ultraviolet radiation cause oxidative stress and inhibit photosynthesis in symbiotic dinoflagellates. Limnol Oceanogr(41):271-283

References

Lesser MP and Farrell JH (2004) Exposure to solar radiation increases damage to both host tissues and algal symbionts of corals during thermal stress. Coral Reefs **23**(3):367-377

Lesser MP (2006) Oxidative stress in marine environments: biochemistry and physiological ecology. Annu Rev Physiol **68**:253-278

Lesser MP (2011) Coral bleaching: causes and mechanisms. In: Coral Reefs: An Ecosystem in Transition. New York, Springer**:**405-419

Lessios H, Glynn P and Robertson D (1983) Mass mortalities of coral reef organisms. Science **222**:715

Lobban C (2002) Ciliate-*Symbiodinium* symbiosis spotted on reefs. Coral Reefs **21**(4):332-332

Long S, Humphries S and Falkowski PG (1994) Photoinhibition of photosynthesis in nature. Annu Rev Plant Biol **45**(1):633-662

Loya Y, Sakai K, Yamazato K, Nakano Y, Sambali H and van Woesik R (2001) Coral bleaching: the winners and the losers. Ecol Lett **4**(2):122-131

Mansour MP, Volkman JK, Jackson AE and Blackburn SI (1999) The fatty acid and sterol composition of five marine dinoflagellates. J Phycol **35**(4):710-720

Mattoo AK, Hoffman-Falk H, Marder JB and Edelman M (1984) Regulation of protein metabolism: coupling of photosynthetic electron transport to *in vivo* degradation of the rapidly metabolized 32-kilodalton protein of the chloroplast membranes. Proc Natl Acad Sci USA **81**(5):1380-1384

McGinty ES, Pieczonka J and Mydlarz LD (2012) Variations in Reactive Oxygen Release and Antioxidant Activity in Multiple *Symbiodinium* Types in Response to Elevated Temperature. Microb Ecol **64**(4):1000-1007

Meissner K, Lippmann T and Gupta AS (2012) Large-scale stress factors affecting coral reefs: open ocean sea surface temperature and surface seawater aragonite saturation over the next 400 years. Coral Reefs **31**(2):309-319

Merle PL, Sabourault C, Richier S, Allemand D and Furla P (2007) Catalase characterization and implication in bleaching of a symbiotic sea anemone. Free Radical Biol Med **42**(2):236-246

Middlebrook R, Hoegh-Guldberg O and Leggat W (2008) The effect of thermal history on the susceptibility of reef-building corals to thermal stress. J Exp Biol **211**(Pt 7):1050-1056

Middlebrook R, Anthony KRN, Hoegh-Guldberg O and Dove S (2010) Heating rate and symbiont productivity are key factors determining thermal stress in the reef-building coral *Acropora formosa*. J Exp Biol **213**(7):1026-1034

Mieog JC, van Oppen MJ, Cantin NE, Stam WT and Olsen JL (2007) Real-time PCR reveals a high incidence of *Symbiodinium* clade D at low levels in four scleractinian corals across the Great Barrier Reef: implications for symbiont shuffling. Coral Reefs **26**(3):449-457

References

Moberg F and Folke C (1999) Ecological goods and services of coral reef ecosystems. Ecol Econ **29**(2):215-233

Møller IM (2001) Plant mitochondria and oxidative stress: electron transport, NADPH turnover, and metabolism of reactive oxygen species. Annu Rev Plant Biol **52**(1):561-591

Morgan-Kiss RM, Priscu JC, Pocock T, Gudynaite-Savitch L and Huner NP (2006) Adaptation and acclimation of photosynthetic microorganisms to permanently cold environments. Microbiol Mol Biol Rev **70**(1):222-252

Muller-Parker G and D'Elia CF (1997) Interactions between corals and their symbiotic algae. In: Life and death of coral reefs. New York, Chapman and Hall**:**96-114

Muller-Parker G and Davy SK (2001) Temperate and tropical algal-sea anemone symbioses. Invertebr Biol **120**(2):104-123

Muller P, Li XP and Niyogi KK (2001) Non-photochemical quenching. A response to excess light energy. Plant Physiol **125**(4):1558-1566

Mullineaux C and Kirchhoff H (2010) Role of lipids in the dynamics of thylakoid membranes. In: Lipids in Photosynthesis: Advances in Photosynthesis and Respiration. Amsterdam, Springer. **30:**283-294

Murata N and Wada H (1995) Acyl-lipid desaturases and their importance in the tolerance and acclimatization to cold of cyanobacteria. Biochem J **308**(Pt 1):1-8

Murata N, Takahashi S, Nishiyama Y and Allakhverdiev SI (2007) Photoinhibition of photosystem II under environmental stress. Biochim et Biophys Acta - Bioenergetics **1767**(6):414-421

Murata N, Allakhverdiev SI and Nishiyama Y (2012) The mechanism of photoinhibition i*n vivo*: Re-evaluation of the roles of catalase, α-tocopherol, non-photochemical quenching, and electron transport. Biochim et Biophys Acta - Bioenergetics **1817**(8):1127-1133

Muscatine L (1967) Glycerol excretion by symbiotic algae from corals and *Tridacna* and its control by the host. Science **156**(3774):516-519

Muscatine L and Porter JW (1977) Reef corals: mutualistic symbioses adapted to nutrient-poor environments. Bioscience **27**(7):454-460

Muscatine L, McCloskey LR and Marian RE (1981) Estimating the daily contribution of carbon from zooxanthellae to coral animal respiration. Limnol Oceanogr **26**(4):601-611

Muscatine L, Falkowski PG, Porter JW and Dubinsky Z (1984) Fate of photosynthetic fixed carbon in light-adapted and shade-adapted colonies of the symbiotic coral *Stylophora pistillata*. Proc R Soc Lond B Biol Sci **222**(1227):181-202

Nakano Y and Asada K (1981) Hydrogen peroxide is scavenged by ascorbate-specific peroxidase in spinach chloroplasts. Plant Cell Physiol **22**(5):867-880

References

Nanjo Y, Mizusawa N, Wada H, Slabas AR, Hayashi H and Nishiyama Y (2010) Synthesis of fatty acids *de novo* is required for photosynthetic acclimation of *Synechocystis* sp. PCC 6803 to high temperature. Biochim et Biophys Acta - Bioenergetics **1797**(8):1483-1490

Nicholas K, Nicholas Jr H and Deerfield II D (1997) GeneDoc: analysis and visualization of genetic variation. Embnew News **4**(1):14

Nii CM and Muscatine L (1997) Oxidative stress in the symbiotic sea anemone *Aiptasia pulchella* (Carlgren, 1943): Contribution of the animal to superoxide ion production at elevated temperature. Biol Bull **192**(3):444-456

Nishiyama Y, Allakhverdiev SI and Murata N (2006) A new paradigm for the action of reactive oxygen species in the photoinhibition of photosystem II. Biochim et Biophys Acta - Bioenergetics **1757**(7):742-749

Nixon PJ (2000) Chlororespiration. Phil Trans R Soc B 355 (1402): 1541-1547

Niyogi KK (1999) Photoprotection revisited: Genetic and molecular approaches. Annu Rev Plant Physiol Plant Mol Biol **50**:333-359

Okuyama H, Orikasa Y and Nishida T (2008) Significance of antioxidative functions of eicosapentaenoic and docosahexaenoic acids in marine microorganisms. Appl Environ Microbiol **74**(3):570-574

Orr JC, Fabry VJ, Aumont O, Bopp L, Doney SC, Feely RA, Gnanadesikan A, Gruber N, Ishida A and Joos F (2005) Anthropogenic ocean acidification over the twenty-first century and its impact on calcifying organisms. Nature **437**(7059):681-686

Ort DR (2001) When there is too much light. Plant Physiol **125**(1):29-32

Ort DR and Baker NR (2002) A photoprotective role for O_2 as an alternative electron sink in photosynthesis? Curr Opin Plant Biol **5**(3):193-198

Palmer CV, Modi CK and Mydlarz LD (2009) Coral fluorescent proteins as antioxidants. PLoS ONE **4**(10):e7298

Pandolfi JM, Bradbury RH, Sala E, Hughes TP, Bjorndal KA, Cooke RG, McArdle D, McClenachan L, Newman MJH, Paredes G, Warner RR and Jackson JBC (2003) Global trajectories of the long-term decline of coral reef ecosystems. Science **301**(5635):955-958

Pandolfi JM, Connolly SR, Marshall DJ and Cohen AL (2011) Projecting coral reef futures under global warming and ocean acidification. Science **333**(6041):418-422

Papina M, Meziane T and Van Woesik R (2007) Acclimation effect on fatty acids of the coral *Montipora digitata* and its symbiotic algae. Comp Biochem Physiol, Part B: Biochem Mol Biol **147**(4):583-589

Pawlowski J, Holzmann M, Fahrni JF, Pochon X and Lee JJ (2001) Molecular identification of algal endosymbionts in large miliolid Foraminifera: 2. Dinoflagellates. J Eukaryot Microbiol **48**(3):368-373

References

Paxton CW, Davy SK and Weis VM (2013) Stress and death of cnidarian host cells play a role in cnidarian bleaching. J Exp Biol DOI:10.1242/jeb.087858

Perez S and Weis V (2006) Nitric oxide and cnidarian bleaching: an eviction notice mediates breakdown of a symbiosis. J Exp Biol **209**(14):2804-2810

Pinto E, Catalani LH, Lopes NP, Di Mascio P and Colepicolo P (2000) Peridinin as the major biological carotenoid quencher of singlet oxygen in marine algae *Gonyaulax polyedra*. Biochem Biophys Res Commun **268**(2):496-500

Platt T, Gallegos C and Harrison W (1980) Photoinhibition of photosynthesis in natural assemblages of marine phytoplankton. J Mar Res(38):687-701

Pochon X, Pawlowski J, Zaninetti L and Rowan R (2001) High genetic diversity and relative specificity among *Symbiodinium*-like endosymbiotic dinoflagellates in soritid foraminiferans. Mar Biol **139**(6):1069-1078

Pochon X, LaJeunesse T and Pawlowski J (2004) Biogeographic partitioning and host specialization among foraminiferan dinoflagellate symbionts (*Symbiodinium*; Dinophyta). Mar Biol **146**(1):17-27

Pochon X, Montoya-Burgos JI, Stadelmann B and Pawlowski J (2006) Molecular phylogeny, evolutionary rates, and divergence timing of the symbiotic dinoflagellate genus *Symbiodinium*. Mol Phylogenet Evol **38**(1):20-30

Pochon X, Garcia-Cuetos L, Baker A, Castella E and Pawlowski J (2007) One-year survey of a single Micronesian reef reveals extraordinarily rich diversity of *Symbiodinium* types in soritid foraminifera. Coral Reefs **26**(4):867-882

Pochon X and Gates RD (2010) A new *Symbiodinium* clade (Dinophyceae) from soritid foraminifera in Hawai'i. Mol Phylogenet Evol **56**(1):492-497

Pochon X, Stat M, Takabayashi M, Chasqui L, Chauka LJ, Logan DDK and Gates RD (2010) Comparison of endosymbiotic and free living *Symbiodinium* (Dinophyceae) diversity in a Hawaiian reef environment. J Phycol **46**(1):53-65

Porter JW, Battey JF and Smith GJ (1982) Perturbation and change in coral reef communities. Proceedings of the National Academy of Sciences **79**(5):1678-1681

Porter JW, Fitt WK, Spero HJ, Rogers CS and White MW (1989) Bleaching in reef corals: physiological and stable isotopic responses. Proc Natl Acad Sci USA **86**(23):9342

Potts D (1984) Generation times and the Quaternary evolution of reef-building corals. Paleobiology:48-58

Powles SB (1984) Photoinhibition of photosynthesis induced by visible light. Annu Rev Plant Physiol **35**(1):15-44

Precht WF and Aronson RB (2004) Climate flickers and range shifts of reef corals. Front Ecol Environ **2**(6):307-314

References

Putnam HM, Stat M, Pochon X and Gates RD (2012) Endosymbiotic flexibility associates with environmental sensitivity in scleractinian corals. Proc R Soc Lond B Biol Sci **279**(1746):4352-4361

Ragni M, Airs RL, Leonardos N and Geider RJ (2008) Photoinhibition of PSII in *Emiliania huxleyi* (Haptophyta) under high light stress: the roles of photoacclimation, photoprotection, and photorepair. J Phycol **44**(3):670-683

Ragni M, Airs RL, Hennige SJ, Suggett DJ, Warner ME and Geider RJ (2010) PSII photoinhibition and photorepair in *Symbiodinium* (Pyrrhophyta) differs between thermally tolerant and sensitive phylotypes. Mar Ecol Prog Ser **406**:57-70

Ralph PJ, Gademann R and Larkum AWD (2001) Zooxanthellae expelled from bleached corals at 33°C are photosynthetically competent. Mar Ecol Prog Ser **220**:163-168

Ralph PJ and Gademann R (2005) Rapid light curves: a powerful tool to assess photosynthetic activity. Aquat Bot **82**(3):222-237

Ralph PJ, Larkum AW and Kühl M (2005) Temporal patterns in effective quantum yield of individual zooxanthellae expelled during bleaching. J Exp Mar Biol Ecol **316**(1):17-28

Reaka-Kudla ML (1997) The global biodiversity of coral reefs: a comparison with rain forests. In: Biodiversity II: understanding and protecting our biological resources. Washington, DC, Joseph Henry Press

Reaka-Kudla ML (2005) Biodiversity of Caribbean coral reefs. In: Caribbean Marine Biodiversity: The Known and the Unknown. Lancaster, Pennsylvania, DEStech Publications

Reitan KI, Rainuzzo JR and Olsen Y (1994) Effect of nutrient limitation on fatty acid and lipid content of marine Microalgae. J Phycol **30**(6):972-979

Reynolds JM, Bruns BU, Fitt WK and Schmidt GW (2008) Enhanced photoprotection pathways in symbiotic dinoflagellates of shallow-water corals and other cnidarians. Proc Natl Acad Sci USA **105**(36):13674-13678

Richardson DL, Harriott VJ and Harrison PL (1997) Distribution and abundance of giant sea anemones (Actiniaria) in subtropical eastern Australian waters. Mar Freshw Res **48**(1):59-66

Richier S, Merle PL, Furla P, Pigozzi D, Sola F and Allemand D (2003) Characterization of superoxide dismutases in anoxia- and hyperoxia-tolerant symbiotic cnidarians. Biochim Biophys Acta - General Subjects **1621**(1):84-91

Richier S, Furla P, Plantivaux A, Merle PL and Allemand D (2005) Symbiosis-induced adaptation to oxidative stress. J Exp Biol **208**(Pt 2):277-285

Richier S, Cottalorda JM, Guillaume MMM, Fernandez C, Allemand D and Furla P (2008) Depth-dependant response to light of the reef building coral, *Pocillopora verrucosa*: Implication of oxidative stress. J Exp Mar Biol Ecol **357**(1):48-56

Riegl B (2003) Climate change and coral reefs: different effects in two high-latitude areas (Arabian Gulf, South Africa). Coral Reefs **22**(4):433-446

Ritchie RJ (2006) Consistent sets of spectrophotometric chlorophyll equations for acetone, methanol and ethanol solvents. Photosynth Res **89**(1):27-41

Robison JD and Warner ME (2006) Differential impacts of photoacclimation and thermal stress on the photobiology of four different phylotypes of *Symbiodinium* (Pyrrhophyta). J Phycol **42**(3):568-579

Rodriguez-Lanetty M, Loh W, Carter D and Hoegh-Guldberg O (2001) Latitudinal variability in symbiont specificity within the widespread scleractinian coral *Plesiastrea versipora*. Mar Biol **138**(6):1175-1181

Rodriguez-Lanetty M, Chang SJ and Song JI (2003) Specificity of two temperate dinoflagellate-anthozoan associations from the north-western Pacific Ocean. Mar Biol **143**(6):1193-1199

Roopin M, Henry RP and Chadwick NE (2008) Nutrient transfer in a marine mutualism: patterns of ammonia excretion by anemonefish and uptake by giant sea anemones. Mar Biol **154**(3):547-556

Rosenberg E, Koren O, Reshef L, Efrony R and Zilber-Rosenberg I (2007) The role of microorganisms in coral health, disease and evolution. Nature Rev Microbiol **5**(5):355-362

Roth MS, Goericke R and Deheyn DD (2012) Cold induces acute stress but heat is ultimately more deleterious for the reef-building coral *Acropora yongei*. Sci Rep **2**, DOI:10.1038/srep00240

Rowan R and Powers DA (1991) Molecular genetic identification of symbiotic dinoflagellates (zooxanthellae). Mar Ecol Prog Ser **71**:65-73

Rowan R and Knowlton N (1995) Intraspecific Diversity and Ecological Zonation in Coral Algal Symbiosis. Proc Natl Acad Sci USA **92**(7):2850-2853

Rowan R, Whitney SM, Fowler A and Yellowlees D (1996) Rubisco in marine symbiotic dinoflagellates: form II enzymes in eukaryotic oxygenic phototrophs encoded by a nuclear multigene family. The Plant Cell Online **8**(3):539-553

Rowan R (2004) Coral bleaching - Thermal adaptation in reef coral symbionts. Nature **430**(7001):742-742

Rumeau D, Peltier G and Cournac L (2007) Chlororespiration and cyclic electron flow around PSI during photosynthesis and plant stress response. Plant, Cell Environ **30**(9):1041-1051

Salih A, Larkum A, Cox G, Kühl M and Hoegh-Guldberg O (2000) Fluorescent pigments in corals are photoprotective. Nature **408**(6814):850-853

References

Sampayo E, Dove S and LaJeunesse T (2009) Cohesive molecular genetic data delineate species diversity in the dinoflagellate genus *Symbiodinium*. Mol Ecol **18**(3):500-519

Sampayo EM, Franceschinis L, Hoegh-Guldberg O and Dove S (2007) Niche partitioning of closely related symbiotic dinoflagellates Mol Ecol **16**(17):3721-3733

Sampayo EM, Ridgway T, Bongaerts P and Hoegh-Guldberg O (2008) Bleaching susceptibility and mortality of corals are determined by fine-scale differences in symbiont type. Proc Natl Acad Sci USA **105**(30):10444-10449

Santos SR, Taylor DJ, Kinzie Iii RA, Hidaka M, Sakai K and Coffroth MA (2002) Molecular phylogeny of symbiotic dinoflagellates inferred from partial chloroplast large subunit (23S)-rDNA sequences. Mol Phylogenet Evol **23(**2):97-111

Santos SR, Toyoshima J and Kinzie III RA (2009) Spatial and temporal dynamics of symbiotic dinoflagellates (*Symbiodinium*: Dinophyta) in the perforate coral *Montipora capitata*. Galaxea, Journal of Coral Reef Studies **11**(2):139-147

Savage A, Goodson M, Visram S, Trapido-Rosenthal H, Wiedenmann J and Douglas A (2002) Molecular diversity of symbiotic algae at the latitudinal margins of their distribution: dinoflagellates of the genus *Symbiodinium* in corals and sea anemones. Mar Ecol Prog Ser **244**:17-26

Saxby T, Dennison WC and Hoegh-Guldberg O (2003) Photosynthetic responses of the coral *Montipora digitata* to cold temperature stress. Mar Ecol Prog Ser **248**:85-97

Sayanova O, Smith MA, Lapinskas P, Stobart AK, Dobson G, Christie WW, Shewry PR and Napier JA (1997) Expression of a borage desaturase cDNA containing an N-terminal cytochrome b5 domain results in the accumulation of high levels of Δ6-desaturated fatty acids in transgenic tobacco. Proc Natl Acad Sci USA **94**(8):4211-4216

Schoenberg DA and Trench RK (1980a) Genetic variation in *Symbiodinium* (=*Gymnodinium microadriaticum* Freudenthal), and specificity in its symbiosis with marine invertebrates. I. Isoenzyme and soluble protein patterns of axenic cultures of *Symbiodinium microadriaticum*. Proc R Soc Lond B Biol Sci **207**(1169):405-427

Schoenberg DA and Trench RK (1980b) Genetic variation in *Symbiodinium* (=*Gymnodinium microadriaticum* Freudenthal), and specificity in its symbiosis with marine invertebrates. II. Morphological variation in *Symbiodinium microadriaticum*. Proc R Soc Lond B Biol Sci **207**(1169):429-444

Scott A, Malcolm HA, Damiano C and Richardson DL (2011) Long-term increases in abundance of anemonefish and their host sea anemones in an Australian marine protected area. Mar Freshw Res **62**(2):187-196

Shick J, Lesser M, Dunlap W, Stochaj W, Chalker B and Won JW (1995) Depth-dependent responses to solar ultraviolet radiation and oxidative stress in the zooxanthellate coral *Acropora microphthalma*. Mar Biol **122(**1):41-51

Shick JM and Dunlap WC (2002) Mycosporine-like amino acids and related gadusols: Biosynthesis, accumulation, and UV-protective functions in aquatic organisms. Annu Rev Physiol **64**:223-262

Shiffler RE (1988) Maximum Z scores and outliers. Am Stat **42**(1):79-80

Sies H (1991) Oxidative Stress II. Oxidants and Antioxidants. London, Academic Press

Silverstein RN, Correa AM, LaJeunesse TC and Baker AC (2011) Novel algal symbiont (*Symbiodinium* spp.) diversity in reef corals of Western Australia. Mar Ecol Prog Ser **422**:63-75

Silverstein RN, Correa AM and Baker AC (2012) Specificity is rarely absolute in coral–algal symbiosis: implications for coral response to climate change. Proc R Soc Lond B Biol Sci **279**(1738):2609-2618

Smith-Keune C and Dove S (2008) Gene expression of a green fluorescent protein homolog as a host-specific biomarker of heat stress within a reef-building coral. Mar Biotechnol **10**(2):166-180

Smith DJ, Sugett DJ and Baker NR (2005) Is photoinhibition of zooxanthellae photosynthesis the primary cause of thermal bleaching in corals. Glob Change Biol **11**:1-11

Solomon S, Qin D, Manning M, Chen Z, Marquis M, Averyt K, Tignor M and Miller H (2007) IPCC Fourth Assessment Report (AR4)–Climate Change 2007: The Physical Science Basis, Contribution of Working Group I to the Fourth Assessment Report of the Intergovernmental Panel on Climate Change. Cambridge University Press, ISBN **978**(0521):70596-70597

Somero GN (1995) Proteins and temperature. Annu Rev Physiol **57**(1):43-68

Stambler N (2010) Coral symbiosis under stress. In: Symbioses and Stress. Dordrecht, Springer**:**197-224

Stambler N (2011) Zooxanthellae: The Yellow Symbionts Inside Animals. In: Coral Reefs: An Ecosystem in Transition. New York, Springer**:**87-106

Stanley GD and Swart PK (1995) Evolution of the coral zooxanthellae symbiosis during the triassic - a geochemical approach. Paleobiology **21**(2):179-199

Stat M, Carter D and Hoegh-Guldberg O (2006) The evolutionary history of *Symbiodinium* and scleractinian hosts - Symbiosis, diversity, and the effect of climate change. Perspect Plant Ecol Evol Syst **8**(1):23-43

Stat M, Pochon X, Cowie ROM and Gates RD (2009) Specificity in communities of *Symbiodinium* in corals from Johnston Atoll. Mar Ecol Prog Ser **386**:83-96

Stat M, Bird CE, Pochon X, Chasqui L, Chauka LJ, Concepcion GT, Logan D, Takabayashi M, Toonen RJ and Gates RD (2011) Variation in *Symbiodinium* ITS2 sequence assemblages among coral colonies. PLoS ONE **6**(1):e15854

References

Steen RG and Muscatine L (1987) Low temperature evokes rapid exocytosis of symbiotic algae by a sea anemone. Biol Bull **172**(2):246-263

Steinke M, Brading P, Kerrison P, Warner ME and Suggett DJ (2011) Concentrations of dimethylsulfoniopropionate and dimethyl sulfide are strain-specific in symbiotic dinoflagellates (*Symbiodinium* sp., Dinophyceae). J Phycol **47**(4):775-783

Stimson J and Kinzie RA (1991) The temporal pattern and rate of release of zooxanthellae from the reef coral *Pocillopora damicornis* (Linnaeus) under nitrogen-enrichment and control conditions. J Exp Mar Biol Ecol **153**(1):63-74

Suggett DJ, Warner ME, Smith DJ, Davey P, Hennige S and Baker NR (2008) Photosynthesis and production of hydrogen peroxide by *Symbiodinium* (Pyrrhophyta) phylotypes with different thermal tolerances. J Phycol **44**:948-956

Sunda W, Kieber DJ, Kiene RP and Huntsman S (2002) An antioxidant function for DMSP and DMS in marine algae. Nature **418**(6895):317-320

Takahashi S, Nakamura T, Sakamizu M, van Woesik R and Yamasaki H (2004) Repair machinery of symbiotic photosynthesis as the primary target of heat stress for reef-building corals. Plant Cell Physiol **45**(2):251-255

Takahashi S and Murata N (2005) Interruption of the Calvin cycle inhibits the repair of photosystem II from photodamage. Biochim et Biophys Acta - Bioenergetics **1708**(3):352-361

Takahashi S and Murata N (2008) How do environmental stresses accelerate photoinhibition? Trends Plant Sci **13**(4):178-182

Takahashi S, Whitney S, Itoh S, Maruyama T and Badger M (2008) Heat stress causes inhibition of the *de novo* synthesis of antenna proteins and photobleaching in cultured *Symbiodinium*. Proc Natl Acad Sci USA **105**(11):4203-4208

Takahashi S, Whitney SM and Badger MR (2009) Different thermal sensitivity of the repair of photodamaged photosynthetic machinery in cultured *Symbiodinium* species. Proc Natl Acad Sci USA **106**(9):3237-3242

Takahashi S and Badger MR (2011) Photoprotection in plants: a new light on photosystem II damage. Trends Plant Sci **16**(1):53-60

Takahashi S, Yoshioka-Nishimura M, Nanba D and Badger MR (2013) Thermal acclimation of the symbiotic alga *Symbiodinium* spp. alleviates photobleaching under heat stress. Plant Physiol **161**(1):477-485

Tchernov D, Gorbunov MY, de Vargas C, Yadav SN, Milligan AJ, Haggblom M and Falkowski PG (2004) Membrane lipids of symbiotic algae are diagnostic of sensitivity to thermal bleaching in corals. Proc Natl Acad Sci USA **101**(37):13531-13535

References

Tchernov D, Kvitt H, Haramaty L, Bibby TS, Gorbunov MY, Rosenfeld H and Falkowski PG (2011) Apoptosis and the selective survival of host animals following thermal bleaching in zooxanthellate corals. Proc Natl Acad Sci USA **108**(24):9905-9909

Tewksbury JJ, Huey RB and Deutsch CA (2008) Putting the heat on tropical animals. Science **320**(5881):1296-1297

Thornhill DJ, LaJeunesse TC, Kemp DW, Fitt WK and Schmidt GW (2006) Multi-year, seasonal genotypic surveys of coral-algal symbioses reveal prevalent stability or post-bleaching reversion. Mar Biol **148**(4):711-722

Thornhill DJ, Kemp DW, Bruns BU, Fitt WK and Schmidt GW (2008) Correspondence between cold tolerance and temperate biogeography in a western atlantic *Symbiodinium* (Dinophyta) lineage. J Phycol **44**(5):1126-1135

Thornhill DJ, Rotjan RD, Todd BD, Chilcoat GC, Iglesias-Prieto R, Kemp DW, LaJeunesse TC, Reynolds JM, Schmidt GW and Shannon T (2011) A connection between colony biomass and death in Caribbean reef-building corals. PLoS ONE **6**(12):e29535

Timmermann A, Oberhuber J, Bacher A, Esch M, Latif M and Roeckner E (1999) Increased El Niño frequency in a climate model forced by future greenhouse warming. Nature **398**:694-697

Tolosa I, Treignier C, Grover R and Ferrier-Pagès C (2011) Impact of feeding and short-term temperature stress on the content and isotopic signature of fatty acids, sterols, and alcohols in the scleractinian coral *Turbinaria reniformis*. Coral Reefs **30**(3):763-774

Trench RK (1971) The physiology and biochemistry of zooxanthellae symbiotic with marine coelenterates. II. Liberation of fixed ^{14}C by zooxanthellae *in vitro*. Proc R Soc Lond B Biol Sci **177**(1047):237-250

Trench RK (1979) Cell biology of plant-animal symbiosis. Annu Rev Plant Physiol Plant Mol Biol **30**:485-531

Tytler E and Trench R (1986) Activities of enzymes in beta-carboxylation reactions and of catalase in cell-free preparations from the symbiotic dinoflagellates *Symbiodinium* Spp. from a coral, a clam, a zoanthid and two sea anemones. Proc R Soc Lond B Biol Sci **228**(1253):483-492

Tyystjärvi E (2008) Photoinhibition of photosystem II and photodamage of the oxygen evolving manganese cluster. Coord Chem Rev **252**(3):361-376

Ulstrup KE, Hill R, van Oppen MJH, Larkum AWD and Ralph PJ (2008) Seasonal variation in the photo-physiology of homogeneous and heterogeneous *Symbiodinium* consortia in two scleractinian corals. Mar Ecol Prog Ser **361**:139-150

Van Alstyne K, Dominique VJ and Muller-Parker G (2009) Is dimethylsulfoniopropionate (DMSP) produced by the symbionts or the host in an anemone-zooxanthella symbiosis? Coral Reefs **28**(1):167-176

References

Van Hooidonk R, Maynard J and Planes S (2013) Temporary refugia for coral reefs in a warming world. Nature Clim Change **3**:508-511

van Oppen MJH, Palstra FP, Piquet AM-T and Miller DJ (2001) Patterns of coral-dinoflagellate associations in *Acropora*: significance of local availability and physiology of *Symbiodinium* strains and host-symbiont selectivity. Proc R Soc Lond B Biol Sci **268**:1759-1767

Vass I, Styring S, Hundal T, Koivuniemi A, Aro E and Andersson B (1992) Reversible and irreversible intermediates during photoinhibition of photosystem II: stable reduced QA species promote chlorophyll triplet formation. Proc Natl Acad Sci USA **89**(4):1408-1412

Venn AA, Wilson MA, Trapido-Rosenthal HG, Keely BJ and Douglas AE (2006) The impact of coral bleaching on the pigment profile of the symbiotic alga, *Symbiodinium*. Plant Cell Environ **29**(12):2133-2142

Venn AA, Loram JE and Douglas AE (2008) Photosynthetic symbioses in animals. J Exp Bot **59**(5):1069-1080

Veron J and Done T (1979) Corals and coral Communities of Lord Howe Island. Mar Freshw Res **30**(2):203-236

Veron J, Hoegh-Guldberg O, Lenton T, Lough J, Obura D, Pearce-Kelly P, Sheppard C, Spalding M, Stafford-Smith M and Rogers A (2009) The coral reef crisis: The critical importance of <350ppm CO_2. Mar Pollut Bull **58**(10):1428-1436

Veron JEN and Stafford-Smith M (2000) Corals of the world. 3 Volumes. Townsville, Australian Institute of Marine Science

Wada H, Gombos Z and Murata N (1994) Contribution of membrane lipids to the ability of the photosynthetic machinery to tolerate temperature stress. Proc Natl Acad Sci USA **91**(10):4273-4277

Wagner D, Przybyla D, op den Camp R, Kim C, Landgraf F, Lee KP, Würsch M, Laloi C, Nater M and Hideg E (2004) The genetic basis of singlet oxygen–induced stress responses of *Arabidopsis thaliana*. Science **306**(5699):1183-1185

Wakefield TS, Farmer MA and Kempf SC (2000) Revised description of the fine structure of in situ" zooxanthellae" genus *Symbiodinium*. Biol Bull **199**(1):76-84

Wakefield TS and Kempf SC (2001) Development of host-and symbiont-specific monoclonal antibodies and confirmation of the origin of the symbiosome membrane in a cnidarian–dinoflagellate symbiosis. Biol Bull **200**(2):127-143

Warner M, Lesser M and Ralph P (2010) Chlorophyll Fluorescence in Reef Building Corals. In: Chlorophyll *a* fluorescence in aquatic sciences: methods and applications. Amsterdam, Springer **4:**209-222

References

Warner ME, Fitt WK and Schmidt GW (1996) The effects of elevated temperature on the photosynthetic efficiency of zooxanthellae *in hospite* from four different species of reef coral: A novel approach. Plant Cell and Environment **19**(3):291-299

Warner ME, Fitt WK and Schmidt GW (1999) Damage to photosystem II in symbiotic dinoflagellates: A determinant of coral bleaching. Proc Natl Acad Sci USA **96**(14):8007-8012

Warner ME and Berry-Lowe S (2006) Differential xanthophyll cycling and photochemical activity in symbiotic dinoflagellates in multiple locations of three species of Caribbean coral. J Exp Mar Biol Ecol **339**(1):86-95

Weis VM (2008) Cellular mechanisms of Cnidarian bleaching: stress causes the collapse of symbiosis. J Exp Biol **211**(19):3059-3066

Wicks L, Sampayo E, Gardner JPA and Davy S (2010a) Local endemicity and high diversity characterise high-latitude coral–*Symbiodinium* partnerships. Coral Reefs **29**(4):989-1003

Wicks LC, Hill R and Davy SK (2010b) The influence of irradiance on tolerance to high and low temperature stress exhibited by *Symbiodinium* in the coral, *Pocillopora damicornis*, from the high-latitude reef of Lord Howe Island. Limnol Oceanogr **55**(6):2476-2486

Wiedenmann J, Schenk A, Röcker C, Girod A, Spindler K-D and Nienhaus GU (2002) A far-red fluorescent protein with fast maturation and reduced oligomerization tendency from *Entacmaea quadricolor* (Anthozoa, Actinaria). Proc Natl Acad Sci USA **99**(18):11646-11651

Wilkerson F, Kobayashi D and Muscatine L (1988) Mitotic index and size of symbiotic algae in Caribbean reef corals. Coral Reefs **7**(1):29-36

Wilkinson C (2004) Status of coral reefs of the world: 2004. Volume 1 and 2. Townsville, Australia, Australian Institute of Marine Science

Williams SE, Shoo LP, Isaac JL, Hoffmann AA and Langham G (2008) Towards an integrated framework for assessing the vulnerability of species to climate change. PLoS Biol **6**(12):e325

Wingler A, Lea PJ, Quick WP and Leegood RC (2000) Photorespiration: metabolic pathways and their role in stress protection. Proc R Soc Lond B Biol Sci **355**(1402):1517-1529

Wise RR (1995) Chilling-enhanced photooxidation: the production, action and study of reactive oxygen species produced during chilling in the light. Photosynth Res **45**(2):79-97

Yakovleva I, Bhagooli R, Takemura A and Hidaka M (2004) Differential susceptibility to oxidative stress of two scleractinian corals: antioxidant functioning of mycosporine-glycine. Comp Biochem Physiol, B: Comp Biochem **139**(4):721-730

Yakovleva IM, Baird AH, Yamamoto HH, Bhagooli R, Nonaka M and Hidaka M (2009) Algal symbionts increase oxidative damage and death in coral larvae at high temperatures. Mar Ecol Prog Ser **378**:105-112

References

Yamano H, Hori K, Yamauchi M, Yamagawa O and Ohmura A (2001) Highest-latitude coral reef at Iki Island, Japan. Coral Reefs **20**(1):9-12

Yamano H, Sugihara K and Nomura K (2011) Rapid poleward range expansion of tropical reef corals in response to rising sea surface temperatures. Geophys Res Lett **38**(4):L04601

Yazu K, Yamamoto Y, Niki E, Miki K and Ukegawa K (1998) Mechanism of lower oxidizability of eicosapentaenoate than linoleate in aqueous micelles. II. Effect of antioxidants. Lipids **33**(6):597-600

Yost DM and Mitchelmore CL (2009) Dimethylsulfoniopropionate (DMSP) lyase activity in different strains of the symbiotic alga *Symbiodinium microadriaticum*. Mar Ecol Prog Ser **386**:61-70

Yost DM, Jones RB and Mitchelmore CL (2010) Alterations in dimethylsulfoniopropionate (DMSP) levels in the coral *Montastraea franksi* in response to copper exposure. Aquat Toxicol **98**(4):367-373

Zapata M, Rodriguez F and Garrido JL (2000) Separation of chlorophylls and carotenoids from marine phytoplankton: a new HPLC method using a reversed phase C-8 column and pyridine-containing mobile phases. Mar Ecol Prog Ser **195**:29-45

Zhukova NV and Titlyanov EA (2003) Fatty acid variations in symbiotic dinoflagellates from Okinawan corals. Phytochemistry **62**(2):191-195

APPENDIX A:

Sequences

A.1 Cytochrome *c* oxidase (*COI*) subunit I like genes, partial

> **KF194194** Seq1[organism=***Pocillopora damicornis***] isolate PdCOISt1 mitochondrial cytochrome c oxidase subunit I-like gene, partial sequence

GATATTGGTACTTTGTATTTAATTTTCGGAGCAGGAGCTGGTTTAATTGGAACTGCTTTTAGTATGCTT
ATACGATTGGAGCTTTCTGCGCCGGGGGCGATGTTAGGAGATGATCATCTTTATAATGTAATTGTTACA
GCACATGCTTTTATTATGATTTTTTTTTTGGTTATGCCGGTCATGATTGGGGGATTTGGTAATTGATTAG
TCCCATTATATATTGGGGCGCCGGATATGGCGTTTCCTCGATTAAACAATATTAGTTTTTGACTTTTGCC
TCCTGCGCTTTTTTTATTATTAGGCTCTGCTTTTATTGAACAAGGGGCGGGGACGGGGTGAACAGTTTA
TCCTCCTCTTTCTAGTATTCAAGCACACTCCGGAGGTTCTGTTGATATGGTTATTTTTAGTCTTCATTTA
GCTGGGGTTTCTTCTATTTTAGGTGCTATTAACTTTATTACTACAATTTTTAATATGCGAGCCCCGGGTG
TGTCTTTTAATAAACTACCTTTATTTGTTTGATCTATTTTAATAACAGCTTTTTTATTACTTTTATCTTTA
CCTGTTTTAGCTGGTGCTATTACTATGTTGTTAACAGATAGAAACTTTAATACGACTTTTTTCGATCCAG
CGGGTGGCGGGGACCCAATATTATTTCAGCATTTATTTTGATTTTTTGGTC

> **KF194195** Seq2[organism=***Pocillopora damicornis***] isolate PdCOISt2 mitochondrial cytochrome c oxidase subunit I-like gene, partial sequence

CATAAAGATATTGGTACTTTGTATTTAATCTTCGGAGCAGGAGCTGGTTTAATTGGAACTGCTTTTAGT
ATGCTTATACGATTGGAGCTTTTTGCGCCGGGGGCGATGTTAGGAGATGATCATCTTTATAATGTAATT
GTTACAGCACATGCTTTTATTATGATTTTTTTTTTTGGTTATGCCGGTCATGATTGGGGGATTTGGTAATT
GATTAGTCCCATTATATATTGGGGCGCCGGATATGGCGTTTCCTCGATTAAACAATATTAGTTTTTGAC
TTTTGCCTCCTGCGCTTTTTTTATTATTAGGCTCTGCTTTTATTGAACAAGGGGCGGGGACGGGGTGAA
CAGTTTATCCTCCTCTTTCTAGTATTCAAGCACACTCCGGAGGTTCTGTTGATATGGTTATTTTTAGTCT
TCATTTAGCTGGGGTTTCTTCTATTTTAGGTGCTATTAACTTTATTACTACAATTTTTAATATGCGAGCC
CCGGGTGGGTCTTTTAATAAACTACCTTTATTTGTTTGATCTATTTTAATAACAGCTTTTTTATTACTTTT
ATCTTTACCTGTTTTAGCTGGTGCTATTACTATGTTGTTAACAGATAGAAACTTTAATACGACTTTTTTC
GATCCAGCGGGTGGCGGGGACCCAATATTATTTCAGCATTTATTTTGATTTTTTGGTCACCCTGGAAGT
T

> **KF194196** Seq3[organism=***Pocillopora damicornis***] isolate PdCOISt3 mitochondrial cytochrome c oxidase subunit I-like gene, partial sequence

AAAGATATTGGTACTTTGTATTTAATTTTCGGAGCAGGAGCTGGTTTAATTGGAACTGCTTTTAGTATG
CTTATACGATTGGAGCTTTTTGCGCCGGGGGCGATGTTAGGAGATGATCATCTTTATAATGTAATTGTT
ACAGCACATGCTTTTATTATGATTTTTTTTTTTGGTTATGCCGGTCATGATTGGGGGATTTGGTAATTGAT
TAGTCCCATTATATATTGGGGCGCCGGATATGGCGTTTCCTCGATTAAACAATATTAGTTTTTGACTTTT
GCCTCCTGCGCTTTTTTTATTATTAGGCTCTGCTTTTATTGAACAAGGGGCGGGGACGGGGTGAACAGT
TTATCCTCCTCTTTCTAGTATTCAAGCACACTCCGGAGGTTCTGTTGATATGGTTATTTTTAGTCTTCAT
TTAGCTGGGGTTTCTTCTATTTTAGGTGCTATTAACTTTATTACTACAATTTTTAAAATGCGAGCCCCGG
GTGTGTCTTTTAATAAACTACCTTTATTTGTTTGATCTATTTTAATAACAGCTTTTTTATTACTTTTATCT

TACCTGTTTTAGCTGGGGCTATTACAATGTTGTTAACAGATAGAAACTTTAATACAACTTTTTTCGATC
CAGCGGGGGGCGGGGACCCAATATTATTTCAGCATTTATTTTGATTTTTTGG

> **KF194197** Seq4[organism=***Pocillopora damicornis***] isolate PdCOISt5 mitochondrial cytochrome c oxidase subunit I-like gene, partial sequence

TCTTCGGAGCCAGGAGCTGGTTTAATTGGAACTGCTTTTAGTATGCTTATACGATTGGAGCTTTCTGCG
CCGGGGGCGATGTTAGGAGATGATCATCTTTATAATGTAATTGTTACAGCACATGCTTTTATTATGATT
TTTTTTTTGGTTATGCCGGTCATGATTGGGGGATTTGGTAATTGATTAGTCCCATTATATATTGGGGCGC
CGGATATGGCGTTTCCTCGATTAAACAATATTAGTTTTTGACTTTTGCCTCCTGCGCTTTTTTTATTATT
AGGCTCTGCTTTTATTGAACAAGGGGCGGGGACGGGGTGAACAGTTTATCCTCCTCTTTCTAGTATTCA
AGCACACTCCGGAGGTTCTGTTGATATGGTTATTTTTAGTCTTCATTTAGCTGGGGTTTCTTCTATTTTA
GGTGCTATTAACTTTATTACTACAATTTTTAATATGCGAGCCCCGGGTGTGTCTTTTAATAAACTACCTT
TATTTGTTTGATCTATTTTAATAACAGCTTTTTTATTACTTTTATCTTTACCTGTTTTACCTGGTGCTATT
ACAATGTTGTTAACAGATAGAAACTTTAATACGACTTTTTTCAATCCAGCGGGGGGCGGGGACCCAAT
ATTATTTCAGCATTTATTTTGATTTTTTGG

> **KF194198** Seq5[organism=***Stylophora*** sp.] isolate PdCOISy2 mitochondrial cytochrome c oxidase subunit I-like gene, partial sequence

CCGGGCTTGGGCCGGGTTTTTTCCTTTGGTCAACCAAATCATAAAGATATTGGTAGTTTGTATTTAATT
TTTGGTGGAGGTGCTGGTTTAATTGGAACGGCGTTTAGTATGCTTATACGACTAGAGCTTTCTGCGCCC
GGAGCGATGTTAGGAGATGATCATCTTTATAATGTAATTGTTACAGCACATGCTTTTATTATGATTTTT
TTTTTGGTTATGCCGGTAATGATTGGGGGGTTTGGTAATTGATTGGCCCCATTATATATTGGGGCGCCG
GATATGGCGTTTCCCCGACTAAACAATATTAGTTTTTGACTTTTGCCCCCTGCGCTTTTTTTATTATTAG
GCTCTGCTTTTATTGAACAAGGGGCGGGGACGGGATGAACAGTTTATCCTCCTCTTGCTAGTATTCAAG
CACACTCTGGAGGTTCGGTTGATATGGTTATTTTTAGTCTTCATTTAGCTGGGGTTTCTTCTATTTTAGG
TGCTATAAACTTTATTACTACAATTTTAAATATGCGAGCCCCGGGTGTGTCTTTTAATAAACTACCTTT
ATTTGTTTGATCTATTTTAATAACAGCTTTTTTATTACTT

> **KF194199** Seq6[organism= ***Stylophora*** sp.] isolate PdCOISy3 mitochondrial cytochrome c oxidase subunit I-like gene, partial sequence

GATATTGGTAGTTTGTATTTAATTTTTGGTGGAGGTGCTGGTTTAATTGGAACGGCGTTTAGTATGCTT
ATACGACTAGAGCTTTCTGCGCCCGGAGCGATGTTAGGAGATGATCATCTTTATAATGTAATTGTTACA
GCACATGCTTTTATTATGATTTTTTTTTTGGTTATGCCGGTTATGATTGGGGGGTTTGGTAATTGATTGG
TCCCATTATATATTGGGGCGCCGGATATGGCGTTTCCCCGACTAAACAATATTAGTTTTTGACTTTTGC
CCCCTGCGCTTTTTTTATTATTAGGCTCTGCTTTTATTGAACAAGGGGCGGGGACGGGATGAACAGTTT
ATCCTCCTCTTGCTAGTATTCAAGCACACTCTGGAGGTTCGGTTGATATGGTTATTTTTAGTCTTCATTT
AGCTGGGGTTTCTTCTATTTTAGGTGCTATAAACTTTATTACTACAATTTTAAATATGCGAGCCCCGGG
TGTGTCTTTTAATAAACTACCTTTATTTGTTTGATCTATTTTAATAACAGCTTTTTTATTACTTTTATCTT
TACCTGTTTTAGCTGGTGCTATTACTATGTTGTTAACAGATAGAAACTTTAATACGACTTTTTTCGATCC
AGCGGGTGGCGGGGACCCAATATTATTTCAGCATCTATTTTGATTTTTTGGT

>Seq7[organism=*Pocillopora damicornis*] isolate PdCOISy5 mitochondrial cytochrome c oxidase subunit I-like gene, partial sequence

TCGAGGACTGTACAGAACAGCGCGGGGCACAAATGAAGCATAAGAACTGCTTTTAGTATGCTTATACG
ATTGGAGCTTTCTGCGCCGGGGGCGATGTTAGGAGATGATCATCTTTATAATGTAATTGTTACAGCACA
TGCTTTTATTATGATTTTTTGGTCACCCTGAAGTTTAAAGAT

A.2 Mitochondrial open reading frame (ORF), partial

> **KF194192** Seq1[organism=***Pocillopora damicornis***] isolate PdORFSt1 ATP synthase subunit 6 (atp6) and hypothetical protein genes, partial cds; mitochondrial

GTCTGGTTTTTAAATTTGCAATGTTTATAATGGTGTTTATTACGCTATTAGAGGTGGCAGTTGCAATAA
TACAGGCCTATGTGTTTTGTCTGTTGGTACAAATTTATTTAACAGATACAATTTTTTTACATTAAAAATG
ACAGCCGTATAAATTTTTTTATGCACAATTGTAGGTATATCGTTAACGGTGAATTATGGATTTGGTATT
GGGTGATATGGTAGTTCTTCTCAAGCCTGGTTAAGGCACCAAATGGGCATAGACGGTGCAGAGAGGGT
CCATCCTTGAGCTTATTTTAATTATGTGCGCCAGCATTCTATTGCTCGTAATGTTGGGGTACAAGTGAA
TCTAGATTCAACTGAAGGACCAAATGATGTTGGGGTACAAGTGAATCAAGAGTCTGAACAGTCTGTGG
ATGTTGTTTTTATAGAATTGGAAGGGCGAAGGGTCCCCGTAAGGGGGGTGACTCTACATGTTGAGCGG
CGTGGTTATTTGGATAATCGGTCTAATCAAGAAGGTGTTGAGAATAGTTTAGGAGATCAATTTGAAGA
TGTGGCTTTTTTAAGAGAGAGTACAAGTACAATTACACCAGAAAGTGTAAATAGGGGCGCTCCAAGTG
GTAATATAAGAAATGTATTAAGTGATTCATTAATAGAGAAGAGAGGCCAAGACCAAACTTTAAGTGA
AATAAAGGTAGAAACACCTCCAGGTGCTTCAAGGGGTGGCCGATGAGCCAGTATAAATCAAGGTGAG
GCTTTAAGAGAAAACAAGGTAGAAATTGGGGTTTTAAGAGAAAACAAAGTAGAAATTGATGAGGTAG
TTGGCTCGACTTTTAGTTCGATCCCCTTAGAGGTTGAAGGGATGATGGCTCATGTGGAAAACAAATTTG
ACATCTGACCCACACTTGTGATAGAGAAAAAAATAAAAAAAAAAAAAAA

> **KF194193** Seq2[organism=**Stylophora** sp.] isolate PdORFSy3 ATP synthase subunit 6 (atp6) and hypothetical protein genes, partial cds; mitochondrial

GTTTTTAAATTAGCAATGTCTATAATGGTGTTTATTACGTTATTGGAGGTGGCCGTTGCGGTGATCCAA
GCGTATGTGTTTTGTCTGCTGACATTAATTTATTTAGCAGACACAATTTTTTTACATTAATCATGAGCGG
GGTAGAAATTTTTTTATGTTCATTAATGGGTGTGTCGGTGTGTTTTAATTATGCGTTCATGATGGCTTGA
TACAGCCAGTCTTCTCAAAGGTGACTTCAGCATCAAATGGATCTTCCAGAGAATACTGAATACGTGCA
TCCTTGAACTTATTATAGTTATGTGCGCCGTCATGGTATTGTTCATAATGGTGGTGCTGATCGGCCAAG
AGATGTTATTTTTATCGATCTAGAAGGGCGACAAGTGCCCTTAAGAAGTCGGCGAGTTTTTAGGGTGG
CGGAGAATGACGAGAGTTTGTGTGATAATGGTAATCGTTTGTGTCATGACGAGGGTTTGTGTGATAAT
GATGATCGTTTGTGTGTTCATGGCGAGAGTTTGTGTGATGATGATAGTTTGTGTGATAATGACGAGTTT
CAAGATGGGGTTTTGCATTTAAGTAAAAGTGCAAGTGAGTCAGAAAGTAGAGGTAGTTTGAGGGAAA
GTGTAATTAAGGGATTAAGTGAGTCAGAAAGTAGAGGTAGTTTGAGGGAAAGTGTAATTAAGGGATT
AAGTGAGTCAGAAAGTAGAGGTAGTTTGAGGGAAAGTGTAATTAAGGGGATTAAGTGATTCAAGAAG
CGAAGACGAAGCGTTAAGGGCAGTAGAGGTAGAAACACATTCAAGTACTGGCCAGTTAGCGCGTACC
ACTCTTGGTGACGCTGCTTGAATCAACTCTTAACCCGATCCCGTCTGAAGTTCAAATGAATGATGGCTC
CTGTGAGAGATCTACTGCTCACGCATTCCACAAAAAAATTGGCAAAAACCCC

A.3 Internal transcribed spacer 2 (ITS2) sequences derived from *Symbiodinium* cells harboured in Lord Howe Island scleractinian corals

> **KF194186** Seq1[organism=*Symbiodinium* sp.] *Symbiodinium* clade C isolate **C111*** 5.8S ribosomal RNA gene (partial) and internal transcribed spacer 2 (complete) and 28S ribosomal RNA gene (partial); isolated from ***Porites heronensis*** in 2010.

AACCAATGGCCTCCTGAACATGCGTTGCACTCTTGGGATTTCCTGAGAGTATGTCTGCTTCAGTGCTTA
ACTTGCCCCACCTTTGCAAGCAGGATGTGTTCTGCCTTGCGTTCTTATGAGCTATTGCCCTCTGAGCCA
ATGGCTTGTTAATTGCTTGGTTCTTGCAAAATGCCTTGCGCGCTGTTATTCAAGTTTCTACCTTCGTGGT
TTTACTTGAGTGACCCTGCTCATGCTTGCAACCGCTGGGATGCAGGTGCATGCCTCTAGCATGAAGTCA
GACAA

> **KF194187** Seq2[organism=*Symbiodinium* sp.] *Symbiodinium* clade C isolate **C111*** 5.8S ribosomal RNA gene (partial) and internal transcribed spacer 2 (complete) and 28S ribosomal RNA gene (partial); isolated from ***Acropora yongei*** in 2010.

AACCAATGGCCTCCTGAACATGCGTTGCACTCTTGGGATTTCCTGAGAGTATGTCTGCTTCAGTGCTTA
ACTTGCCCCACCTTTGCAAGCAGGATGTGTTCTGCCTTGCGTTCTTATGAGCTATTGCCCTCTGAGCCA
ATGGCTTGTTAATTGCTTGGTTCTTGCAAAATGCCTTGCGCGCTGTTATTCAAGTTTCTACCTTCGTGGT
TTTACTTGAGTGACCCTGCTCATGCTTGCAACCGCTGGGATGCAGGTGCATGCCTCTAGCATGAAGTCA
GACAA

> **KF194188** Seq3[organism=*Symbiodinium* sp.] *Symbiodinium* clade C isolate **C3** 5.8S ribosomal RNA gene (partial) and internal transcribed spacer 2 (complete) and 28S ribosomal RNA gene (partial); isolated from ***Acropora yongei*** in 2010.

AACCAATGGCCTCCTGAACGTGCGTTGCACTCTTGGGATTTCCTGAGAGTATGTCTGCTTCAGTGCTTA
ACTTGCCCCAACTTTGCAAGCAGGATGTGTTTCTGCCTTGCGTTCTTATGAGCTATTGCCCTCTGAGCC
AATGGCTTGTTAATTGCTTGGTTCTTGCAAAATGCTTTGCGCGCTGTTATTCAAGTTTCTACCTTCGTGG
TTTTACTTGAGTGACGCTGCTCATGCTTGCAACCGCTGGGATGCAGGTGCATGCCTCTAGCATGAAGTC
AGACAA

> **KF194189** Seq4[organism=*Symbiodinium* sp.] *Symbiodinium* clade C isolate **C100** 5.8S ribosomal RNA gene (partial) and internal transcribed spacer 2 (complete) and 28S ribosomal RNA gene (partial); isolated from ***Pocillopora damicornis*** in 2010.

AACCAATGGCCTCCTGAACGTGCGTTGCACTCTTGGGATTTCCTGAGAGTATGTCTGCTTCAGTGCTTA
ACTTGCCCCAACTTTGCAAGCAGGATGTGTTTCTGCCTTGCGTTTTTATGAGCTATTGCCCTCTGAGCC
AATGGCTTGTTAATTGCTTGGTTCTTGCAAAATGCTTTGCGCGCTGCTATTCAAGTTTCTACCTTCGTGG
TTTTACTTGAGTGACACCGCTCATGCTTGCAACCGCTGGGATGCAGGTGCATGCCTCTAGCATGAAGTC
AGACAA

Appendix

> **KF194190** Seq5[organism=*Symbiodinium* sp.] *Symbiodinium* clade C isolate **C118** 5.8S ribosomal RNA gene (partial) and internal transcribed spacer 2 (complete) and 28S ribosomal RNA gene (partial); isolated from ***Pocillopora damicornis*** in 2010.

AACCAATGGCCTCCTGAACGTGCGTTGCACTCTTGGGATTTCCTGAGAGTATGTCTACTTCAGTGCTTA
ACTTGCCCCAACTTTGCAAGCAGGATGTGTTTCTGCCTTGCGTTCTTATGAGCTATTGCCCTCTGAGCC
AATGGCTTGTTAATTGCTTGGTTCTTGCAAAATGCTTTGCGCGCTGTTATTCAAGTTTCTACCTTCGTGG
CTTTACTTGAGTGACGCTGCTCATGCTTGCAACCGCTGGGATGCAGGTGCATGCCTCTA

> **KF194191** Seq6[organism=*Symbiodinium* sp.] *Symbiodinium* clade C isolate **C118** 5.8S ribosomal RNA gene (partial) and internal transcribed spacer 2 (complete) and 28S ribosomal RNA gene (partial); isolated from ***Stylophora* sp.** in 2010.

AACCAATGGCCTCCTGAACGTGCGTTGCACTCTTGGGATTTCCTGAGAGTATGTCTACTTCAGTGCTTA
ACTTGCCCCAACTTTGCAAGCAGGATGTGTTTCTGCCTTGCGTTCTTATGAGCTATTGCCCTCTGAGCC
AATGGCTTGTTAATTGCTTGGTTCTTGCAAAATGCTTTGCGCGCTGTTATTCAAGTTTCTACCTTCGTGG
CTTTACTTGAGTGACGCTGCTCATGCTTGCAACCGCTGGGATGCAGGTGCATGCCTCTAGCATGAAGTC
AGACAG

> Seq7[organism=*Symbiodinium* sp.] *Symbiodinium* clade C isolate **C117** 5.8S ribosomal RNA gene (partial) and internal transcribed spacer 2 (complete) and 28S ribosomal RNA gene (partial); isolated from ***Porites heronensis*** in 2011.[1]

AACCAATGGCCTCCTGAACGTGCGTTGCACTCTTGGGATTTCCTGAGAGTATGTCTGCTTCAGTGCTTA
ACTTGCCCCAACTTTGCAAGCAGGATGTGTTTCTGCCTTGCGTTCTTATGAGCTATTGCCCTCTGAGCC
AATGGCTTGCTAATTGCTTGGTTCTTGCAAAATGCTTTGCGCGCTGTTATTCAGGTTTCTACCTTCGTGG
TTTTACTTGAGTGACGCTGCTCATACTTGCAACCGCTGGGATGCAGGTGCATGCCTCTAGCATGAAGTC
AGACAA

> Seq8[organism=*Symbiodinium* sp.] *Symbiodinium* clade C isolate **similar to C3** 5.8S ribosomal RNA gene (partial) and internal transcribed spacer 2 (complete) and 28S ribosomal RNA gene (partial); isolated from ***Isopora palifera*** in 2011.[1]

AACCAATGGCCTCCTGAATGTGCGTTGCACTCTTGGGATTTCCTGAGAGTATGTCTGCTTCAGTGCTTA
ACTTGCCCCAACTTTGCAAGCAGGATGTGTTTCTGCCTTGCGTTCGTATGAGTTATTGCCCTCTGAGCC
AATGGCTTGTTAATTGCTTGGTTCTTGCAAAATGCTTTGCGCGCTGTTATTCAAGTTTCTACCTTCGTGG
TTTTACTTGAGTGACGCTGCTCATGCTTGCAACCGCTGGGATGCAGGTGCATGCCTCTAGCATGAAGTC
AGACAA

[1] Note: ITS2 sequences Seq7 – Seq10 have not been submitted to GenBank yet due to a closedown of data submission on GenBank (caused by a lapse of government funding) at the time of writing.

Appendix

> Seq9[organism=*Symbiodinium* sp.] *Symbiodinium* clade C isolate **similar to C3** 5.8S ribosomal RNA gene (partial) and internal transcribed spacer 2 (complete) and 28S ribosomal RNA gene (partial); isolated from ***Acropora solitariensis*** in 2011.[1]

AACCAATGGCCTCCTGAATGTGCGTTGCACTCTTGGGATTTCCTGAGAGTATGTCTGCTTCAGTGCTTA
ACTTGCCCCAACTTTGCAAGCAGGATGTGTTTCTGCCTTGCGTTCGTATGAGTTATTGCCCTCTGAGCC
AATGGCTTGTTAATTGCTTGGTTCTTGCAAAATGCTTTGCGCGCTGTTATTCAAGTTTCTACCTTCGTGG
TTTTACTTGAGTGACGCTGCTCATGCTTGCAACCGCTGGGATGCAGGTGCATGCCTCTAGCATGAAGTC
AGACAA

> Seq10[organism=*Symbiodinium* sp.] *Symbiodinium* clade C isolate **similar to C131** 5.8S ribosomal RNA gene (partial) and internal transcribed spacer 2 (complete) and 28S ribosomal RNA gene (partial); isolated from ***Porites heronensis*** in 2012.[1]

AACCAATGGCCTCCTGAACATGCGTTGCACTCTTGGGATTTCCTGAGAGTATGTCTGCTTCAGTGCTTA
ACTTGCCCCAACTTTGCAAGCAGGATGTGTTTCTGCCTTGCGTTCTTATGAGCTATTGCCCTCTGAGCC
AATGGCTTGTTAATTGCTTGGTTCTTGCAAAATGCTTTGCGCGCTGTTATTCAAGTTTCTACCTTCGTGG
TTTTACTTGAGTGACGCTGCTCATGTTTGCAACCGCTGGGATGCAGGTGCATGCCTCTAGCATGAAGTC
AGACAA

A.4 Internal transcribed spacer 2 (ITS2) sequences derived from *Symbiodinium* cells harboured in *Entacmaea quadricolor*

> **KF134172** Seq1[organism=*Symbiodinium* sp.] *Symbiodinium* clade C isolate **C42(type2).1** 5.8S ribosomal RNA gene (partial) and internal transcribed spacer 2 (complete) and 28S ribosomal RNA gene (partial); isolated from ***Entacmaea quadricolor*** in 2012.

AAGCAATGGCCTCCTGAACCTGCGTTGCACTCTTGGGATTTCCTGAGAGTATGTCTGCTTCAGTGCTTA
ACTTGCCCCAACTTTGCAAGCAGGATGTGTTTCTGCCTTGCGTTCTTATGAGCTATTGCCCTCTGAGCC
AATGGCTTGTGAATTGCTTGGTTCTTGCAAAATGCTTTGCGCGCTGTTATTCAGGTTTCTACCTCCTTCG
TGGTTTTACTTGAATGACGCTGCTCATGCTTGCAACCGCTGGGATGCAGGTGCATGCCTCTAGCATGAA
GTCAAACAA

> **KF134173** Seq1[organism=*Symbiodinium* sp.] *Symbiodinium* clade C isolate **C42(type2).2** 5.8S ribosomal RNA gene (partial) and internal transcribed spacer 2 (complete) and 28S ribosomal RNA gene (partial); isolated from ***Entacmaea quadricolor*** in 2012.

AATCAATGGCCTCCTGAACGTGCGTTGCACTCTTGGGATTTCCTGAGAGTATGTCTGCTTCAGTGCTTA
ACTTGCCCCAACTTTGCAAGCAGGATGTGTTGCTGCCTTGCGTGCTTATGAGCTATTGCCCTCTGAGCC
AATGGCTTGTGAATTGCTTGGTTCTTGCAAAATGCTTTGTGCGCTGTTATTCAGGTTTCTACCTTCGTGG
TTTTACTTGAGTGACGCTGCTCATGCTTGCAACCGCTGGGATGCAGGTGCATGCCTCTAGCATGAAGTC
AGACAA

> **KF134172** Seq1[organism=*Symbiodinium* sp.] *Symbiodinium* clade C isolate **C25.1** 5.8S ribosomal RNA gene (partial) and internal transcribed spacer 2 (complete) and 28S ribosomal RNA gene (partial); isolated from ***Entacmaea quadricolor*** in 2012.

AATCAATGGCCTCCTGAACGTTCGTTGCACTCTTGGGATTTCCTGAGAGTATGTCTGCTTCAGTGCTTA
ACTTGCCCCAACTTTGCAAGCAGGATGTGTTTCTGCCTTGCGCTCTTATGAGCCATTGCCCTCTGAGCC
AATGGCTTGTTAGTTGCTTGGCTCTTGCAAAATGCTTTGCGCGCTGTTATTCACGTTTCTACCTTCGTGG
TTTTACTTGAGTGACACGCTGCTCATGCTTGCAACCGCTGGGATGCAGGTGCATGCCTCTAGCATGAAG
TCAGACAA

> **KF134172** Seq1[organism=*Symbiodinium* sp.] *Symbiodinium* clade C isolate **C3.25** 5.8S ribosomal RNA gene (partial) and internal transcribed spacer 2 (complete) and 28S ribosomal RNA gene (partial); isolated from ***Entacmaea quadricolor*** in 2012.

AACCAATGGCCTCCTGAACGTGCGTTGCACTCTTGGGATTTCCTGAGAGTATGTCTGCTTCAGTGCTTA
ACTTGCCCCAACTTTGCAAGCAGGATGTGTTTCTGCCTTGCGTTCTTATGAGCTATTGCCCTCTGAGCC
AATGGCTTGTTAATTGCTTGGTTCTTGCAAAATGCTTTGCGCGCTGTTATTCAAGTTTCTACCTTCGTGG
TTTTACTTGAGTGACACGCTGCTCATGCTTGCAACCGCTGGGATGCAGGTGCATGCCTCTAGCATGAAG
TCAGACAA

APPENDIX B:

Bleaching descriptors (Chapter 5)

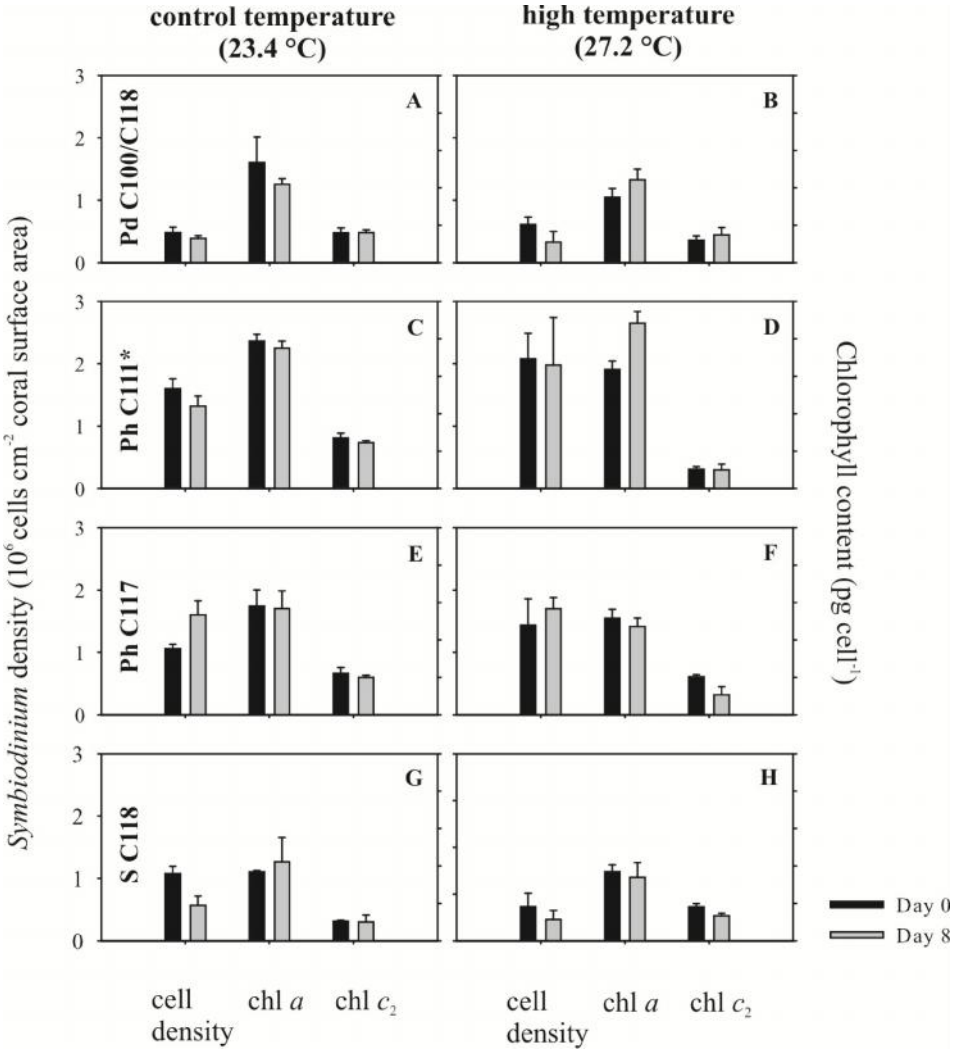

Figure B.1: *Symbiodinium* density in 10^6 cells cm^{-2} coral surface area (left y-axis) as well as chlorophyll *a* and c_2 content in pg $cell^{-1}$ (right y- axis) for Day 0 (black bars) and Day 8 (grey bars) at the control temperature of 23.4 °C (left vertical lane) and at high temperature of 27.2 °C (right vertical lane) in the coral species *Pocillopora damicornis* hosting *Symbiodinium* ITS2 types C100 and C118 (first horizontal lane), *Porites heronensis* hosting *Symbiodinium* C111* (second horizontal lane), *Porites heronensis* hosting *Symbiodinium* C117 (third horizontal lane) and *Stylophora* sp. hosting *Symbiodinium* C118 (forth horizontal lane). No significant change ($p > 0.05$) in any of the parameters has been revealed by rmANOVA.